The productivity of coral reef fishes

Renato Morais Araujo

February 2020

For the Degree of Doctor of Philosophy

College of Science and Engineering

ARC Centre of Excellence for Coral Reef Studies

James Cook University

Dedico esta tese ao Vovô Manoel,

avô, pai, herói

Acknowledgements

I thank my supervisor, David Bellwood, for continued guidance, counselling, and unconditional availability and support throughout the thesis; for those long hours of brain-draining, incredibly insightful meetings, and for not minding my artful representations of him in presentations. Thanks also to Sean Connolly for his disproportional contribution to the theoretical development of this thesis, which happened in the context of a particularly challenging chapter.

Thanks to all who kindly helped me during field work: Pauline Narvaez, Victor Huertas, Ale Siqueira, Chris Hemingson, Sterling Tebbett, Rob Streit, Joshua Phua, Sam Shu Quin and Sabrina Inderbitzi. Special thanks to 'my' rusty chain field crew, Pauline, Victor and Ale, for taking over big responsibilities while I eternally counted 68,656 big or small fish. You tamed quaddie and marinated chains (just enough rustiness), spending days at depths deeper than the height of a (short) person. That happened despite broken ears, fingers, cameras and unplanned alarms. Thank you very much.

Thanks to my academic mentors, Sergio Floeter and Cadu Ferreira, who, since 2007 (back in the Holocene), taught me to think geographically and energetically. The opportunities you provided me opened doors I did not think existed. Conversations with Michel Kulbicki and Howard Choat, back in 2015, were instrumental in my will to pursue the merging of fish demography and visual surveys to investigate coral reef production. Howard also provided great many insights over coffee during my candidature. Murray Logan pointed the way to the newly accessible Bayesian world and influenced much of the analytical reasoning of this thesis.

Thank you to the Centre of Mediocrity for Coral Reef Studies folks: Ale Siqueira, Arun Oakley-Cogan, Chris Hemingson, François Latrille, Mike Mihalitsis, Rob Streit, Victor Huertas, Sterling Tebbett. Our adventures, from the Tin Box to the ATSIP, including French Polynesia, Canberra, Sydney, Brisbane, Finch Hatton, and, obviously, fossicking in the desertic Richmond, will never be forgotten. Many of this thesis' concepts and solutions were triggered by coffee break conversations on workdays (sometimes coffee days on work breaks). Thanks also to Bellwood Lab people, past and present: Orpha Bellwood, Martial Depczynski, Simon Brandl, Chris Fulton, Roberta Bonaldo, Michael Marnane. Martial Depczynski's work was the foundation stone on which this thesis developed.

Fieldwork for this thesis was made possible by a Lizard Island Doctoral Fellowship provided by the Lizard Island Reef Research Foundation, with the support of the Australian Museum Lizard Island Research Station. Special thanks to Anne Hogget, Lyle Vail, Marianne and John Dwyer for making Lizard Island the best place on Earth to do coral reef research.

Staff at JCU and the Centre of Excellence for Coral Reef Studies supported aspects of my candidature, particularly Janet Swanson, Vivian Doherty, Greg Suosaari, Glenn Ewels, Claire Meade, Prof. Garry Russ, Prof. Andy Hoey, Tammy Walsh, Rick Abom and Liz Tynan. Also, special thanks to the amazing staff of the Damai II for all the field support.

Friends from Lavras, Floripa, Townsville and elsewhere have endured my absolute incapacity to read, respond to or send messages. Thank you for persisting (I hope). Also, to my French family, who have received me with open arms, tolerated repeated mumblings of a very narrow vocabulary, and still want to see me back: merci beaucoup.

I will always be grateful to my family. My grandpa Manoel and my grandma Zulma were much more than grandparents, they offered me infinite love and the best childhood I could ask. They were role models for life and will forever live in my heart. This thesis is dedicated to my grandpa, who sadly passed away during this thesis, but who will remain my eternal inspiration. My mom Débora, my dad Fábio and my brother Fabinho have provided enormous support throughout my life, and have coped with excessively long absences. My uncle Luís Cesar unveiled the world for me and lovingly provided me with opportunities that eventually brought me here. Muito obrigado a vocês por tudo, sempre. Finally, Lizard Island gave me more than fish data: to my partner Pauline, thank you for enduring stressful deadlines, and for sharing a life, good and bad times, love, plans and dreams with me.

Statement of the Contribution of Others

This thesis was supported by funds provided to me by the Lizard Island Reef Research Foundation (Lizard Island Doctoral Fellowship) and the Graduate Research School, James Cook University (HDR Competitive Research Training Grant), as well as funds provided to David Bellwood by the Australian Research Council (ARC Discovery, ARC Centre of Excellence and ARC Laureate Fellowship). Part of the fieldwork was also supported by an invitation from the Ocean Geographic Society to integrate the Elysium Heart of the Coral Triangle Expedition. During the course of my degree, I was supported by a James Cook University Postgraduate Research Scholarship.

This thesis was conducted under the supervision of David Bellwood, and all chapters benefited from his conceptual guidance and editorial assistance. In **Chapter 5**, Martial Depczynski, Christopher Fulton, Michael Marnane, Pauline Narvaez and Victor Huertas participated in the data collection and data analysis, and Simon Brandl participated in the data analysis and conceptual development. All co-authors provided editorial assistance. **Chapter 6** was conducted under the shared supervision of David Bellwood and Sean Connolly. Sean Connolly contributed conceptual guidance, data analysis advice and editorial assistance.

All work reported in this thesis has been conducted in accordance with Great Barrier Reef Marine Park Authorization Permit number G17/38142.1 to David Bellwood, and JCU Animal Ethics Committee Approval A2375 to myself.

Abstract

Coral reefs are undergoing profound climate-driven structural and functional changes. These changes are expected to affect the fish and fisheries production that provide food for millions of people. However, the energetic processes that lead from solar energy to fish production on coral reefs are still poorly understood. This raises the question: will coral reefs maintain their capacity to provide this critically important ecosystem service? Answering this question will require innovative strategies to measure food production potential on reefs and to identify the impacts of ecosystem change. In this thesis, I first developed a framework for quantifying reef fish productivity from common field survey data and life-history traits. Combining this framework with detailed reef fish surveys, I then addressed three key ecological questions: What are the main trophic pathways fuelling reef fish productivity? What are the effects of coral loss, reduced topographic complexity and overfishing on productivity? And, what are the potential causal mechanisms underpinning potential productivity changes?

Growth is a fundamental process of life, but little is known about what drives reef fish growth at macroecological scales. Given the practical challenges of collecting growth data for all 6,000+ reef fish species, universal relationships would be useful for predicting growth trajectories. My first objective was, therefore, to evaluate the drivers of reef fish growth across large spatial and environmental gradients and across a range of morphological and behavioural traits. I compiled, filtered and standardised a dataset of almost 2,000 Von Bertalanffy Growth Model curves from 588 reef fish species. These were used to test the influence of environmental variables and species traits on growth, while also accounting for phylogenetic structure. Body size was found to be the main driver of reef fish growth curves, followed by temperature. Alongside diet and reef dependence, these provided the basis for a machine learning model that predicted reef fish growth trajectories with high accuracy and precision.

Although there is increasing interest in the productivity of coral reef fisheries, there are currently no standardised methods to explore assemblage-level reef fish production. My second objective was, therefore, to develop a robust and easily applicable framework to quantify fish productivity in high-diversity systems, such as coral reefs. I started by integrating the model developed to predict growth trajectories into an existing approach to estimate individual and species-level somatic growth, and then

expanding this approach by incorporating mortality in the growth functions. This resulted in a framework that yielded fisheries-independent fish productivity from routinely-collected fish survey data. A step by step guide and an easy to use interface (R package) are provided, highlighting the utility of this approach as a tool for managing coral reef resources.

Building on this approach, I used a high-definition survey dataset to generate the first energetic roadmap of a full coral reef fish assemblage, from the smallest to the largest fishes. Specifically, I identified the trophic pathways determining fish productivity on a windward coral-degraded reef. Because of its reduced coral cover and high abundance of algal turfs, this reef represents the conditions expected for most future coral reefs. Despite the reduced coral cover, 41% of all fish productivity was still supported by species feeding in the water column on external food sources, i.e. plankton from pelagic pathways. The critical energetic contribution of these pelagic subsidies would remain largely undetected if considering standing biomass alone, since this high productivity originated from a relatively small fish biomass. Thus, coral-degraded reefs can still maintain considerable fish productivity, with planktivorous fishes providing major pelagic subsidies.

The global coral bleaching events of 2015-2017 reconfigured coral reefs, sparking the need to understand how multiple ecosystem functions respond to coral loss. I evaluated four metrics of the functioning of reef fish assemblages (standing biomass, productivity, consumed biomass and turnover) on a coral reef in the Great Barrier in two time periods: in 2003/04 and 2018/19. During this 15-year period, the reef was hit by two cyclones and two severe bleaching events leading to habitat-specific coral losses of up to 83%. Family-level responses to coral loss were similar to previous studies, but there were unexpected assemblage-wide responses. Reef fish biomass, productivity and consumed biomass increased after 15 years, indicating a trajectory of biomass accumulation after the observed coral loss. However, this biomass build-up was not matched by renewal rates, as turnover declined over the same period. The resulting slower-paced reef fish assemblages suggest enhanced production might be due to the growth of previously present individuals, questioning the long-term stability of the observed energetic shifts.

I then expanded the thesis to explore the potential relationship between coral reef fish productivity and standing biomass on a macroecological scale. Although standing biomass is a widely used, static,

proxy for inherently dynamic biomass production rates, the equivalence between coral reef fish biomass and productivity has never been tested. I therefore investigated the relationship between biomass and productivity in a key reef fish group, using a 15,000 km wide Indo-Pacific dataset, which revealed evidence for distinct transect-level productivity-biomass relationships in high-biomass vs. low-biomass regions. These differences were due to smaller fishes with higher production per unit biomass in low-biomass regions. Importantly, increased human population densities explained reduced fish size and decreased biomass in these regions, but was not related to productivity. A modelling framework that simulates the impacts of overexploitation on reef fish biomass and productivity showed that, as size-selective fishing depleted fish biomass, it triggered increased production per unit biomass. Thus, compensatory productivity at low biomass may help to explain why some biomass-depleted fish assemblages still sustain fisheries catches and provide ecosystem goods under continued exploitation.

The productivity estimates obtained from the frameworks developed herein are intuitive, easy to obtain, and independent from fisheries surveys. They, therefore, offer an opportunity to explore ecological questions that directly address resource production patterns on coral reefs. In this thesis, this approach revealed that on coral reefs: 1) external pelagic subsidies are key to coral reef fish production, even on reefs with low coral cover; 2) reef fish assemblages exposed to severe coral loss may undergo energetic shifts to a more productive, but potentially more unstable, state; and 3) overexploitation drives stronger declines in reef fish biomass than productivity, due to compensatory production at low biomass levels, potentially helping to explain sustained fisheries yields despite depleted biomass. By bridging the gap between common survey data and traditional resource production models, this thesis lays the foundation for a new resource assessment paradigm on coral reefs.

Table of Contents

List of Tables

List of Figures

Chapter 1: General Introduction

Coral reefs are among the most productive ecosystems on Earth, with gross carbon fixation commonly exceeding 2,500 g C m^{-2} $year^{-1}$ (Crossland, Hatcher, & Smith, 1991; Kinsey, 1985; Odum & Odum, 1955). However, this exceptional food production is almost entirely consumed by reef residents, with respiration rates often matching carbon fixation (Kinsey, 1985; Odum & Odum, 1955; Sargent & Austin, 1954). The discovery of this fine energetic balance in the early 1950s led ecosystem ecologists to believe that coral reefs were closed systems, subsisting in nutrient-scarce tropical waters by means of elaborate mechanisms of internal recycling (e.g. Hatcher, 1988; Kinsey, 1985; Lewis, 1977; Odum & Odum, 1955). This apparent contradiction of high internal photosynthesis in crystal clear, 'desert' oceans has garnered enough attention as to merit its own term, the 'Darwin's Paradox' (e.g. Mumby & Steneck, 2018; Richter, Wunsch, Rasheed, Kötter, & Badran, 2001), although Darwin's connection to this paradox is, at best, circumstantial (see **Appendix A** for an investigation on the origins of the 'Darwin's Paradox'). Only later in the 20th Century, did quantification of energy flows in detritus-based food webs provide a potential mechanistic explanation for high photosynthesis and high recycling (e.g. Arias-González, Delesalle, Salvat, & Galzin, 1997; Crossland et al., 1991; Opitz, 1996).

The 'closed-system' paradigm of coral reefs was soon confronted by observations of zooplankton depletion and extensive zooplankton-feeding by reef fishes (e.g. Emery, 1968; Hiatt & Strasburg, 1960; Randall, 1967). The closed-system paradigm persisted, however, because the low concentrations of plankton measured in surface waters around coral reefs were deemed insufficient to contribute to the extensive energetic requirements of coral reef consumers (Glynn, 1973; Lewis, 1977). Later research employing fine-scale mapping of water movement and plankton transport revealed that the 'plankton insufficiency' on coral reefs was only superficial. Cross-depth water transport mechanisms, such as upwelling, downwelling and internal waves were found to bring nutrients and biological productivity from deeper oceanic waters and concentrate them in the shallows near land masses (Andrews & Gentien, 1982; Genin, Jaffe, Reef, Richter, & Franks, 2005; Gove et al., 2016; Hamner & Hauri, 1981; Rougerie & Wauthy, 1993; Wyatt, Lowe, Humphries, & Waite, 2010). These mechanisms allow the pelagic production reaching coral reefs to attain values orders of magnitude larger than those found in

surface ocean waters (Genin, 2004; Gove et al., 2016; Hamner & Hauri, 1981; Hamner, Jones, Carleton, Hauri, & Williams, 1988; Wyatt et al., 2010). Upward water transport, thus, offered the missing piece in the coral reef productivity puzzle, highlighting the need to simultaneously consider both internal primary production and inputs from adjacent ecosystems, particularly those from the pelagic realm.

Coral reef productivity is exploited by a wide array of consumers, with fishes being a dominant element in both diversity and biomass. Reef fishes *sensu lato* comprise over 6,000 species (Kulbicki et al., 2013; V. Parravicini et al., 2013) covering a vast array of forms and functions, and featuring numerous interactions that underpin their role as dominant actors in the energetic landscape of coral reefs (Bellwood & Wainwright, 2002; Wainwright & Bellwood, 2002). Not surprisingly, humans took advantage of coral reef productivity through harvesting of reef resources very early. This is indicated by early evidence of seafaring and fishing (Erlandson, 2001; Erlandson & Rick, 2010), including reef fish remains in shelters as old as 42,000 years from coral areas in East Timor, and 28,000 years in the Solomon Islands (S. O'Connor, Ono, & Clarkson, 2011; Wickler & Spriggs, 1988). Later on, the Polynesian island-hopping in the Pacific could hardly be made possible without relying on the predictability of coral reef resources (e.g. Craig, Green, & Tuilagi, 2008; Giovas, Lambrides, Fitzpatrick, & Kataoka, 2017; Longenecker et al., 2014). The strong cultural and ecological ties established between humans and coral reefs has resulted in a high contemporary dependence on reef resources. Over 400 million people live close to coral reefs (Donner & Potere, 2007), at least 6 million actively engage in coral reef fishing (Teh, Teh, & Sumaila, 2013), with many more benefitting indirectly from these activities. Thus, the overall importance of coral reefs in sustaining the livelihoods of people, particularly in low-income tropical countries, cannot be overstated.

Until recently, most of the research focused on understanding the relationship between coral reef resources and people's livelihoods addressed the impacts of overharvesting (including overexploitation or overfishing). Marine Protected Areas were largely advocated, planned and implemented as a management instrument aimed not only at maintaining and rebuilding fish stocks (Edgar et al., 2014; Halpern, 2003; Mora et al., 2006; Sale et al., 2005; Worm et al., 2009), but also as a means of enhancing the resilience of marine ecosystems. Enhanced resilience was thought to increase the chances of coral reefs resisting and recovering from impacts of other stressors (the "resilience-based paradigm", e.g.

Bellwood, Hughes, Folke, & Nyström, 2004; Bruno, Côté, & Toth, 2019; Hughes, Graham, Jackson, Mumby, & Steneck, 2010; Mumby et al., 2006). However, the unprecedented global El-Niño event of 2014-2016 had an important role in changing convictions and redirecting priorities in coral reef research (e.g. Bellwood, Pratchett, et al., 2019; Hughes, Barnes, et al., 2017), including this thesis. Indeed, in 2015, when I first proposed this research program, my focus was primarily on understanding how trophic pathway partitioning could affect the spatial patterns of coral reef fish productivity. But the severe global coral mortality event that followed resulted in profound changes to coral reefs, including, presumably to productivity patterns.

The impacts of the 2014-2016 marine were particularly well documented – and striking – on the Great Barrier Reef (GBR), Australia. Until then, the largest reef system in the planet had escaped from two bleaching events and a series of cyclones with only limited damage (Hughes, Kerry, et al., 2017). However, in 2016, over 90% of the reefs in the GBR suffered some level of bleaching, with over 50% suffering severe bleaching (> 60% of the corals bleached) (Hughes, Kerry, et al., 2017). This massive impact was not evenly spread in spatial or taxonomic scales, being concentrated in the northern part of the GBR and in fast-growing, staghorn and tabular corals (Hughes, Kerry, et al., 2017, 2018). Overall, coral cover declined by 30% throughout the GBR, with over 50% decreases on reefs in the northern portion, and over 75% cover reduction for staghorn and tabular forms (Hughes, Kerry, et al., 2018). These catastrophic coral population reductions and species composition changes were followed, not surprisingly, by plummeting coral recruitment (Hughes et al., 2019). Although the responses of reef fish assemblages to coral mortality often occur in longer time frames (e.g. Graham et al., 2007; Pratchett et al., 2008), acute changes in the abundance, spatial and trait distribution of some groups have already been documented (Richardson, Graham, Pratchett, Eurich, & Hoey, 2018; Stuart-Smith, Brown, Ceccarelli, & Edgar, 2018; but see Wismer, Tebbett, Streit, & Bellwood, 2019 for how coral-fish responses can be spatially decoupled at local scales).

The pervasive 2014-2016 El-Niño had a global extent and its damage to coral reefs in other parts of the world mirrored what was seen on the GBR (Hughes, Anderson, et al., 2018; McClanahan et al., 2019). Not only have the effects of climate change now reached coral reefs globally, they have also become more frequent and more intense (Hughes, Anderson, et al., 2018). Although coral mortality is

the main mechanism through which coral reef fishes are expected to respond to marine heatwaves, mismatching responses of fishes and corals have suggested that direct heatwave effects on fishes might already be occurring (Stuart-Smith et al., 2018). Indeed, tropical species, including most coral reef fishes, live dangerously close to their metabolic optima (Barneche et al., 2014; Rummer et al., 2014; Tewksbury, Huey, & Deutsch, 2008). While further temperature increases from heatwaves are predicted to generate severe physiological impacts (Rummer et al., 2014) expected physiological impacts might be ameliorated to some extent by changes in metabolic optima driven by transgenerational acclimation and adaptation (Donelson, Munday, McCormick, & Pitcher, 2012; Donelson, Salinas, Munday, & Shama, 2018).

Nevertheless, temperature is a critical ecological driver that dictates not only individual-level processes, such as metabolic requirements (Brown, Gillooly, Allen, Savage, & West, 2004; Gillooly, Brown, West, Savage, & Charnov, 2001), but also higher order phenomena, such as species range limits (Stuart-Smith, Edgar, & Bates, 2017), abundance-distribution patterns (Waldock, Stuart-Smith, Edgar, Bird, & Bates, 2019), and ecosystem energetic fluxes (Barneche et al., 2014). Multiple modelling forecasts have now been developed to evaluate the impact of present and future temperature increases on fisheries productivity at a global level (e.g. Barange et al., 2014; Blanchard et al., 2012; Cheung et al., 2010; Lotze et al., 2019; Thiault et al., 2019). These models generally forecast a redistribution of global fisheries catches under global warming, with increased catches in temperate latitudes and decreased in the tropics (e.g. Blanchard et al., 2012; Cheung et al., 2010; Thiault et al., 2019). This prediction is worrisome because of the dependence of low-income countries on tropical fisheries and, particularly, on reef fisheries (Barange et al., 2014; Newton et al., 2007).

Global-scale fisheries forecast models, however, cannot capture complex processes that emerge at lower spatial scales on coral reefs (e.g. Jennings & Collingridge, 2015). Of particularly significance, the structural complexity of the coral-accreted reef matrix provides numerous niche opportunities for coral reef organisms (Graham & Nash, 2013), but tends to decline sharply after extensive coral mortality (Pratchett et al., 2008). Smaller-scale models that explicit consider aspects such as diversity and abundance of prey refuges have been used to examine the effects of structural complexity loss on reef fish productivity (Rogers, Blanchard, & Mumby, 2014, 2018; Rogers, Blanchard, Newman, Dryden, &

Mumby, 2018) These models predict short-term increases in fish productivity after coral loss, mainly due to herbivores benefitting from expanding algal turfs, followed by long-term declines in productivity after the erosion and collapse of prey refuges (Rogers, Blanchard, & Mumby, 2018; Rogers, Blanchard, Newman, et al., 2018).

Contrasting with these models, empirical resource assessment on coral reefs has been traditionally focused on static metrics such as fish abundance and standing biomass (D'agata et al., 2016; Duffy, Lefcheck, Stuart-Smith, Navarrete, & Edgar, 2016; Mora et al., 2011; Nash & Graham, 2016) These are often used as a proxy for the real quantity of interest, i.e. the rates of production of new biomass. Although the limitations of using standing biomass to estimate biomass production were recognised early in coral reef ecology (Bardach, 1959), difficulties in quantifying the dynamic process of biomass production (K. R. Allen, 1971) resulted in standing biomass being used as a popular resource assessment tool. Unfortunately, to-date, there is no unequivocal evidence to indicate that a resource pool metric (standing biomass) can be used to predict its underlying build-up rate (productivity). This would be the same as judging the chance of a family running out of food solely by the size of their fridge, without accounting for how fast they eat or visit the shops. Indeed, a comprehensive meta-analysis showed that, across multiple types of ecosystems, rarely were standing biomass and productivity directly proportional (Jenkins, 2015). If biomass is a questionable proxy, then there is an ever-increasing necessity to focus on quantifying resource production. However, present methods to estimate reef fish productivity are burdensome, either computationally (i.e. ecosystem or trophic models) or logistically (i.e. field-intensive monitoring of catches), and thus productivity estimates remain largely unavailable to most reef ecologists. Unfortunately, the lack of an alternative, general and accessible method to quantify resource production is now a major obstacle to our understanding of coral reef fisheries responses to global warming, stymying management progress and jeopardising the future of coral reef fisheries.

Thesis outline

The unprecedented worldwide reshaping of marine ecosystems has created an ecological crisis that threatens the livelihoods of millions of people that rely on reef fish production for food. Addressing this emergency will require innovative strategies to measure food production potential and to identify the impacts of ecosystem change. The main aim of this thesis, therefore, is to develop a simple and effective framework to quantify coral reef fish productivity, and then use it to evaluate ecological patterns of productivity and their susceptibility to global changes and human impacts. In **Chapter 2**, I develop a machine learning-based model to predict reef fish growth coefficients for combinations of traits and environmental settings. This model both standardises existing growth data, ensuring comparability, and predicts somatic growth for data deficient species. In doing so, it bridges the gap between individual somatic growth and community-wide biomass production on reef systems. In **Chapter 3**, I provide a framework for easily estimating fish productivity for high species diversity ecosystems, such as coral reefs. This framework is anchored on somatic growth and mortality probability, and is facilitated by the model from the previous chapter. I also consider the use of fish productivity as a tool for monitoring and managing high-diversity aquatic systems, for which I provide an easy-to-use R software interface. In **Chapter 4**, I combine the model and framework from the previous chapters to quantify the productivity of an entire coral reef fish assemblage for the first time, from the smallest to the largest fishes. I then partition this productivity according to habitat and distinct trophic pathways and test a conceptual model in which reef fish productivity is driven by water flow and topographic complexity. In **Chapter 5**, I evaluate the effects of severe coral loss on four metrics of energy flow and storage that underscore biomass production, explicitly testing the hypothesis that coral loss can lead to energetic shifts in fish assemblages. This chapter expands on the previous ones by quantifying multiple aspects of fish production on coral reefs. Finally, in **Chapter 6**, I evaluate the key assumption that fish standing biomass is a surrogate for productivity. I explore potential relationships between biomass and productivity in two spatial scales using a large dataset of a key fisheries target group, simultaneously looking for human impact correlates. I then develop a theory-driven modelling

framework to simulate fishing in coral reef fish assemblages, aimed at replicating the observed patterns while testing for potential explanatory mechanisms.

Chapter 2: Global drivers of reef fish growth

Published as: Morais, R.A., & Bellwood, D.R. (2018) Global drivers of reef fish growth. *Fish and Fisheries, 19*(5), 874–889.

Introduction

Individual growth, *i.e.* increasing body size over time, is a fundamental process of life. If "the primary goal of any organism is to reproduce" (Roff, 1992), there is no doubt that growth is one of the main mechanisms facilitating reproduction. As individuals grow, they experience lower mortality rates and higher reproductive output that increase their reproductive success (Begon, Townsend, & Harper, 2006; Beverton & Holt, 1959; Calder, 1984). Not surprisingly, life histories appear to be adjusted to optimize energetic investments in somatic growth and reproduction (Calder, 1984; Charnov & Gillooly, 2004; Roff, 1992). However, the metabolic costs of synthesizing new molecules and replicating cells increase disproportionally as organisms grow (Bertalanffy, 1938, 1957). As a result, growth rates decrease during ontogeny, resulting in asymptotic or sigmoidal size-at-age curves that tend to stabilize close to the population average maximum body size (Bertalanffy, 1938, 1957; Ricker, 1979).

Somatic growth is one of the most important data types for fisheries stock assessment. There have been, therefore, many theoretical and methodological advances in the study of fish growth in the context of fisheries stock management (e.g. Beverton & Holt, 1957, 1959; Hilborn & Walters, 1992; Pauly, 1979; Ricker, 1979). Yet, fisheries biology has been based largely on temperate fish stocks, with studies often focusing on a single species (Beverton & Holt, 1957; Pauly, 1979). By comparison, tropical fishes have been relatively understudied (Munro & Williams, 1985; Pauly, 1980a). Moreover, there have been few attempts to understand growth patterns of fishes at the community or macroecological level (but see Munro & Williams, 1985; Pauly, 1998). Since growth links assimilated energy to the production of individual biomass (Brown et al., 2004), it incorporates individuals into patterns of community metabolism (Barneche et al., 2014). In this context, the size that an organism attains has physiological implications that scale up to the ecosystem level (Brown et al., 2004; Calder, 1984; Gillooly et al., 2001; Gillooly, Charnov, West, Savage, & Brown, 2002; T. A. McMahon & Bonner, 1983; Schmidt-Nielsen,

1984). High biodiversity fish assemblages, as formed on coral reefs, incorporate numerous functional and life-history types, with a wide range of potential growth trajectories (Bellwood & Wainwright, 2002; Depczynski & Bellwood, 2006). These systems, therefore, offer an exciting opportunity to understand how fish growth varies at a macroecological scale (i.e. among populations or species).

Body size and temperature are the two most important determinants of metabolism (Brown et al., 2004; Gillooly et al., 2001) and are also very likely to be important in shaping reef fish growth (Pauly, 1979; Ricker, 1979). Additionally, growth depends on the energy and nutrient supply available to an individual (Bertalanffy, 1957; West, Brown, & Enquist, 2001). Reef fish acquire resources in a multitude of different ways (Wainwright & Bellwood, 2002), and traits such as dietary preferences (Buesa, 1987; Choat & Robertson, 2002), position in the water column (Bellwood, 1988; Hamner et al., 1988) and schooling behaviour (Kavanagh & Olney, 2006) might also affect their growth. Finally, geometric constraints of body shape could affect the way fish grow, both directly and indirectly (e.g. by affecting their swimming performance Pauly, 1998). Despite important advances in characterizing some of the drivers of reef fish growth (Choat & Axe, 1996; Choat & Robertson, 2002; Gust, Choat, & Ackerman, 2002; Trip, Choat, Wilson, & Robertson, 2008), we still do not know the relative importance of these environmental and functional variables to determine growth patterns at the community level. In addition, we do not know how community-level growth patterns will behave at broader scales. Because characterizing fish growth is such a resource-demanding task, it is unrealistic to expect that ecologists will have access to growth trajectories of all species in high diversity reef communities. This hinders our comprehension of, for example, community-level fish growth and its energetic implications. Better knowledge of the drivers of reef fish growth would allow us to predict growth trajectories of unsampled species and further improve our understanding of the energetics of reefs as a whole.

In this context, this study aims to quantitatively evaluate the drivers of reef fish somatic growth across a large gradient of environmental variables and across a range of morphological and behavioural traits. The basis of this study is the large volume of fish growth (mainly size-at-age) data collected by fisheries researchers over many decades. We first develop a standardization procedure that generates a growth measure that is both intuitive and comparable between species and populations. Then, we evaluate the metabolic predictions that body size and temperature should be the main drivers of reef

fish growth by modelling standardized reef fish growth relative to these variables, while simultaneously accounting for phylogenetic relationships. We also consider, in the same framework, traits that affect resource availability (primary productivity) and energy acquisition by reef fishes (diet, position relative to the reef, schooling behaviour, and body shape). We hypothesize that these factors might be important in explaining residual variance in growth, after accounting for body size and temperature. Finally, we feed the most important variables to a new machine learning routine that accurately predicts this standardized growth measure for the entire range of fish morphological and behavioural traits and environmental variables investigated.

Methods

Setting the stage: bioenergetics of fish growth

A bioenergetic model describing animal growth was developed by Von Bertalanffy (Bertalanffy, 1938, 1949, 1957) and has been extensively applied to fish growth, especially in fisheries biology (e.g. Beverton & Holt, 1957; Hilborn & Walters, 1992; Pauly, 1979). We acknowledge the effectiveness of other more recent growth models (e.g. West *et al.* 2001) but we use Von Bertalanffy's one because: 1) the parameters required are mathematically simple to obtain and easy to interpret; and 2) it has been widely used. Thousands of growth curves have been produced using this model over the last seven decades. In the context of the Von Bertalanffy Growth Model (VBGM), growth is the net result of two opposite metabolic processes: anabolism, the production of body substances; and catabolism, the consumption of body substances. Its underlying mathematical formulation, the Von Bertalanffy Growth Function (VBGF) follows as

$$\frac{dW}{dt} = \eta W^m - \kappa W^n \quad (1)$$

in which $\frac{dW}{dt}$ is the instant rate of change in fish weight over time; ηW^m is a term that represents anabolism and κW^n is a term that represents catabolism. Growth may, thus, be either positive, when the organism increases in body mass, or negative, when the organism decreases in body mass. Biologists

are most frequently interested in positive growth, which, for multicellular organisms, is mainly due to an increasing number of cells (Bertalanffy, 1938). An increase in the number of cells leads to a proportional increase in catabolism because all living cells consume body substances (Bertalanffy, 1938; Pauly, 1979). Therefore, the catabolic term should be proportional to weight, with n = 1. For fishes and other aquatic organisms, it has been proposed that anabolism is limited by the rate at which oxygen can diffuse through the gills and become available for cell synthesis (Bertalanffy, 1957; Pauly, 1979). In this case, the anabolic term would increase proportionally to gill surface area and not to overall body weight (Bertalanffy, 1949; Pauly, 1979), with $m = \frac{2}{3}$ (Pauly 1979). However, empirical evidence strongly suggests that m is closer to $\frac{3}{4}$ than to $\frac{2}{3}$ (Pauly, 1979; Ricker, 1979; Savage, Gillooly, Woodruff, et al., 2004). The most likely explanation to this is that anabolism is proportional to the area of the circulatory network rather than to the gill surface area (West, Brown, & Enquist, 1997). Nevertheless, integrating the VBGF with $m = \frac{2}{3}$ generates a simplified mathematical formulation, the so-called "special VBGF" (Beverton & Holt, 1957; Pauly, 1979). Not surprisingly, the simple formulation of the special VBGF is the most widely employed facet of the VBGM, and the one used by most growth studies.

The integrated special VBGF assumes two forms:

$$L_t = L_\infty\left(1 - e^{-K(t-t_0)}\right) \quad (2)$$

and

$$W_t = W_\infty\left(1 - e^{-K(t-t_0)}\right)^b \quad (3)$$

relating the body size of a fish at time t (in length, L_t, or weight, W_t) to the average asymptotic size of the population to which it belongs (L_∞ and W_∞), the theoretical age when size = 0 (t_0), and the rate at which fish in this population, on average, approach the population asymptotic size (K). Of these parameters, t_0 holds little biological information (Kritzer, Davies, & Mapstone, 2001; Pauly, 1979) and has frequently been constrained to zero or estimated after constraining size when age = 0 to the

settlement size (e.g. Berumen, 2005; Kritzer et al., 2001). The exponent b on equation (3) is equal to the species-specific length-weight regression parameter b (Froese, 2006). The most fundamental parameters to characterize growth are, thus, L_∞ (or W_∞) and K, which can also be used to statistically estimate t_0 (Pauly, 1979, 1980a).

A database of VBGF parameters: assembling and processing

The VBGM can be fitted to individual or population-level growth data. Individual-level data include repeated measures of the same individual over time, as in captivity or mark-recapture studies (Francis, 1988). Population-level data include length-frequency analysis (Pauly & Morgan, 1987) and size-at-age data from temporally deposited rings in hard structures such as vertebrae, dorsal spines, scales, but mainly otoliths (Campana, 2001; Choat & Robertson, 2002). However, caution should be exercised when comparing growth data derived from different methods for two reasons. Firstly, because in the VBGM from individual or population-level data, L_∞ values have distinct meanings (Francis, 1988). For individual-level data it is the length at which the expected growth increment of an individual is zero, whereas for population-level it is the average asymptotic size of a population (Francis, 1988). Secondly, because different methods can derive different VBGF parameters' estimates, even from the same population (e.g. Schwamborn & Ferreira, 2002). Indeed, length-frequency and age-based methods have been used simultaneously to improve VBGF parameter estimates (Campana, 2001; Morales-Nin, 1989). In the present paper, we compiled an extensive reef fish growth database that includes both individual and population-level growth data. We accounted for the potential issues listed above by first standardizing K relative to the maximum size of a species instead of L_∞, and then explicitly considered the type of data used for fitting the VBGM as a covariate in our model. Details of both procedures are given below. We then examine the effects of environmental factors and species morphological and behavioural traits on growth.

The assembled database included the VBGF parameters, length-weight regression parameters, species morphological and behavioural traits and environmental variables associated with the geographic location of the compiled reef fish growth curves. We used the family list provided by

Bellwood & Wainwright (2002) to define a minimum list of "reef fish" families, with the addition of important commercial groups that eventually use reef habitats: Rachycentridae, Scombridae and Sebastidae. It is important to make clear that we use a broad concept of "reef fish" that encompasses both coral reef taxa and families restricted to the rocky coasts of temperate regions (i.e. Sebastidae). Within the selected families, we kept only those genera and species known to use reefs or that are likely to be seen in the vicinity of a reef. The main source of data was FishBase (Froese & Pauly, 2018) and the references therein, but we included 151 additional growth curves. Some of the growth curves from short-lived small cryptobenthic fishes were modelled by linear regressions in the original references (Depczynski & Bellwood, 2006; Kritzer, 2002; Winterbottom, Alofs, & Marseu, 2011; Winterbottom & Southcott, 2008). However, linear growth can be expected under the VBGM if longevity is smaller than that necessary to reach the asymptotic size. Thus, we fitted a VBGM to raw data extracted from the graphs in these studies.

With the whole VBGF parameters dataset, we implemented a multi-step quality control procedure, excluding curves that were:

1. obtained from individuals in captivity (aquarium and aquaculture);
2. without clear information on the type of length measure employed (i.e. total length, standard length);
3. outliers, *i.e.* where L_∞ exceeded the reported maximum size of the species by 50% or more; or K deviated from a K value typical of the family by 50% or more (unless differences in values could clearly not be explained by methodological approaches);
4. from an inadequately circumscribed geographic locality (precluding access to environmental data);

We converted all estimates of the parameter L_∞ to TL (Total Length in cm) using length-length conversion factors obtained from FishBase or directly from photographic records. When both sex-specific and combined growth curves were reported, we used only the combined curve; when only sex-specific curves were reported, we averaged parameters between males and females to exclude the influence of sex. We acknowledge that this procedure places equal weights on sample sizes that might have differed between sexes. However, in many cases this information was not accessible. We therefore

averaged growth parameters to reduce the effect of differences in growth between sexes. Following these quality control criteria, 484 curves were excluded or aggregated, leaving a final database with 1,921 growth curves from 588 species of reef associated fish (**Appendix B**; Morais & Bellwood, 2018a).

Compiling and processing of explanatory variables

We modelled reef fish growth as a function of morphological and behavioural traits (*i.e.* maximum body size, diet, schooling behaviour, position relative to the reef and body form), environmental variables (*i.e.* sea surface temperature and pelagic primary productivity), and the method used to obtain the growth data).

Maximum body size is the maximum recorded length (TL in cm) for a referred species, either based on the literature or the authors' unpublished data (**Appendix B**; Morais & Bellwood, 2018a). "Body size" here was taken to be a synonym of "species body size", an evolutionary property of a lineage (often a species). It is explicitly distinguished from "individual body size", which is a property of an individual and a function of both ontogeny and the individual's environment. Moreover, we acknowledge that the VBGM theory and much of the field of allometry quantifies body size in terms of body mass rather than length (Bertalanffy, 1938, 1949, 1957), however, we chose to use length because: 1) growth has been traditionally expressed in terms of length in fisheries biology; and 2) because reef ecologists primarily collect length data of fish (*e.g.* from underwater visual census). Seven dietary categories were considered: herbivores/detritivores, herbivores/macroalgivores, omnivores, planktivores, sessile invertivores, mobile invertivores, and fish and cephalopod predators (Mouillot et al., 2014; Valeriano Parravicini et al., 2014). Schooling behaviour (or gregariousness) measures the extent of intraspecific aggregations in five levels: solitary, pair, small groups (3-20 individuals), medium groups (20-50 individuals) or large groups (>50 individuals) (Mouillot et al., 2014; Valeriano Parravicini et al., 2014). Position relative to the reef combines horizontal and vertical components, resulting in six levels (Bellwood, 1988). The horizontal component represents the degree of association of a fish to the reef: reef dwelling (more likely to be found on the reef than in other adjacent habitats) and reef associated (more likely to be found in adjacent non-reef habitats than on the reef). The vertical

component represents the position in the water column: benthic, bentho-pelagic and pelagic (Mouillot et al., 2014). The body shape factor is a continuous variable derived from the length-weight regression coefficients of fish (termed "body form factor" in Froese, 2006) that measures the extent to which a fish is elongated or deep-bodied. It can be perceived as the a parameter value a fish species should have if its $b = 3$. Since a and b can be sensitive to methodological issues (Froese, 2006), we compiled a database on these parameters estimated from the Bayesian Hierarchical Model described by Froese, Thorson, & Reyes (2014). This model starts with priors reflecting broad shape categories and is improved by the hierarchical addition of length-weight parameters from studies of closely related species or from different populations of the species of interest. The parameter estimates are given in (**Appendix B**; Morais & Bellwood, 2018a). The logical basis of the shape factor calculation is provided in Froese (2006).

Environmental data (sea surface temperature and pelagic net primary productivity) were acquired by georeferencing the locality of each of the growth curves. Growth curves were only included if the referred areas were biogeographically discrete with no major disparities in oceanographic features, regardless of size. Thus, "Ionian Sea" was acceptable, but not "Eastern Australia". Within the area, the centroid was estimated, and its coordinates used to extract mean sea surface temperature, mean chlorophyll concentration and mean photosynthetically active radiation from Bio-ORACLE (Tyberghein et al., 2012). To decrease the chance of bias due to the centroid estimate, we averaged the values from across the closest four cells (each cell has a width of ~9.2 km in Bio-ORACLE). Pelagic net primary productivity was estimated from chlorophyll concentration and photosynthetically active radiation by using the model described in Behrenfeld & Falkowski (1997). Details on the calculation of productivity can be found in (Morais & Bellwood, 2018b).

Finally, given the possibility that the method used to derive the growth curves would affect the final VBGF parameter estimates (see above in *A database of VBGF parameters: assembling and processing*), we included method as a covariate in our model. Method consisted of six levels: mark-recapture, length-frequencies, scale rings, otoliths rings, rings from other structures and unknown. Although we aimed to tease apart the confounding effects that different methods can have on growth

estimates, we were mainly interested in predicting for otoliths rings only, since this is the most widely used aging technique nowadays (e.g. Campana, 2001; Choat & Robertson, 2002).

Accounting for phylogenetic non-independence

Our dataset included species with varying degrees of shared ancestry, as well as multiple observations from the same species. These features result in non-independence among observations and require a phylogenetic correlation structure to be specified (Symonds & Blomberg, 2014). To do this, we first created a super tree by combining phylogenies that included our species using the ''rotl' package (Michonneau, Brown, & Winter, 2016) in the software R (R Core Team, 2019). This package is an interface to the Open Tree of Life (Hinchliff et al., 2015). Non-matching species were manually included in the phylogeny alongside congeneric species (e.g. the Doederlein's cardinalfish (*Ostorhinchus doederleini*, Apogonidae) with the Yellowstriped cardinalfish (*Ostorhinchus cyanosoma*, Apogonidae) or the Fusca drum (*Umbrina ronchus*, Sciaenidae) with the Shi drum (*Umbrina cirrosa*, Sciaenidae) or with the most closely-related families according to (Betancur-R et al., 2017) (Morais & Bellwood, 2018b). Branch lengths were computed using the method of Grafen (1989). Each species was represented in the phylogeny by as many tips as its number of growth curves, and intraspecific branch lengths were set to zero. Finally, we used the phylogeny to generate a correlation structure by applying a Brownian motion model of trait evolution (Symonds & Blomberg, 2014). All phylogenetic procedures and manipulations were carried out with the packages 'ape' (Paradis, Claude, & Strimmer, 2004) and 'phytools' (Revell, 2012) in R.

Different populations of the same species vary in their growth trajectories depending on environmental factors, such as temperature and food availability (Bertalanffy, 1957; Choat & Robertson, 2002; Pauly, 1980a; Ricker, 1979). VBGF parameters' estimates can also be affected by methodological issues such as small sample sizes and underrepresented body-size ranges (Berumen, 2005; Kritzer et al., 2001). This can result in large disparities in L_∞ (or W_∞) and K among populations of the same species (**Figure 1**A) or even among studies of the same population. Although these disparities could preclude direct comparisons, it has been argued that they conform to a theoretical and

empirical pattern. Pauly (1979) suggested that, in the special VBGF, K varies with W_∞ with a slope of $s_w = -\frac{2}{3}$ and with L_∞ with a slope of $s_L = -2$, when all parameters are $\log_{10}$ transformed (Munro & Pauly, 1983; Pauly, 1979, 1980a). If we assume a VBGF with $m \neq \frac{2}{3}$ (Pauly, 1979; Savage, Gillooly, Woodruff, et al., 2004), then K should vary with W_∞ and L_∞ with s_w and s_L slopes that differ from the values above. Following Pauly (1979) reasoning, we can define

$$s_w = -m \text{ and } s_L = -\frac{m}{b} \quad (4)$$

where m is the VBGM anabolic term exponent and b is the species length-weight regression exponent (for simplicity, we will only refer to the length slope s_L from now on). The anabolic exponent can be taken as the metabolic scaling exponent, which (Savage, Gillooly, Woodruff, et al., 2004) found out to be on average 0.761 (CI_{95} 0.68-0.86) for fishes. Froese et al. (2014) found that, for all body types of fish, b averages 3.04 (CI_{95} 2.81-3.27). Substituting the mean and extreme (CI_{95}) values of these parameters in Pauly's equation results in the average slope, $\overline{s_L}$, being -2.31 (CI_{95} from -2.75 to -1.91). Since b can vary among species, s_L is probably better characterized by a distribution centred on -2.31 and ranging from -2.75 to -1.91 (**Figure 1**B).

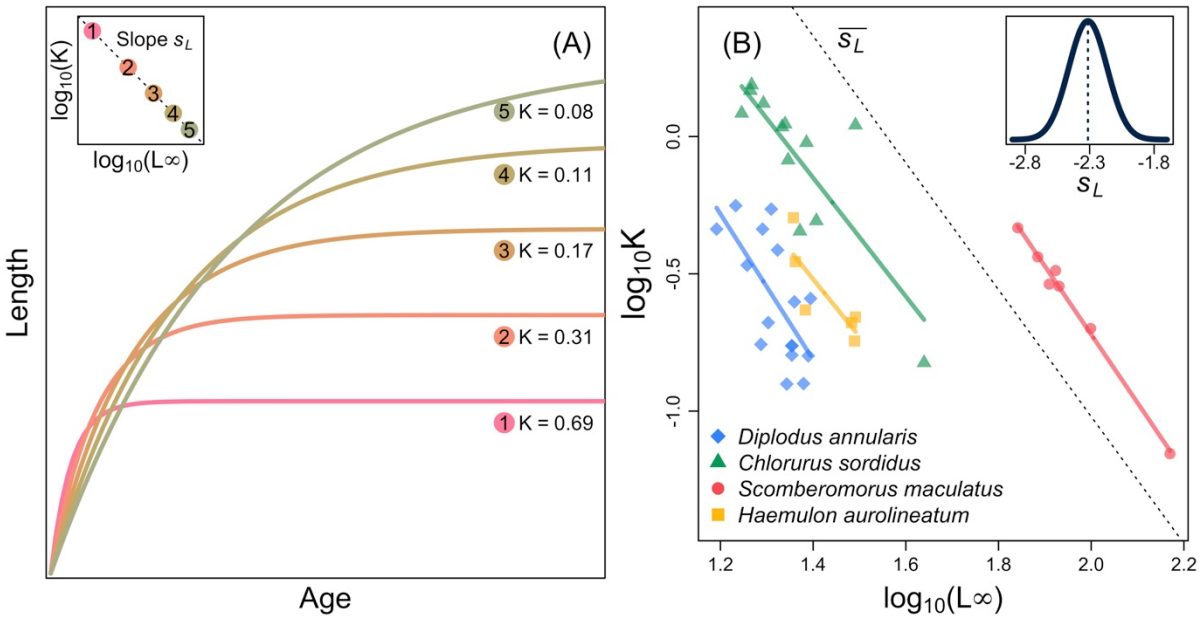

Figure 1: (A) *Growth curves from populations of the same species that vary in asymptotic size and in the Von Bertalanffy growth parameter K. The insert shows the theoretical relationship among these curves in a double logarithmic plot of K and L_∞, with a slope of s_L.* ***(B)*** *Empirical relationships between K and L_∞ for multiple populations of four selected species (different shapes). Continuous lines mark the estimated s_L for each species and the dotted line is the theoretical average slope $\overline{s_L}$ of -2.31. The insert shows the theoretical distribution of s_L, with the average, $\overline{s_L}$, indicated by the dotted line. Data source: (**Appendix B**; Morais & Bellwood, 2018a).*

Standardizing growth curves for among-populations and species comparisons: the Ø and K_{max} parameters

The practical meaning of the relationship between K and L_∞ can be better represented in a plot like **Figure 2**. Variation among growth curves of a species along a theoretical line with slope s_L in such a plot could, for example, reflect incomplete sampling of the population size range. However, residual variation, *i.e.* variation in any direction other than along this line, will likely be due to environmental factors (*e.g.* temperature, productivity). This "residual variation" (quoted because it is actually the variation in which we are interested) can be isolated by regressing each growth curve along the theoretical line towards a specific size value (**Figure 2**). By regressing the curves towards the y-axis, we obtain the rate at which a fish population with the VBGF parameters specified would converge to

its asymptotic size, L_∞, if it grew to $L_\infty = 1cm$ (**Figure 2**A). This approach is a standardization procedure that allows one to compare growth among populations at a constrained minimum body size. The resulting parameter has been named the growth performance index by Pauly (1979) and has been represented by the characters P, a, φ or Ø. It will be hereafter referred as Ø. In practical terms, Ø is calculated as

$$Ø = log_{10}K - s_L.log_{10}L_\infty \quad (5)$$

for length data (Froese & Binohlan, 2003).

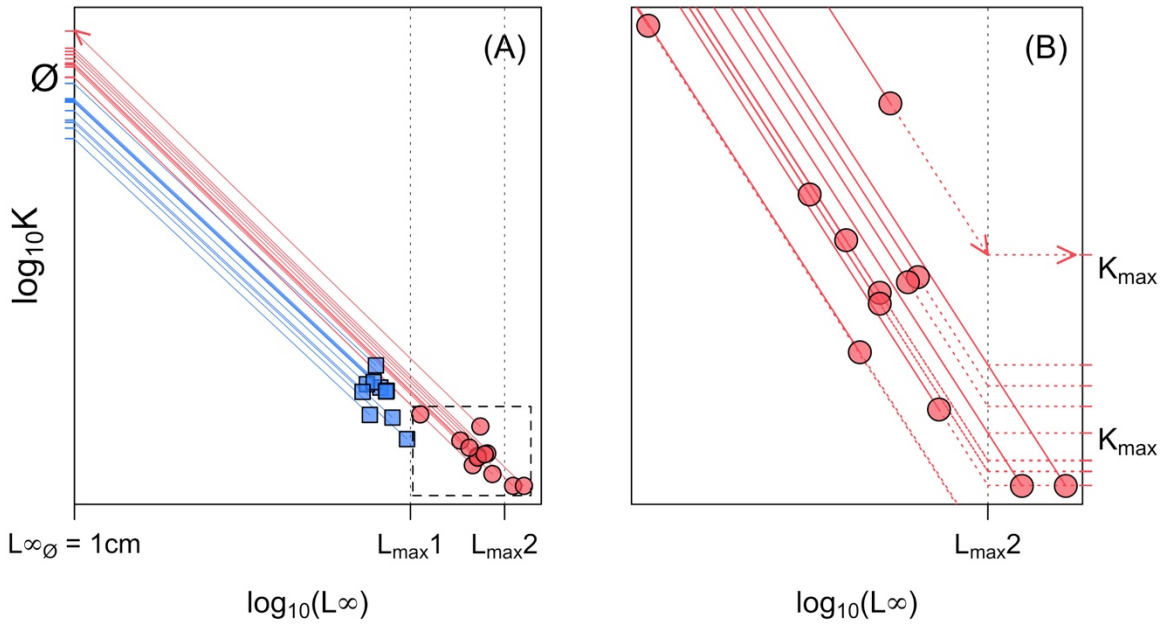

Figure 2: *Growth curves from populations of the same species (same shaped dots) can vary in their parameters K and L_∞, although they tend to depict a negative relationship in a double logarithmic plot. These curves can be standardized by regressing each data point along a line that crosses the point with a slope s_L. This can be done either towards the y-axis **(A)**, obtaining the growth performance index (Ø) when $L_\infty = 1cm$; or towards a line perpendicular to the species maximum size L_{max}, obtaining K_{max} **(B)**.*

Alternatively, one can regress each growth curve towards the point where it intercepts a line projecting the maximum size reported for that species (L_{max}, **Figure 2**B). This standardization

procedure results in an estimate of the rate at which a fish population with the specified VBGF parameters would approach its L_∞ if $L_\infty = L_{max}$, and is termed K_{max}. Mathematically, it is obtained by

$$log_{10}K_{max} = Ø + s_L . log_{10}L_{max} \quad (6)$$

It is important to clearly distinguish between the meanings of K, K_{max} and Ø. K is the rate of convergence towards a population (or individual) asymptotic body size, with meanings as discussed above (section *A database of VBGF parameters: assembling and processing*). K_{max} and Ø, however, are theoretical projections of K at specific body lengths. By standardizing K to a constrained body length ($L_\infty = 1\ cm$ or $L_\infty = L_{max}$), the derived parameters (K_{max} or Ø) concentrate all growth information and allow for comparisons across populations and species.

The growth performance index (Ø) and the expected growth coefficient at the theoretical maximum species size (K_{max}) are, for any one species, opposite ends of the same line (**Figure 2**). Since we consider K_{max} to be easier to interpret biologically than Ø, K_{max} will be the main focus of this work. A potential caveat is that K_{max} is first standardized by species maximum size, and then modelled by this same variable. We evaluate possible issues of this approach by, first, checking the relationship between K_{max} and Ø (see below in *Procedures for modelling K_{max} and Ø*), and then perform all modelling procedures using Ø as well as the response variable. We report all the alternative modelling results in the **Appendix B**.

Contrasting theoretical and empirical estimates of s_L

To check if the theoretical range of s_L values is supported by our data, we first filtered our growth curves dataset to retain all species that had six or more growth curves. This resulted in 74 species for which s_L could be estimated by regressing $\log_{10}$ transformed K and L_∞ values. Then we calculated a weighted average of these estimated $s_L$values in a meta-analytical Bayesian framework using the R package 'brms' (Bürkner, 2017). This procedure incorporates standard errors, weights, and a prior

distribution when averaging values of a variable. We used the standard errors of the s_L estimates from the K and L_∞ regressions; and also included the R^2 of these regressions as the weights. The theoretical range of s_L values was used to delimitate the prior distribution of the intercept. The model was run with four chains of 3,000 iterations, with 1,500 warm-up steps and a thinning of every third step for each chain. The output of this procedure is a posterior distribution of s_L values whose 95% credibility interval can be used for inference. To check for mismatches between our data and the posterior distribution, we visually compared the distribution of s_L among the species in our dataset with values simulated from the posterior distribution. Complete overlap between the simulated and the empirical data would reveal that incorporating quality metrics (standard errors and weights) to the species s_L estimates did not affect the posterior distribution, *i.e.* the data quality was uniform, and no meta-analysis was required.

Procedures for modelling K_{max} and Ø

Prior to fitting the model, we checked the explanatory variables for collinearity using two approaches. First, we plotted the relationship among these variables using Local Weighted Scatterplot Smoothing regressions (LOWESS, **Figure B1** in **Appendix B**) and also checked for correlations. Second, we fitted a simple linear regression with all the covariates and calculated the Variance Inflation Factor (VIF). Only one correlation higher than 0.5 was found, between schooling and position. Further checking the VIF suggested that both of these variables and diet had some degree of collinearity. The exclusion of schooling resulted in all variables remaining with a VIF < 4, a value that we deemed satisfactory. We also assessed the assumptions that the response variable K_{max} included information that was different from the parameters K, L_∞, and Ø. We modelled these relationships by using LOWESS regressions. If these assumptions were true, then K_{max} would be related to both K and L_∞ with a high residual variation, but not be related to Ø.

To determine the main drivers of reef fish growth, we modelled K_{max} and Ø relative to morphological and behavioural traits, and environmental variables, in a Phylogenetic Generalized Least Squares Models (PGLS, Symonds & Blomberg, 2014). Since there are currently no methods to fit a phylogenetic model with a Gamma distribution, we $\log_{10}$ transformed K_{max} to achieve Gaussian

distribution (**Figure B2** in **Appendix B**). We $\log_2$ transformed body size and primary productivity to decrease dispersion. Finally, to assist with model convergence, all continuous variables were centred. We fit the models using the package 'nlme' (Pinheiro, Bates, DebRoy, Sarkar, & R Core Team, 2017) in R. We contrasted the full model with nested submodels by iterating the model fit with one explanatory variable excluded each time. All models were fitted using Maximum Likelihood for comparing fixed effects and the comparisons were based on Akaike Information Criterion (AIC) metrics: ΔAIC and wAIC (Bartoń, 2016; Burnham & Anderson, 2002). Finally, we assessed the importance of each predictive variable by using the proportional change in the R^2 from the full model to submodels excluding each variable. Since GLS techniques do not allow R^2 calculation in the same way as Ordinary Least Squares, we instead calculated a prediction R^2. This was achieved by fitting a linear regression of the raw data values by the predicted values from the PGLS, and then using the R^2 from this regression to do the calculations. After the fitting procedure, we performed model validation as recommended by Zuur, Ieno, Walker, Saveliev, & Smith (2009) and refitted the final model using Restricted Maximum Likelihood.

Predicting growth coefficients for trait combinations and environmental settings and assessing prediction accuracy

We used XGBoost, a Gradient Boosted Regression Tree (GBRT) method to predict reef fish standardised growth coefficients K_{max}. The goal of this step was to derive a table that can be used to predict growth trajectories for unsampled species using the combinations of morphological and behavioural traits, and the environmental settings evaluated here. Machine learning techniques, such as GBRTs, are considered superior in predicting when compared to statistical methods (Elith, Leathwick, & Hastie, 2008). XGBoost, in particular, is regarded as the state-of-the-art tree boosting system, yielding very fast and accurate predictions (Chen & Guestrin, 2016; Mitchell & Frank, 2017). One of the main advantages of GBRTs over statistical methods is the possibility of efficiently modelling multi-level variable interactions (Elith et al., 2008).

The same model structure as in the final PGLS was used for prediction, except that the response variable, K_{max}, was included in its raw form and the XGBoost model was fitted with a Gamma distribution. Two tuning steps were executed before running the prediction model. First, we fit the model multiple times with combinations of model parameters (learning rate, maximum tree depth, gamma and subsampling rate) that were varied systematically, and recorded the combinations that yielded the minimum root mean square error (rmse). These values were: learning rate = 0.15, maximum tree depth = 7, gamma = 0.15 and subsampling = 0.5. Other parameters were kept in their default values. Then, we refit the model multiple times with combinations of values randomly drawn from a uniform distribution bound by the recorded parameter values from the previous round ± 10%, and again selected the parameters that minimized rmse. These tuning steps reduced model rmse from 0.32 to 0.27, a substantial increase in prediction consistency.

To evaluate the accuracy and precision of XGBoost in predicting from our data, we used a cross-validation procedure. This consisted in randomly splitting the growth coefficients database into independent training and testing datasets. The training dataset contained 80% of the data points and was used to refit the final model in order to generate coefficients for prediction. The testing dataset contained the remaining 20% of the data points and was used exclusively to contrast with predictions from the training dataset model. By using different datasets to fit the model and to predict, cross-validation makes these steps independent, and, therefore enhances bias detection. We calculated a bias metric by subtracting each K_{max} predicted by the xgboost from its estimate in the database (the "measured" value). An accurate model would have a bias at or very close to zero. Precision was assessed by a prediction R^2 analogous to the one calculated for the PGLS. These cross-validation procedures were repeated 1,000 times.

Finally, prediction was carried out for all diet and position groups, for body sizes between 2 and 200 cm TL, for sea surface temperatures between 10 and 30 ºC, and for the ageing method of otolith's rings only (see above *Compiling and processing of explanatory variables*). We bootstrapped the model for 1,000 iterations to generate a distribution of K_{max} predictions. All prediction-related analyses were conducted with the R package 'xgboost' (Chen, He, Benesty, Khotilovich, & Tang, 2018).

Results

The average slope of the relationship between K and L_∞ for multiple species in our dataset, $\overline{s_L}$, was estimated at -2.18, with 95% credibility interval ranging between -2.31 and -2.06 (**Figure 3**A). Thus, the posterior distribution just included the theoretical $\overline{s_L}$ of -2.31. Simulating species s_L from this posterior distribution resulted in a distribution of values that had two main differences when compared to the empirical dataset (**Figure 3**B). First, positive s_L values, that is, species for which the parameter K increased as L_∞ increased, were rare in the simulated dataset (**Figure 3**B). Second, values in the vicinity of -2 were much more common in the simulated than in the empirical dataset (**Figure 3**B). Altogether, these findings suggested that the theoretical $\overline{s_L}$ distribution was consistent with the posterior $\overline{s_L}$ estimated from the empirical data after accounting for its highly heterogeneous quality. Thus, we used equation (4) to estimate s_L for all species in our dataset, and then derived Ø and K_{max} from equations (5) and (6).

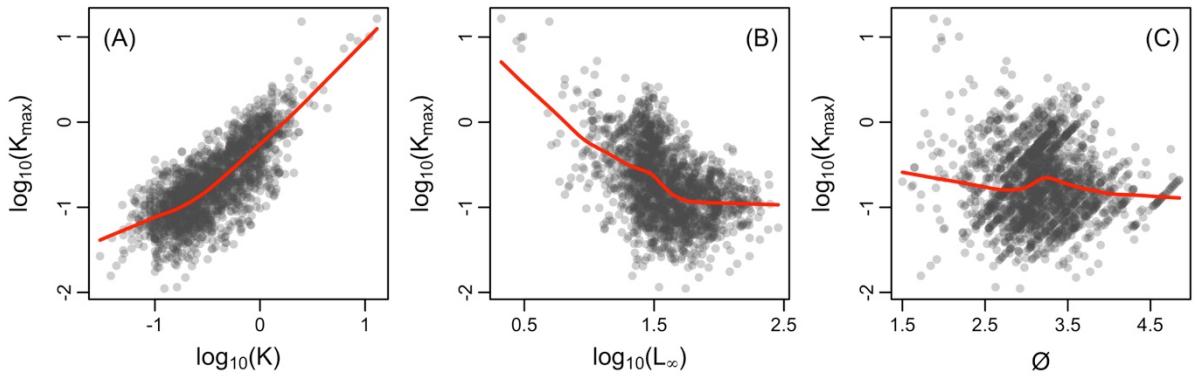

Figure 3: *Relationship between the derived growth coefficient, K_{max}, and the Von Bertalanffy Growth parameters K* ***(A)*** *and L_∞* ***(B)****, as well as the growth performance index, Ø* ***(C)*** *from a global reef fish growth dataset. Trend lines are LOWESS smoothers.*

The growth coefficient K_{max} for all fishes varied from 0.011 to 16.43, while the growth performance index, Ø, varied from 1.50 to 5.85. This range of K_{max} and Ø was distributed across reef fish species varying in size and shape by more than two orders of magnitude (from 1.9 to 320 cm in TL and from 0.0004 to 0.034 in shape factor), living in sea surface temperature regimes ranging from less

than 6 ºC to almost 31ºC and primary productivity from 30 to more than 2,000 gC.m^{-2}.year^{-1}. As expected, K_{max} was positively related to K and negatively related to L_∞, both with high residual variation (**Figure 4**). Also, as expected, K_{max} and Ø were unrelated.

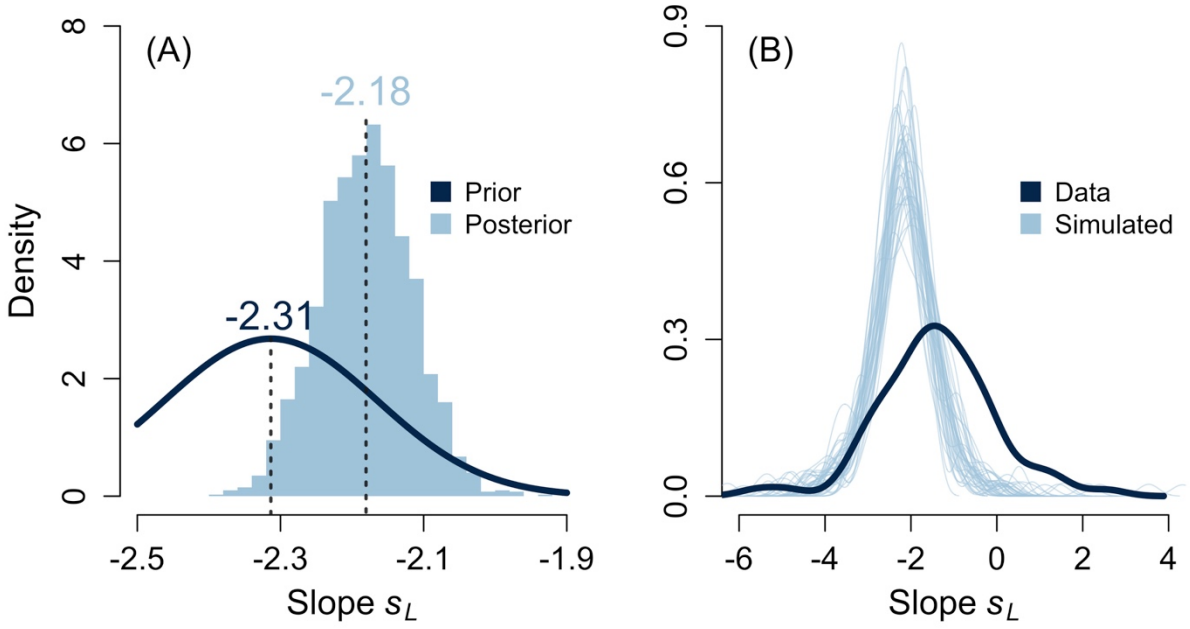

Figure 4: (A) *The prior and posterior s_L distributions from a Bayesian meta-analysis of a global reef fish growth dataset. The prior is the theoretical s_L distribution centered on $\overline{s_L} = -2.31$.* ***(B)*** *Empirical s_L distribution from 74 species in our dataset compared to simulated distributions of species s_L drawn from the posterior distribution.*

Body size was the most important variable in our model, accounting for almost 64% of the explained variability in K_{max} (**Figure 5**). Temperature, diet, method and position relative to the reef explained a smaller portion of the variability in K_{max}, between 6% and 2.5%. The fact that shape factor and pelagic primary productivity explained almost no variability K_{max} suggested that these variables were adding little information to our model. This was further confirmed by comparing nested submodels: the model excluding both shape factor and productivity had an AIC indistinguishable from the full model (**Table B1** in **Appendix B**), and thus we excluded both. The final model explained 61.5% of the variation in K_{max} and contained body size, temperature, diet, method and position relative to the reef (**Table 1**; model validation in **Figures B3** and **B4**, **Appendix B**).

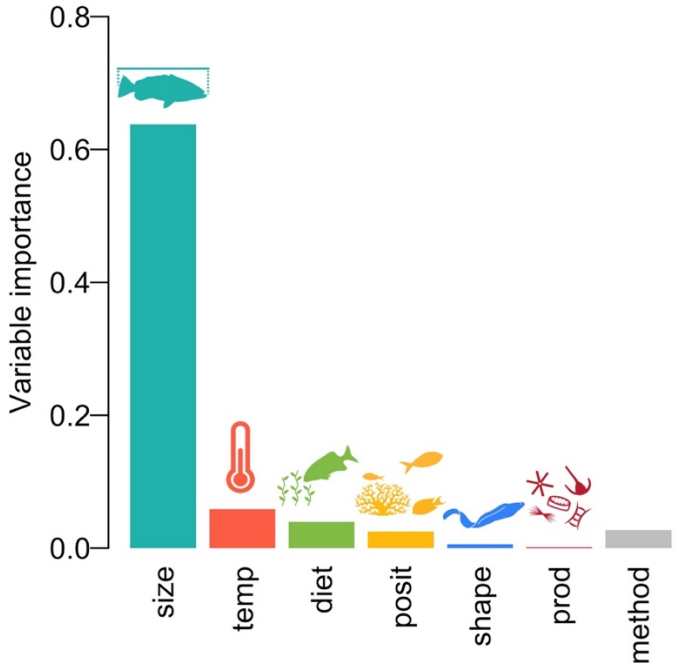

Figure 5: *The importance of each variable in our full model of K_{max} using a global dataset of reef fish growth. This metric represents, for each variable, the proportion of total variability explained. size = body size, temp = mean sea surface temperature, posit = position relative to the reef, shape = body shape factor, prod = mean pelagic net primary productivity, method = method used to derive the growth curves.*

Table 1: *Model coefficients of the final PGLS used to model the growth coefficient K_{max} in reef fishes using a global dataset.*

Variable	Level	Estimate	St. Error	t-value	p-value
Intercept	-	0.032	0.152	0.21	0.8341
Body size	-	-0.330	0.013	-26.14	<0.0001
Sea surface temperature	-	0.010	0.002	4.42	<0.0001
Diet	Herbivores/detritivores	-0.338	0.101	-3.33	0.0009
	Omnivores	-0.471	0.103	-4.58	<0.0001
	Planktivores	-0.352	0.102	-3.46	0.0006
	Invertivores sessile	-0.389	0.123	-3.16	0.0016
	Invertivores mobile	-0.317	0.098	-3.23	0.0013
	Piscivores	-0.205	0.100	-2.05	0.0402
Position	Pelagic reef dwelling	-0.253	0.074	-3.43	0.0006
	Bentho-pelagic reef associated	-0.239	0.055	-4.34	<0.0001
	Bentho-pelagic reef dwelling	-0.249	0.052	-4.79	<0.0001
	Benthic reef dwelling	-0.231	0.056	-4.11	<0.0001
	Benthic reef associated	-0.274	0.053	-5.14	<0.0001
Method	Mark-recapture	-0.074	0.038	-1.96	0.0505
	Otoliths rings	-0.166	0.016	-10.22	<0.0001
	Unknown	-0.136	0.017	-7.85	<0.0001
	Other rings	-0.166	0.032	-5.17	<0.0001
	Scale rings	-0.160	0.024	-6.68	<0.0001

The effects of the explanatory variables on K_{max} are depicted in **Figure 6** (see **Appendix B**, **Figure B5** for data points). K_{max} decreased steeply with maximum body size and increased with temperature. Among the diet categories, herbivores/macroalgivores had the highest K_{max} values, followed by fish and cephalopod predators. All other dietary groups had lower values (**Figure 5**, **Table 1**). In terms of the position relative to the reef, pelagic reef-associated fishes showed the highest K_{max}, while the remaining groups showed broad overlap in values (**Figure 5**, **Table 1**). Growth curves

obtained from length-frequency methods tended to overestimate K_{max} compared to all other methods except mark-recapture (**Table 1**, **Figure B4** in **Appendix B**). The model of Ø was almost identical to the one of K_{max} in most outputs, except for a positive, instead of negative, relationship with body size (details in **Tables B2** and **B3**, and **Figures B6-B10** in **Appendix B**).

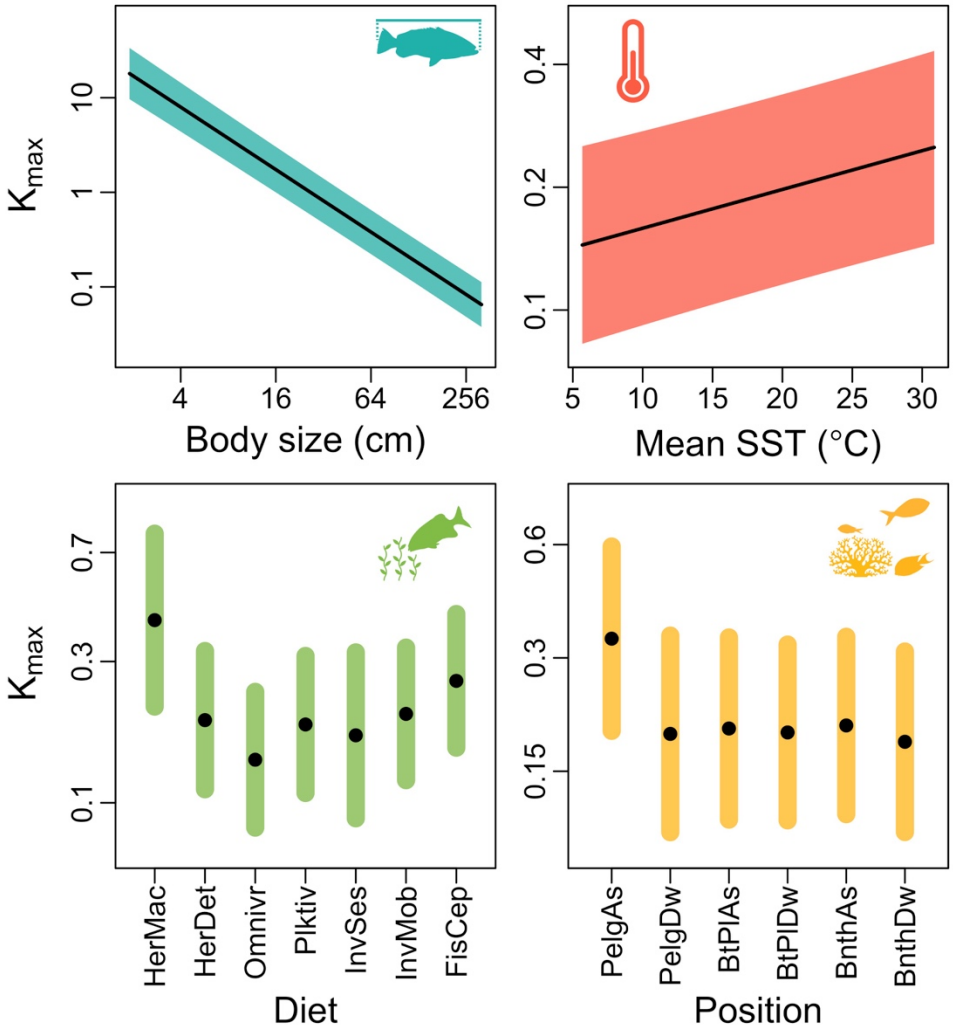

Figure 6: *Relationship between K_{max} and body size, temperature, diet and position relative to the reef for reef fishes in a PGLS using a global dataset of growth. Note the different y-axis scales. Black lines and black dots indicate model predictions, and bands indicate the 95% confidence intervals of model predictions calculated from model standard errors. HerMac = herbivores/macroalgivores; HerDet = herbivores/detritivores; Omnivr = omnivores; InvSes = sessile invertivores; InvMob = mobile invertivores; FisCep = fish and cephalopod predators; PelgAs = pelagic reef associated; PelgDw = pelagic reef dwelling;*

BtPlAs = bentho-pelagic reef associated; BtPlDw = bento-pelagic reef dwelling; BnthAs = benthic reef associated; BnthDw = benthic reef dwelling.

Cross-validation of the XGBoost predictions is summarized in **Figure B11**, **Appendix B**. The median bias (measured minus predicted K_{max}) across the iterations was very close to, and not significantly different from zero (**Figure B11**). The bootstrapped R^2 distribution was bimodal, indicating that predictive power varied across iterations (**Figure B11**). This suggested that a median would be more adequate than a mean to represent the bootstrapped values. Predictions were, in median, related to the K_{max} values from our dataset with an R^2 of 0.81 (**Figure B11**). The prediction table for K_{max} values using the bootstrapped XGBoost model for different combinations of traits and temperature values is available from (Morais & Bellwood, 2018a).

Discussion

Of the broad spectrum of morphological and behavioural traits and environmental variables examined, body size was the main driver of reef fish growth. This variable alone accounted for 64% of the explained variation in reef fish growth as represented by K_{max}. By comparison, the other variables in our final model accounted for between 6% and 2.5% of the variation. Of these variables, temperature was the most important. These findings strongly agree with metabolic models of growth (e.g. Bertalanffy, 1938, 1957; West et al., 2001) and the Metabolic Theory of Ecology (Brown et al., 2004) in concluding that body size and temperature are the most important drivers of biological processes, including growth rates (Brown et al., 2004; Charnov & Gillooly, 2004; Ernest et al., 2003; Gillooly et al., 2001, 2002; Savage, Gillooly, Brown, West, & Charnov, 2004). Thus, reef fish should grow as predicted by their body size and their environmental temperature, assuming that they have access to energetic supplies exceeding metabolic costs for a substantial part of their ontogeny. Nevertheless, access to this energetic surplus can be constrained by resource availability or acquisition mode (Beverton & Holt, 1959; Ricker, 1946): for example, fish that feed on macroalgae are not expected to derive the same amount of energy per unit of food ingested as fish that feed on invertebrates (Choat & Clements, 1998; Clements, Raubenheimer, & Choat, 2009; Horn, 1989). Consequently, reef fish of a particular body size living at a given temperature could vary in the way they grow depending on access

to food resources. This potential influence of trophic resources is supported by our data, since diet and position relative to the reef were invariably kept in our final model. These variables were important to explain deviances from predictions based solely on body size and temperature.

Body size and temperature effects

The fact that reef fish growth rates depend on body size and temperature is a reflection of underlying physiological processes: all mass-specific physiological rates follow body size and temperature, since these factors determine metabolism (Gillooly et al., 2001). Consequently, they also determine energetic demands. Mass-specific metabolic rates decrease with size and increase with temperature (Brown et al., 2004), the same trends we observed for K_{max}. This relationship between rates and body size stems from physiological constraints on molecule transport (e.g. amino-acids or carbohydrates) across body surfaces to individual cells (West et al., 1997). By contrast, the temperature dependence of physiological rates follows a simple kinetic relationship: higher temperatures increase the rates of chemical reactions (Brown et al., 2004; Gillooly et al., 2001). All types of chemical reactions, from lyses to syntheses, are kinetically affected. As a result, organisms in warmer temperatures have higher metabolic rates, and also higher growth rates, than similar-sized organisms in cooler temperatures.

Resource availability and acquisition effects

Although the energetic demands of an organism are determined by size and temperature (Bertalanffy, 1957; Brown et al., 2004), its energetic supply is mediated by resource acquisition. Reef fishes encompass a wide array of morphological, physiological and behavioural traits that allow them to explore a broad spectrum of feeding resources (Wainwright & Bellwood, 2002). Feeding resources also vary largely in space and time. Thus, the interplay between resource availability and traits used to explore them should result in some level of growth disparities among feeding modes (Beverton & Holt, 1959; Ricker, 1946). Our results partially support this expectation: diet and the degree of association with the reef affected reef fish growth coefficients. Remarkably, after accounting for body size and

temperature, herbivores/macroalgivores had higher growth coefficients than all other trophic groups. This includes fish with "better quality" diets (sensu Harmelin-Vivien, 2002), such as planktivores or fish and cephalopod predators.

Marine prey items exhibit considerable variability in energetic and protein content (Bowen, Lutz, & Ahlgren, 1995; Brey, Müller-Wiegmann, Zittier, & Hagen, 2010; Choat & Clements, 1998), as well as in their structural and chemical defences against predation (Burns, Ifrach, Carmeli, Pawlik, & Ilan, 2003; Hay, 1991). Depending on these factors, food resources for marine organisms have been categorized as "low-quality" or "high-quality" (Choat & Clements, 1998; Harmelin-Vivien, 2002). Low-quality items include sessile invertebrates and macroalgae that have low protein and/or energy content, and frequently also structural and/or chemical defences. High-quality items, such as mobile invertebrates and fish, have a high protein and energy content and relatively few structural or chemical defences. One may therefore assume, based on these differences, that fishes with "high-quality" diets would grow faster than fishes with "low-quality" diets (Harmelin-Vivien, 2002). However, "low-quality" dietary items are readily available on reefs, and exploiting them may be a trophic opportunity rather than a constraint (Harmelin-Vivien, 2002). Niche expansion from "high-quality" to "low-quality" diets in reef fish lineages has, for instance, been followed by rapid evolutionary diversification (Lobato et al., 2014). Fishes have many behavioural and physiological mechanisms to deal with their preferred food (Choat & Clements, 1998; Clements et al., 2009). The fact that many fishes rely on apparently "low-quality" diets such as algae and particulates suggest that the purported obstacles posed by these diets (i.e. defences, scarcity of nutrients) are generally overcome. A possible trade-off between lower nutrient levels but higher and more predictable availability may mean that these "low-quality" items may indeed provide fishes with superior nutritional rewards (e.g. Choat, Clements, & Robbins, 2002; Wilson, Bellwood, Choat, & Furnas, 2003). There is increasing evidence that feeders of "low-quality" diets, such as herbivores and detritivores, do not grow markedly slower than feeders of "high-quality" diets (Choat & Axe, 1996; Choat & Robertson, 2002; Trip, Raubenheimer, Clements, & Choat, 2011). Our results add further support to these findings. After accounting for differences due to other factors (mainly body size and temperature), sessile invertivores and herbivores/detritivores grew similarly to planktivores or mobile invertivores, whereas herbivores/macroalgivores grew faster than the other

trophic groups. Clearly, the constraints imposed by an herbivorous diet are not as severe as previously thought.

We see a similar but unexpected pattern in pelagic primary productivity, a component of resource availability for fishes. Although pelagic fishes associated with reefs had higher growth coefficients than all other position categories, we did not find a relationship between growth and pelagic primary productivity. This pattern, again, disconnects apparent food quality/availability from potential for growth. The gradient in primary productivity here investigated included very productive temperate reefs and also oligotrophic tropical coral reefs. The fact that fish growth did not respond to this gradient shows that, in the scale investigated, the different strategies that fish employ to acquire resources are optimized to deal with resource availability.

Pelagic primary productivity can play an important role in the energetics of both temperate and tropical reefs (e.g. Truong, Suthers, Cruz, & Smith, 2017; Wyatt, Waite, & Humphries, 2012). However, some of the most productive marine habitats frequently occur in tropical oligotrophic waters: coral reefs (Crossland et al., 1991; Hatcher, 1988). This observation is partially explained by coral reefs' high efficiency in uptake rates and recycling of nutrients, especially through the detritus pathway (Arias-González et al., 1997; Crossland et al., 1991; de Goeij et al., 2013). There may also be scale-dependent factors involved, for example, the use of the pelagic environment adjacent to reefs. Ocean currents provide reef food chains with large transient zooplankton from the open ocean (Hamner et al., 1988; Hobson, 1991). As currents move closer and through the reef, this large zooplankton is depleted by feeding from planktivorous fishes, i.e. the "wall of mouths" (Hamner et al., 1988). Thus, the pelagic environment adjacent to reefs provides a highly rewarding food source for those fishes capable of exploring it (Bellwood, 1988; Hamner et al., 1988). This pelagic environment also provides predators with the opportunity to feed on fishes that live far from the protection of the reef structure (Hobson, 1991). Fish that live in the open have few chances of escaping predators other than schooling, swimming fast or getting large quickly (Hobson, 1991). A similar reasoning might be applied to the predators themselves. It seems likely that growing fast in the pelagic environment adjacent to reefs is an outcome of opportunities and pressures: opportunities provided by abundant, high quality feeding resources

(zooplankton and zooplanktivorous fishes); and the need to quickly achieve large body sizes to escape predation.

Reef fish growth in a changing world

This study has demonstrated the major importance of body size and, to a smaller degree, also of temperature on reef fish growth, as predicted by theory. Rising sea temperatures and disruption of fish size structure are ongoing threats to tropical reefs (Hughes, Kerry, et al., 2017; Jackson et al., 2001). Both are likely to disturb normal fish growth trajectories. For example, although fish growth coefficients increased with temperature in the present study, the temperature range investigated herein only encompasses present sea conditions (up to ~31ºC). Many tropical reef fishes already live in temperatures close to their metabolic optimum, with further temperature increases resulting in diminished aerobic scope (Barneche et al., 2014; Rummer et al., 2014). Despite the fundamental ties between metabolism and growth, it is unlikely that reef fish growth coefficients will keep on increasing linearly with further rises in sea temperature. Moreover, reef fish size structure can be severely disrupted by size-selective fishing activities (Jennings & Blanchard, 2004; Jennings & Kaiser, 1998; Robinson et al., 2017). This type of fishing can also induce non-random genetic changes to fish populations, for example, by selecting for lineages that grow to smaller sizes, mature, and attain their asymptotic sizes more quickly (Kuparinen & Merilä, 2007). Although this scenario could potentially result in either increased or decreased growth rates (Kuparinen & Merilä, 2007), any potential benefits may be outweighed by detrimental consequences to reproductive output or larval survival (e.g. Birkeland & Dayton, 2005; Hixon, Johnson, & Sogard, 2014). Hence, exploring the links between population asymptotic size, growth rates, rising sea temperatures, and fishing-induced size changes is likely to be of increasing interest to reef fish ecologists in the near future.

Variables that represent resource availability and acquisition had a minor, albeit significant role on growth in this study. We expect that downscaling from the global reef fish assemblage, examined herein, to local assemblages will increasingly emphasize links between growth and resource-related variables. For example, Gust et al. (2002) documented abrupt demographic changes between populations of parrotfishes and a surgeonfish from outer and mid-shelf reefs in the Great Barrier Reef.

Populations from outer-shelf reefs had smaller asymptotic size and higher growth coefficients, as well as higher abundances, when compared to mid-shelf reefs. The authors concluded that differences in growth were an outcome of density-dependent processes triggered by limited production of detritus, the main feeding resource of the species evaluated (Gust et al., 2002). On an even smaller spatial scale, Clifton (1995) observed varying growth rates of a Caribbean parrotfish between adjacent reefs subject to distinct wave action. This was attributed to wave action mediating the population dynamics of benthic filamentous algae targeted by that parrotfish species, thus determining its growth rates. Moreover, local communities include only a small subset of the potential environmental variability and, most often, also of the size range used in this study. Hence, resource-related variables are likely to be more important, and useful, to explain differences in growth at a reduced scale. Some of the most interesting departures from expectations in this paper resulted from investigating resource variables. Particularly, our model showed that growth rates of herbivores/macroalgivores, theoretically "low-quality" feeders, were higher than fish and cephalopod, and mobile invertebrate predators, considered as "high-quality" feeders. This supports the idea that fish have developed behavioural, physiological and anatomical mechanisms to deal with their preferred food and illustrates how studying fish growth might help to clarify other aspects of reef ecology.

Predicting growth coefficients

In addition to identifying the drivers of reef fish growth, we apply a state-of-the-art machine learning technique to predict growth coefficients for combinations of these drivers. Thus, we provide an accurate and precise means of estimating the growth trajectories of unsampled reef fish species. This can be particularly useful if one wishes to characterize whole-assemblage patterns of fish growth (e.g. Depczynski, Fulton, Marnane, & Bellwood, 2007). To facilitate this use, we provide the raw growth dataset (**Appendix B**; Morais & Bellwood, 2018a) and an easy-to-use table with predicted coefficients (**Appendix B**; Morais & Bellwood, 2018a). The prediction table includes most of the range of morphological and behavioural traits and environmental variables that tropical and temperate reef fishes are likely to encounter.

Ours is not the first study to provide predictions of fish life-history traits. Thorson, Munch, Cope, & Gao (2017), for example, used a multivariate probabilistic model to derive estimates of four life-history traits, including growth parameters, of all fish species. This impressive task was not without challenges, and the authors recognize three drawbacks of their approach: 1) the use of a taxonomic, rather than phylogenetic, structure to model correlations among species; 2) the absence of resource-related variables in their model; and 3) the lack of discrimination between high and low quality input data. We believe that, by focusing our attention to reef fishes, we were able to overcome these three drawbacks and, as such, to provide more accurate growth predictions for our targeted group.

Growth is primarily a physical phenomenon driven by body size and temperature. Biological features related to resource acquisition are important but only to a minor extent, and some do not affect growth as expected. The model derived herein can be used as an easily available method for estimating growth trajectories of unsampled species and, as such, to bridge the gap between individual and community-level growth patterns. This will contribute to a better understanding of the role of fish growth in ecosystem processes, such as energy flow and nutrient cycling, which ultimately result in biomass accumulation.

Chapter 3: Principles for estimating fish productivity on coral reefs

Publishe as: Morais, R.A., & Bellwood, D.R. Principles for estimating fish productivity on coral reefs. *Coral Reefs. doi: 10.1007/s00338-020-01969-9.*

Introduction

Overfishing and global warming are rapidly reshaping earth's marine and freshwater ecosystems, changing species composition and altering fluxes of energy and matter (Norström et al., 2016). Some of these ecosystems are experiencing widespread structural and functional changes (Bellwood, Pratchett, et al., 2019; Hughes, Barnes, et al., 2017), with new configurations that are now considered irreversible. Importantly, we are only starting to understand the functional implications of these new ecosystem configurations (**Figure 7**A,B) (Bellwood, Pratchett, et al., 2019; Brandl, Rasher, et al., 2019). With the onset of the Anthropocene, management of natural resources requires new strategies to accurately measure and then prepare for the impacts of contemporary drivers of change on critical ecosystem services (Norström et al., 2016). Aquatic natural resources support significant subsistence, economic and well-being activities (Lynch et al., 2016; Moberg & Folke, 1999). In particular, tropical inland and reef resources are overwhelmingly exploited by small-scale fisheries, and provide food for many hundred millions of people (Cinner, 2014; Deines et al., 2017; Lynch et al., 2016). Will tropical aquatic ecosystems in the Anthropocene be able to keep on sustaining the livelihoods of people that depend on them?

Fish standing biomass has been widely used as a simple, practical means of quantifying resource availability for management purposes, particularly in marine systems (Nash & Graham, 2016). Biomass is an inherently intuitive concept (i.e. more biomass means more and larger fish) easily estimated combining fish abundance and size data with widely available length-weight regression parameters (Froese, 2006). Moreover, fish biomass has been tightly linked to impacts from human activities, such as fishing (e.g. Jennings & Lock, 1996; Nash & Graham, 2016). Spikes in fishing effort, for example, can lead to biomass depletion, whereas fishing closures have been observed to trigger biomass build-

up (Russ & Alcala, 2003). Thus, it may seem logical that fish standing biomass be taken as good indicator of potential fisheries yields, particularly in data-deprived coral reef fisheries.

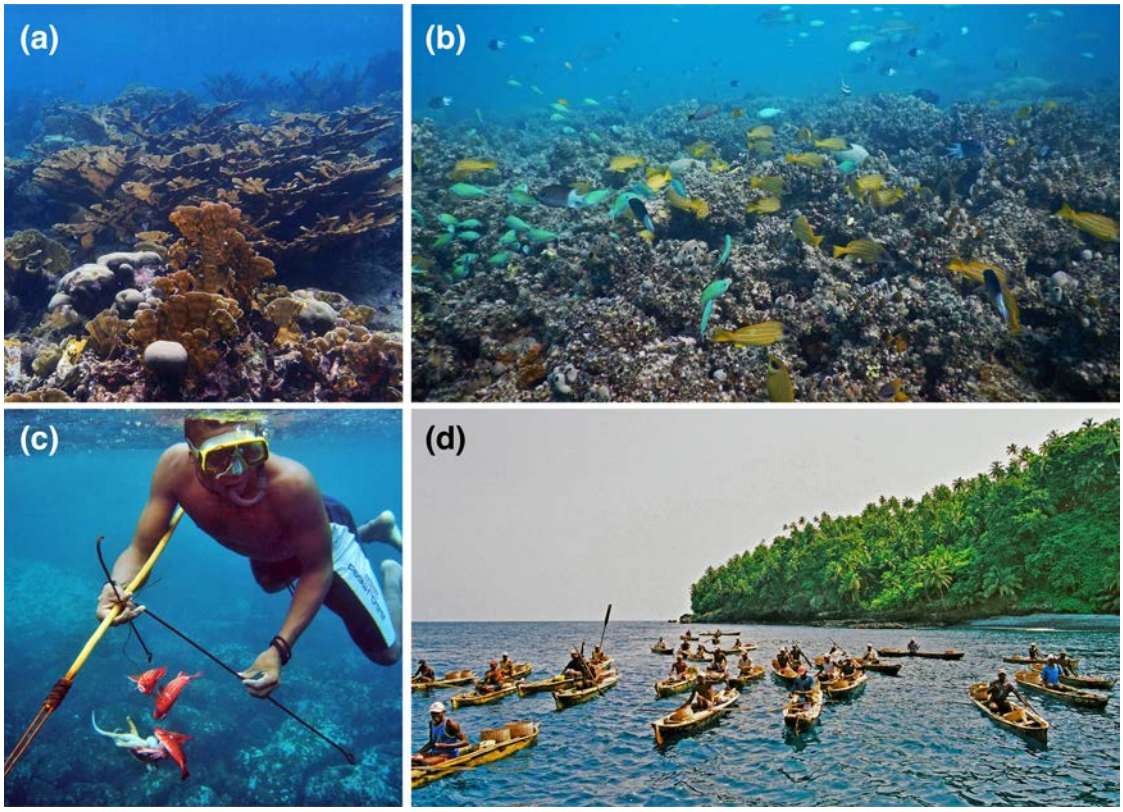

Figure 7: *Aquatic ecosystems are rapidly reconfiguring in response to global changes. Coral reefs, for example, are moving from coral-dominated* ***(A)*** *to alternate states* ***(B)****. Still many people depend on reef resources as a source of food and income* ***(C, D)****. Will reefs and other aquatic systems in the Anthropocene still be able to sustain peoples' livelihoods?* ***(A, B)*** *RA Morais;* ***(C, D)*** *JL Gasparini.*

However, standing biomass is only one of the components required to understand fisheries yields (Worm et al., 2009). Fisheries rely on constant resource production, rather than on its abundance at any one point in time. Thus, it is possible that the perceived utility of standing biomass to inform coral reef fisheries yields has persisted without detailed scrutiny. Recent research has unveiled a general decoupling between fish biomass or fisheries yiels in these systems (Morais & Bellwood, 2019; Morais, Connolly, & Bellwood, 2020; Rogers, Blanchard, Newman, et al., 2018). Even biomass-depleted ecosystems can provide considerable fish productivity and, consequently, support significant fisheries

(Condy, Cinner, McClanahan, & Bellwood, 2015; McCann et al., 2016; Newton, Côté, Pilling, Jennings, & Dulvy, 2007). This decoupling between standing biomass and productivity might also affect perceptions of depletion, reinforcing the need to quantify productivity directly (Embke et al. 2019; Morais et al., 2020). However, despite the clear management benefits and the recent increased interest on quantifying reef fish productivity (e.g. Benkwitt, Wilson, & Graham, 2020; Bozec, O'Farrell, Bruggemann, Luckhurst, & Mumby, 2016; MacNeil et al., 2015; McClanahan, 2018; Morais et al., 2020; Robinson, Wilson, Robinson, et al., 2019; Rogers et al., 2014), we currently lack a robust and easily applicable framework to estimate fish productivity on high species-diversity contexts. As a result, studies have diverged considerably in what they consider productivity to be and how they estimate it (McClanahan, 2018; Morais & Bellwood, 2019; Mourier et al., 2016; Rogers, Blanchard, Newman, et al., 2018).

Here, we outline principles and present a generalised, fisheries-independent approach to estimate community-level reef fish productivity. Our approach combines well-established research methods in fisheries biology, ecology and marine research: demographic models and underwater fish counts. Although the framework here presented is particularly relevant for reef systems in the marine realm, we foresee applications to any high-diversity aquatic ecosystems for which fish abundances and individual weights can be obtained, and age estimated. This includes tropical lakes (Takeuchi, Ochi, Kohda, Sinyinza, & Hori, 2010), rivers and streams (Nunes, Morais, Longo, Sabino, & Floeter, 2020) and other coastal marine habitats (Hemingson & Bellwood, 2018) where underwater fish counts have been used.

From individual to communities: pathways to the production of biomass

From the perspective of an individual fish, biomass is produced through the growth of its tissues (somatic growth, *i.e.* muscles and bones, and 'fattening') and reproductive output. Both processes require energy, and the balance between how much energy is devoted to growth and reproduction changes with ontogeny, *i.e.* as individuals age (**Figure 8**). All fishes undertake a phase of intensive somatic growth and no gamete production early in their ontogeny, before sexual maturation (Phase 1, **Figure 8**). This leads to a transitional phase where somatic growth rates decline and investment on

reproduction quickly increases (Phase 2, **Figure 8**). Although some species continue to grow at similar rates throughout their lives (i.e. linear growth, Depczynski & Bellwood, 2006), most fishes eventually decelerate or even cease to grow, focusing solely on reproduction (Phase 3, **Figure 8**). This directed energetic investment allows reproductive rates to reach a maximum value, although reproduction often continues throughout a fish's lifespan (which can last for many decades, Choat & Robertson, 2002). The total biomass production over the lifespan of a fish equals to its total somatic mass production plus its lifetime reproductive output (i.e. the total number of gametes produced throughout its life).

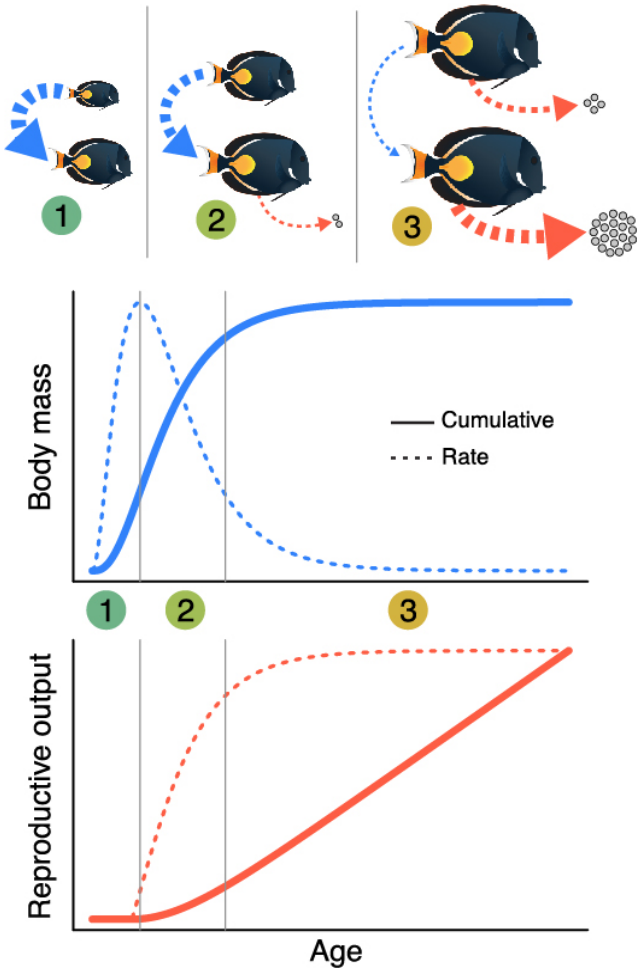

Figure 8: *Fish produce biomass through somatic growth (blue) and reproductive output (red). Early in the ontogeny* ***(1)****, growth rates increase rapidly up to a maximum (dashed blue line), while reproductive rates are null or incipient (dashed red line). As the fish grows (continuous blue line), growth rates decrease and reproductive rates increase* ***(2)****, until growth decelerates near the asymptotic size* ***(3)****. In this phase,*

reproductive rates are maximum, although the cumulative reproductive output increases until mortality (continuous red line).

Upscaling the biomass production of individual fish to the whole community (**Figure 9**) requires considering both the temporal and spatial processes that emerge at this scale. These are mainly represented by mortality, inflow of larvae and recruits from outside the system (exogenous), and outflow of eggs and larvae (endogenous). Together, these processes link productivity across trophic levels (i.e. the consumption of a prey fish is the start of biomass production for a predator), connect adjacent ecosystems, and determine the degree of temporal stability of productivity (e.g. are fully grown fishes replaced by new recruits that can continue growing?). From an energetic perspective, the production of fish biomass is a costly end goal that requires vast amounts of energy spent in foraging, processing and assimilating food, and tissue-building (Barneche & Allen, 2018; Clarke, 2019). For fishes and other ectotherms, these processes involve an energetic expenditure of ~4.4 times the energy stored in the form of biomass (Clarke, 2019) .

Although individuals experience mortality as the outcome of a binary process (*i.e.* death or survival), populations and cohorts (*i.e.* individuals that settled at the same time interval) experience, instead, rates of mortality. Natural mortality rates, which can also be viewed as the instantaneous probability of death of an individual due to natural causes, decrease exponentially as fish cohorts age, mainly because of the correlation between age and size in young fish. Initial life-history phases of reef fishes, such as settlers, suffer extensive mortality (Almany & Webster, 2006; Victor, 1986). Although the exact mortality rates are unknown for reef fish larvae, more than 50% of recruits tend to die in the first two days after settlement (Almany & Webster, 2006; Goatley & Bellwood, 2016). As a result of sharply reduced mortality rates, some reef fishes can live for decades (Choat & Axe, 1996; Choat, Axe, & Lou, 1996; Choat & Robertson, 2002). Others, however, remain exposed to relatively high mortality rates (albeit substantially reduced from post-settlement) throughout their lives and only live for a few months (Depczynski & Bellwood 2006; Kingsford, O'Callaghan, Liggins, & Gerlach, 2017). Nevertheless, the fate of the biomass from individuals that die is challenging to detect, and normally goes unnoticed by researchers (the 'dark productivity' in Brandl, Tornabene, et al., 2019). Individuals

that die get consumed, either before dying, through predation, or after, through scavenging and decomposition (but not necessarily by fishes). The energy contained in their biomass is, thus, channelled to different pathways and end up indirectly fuelling the growth and biomass production of other reef (or non-reef mobile) consumers (Brandl, Tornabene, et al., 2019).

Exogenous inflow of larvae and settlers can supplement the biomass production of local reef fish assemblages (Allgeier, Speare, & Burkepile, 2018; Brandl, Tornabene, et al., 2019). Although exogenous inflow can drive the replenishment of fish assemblages, the direct contribution of settlers to total biomass production is small. Settlers weigh several orders of magnitude less than adults and, hence, almost all of the biomass produced by an individual is due to post-settlement growth. This becomes obvious by comparing, for example, the weight of a recruit parrotfish (0.01-0.08 g, Grutter et al., 2017; Froese & Pauly, 2018) with a fully grown adult (750-5,400 g for most species, Randall, 1997). Although such a magnitude of difference in size between adults and settlers (over 60,000-fold) may be extreme, it is not restricted to parrotfishes, since most recruits of reef fishes are also very small (smaller than 2 cm, Grutter et al., 2017). Even the smallest coral reef fish for which the whole life-cycle is known, the tiny *Eviota sigillata*, produces over 95% of its maximum body weight of ~0.045 g after settlement (Depczynski & Bellwood, 2005; RAM unpub. data). Nevertheless, endogenous eggs and larvae can also enter local biomass production indirectly, if recycled within the ecosystem (e.g. reef planktivores feeding on fish eggs), or if larvae return to settle in their natal areas (Almany et al., 2017). However, these cases have little direct (but high indirect) relevance for fisheries because eggs and larvae are typically too small to be harvested.

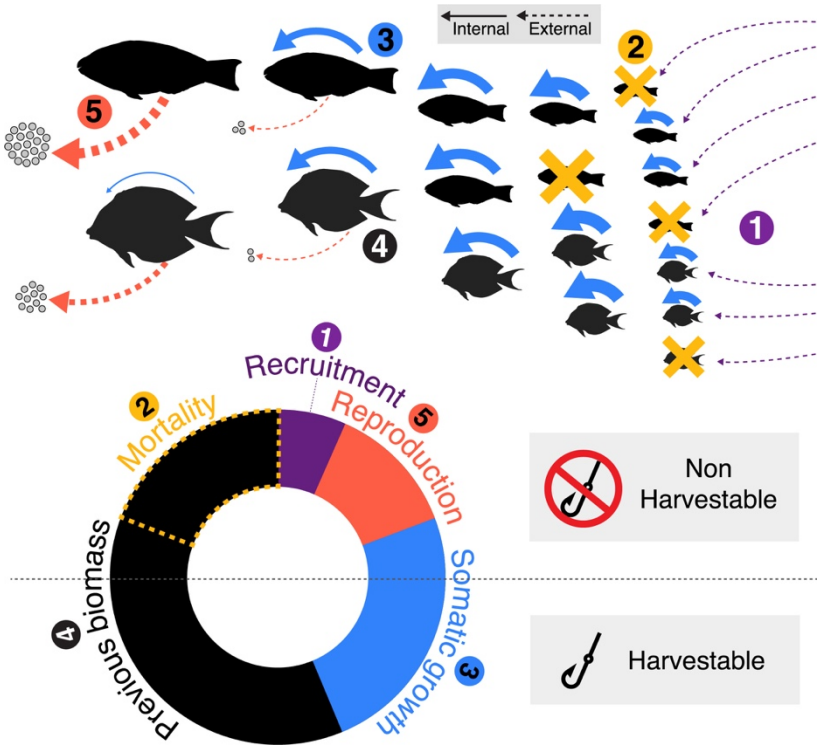

Figure 9: *Biomass production at the community scale includes processes that transcend the individual, such as mortality, inflow of larvae and recruits, and outflow of eggs and larvae. These processes move productivity between ecosystems and link it across trophic levels. Biomass recycled via mortality (and consumption), added through recruitment, broadcasted as reproductive output (i.e. eggs and larvae) and proportions of standing biomass and somatic growth stored in small individuals cannot or are not directly harvested.*

Finally, movements of prey and predators may blur the spatial boundaries of ecosystems, potentially decoupling the productivity of fish assemblages from their trophic structure (e.g. Mourier et al., 2016; Trebilco, Baum, Salomon, & Dulvy, 2013). This may happen, for example, through feeding incursions from reef predators into non-reef habitats (McCauley et al., 2012), through prey fish movements that result in temporary aggregations (Mourier et al., 2016), or through the transport of external food subsidies to reef consumers via ocean currents (Morais & Bellwood, 2019). These mechanisms incorporate productivity from larger areas into coral reef food webs, but their effects are often confounded by the interaction between fish movements and the restricted spatial scale inherent to the method (i.e. underwater visual surveys) (Heenan, Williams, & Williams, 2019; Ward-Paige,

Flemming, & Lotze, 2010). Coral reefs also include food web compartments that are independent of fish, and, thus, not quantified in fish surveys (although these may be part of ecosystem trophic models, e.g. Arias-González et al., 1997; Blanchard et al., 2009; Rogers et al., 2014); as well as cryptic fish compartments that are also not quantified in visual surveys (e.g. Ackerman and Bellwood 2000; Brandl et al. 2019b; Morais and Bellwood 2019). Overall, these points highlight some of the difficulties in capturing the productivity of entire food webs on coral reefs.

Assessing fish and fisheries productivity on tropical reefs

In contrast to biomass, productivity is a dynamic measure, and hence not easy to directly quantify (K. R. Allen, 1971). Until the early 1980s, the only tractable method for estimating the productivity of fish assemblages was through monitoring of fisheries catches (Munro & Williams, 1985). Catches, however, depend on habitat, seasons, years, economic and even cultural factors (Dalzell, Adams, & Polunin, 1996), and it is often hard to define the area from where a specific catch derives (Bellwood, 1988). This enormous variability made meaningful geographic comparisons of wild fish productivity difficult. The development of mass-balanced trophic (or ecosystem) models, such as ECOPATH, provided an alternative approach to quantify reef fish productivity (Christensen & Pauly, 1992), but this was often subject to similar constraints (i.e. delimiting reef and other habitats in a mosaic area, Polunin, 1996).

More recently, reef fish productivity has been estimated using individual size-structured trophic models (Rogers, Blanchard, & Mumby, 2018; Rogers, Blanchard, Newman, et al., 2018; Rogers et al., 2014), stock-production models (Bozec et al., 2016; McClanahan, 2018), bioenergetic models (Mourier et al., 2016), individual age models (Benkwitt et al., 2020; Brandl, Tornabene, et al., 2019; Depczynski et al., 2007; Morais et al., 2020; Morais & Bellwood, 2019), or empirical biomass gradients in protected areas (MacNeil et al., 2015). If the main goal is to popularise the use of fish productivity as a metric to quantify resource production and ecosystem function, the ideal method should be powerful, unbiased, simple and user-friendly. Each of the above-mentioned methods was developed for specific contexts, and we summarise some of their main features below. However, it is beyond the scope of this article to quantitatively evaluate their performance or accuracy.

Trophic models are useful in that they allow for estimates of ecosystem properties, in addition to fish productivity, such as consumption rates and trophic efficiencies (Blanchard et al., 2009; Christensen & Pauly, 1992). Because they incorporate trophodynamic processes, trophic models can generate long-term estimates of production, and also predict productivity under multiple scenarios of ecosystem change (Rogers, Blanchard, Newman, et al., 2018; Rogers et al., 2014). However, to be able to do that, trophic models require the input of multiple parameters describing trophic relationships, dependencies and rates. Many of these parameters can be uncertain or, more often, unknown for high-diversity ecosystems such as coral reefs.

Stock-production models are based on population trends over time (Pella & Tomlinson, 1969; Schnute & Richards, 2002). Because stock-production models work at the stock level, they require no inputs of trophic relationships and demand less input parameters. These models, however, have been developed for modelling single species dynamics and do require knowledge of intrinsic population growth rates (Pella & Tomlinson, 1969), or intensive model optimisation (Bozec et al., 2016). Population growth rates can be unknown for many species, especially when assessments do not cover extended time scales. Similarly, optimisation routines might not be easily accessible for field ecologists or managers (Bozec et al., 2016). Although simple stock-production models have been used on coral reefs by considering the whole fish community as the stock (McClanahan, 2018), their performance for multi-species contexts in these ecosystems has, to the best of our knowledge, not been evaluated.

Individual age models do not require inputs of trophic relationships or population trends (e.g. Depczynski et al., 2007; Morais & Bellwood, 2019). Instead, these models combine species and size data with life-history traits to predict the age, and then growth and natural mortality rates for individuals. As a result, individual models provide a practical interface with multispecies field data. These models rely on principles to quantify the productivity of fish cohorts using somatic growth models (e.g. the Von Bertalanffy Growth Model, VBGM) and mortality functions (e.g. exponential mortality rates) that were established more than 70 years ago (K. R. Allen, 1971; Beverton & Holt, 1957; Ricker, 1946). However, their key conceptual breakthrough was that visual survey data, which includes individual fish sizes and abundance, can be used to estimate somatic productivity if species-specific growth trajectories are known. In essence, this involves determining the 'expected' age of each fish at the moment they are

surveyed by positioning them in their known (or predicted) growth trajectory, based on their body length. This expected or 'operational' age can be unrelated to the real age, but nonetheless allows precise estimates of the expected growth after a time interval.

This individual approach was first used by Depczynski et al. (2007), providing a simple but critical advancement in applying methods traditionally used in fisheries studies to coral reef ecology. Natural mortality rates were incorporated by Morais and Bellwood (2019), but here we expand this idea by including an ontogenetic, size-based mortality risk function. We formalise the individual age framework for estimating productivity as a series of steps, starting with the acquisition of field data, summarised below. We also provide the underlying model equations, as well as an R language package, *rfishprod*, with functions to implement all calculations and to predict (or access) the required life-history data for reef fishes (see **Appendix C**). A beta version of the package can be downloaded from http://github.com/renatoamorais/rfishprod.

A framework for estimating fish productivity for high-diversity ecosystems

Marine ecologists typically conduct underwater field surveys that cover areas of tens to a few hundred square metres. They identify the fish species within those areas and estimate their abundance, also tallying the approximate body length of each individual. This type of field data is the first step of our framework (**Figure 10**, Step 1). Species identities can be used to access species-specific length-weight conversion coefficients, as well as life-history traits, such as growth and mortality coefficients (**Figure 10**, Step 2). These are normally obtained from databases (FishBase, Froese & Pauly, 2018), or from predictive models (e.g. Gislason, Daan, Rice, & Pope, 2010; Morais & Bellwood, 2018b; Thorson et al., 2017) that employ as inputs other species-specific traits and environmental variables such as temperature.

Length-weight coefficients can then be used in conjunction with field-derived fish lengths to predict individual body mass values (**Figure 10**, Step 3). When species-specific coefficients are not available, data from phylogenetically related or morphologically similar species is normally used. Standing biomass is simply the cumulative body mass of individuals within a taxonomic or ecological unit, per unit area surveyed. Taxonomic or ecological units are normally species, size classes, trophic

groups, or the whole assemblage. Standing biomass can also be spatially aggregated to represent larger areas such as habitats, sites, islands, regions, etc.

Individual body mass is also the starting point for estimating growth and productivity (**Figure 10**, Step 4). Growth models, such as the Von Bertalanffy Growth Model (VBGM), use mathematical equations to describe average body size increments as individuals age. The most common size metric used in these models is length, which can be converted to mass following the previous step. These size-at-age relationships can be used to forecast the expected size of a fish after a specific time interval (Choat & Robertson, 2002; Depczynski et al., 2007; Morais & Bellwood, 2018b). Somatic growth can then be approximated by subtracting the body mass of an individual at two time points. Because some fish are likely to die between time points, natural mortality has to be considered when calculating net productivity.

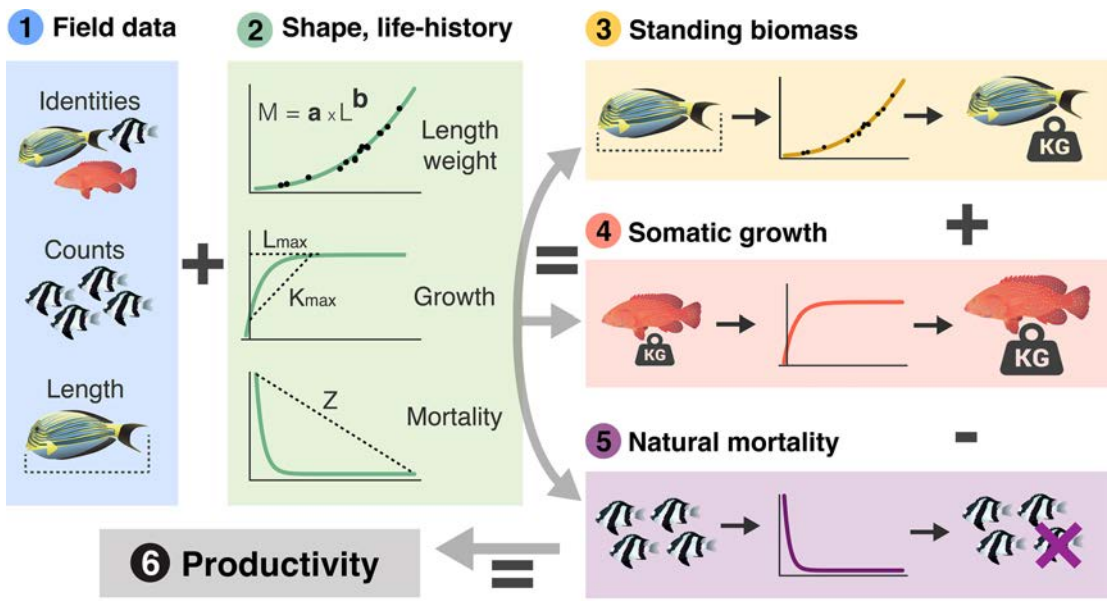

Figure 10: *Steps leading from the acquisition of underwater survey field data* ***(1)*** *to estimating fish productivity* ***(6)****. Shape and life-history species traits predict growth trajectories and mortality probabilities* ***(2)*** *(see* ***Appendix C****). Length-weight relationships convert field-obtained lengths to body mass values* ***(3)****, which are used with growth trajectories to predict body mass increments over a time interval* ***(4)****. Finally, exponential mortality rates define the expected per capita weight losses due to natural mortality. Productivity is the resulting growth minus losses due to mortality (see main text).*

The probability of a fish dying can be obtained empirically or from statistical and theoretical relationships (Brown et al., 2004; Gislason et al., 2010). From the perspective of an individual fish, the probability of mortality decreases exponentially as the fish ages and grows (Goatley & Bellwood, 2016; Jørgensen & Holt, 2013). From the perspective of a cohort of individuals settling, mortality rates decrease exponentially with time and have been predicted by the growth trajectory and maximum size of the species, and water temperature (Brown et al., 2004; Gislason et al., 2010). Natural mortality can be incorporated in the framework described herein in either of two ways: a probabilistic routine that randomly removes individuals, given their estimated mortality probabilities (e.g. daily or yearly, **Figure 10**, Step 5); or a deterministic routine that removes the expected biomass loss due to mortality for each individual (**Appendix C**). The choice between stochastically or deterministically accounting for mortality will depend on the goal of the study. Whilst the deterministic routine allows estimating net productivity at the individual level by incorporating per capita losses, the probabilistic routine permits tracing the fate of individuals on a population. Because the choice of which individuals die is random (although probabilistic), the stochastic method only makes sense iteratively (i.e. after hundreds of independent simulations) and is most useful for simulating scenarios and outcomes. Conversely, the deterministic method avoids aggregating random variability, and, thus, facilitates comparisons (e.g. between reefs, years, etc.). However, the use of 'expected per capita loss of biomass due to mortality' might not be adequate in all scenarios, for it suggests a philosophically counter-intuitive process, i.e. that individual fishes die 'a little bit' every day. Regardless of the chosen method, productivity then equals the total somatic growth minus the losses due to mortality after a given time interval. Productivity can be aggregated in multiple levels, not only spatially, but also temporally.

Validating productivity estimates and data quality

Empirically measuring dynamic quantities, such as absolute productivity, requires closely controlled conditions (K. R. Allen, 1971). Two possible approaches would be to operate controlled fishing experiments on whole fish assemblages (R. E. Brock, Lewis, & Wass, 1979), or to simulate complete fish assemblages in captivity. Both approaches face substantial challenges (e.g. quantifying fishing intensity or the adequacy of simulating natural food provision to captive fish spanning multiple

trophic levels), with consequential low feasibility in the real-world. Estimated productivity must, therefore, be validated by ground-truthing its main empirical variables: growth and mortality rates.

Because empirical VBGM parameters do not exist for all species, they need to be estimated (**Chapter 2**; Morais & Bellwood, 2018b). Previously, we have shown that the machine learning-based method for forecasting growth trajectories from species traits and water temperature can generate precise and unbiased estimates for reef fishes (**Chapter 2**; **Appendix D**; Morais & Bellwood, 2018a,b, 2019). In that case, calculating productivity with estimated vs. empirical VBGM parameters generated nearly identical results (see the sensitivity analyses in **Appendix D** and Morais & Bellwood, 2019). Overall, this suggests that the cumulative growth potential estimated at the individual level is an accurate way to estimate the gross productivity of reef fish populations and assemblages.

Mortality rates for wild fishes are difficult to obtain in the field, with empirical mortality data still lacking for most species (Depczynski & Bellwood, 2006; Goatley & Bellwood, 2016). However, these rates do obey theoretical and empirical trends, and therefore can be estimated from previously determined statistical relationships (Brown et al., 2004; Gislason et al., 2010; Pauly, 1980b). Concordant results have been found when reef fish mortality estimates using these methods were compared among one another or with field data (Depczynski & Bellwood, 2006; Hart & Russ, 1996; Thillainath, McIlwain, Wilson, & Depczynski, 2016). Although much more research is needed to unveil taxonomic and trait-level patterns of fish mortality, existing methods can provide initial approximations of mortality rates (Gislason et al., 2010). In the **Appendix C**, we explore different possible ways of incorporating both the cohort/population and the ontogenetic component of natural mortality (as referred in the previous section).

Importantly, the quality of the productivity estimates obtained by the individual age framework will depend on the quality of both the survey data and the life-history data or predictions used. For example, due to strong method and observer bias, it is essential that counts be consistently derived from the same method (i.e. not mixing tape-first with simultaneous tape winding surveys, Dickens, Goatley, Tanner, & Bellwood, 2011; Emslie, Cheal, MacNeil, Miller, & Sweatman, 2018) and, preferentially, same observer, unless the observer effect can be eliminated or minimised (i.e. through extensive training, Thompson & Mapstone, 1997). Complementary techniques may also help to reduce bias such

as, for example, the use of stereo-video to improve size estimates (e.g. Harvey, Fletcher, & Shortis, 2002) or implementing instantaneous surveys to account for very mobile species (Ward-Paige et al., 2010). Likewise, it is imperative that life-history data from large databases (such as FishBase) be consistently checked for quality (e.g. Robertson, 2008; Thorson, Cope, & Patrick, 2014) and that methods to predict life-history traits be thoroughly tested and validated (e.g. Morais & Bellwood, 2018, 2019).

Forecasting population dynamics by considering recruitment

Expanding the individual age productivity framework to forecast population dynamics requires considering recruitment besides growth and mortality (**Figure 9**). Contrary to somatic growth or mortality rates, recruitment rates cannot be predicted, for open systems such as coral reefs, from environmental or individual features (*e.g.* body size, temperature). Reef fishes have a bipartite lifecycle in which reef-inhabiting adults broadcast larvae to the open ocean. In the open ocean, large mortalities, water-driven transport and fish behaviour make predicting the fate of individual larvae virtually impossible. Thus, there is a large potential for spatial decoupling between where fishes reproduce and where they settle (Almany et al., 2017). Directly incorporating recruitment into fish productivity estimates would, thus, require data on recruitment rates, including abundance of recruits and frequency of recruitment pulses (e.g. as in Brandl, Tornabene, et al., 2019).

A theoretical solution would be to employ stock-recruitment relationships, which assume that the number of recruiting fishes is a function of population spawning biomass or reproductive adults (e.g. Beverton & Holt, 1957; Ricker, 1954). In practice, evidence suggests that large density-dependent mortality in the pelagic phase or immediately after settling may weaken stock-recruitments for coral reef fishes (Caley et al., 1996; Doherty, 1991; Meekan, Milicich, & Doherty, 1993; Robertson, 1990), but this still remains under investigated. Furthermore, recruitment data with which to derive stock-recruitment relationships is scarce for most reef fishes (Caley et al., 1996). To partially circumvent this, (Brandl, Tornabene, et al., 2019) assumed recruitment to be constant and proportional to the relative abundance of fish larvae from different families found near reefs, from different studies. However, this

is likely to apply mainly to small fishes with year-round reproduction, such as in their case. This procedure also generates abundances that cannot be scaled with empirical densities.

Alternatively, Bozec et al. (2016) have assumed that recruit densities level-out to conform to the overall reef fish size-structure immediately after recruitment, and that size structure is constant through time. Community size-structure is known to change in response to disturbances such as fishing or coral loss (Dulvy, Polunin, Mill, & Graham, 2004; Morais et al., 2020; Robinson et al., 2017; Rogers, Blanchard, Newman, et al., 2018). Some of these size-structure changes in response to disturbance may be predictable, i.e. the expected steepening of the size spectrum from size-selective fishing (Dulvy et al., 2004; Jennings & Blanchard, 2004) and, could, in theory be accounted for. However, how stable community size-structure is in the absence of disturbance remains unclear. This topic thus remains open and will benefit from further developments. Long-term empirical datasets of recruitment dynamics and community size-structures will be key to assess how robust the above assumptions are, and the power of individual models in forecasting population dynamics beyond near-future productivity.

Managing for coral reef fish productivity

For decades, biomass-based targets and evaluations of ecosystem health have dominated management recommendations on coral reefs (e.g. R. E. Brock et al., 1979; Friedlander & Parrish, 1998; McClanahan et al., 2014; Russ, Stockwell, & Alcala, 2005; Sandin et al., 2008). But what can coral reef fish productivity tell fisheries managers and stakeholders that standing biomass cannot? Fishing activities rely on constantly harvesting standing biomass. New biomass must be produced to replace what has been harvested, otherwise standing biomass will diminish and, eventually, be depleted. This suggests a fundamental conceptual decoupling of productivity, a dynamic ecosystem rate; from standing biomass, an ecosystem pool that is the consequence of accumulating productivity over time (A. P. Allen & Gillooly, 2009; Brown et al., 2004; Jenkins, 2015). Indeed, such a decoupling between fish standing biomass and productivity has been shown for reef fishes, both theoretically and empirically (Barneche et al., 2014; Morais & Bellwood, 2019; Morais et al., 2020).

Biomass production rates, just like any other biological rates, are proportional to metabolism and, thus, depend on temperature and body size (Brown et al., 2004; Yvon-Durocher & Allen, 2012). Hence, the same standing biomass can be sustained by different production rates in different contexts. For instance, a higher metabolism, and thus productivity, is required to maintain the same standing biomass of small fishes compared to large fishes, and in warm compared to cold waters (Barneche et al., 2014). This is also evident from the increased productivity per unit biomass triggered by reductions in average size from intense size-selective fishing (Morais et al., 2020). Furthermore, many reef fish species have exceptionally high longevity (e.g. Choat & Axe, 1996; Choat & Robertson, 2002), with the biomass accumulated in these species potentially reflecting production amassed over decades, rather than their current productivity. Because of that, the temporal scope over which biomass has accumulated may not be obvious, and, thus, assuming that standing stocks are proportional to resource production can be risky.

Fish productivity, conversely, provides a more direct link to fisheries yields and biomass build-up (MacNeil et al., 2015) than standing biomass. Indeed, assuming negligible loss due to other sources (e.g. emigration), the productivity of a fish assemblage as quantified using the individual age framework described herein represents the potential fisheries yield of that fish assemblage. This is analogous to the concept of 'surplus production' (Beverton & Holt, 1957; Hilborn & Walters, 1992; Schnute & Richards, 2002; Zottoli, Collie, & Fogarty, 2020). In doing so, this method may provide a long sought-after, fisheries-independent method of quantifying potential yields/surplus production in high-diversity tropical ecosystems (e.g. Jennings & Polunin, 1996). From it, one can, for example, determine species-specific annual production and redirect fishing effort under a balanced harvest approach (e.g. Jacobsen, Gislason, & Andersen, 2014; Zottoli et al., 2020). The individual age framework thus offers a relevant tool with the potential to inform the management of tropical multispecies coral reef fisheries in a way that standing biomass simply cannot (see Morais et al., 2020).

In summary, here we provide a simple, fisheries-independent framework to estimate fish productivity that can help to bridge the gap between biomass-based targets and process-based management. Because it arises from non-destructive visual surveys, the resulting productivity metric are particularly useful in a management context for monitoring fish productivity from repeated surveys.

Furthermore, this framework avoids the requirements from other methods of multiple unknown or uncertain ecosystem-level trophic relationships. Instead, it relies on relatively easily accessible life-history parameters. Thus, this framework is ideal for high-diversity tropical aquatic ecosystems, such as coral reefs, in which many such parameters are unknown, or difficult and costly to obtain.

Coral reef ecology is now expanding to embrace process-based management approaches (Bellwood, Pratchett, et al., 2019; Hughes et al., 2017), a response to worldwide mass loss of corals that is likely to intensify. Quantifying key ecological functions and services provided by these systems is now more critical than ever to detect changes, predict trends, and trigger management responses (Bellwood, Pratchett, et al., 2019). Given the renewed interest in methods to assess ecosystem health and resource availability, the framework presented here could facilitate the use of fish productivity as a robust tool to assist the management of coral reef resources and ecosystem functions, and contribute to a broader understanding of harvested coral reefs.

Chapter 4: Trophic pathways and the fish productivity of a degraded coral reef

Published as: Morais, R.A., & Bellwood, D.R. (2019) Pelagic subsidies underpin fish productivity on a degraded coral reef. *Current Biology, 29*(9), 1521–1527.e6

Introduction

Coral reefs harbour high productivity in nutrient-poor tropical oceans. This exceptional productivity can be explained by high recycling rates (de Goeij et al., 2013; Wild et al., 2004), deep-water nutrient enrichment (Gove et al., 2016), and assimilation of external production (Hamner et al., 1988). Fishes consume this productivity through multiple trophic pathways and, as a result, dominate consumer biomass. Their reliance on pelagic vs. benthic productivity pathways has been quantified from the tissues of individual fish (K. W. McMahon, Thorrold, Houghton, & Berumen, 2016; Wyatt et al., 2012), but the contribution of different energetic pathways to the total productivity of coral reef fish assemblages remains unquantified. Here, we combined high-resolution surveys and individual biomass production estimates to generate the first energetic map of a full coral reef fish assemblage, from the smallest to the largest fishes (Ackerman & Bellwood, 2000; Ackerman, Bellwood, & Brown, 2004).

Specifically, we investigated the major trophic pathways that sustain the productivity of this entire coral reef fish assemblage. We define trophic pathways as ensembles of trophic interactions leading from resources to consumers, incorporating ecological and spatial components (see Methods). We used high-resolution surveys of fish assemblages from the windward face of a mid-shelf reef in the northern Great Barrier Reef (GBR), incorporating gobies to large apex predators. Surveys combined nested visual surveys and enclosed clove oil stations (Ackerman & Bellwood, 2000; Depczynski et al., 2007) using a sampling algorithm that integrates survey area, fish size and abundance. This allowed us to model individual-level somatic growth and mortality probability for the entire fish assemblage and, for the first time, to obtain the area-specific total fish productivity of a coral reef. We then partitioned this fish productivity by reef zone (from the exposed slope to the sheltered lagoonal back reef, **Figure 11**), and by six reef and off-reef trophic pathways.

The 18,271 fish recorded included 309 species, spanning 7 orders of magnitude in body mass (0.002 to 19,300 g). We used the resulting dataset to: (1) estimate fish productivity for each reef zone and trophic pathway; (2) describe how the importance of each trophic pathway changes using fish standing biomass vs. productivity; and (3) to test a conceptual model of coral reef productivity based on water flow and topographic complexity. Our streamlined approach requires few model parameters and offers new insights into the drivers of coral reef fish productivity.

Methods

Study locality and design

We conducted this study at Lizard Island (14.7°S; 145.46°E), a mid-shelf granitic island located *c*. 30 km from the Australian coast, in the northern section of the Great Barrier Reef. Our sampling design encompassed three sites at a well-developed windward section of the reef stretching from the lagoon entrance and Bird Islet, to South Island (**Figure 11**). At each of these sites, we surveyed coral reef fishes along a gradient of reef zones, from the exposed outer slope, reef crest and front flat, to the sheltered lagoonal back reef (**Figure 11**). Survey depths varied along with the zones, but were 6.9 ± 0.7 m for the slopes, 3.7 ± 0.6 m for the crests, 1.9 ± 0.3 m for the front flats and 1.9 ± 0.6 m for the lagoonal back reefs. Within each reef zone at each site, we performed three sets of visual surveys (in a total of 36 surveys), and one transect of eight enclosed clove oil stations, hereafter referred to as a 'deployment' (in a total of 12 deployments and 96 stations). All surveys took place during a five-week time period between January and February of 2018.

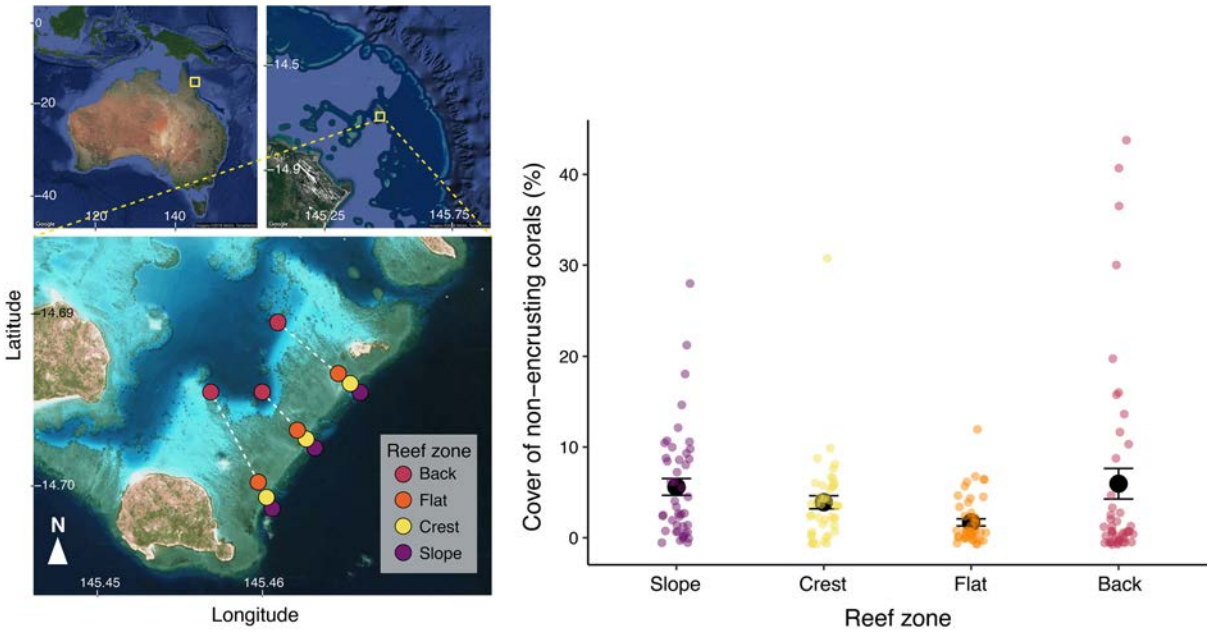

Figure 11: *The studied reef at Lizard Island, northern Great Barrier Reef, with the reef zones surveyed (left panels). The right panel shows the cover of non-encrusting scleractinian corals on the different reef zones. Black circles are the mean cover, while coloured dots indicate the cover of each individual photoquadrat (n = 45 per reef zone). Error bars represent the standard error of the mean.*

Survey procedures

Our surveys of coral reef fishes combined two sampling methods: underwater visual surveys and enclosed clove oil stations (Ackerman & Bellwood, 2000). The underwater visual surveys consisted in four nested sub surveys, designed to maximise the detection of fishes with distinct body sizes and behaviours. During each of the sub surveys, a single diver (RAM) identified, counted and estimated the length (TL, to the nearest cm) of a specific set of fish species within the count area. During the first phase, the diver swam while stretching a tape for 50 m and surveying fishes in an area that extended from the tape to 2.5 m at each side of it. In this phase, the diver surveyed large (>25 cm TL), conspicuous, water column-positioned or quick-swimming fishes likely to be scared away by the diver and to abandon the survey area. Large parrotfishes, surgeonfishes, rabbitfishes, jacks, fusiliers, groupers, emperors and snappers would normally be included within this category. During the second phase, the diver swam back along the tape for 30 m, while also surveying an area that extended from the tape to 2.5 m at each side of it. During this phase the diver surveyed smaller, but nonetheless mobile

fishes likely to be displaced by the diver's passage during the first phase, but either unlikely to go far out of the area, or likely to return after a few seconds. This normally included small to medium-sized surgeonfishes, parrotfishes, rabbitfishes, groupers, most wrasses, small fusiliers, sergeant fishes and puller species (genus *Chromis*) feeding more than 1 m away from the substrate. Then the diver changed direction again, swimming towards the end of the tape for 30 m, while surveying an area that extended from the tape to 0.5 m at each side of it. During the third phase the diver surveyed small, non-cryptic, site-attached fishes, normally straight over the substrate or about a metre up the water column. This included mainly damselfishes and cardinalfishes, but also most small wrasses (e.g. *Stethojulis*, *Pseudocheilinus*). Finally, the diver started recoiling the tape and swimming back for another 30 m-stretch while surveying holes, crevices and overhangs located between the tape and 0.5 m to each side. During this phase, the diver surveyed any fish hidden in these structures that would not have been detected in the previous surveys, such as squirrelfishes, soldierfishes and cardinalfishes; as well as small cryptobenthic fishes such as gobies, blennies, triplefins, dottybacks, and pipefishes (Brandl, Goatley, Bellwood, & Tornabene, 2018).

Given the inefficacy of visual survey methods to adequately sample full cryptobenthic fish assemblages, we used enclosed clove oil stations for these taxa (Ackerman & Bellwood, 2000; Ackerman et al., 2004; Brandl et al., 2018). Each clove oil station deployment consisted of a 14 m long transect, along which we systematically laid eight small (0.4 m^2), approximately circular stations at 2 m intervals. Each station consisted of a 2 mm-mesh mosquito net sown in a conic shape, attached to a 2.25 m long steel chain that delimited the circular area at the bottom. The chain links were approximately 5 cm long and the region where the mesh covered the chain was enveloped by a fabric tissue to avoid damage due to possible abrasion with coral substrate. We attached a small nautical float, tied to a string, to the tapered end of the mesh to keep it erect. Within each station, we sprayed approximately 150 mL of a 3:1 ethanol:clove oil mixture following a concentric border-to-centre pattern, until a curtain of the mixture could be seen within the whole station. The mixture was allowed to sit for approximately 2 min for the anaesthetic properties of the clove oil to act before starting the search for cryptobenthic fishes on the substrate within the station (Depczynski et al., 2007). The search followed a gradual pattern from the borders towards the centre. All fishes from each station were placed

within an individual plastic bag and further euthanised on ice with clove oil. Each individual fish was measured and identified in the lab under a stereomicroscope. Animal collection and euthanasia were performed according to the animal ethics permit A2375 from the James Cook University's Animal Ethics Committee to RAM.

Some of the cryptobenthic fish species detected during the fourth phase of the visual surveys were also captured in the enclosed clove oil deployments. This was especially true for gobies, blennies, triplefins, dottybacks and devilfishes. To deal with the different abundance estimates between the visual counts and clove oil collection methods for these species, we used the criterion of the highest abundance. For whichever cryptobenthic species detected in both methods, we kept the abundance estimated by the method that generated the highest value and excluded the other one. This most often involved excluding the data from the visual survey. However, a few gobies from the genera *Amblyeleteotris* and *Valenciennea*, as well as *Koumansetta rainfordi*; and blue and yellow devilfishes (*Assessor macneilli* and *A. flavissimus*) were more frequently detected by visual surveys.

Additional environmental data

In addition to the fish surveys, we also obtained topographic complexity data for each set of surveys, and coral cover and water flow data for each reef zone. Topographic complexity was measured using a modification of the chain method (e.g. Wilson, Graham, & Polunin, 2007) to target larger-scale topographic features. Instead of a chain, we used a 20 m-long rope with 40 g fishing sinkers attached at every 1 m interval. This weighed rope was laid over the reef substrate following a linear pattern and always in parallel to the tape used for the fish surveys, making sure that it conformed to the substrate as much as possible. The ratio between the known length of the weighed rope and the linear distance that it covered while on the substrate provided the rugosity metric herein considered to represent topographic complexity. Although this method provides only a broad overview of complexity, it correlates strongly with features such as the abundance of holes and crevices (Wilson et al., 2007).

Coral cover was obtained by analysing five photoquadrats of 1 m x 1 m taken randomly along the tape at each fish survey. This resulted in 15 quadrats analysed per reef zone, per site (total of 180 photoquadrats), encompassing a total surveyed area of 180 m^2. We specifically aimed to quantify the

total cover of any living non-encrusting hard corals (Anthozoa: Scleractinia). This included mainly massive forms, but also digitate, corymbose and branching forms that provided structural complexity or, in the case of recruits, that could potentially provide future structural complexity. Non-encrusting hard coral cover, hereafter referred as coral cover, was estimated by overlaying 50 randomly assigned points to the area defined by each photoquadrat. Mean and standard deviation of coral cover for each reef zone was calculated from the pool of photoquadrats containing transects and sites.

Net water flow was obtained from (Fulton & Bellwood, 2005) for the same reef zones of the same windward reef stretch at Lizard Island here investigated. These authors combined field dissolution experiments and posterior laboratory flow calibration to translate dissolution rates to linear flow velocities. Gypsum balls were used both in field and laboratory dissolution experiments for replicated 24-h periods (Fulton & Bellwood, 2005). Laboratory calibration of dissolution rates involved exposing the gypsum balls to increasing flow velocities at the same water temperatures measured in the field (Fulton & Bellwood, 2005). Since only average flow and standard deviation per reef zone were available, we used a randomization procedure to incorporate the variability surrounding the average in our analysis (described in the *Quantification and Statistical Analysis section*).

Defining trophic pathways

We depart from the traditional paradigm of assigning each species to a specific trophic group, recognising that one species can perform multiple ecosystem functions and vice-versa (Bellwood, Streit, Brandl, & Tebbett, 2019). Instead, we identify one or multiple trophic pathways to which each individual fish is part in our study system. We define a trophic pathway as the ensemble of trophic interactions leading from a series of resources to a consumer. The trophic pathways we consider here incorporate not only the major recognised ecological compartments of coral reef economies (pelagic and benthic), but also the seascape (reef and off-reef) and the reef surface (epibenthic or cryptobenthic) where these trophic interactions occur. The boundaries of trophic pathways are, therefore, not only defined by the immediate source of primary productivity, but also consider specificities of habitat or microhabitat. For example, whereas most parrotfish species feed exclusively over the reef substratum, some species are known to feed over sand in the sediment apron adjacent to the reef (Bellwood & Choat,

1990). This case epitomises the use of two distinct trophic pathways that might not necessarily differ in the nature of the resource (i.e. particulates are ingested), but in terms of where the resource is located and, therefore, its composition and nutritional value.

Many coral reef predators have generalised feeding habitats and high levels of flexibility, predating on fish in more than one of these trophic pathways and being able to switch between prey types depending on their availability (e.g. Kingsford, 1992). In such cases, only high-definition techniques that quantify the degree of reliance on different energy sources (e.g. stable isotope, comprehensive dietary analyses or DNA barcoding; K. W. McMahon et al., 2016) can confidently assign the main trophic pathway used by an organism. This level of resolution was available only for a handful of species and, thus, in most cases these generalist feeders were included in a 'generalised predation' pathway category. In addition to predators, the main consumers defining each of the trophic pathways considered herein are defined as:

Off-reef water column: fishes that feed on plankton in the water column and that are not directly dependent on the reef structure for sheltering. This includes species that shelter in the reef structure during the night (Russ, Aller-Rojas, Rizzari, & Alcala, 2017) or that are able to move between reefs;

Off-reef sand substrata: fishes that feed on particulates, invertebrates or on other fishes in the sandy substratum at the interface or adjacent to reefs, including lagoonal sediments and rubble surrounding patch reefs;

Reef water column: fishes that feed on plankton in the water column, but that are directly dependent on the reef structure for sheltering;

Reef epibenthic substrata: fishes that feed on macroalgae, turf algae, detritus, cyanobacteria, or on sessile invertebrates attached to the exposed surface of the reef matrix. Some of these fishes, particularly parrotfishes, pierce the reef matrix and, thus, in addition to the epilithic layer, access some of these resources in the endolithic layer immediately underneath it;

Reef cryptobenthic: fishes that feed on turf algae, detritus, cyanobacteria, sessile invertebrates, mobile invertebrates or on other fishes that occupy the concealed surface of the reef matrix. This includes caves, crevices, holes and other microhabitats used as shelter.

Because our definition of pathways includes a spatial component, off-reef pathways involve potential energy subsidies (e.g. Mourier et al., 2016). Also, since this is a windward reef, the predominant transport of materials is assumed to take place from the open water to the reef, rather than the inverse (e.g. Hamner et al., 1988). Therefore, we consider both off-reef and reef water column pathways to represent potential pelagic subsidies to the reef economy. Importantly, we do not intend to quantify the absolute productivity of the trophic pathways here identified (Arias-González et al., 1997; Polovina, 1984). Our study focuses strictly on the portion of these pathways comprised by coral reef fishes. Therefore, the productivity of the different pathways needs to be interpreted as relative to the total fish component, rather than as absolute values. We recognise that some of these pathways are likely to have additional important contributions from other organisms, but we do not quantify these. Thus, we define the term 'pelagic subsidies' as the proportion of the potential total pelagic subsidies that is accessed by fishes, primarily, but not exclusively, in a direct form (i.e. planktivory). These subsidies are measured in units of fish mass produced (i.e. kg ha^{-1} day^{-1}), and not in units of material mass transported.

Furthermore, it is also noteworthy that we do not directly trace carbon flow or energetic pathways (e.g. K. W. McMahon et al., 2016; Wyatt et al., 2012). Instead, we define the relative use of different pathways at the species level based on an extensive compilation of dietary, habitat use and stable isotope analyses. Part of the data used herein suggests the occurrence of interactions between pathways, including: the assimilation of pelagic production by detritivores (Eurich, Baker, & Jones, 2019; K. W. McMahon et al., 2016), likely mediated by inputs and faeces from plankton-feeding fishes to the detritus (Robertson, 1982; Wilson et al., 2003); or feeding on detached benthic algae in the water column by planktivores (e.g. Hamner et al., 1988; Hobson & Chess, 1978; Wyatt et al., 2012).

A matrix of reliance on trophic pathways was obtained based on information compiled from the literature for each of the 309 species examined. For as many species as possible, we used direct or

indirect quantitative evidence of feeding habits (i.e. dietary studies or stable isotopes) and habitat use (i.e. feeding behaviour studies or anecdotal evidence) to assign proportional reliance on each of the trophic pathways described above. When multiple quantitative studies were available, we averaged values across studies, using the standard deviation as a measure of variability. When only one quantitative study was available, the variability reported (e.g. among individuals or among habitats) was included. If no variability was reported, the scale of variability was estimated as a function of the mean value. This allowed uncertainty to be aggregated. For species with only anecdotal evidence of pathway reliance (e.g. descriptions of feeding behaviour with no quantification), both trophic pathway reliance and variability were estimated on a qualitative-quantitative scale, from 0 (negligible proportion) to 1 (almost complete dependence). The trophic reliance matrix for all species, including values, data types, references and notes on the procedures adopted are included in the Data S2.

Quantification and statistical analysis

Combining survey phases using a resampling algorithm

We devised a resampling algorithm to combine the outputs of the four nested phases of the visual surveys and the clove oil stations into a single unit. This algorithm consisted of randomly sampling individuals from the area surveyed at each of these components, proportionally to their expected abundance in a standardised area following:

$$N_{exp_i} = N_{sur_i} \times \left(\frac{A_{sur_i}}{A_{exp}}\right) \quad (7)$$

Where N_{exp_i} is the expected fish abundance in phase i if the area surveyed was equal to A_{exp}, N_{sur_i} is the actual abundance surveyed in phase i, A_{sur_i} is the area surveyed in phase i; and A_{exp} is the standardised area, taken here as 100 m^2. The total fish abundance in the standardised area was then the sum of the N_{exp_i} from the four phases plus the clove oil deployment.

This resampling procedure was applied to the group of three sets of visual surveys and eight clove oil stations of each reef zone at each site. This resulted in one resampled reef area of 100 m^2

including fishes surveyed on all phases, per reef zone per site. For phases 1 and 2 of the visual surveys, the resampling procedure generated subsamples, whereas for phases 3 and 4 and the clove oil deployment, resampling resulted in extrapolated samples. This whole resampling procedure was then repeated 99 times, so to generate a distribution of values from resampled reef areas for each combination of zone and site. Given the number of iterations, we considered these distributions, hereafter 'resampling distributions', to represent most of the variability in standing biomass and productivity of the surveyed assemblages. We could, thus, incorporate the variability of the fish assemblages within and among sites for each reef zone. The median of a resampling distribution was chosen as the reference value cited throughout the text.

Standing biomass and productivity

For all fish species detected in the visual surveys and clove oil deployments, we compiled Bayesian length-weight regression coefficients and coarse species-level traits (maximum length, diet and position relative to the reef) from FishBase, **Chapter 2** and **Appendix B**. We used the length-weight coefficients to estimate individual fish weights and, hence, standing biomass. The expected somatic growth of each individual fish was estimated from its growth trajectory under the Von Bertalanffy Growth Model (VBGM). This involved first using the compiled maximum length, diet and position relative to the reef to estimate VBGM K_{max} coefficients for each species, according to the method and predictive model in **Chapter 2** (Morais & Bellwood, 2018b). K_{max} is a standardised VBGM coefficient that represents the potential growth trajectory of an individual if its population asymptotic length (L_∞) was equal to its reported species maximum length (**Chapter 2**; Morais & Bellwood, 2018b). Then, we used the potential growth trajectory defined by the estimated K_{max} and the maximum length of each species to ascertain the likely age of an individual fish, given its length (Depczynski et al., 2007). This potential growth trajectory was then used to estimate the expected growth, in length units, of the individuals after a one-day time interval. Expected somatic growth, in length, was afterwards converted to expected somatic growth, in mass units, using the length-weight regression coefficients.

We also incorporated into our estimates of fish productivity likely losses due to natural mortality. For a given species, natural mortality was assumed to decrease exponentially as individuals age, following the trajectory depicted by the scale parameter Z (Hilborn & Walters, 1992). The parameter Z was estimated for each species using Pauly's method (Pauly, 1980b), which considers the VBGM parameters L_∞ and K, as well as water temperature. We used the species maximum length and K_{max} obtained previously, and mean sea surface water temperature to estimate Z. Sea surface temperature was retrieved for Lizard Island from the Integrated Marine Observing System (IMOS), a national collaborative research infrastructure supported by the Australian Government, and made available by the Australian Institute of Marine Science (Key Resources Table). IMOS data are obtained by an in-situ autonomous monitoring system, and were based on the mean of daily average temperatures across at least seven years of data collection. We rescaled Z from a yearly to a daily mortality scale parameter (Z_d) by dividing it by 365. We then used a modification of the formula in (Hilborn & Walters, 1992) to estimate the daily probability of survival for each individual fish:

$$P_{surv_n} = e^{-Z_{d_n}} \tag{8}$$

Where a_{t+1_n} is the relative age of the individual n on day $t+1$, with $a_{t+1} = \{0, \dots, 1\}$; and Z_{d_n} the daily mortality parameter for individual n. We simulated natural mortality events for each individual as the outcome of a Bernoulli trial (with 0 = mortality and 1 = survival) using the probability of survival as given by equation (2). Individuals were removed from the sample or kept depending on the outcome of each trial. Since fishing activities are prohibited at Lizard Island for any purposes other than scientific collections, we considered fishing mortality to be indistinguishable from zero and, thus, total mortality to equal natural mortality. The total fish productivity at any given resampled area was the sum of the somatic growth of all surviving individuals over the time interval used. Finally, standing biomass was rescaled from g 100 m^{-2} to ton ha^{-1}, and productivity was rescaled from g 100 m^{-2} day^{-1} to kg ha^{-1} day^{-1}.

Assigning trophic pathways to individual fishes

We used the Dirichlet distribution (also known as the Multivariate Beta distribution) to map trophic pathways to individual fish. A Dirichlet distribution of k dimensions (i.e. levels of a categorical variable) is governed by the parameters $\alpha_1 \dots \alpha_k$ that describe the magnitude of each level; and by α_0, which is the sum of the magnitudes and, hence, the scaling factor. Together, they define the proportional expected values of each level of a categorical value (Balakrishnan & Nevzorov, 2003):

$$E[X_k] = \frac{\alpha_k}{\alpha_0} \tag{9}$$

In our case, the different trophic pathways represent the different k dimensions. There are no independent variance parameters, and thus the α parameters also determine the variance (Balakrishnan & Nevzorov, 2003). We started by estimating, for each species, α_0 for each trophic pathway from the trophic reliance matrix. The proportional reliance was considered to represent $E[X_k]$, and the compiled variability (see above *'Defining trophic pathways'*) to represent the variance $Var[X_k]$. From these terms, we initially calculated multiple α_{0_k} from (Balakrishnan & Nevzorov, 2003):

$$\alpha_{0_k} = \frac{(E[X_k] - E[X_k]^2)}{Var[X_k]} - 1 \tag{10}$$

We then averaged the multiple α_{0_k} to obtain α_0, and, from it, estimated the different α_k by:

$$\alpha_k = \alpha_0 . E[X_k] \tag{11}$$

Finally, we simulated Dirichlet-distributed values by randomly drawing from the Dirichlet distribution defined by the species-specific parameters. We drew as many values per species as individuals from that species in our sample, each composing a stochastic variation of the species proportional trophic reliance vector. The proportional reliance vector for each individual was

subsequently multiplied by the expected somatic growth of that individual to generate a vector of growth, in mass units, attributable to the different trophic pathways.

Data analysis and hypothesis testing

To test the potential effect of pelagic subsidies in driving total productivity, we first modified the resampling algorithm described above to include only the four phases of the visual surveys (i.e. excluding the clove oil stations). This allowed us to resample the fish assemblage at the level of individual surveys, rather than at the level of reef zones and sites. Although excluding the enclosed clove oil stations implied underestimating the cryptobenthic pathway, we found similar productivity values for the cryptobenthic pathway in all reef zones (**Figure 13**). Therefore, doing so likely did not affect our capacity to detect the influence of pelagic subsidies on the total productivity of the different reef zones. Thus, we used the resampled reef areas for the 36 sets of surveys to test whether the proportion of pelagic subsidies, defined as the proportion of total productivity composed by the off-reef and reef water column pathways, was driving total fish productivity. To do so, we first fitted a gaussian Linear Mixed Model with proportion of pelagic subsidies as a fixed factor and site as a random intercept; and then fitted a similar model, but included an additional interaction term between proportion of pelagic subsidies and reef zone. We then compared the two models using the Akaike Information Criterion (AIC) and the derived weight of Akaike (wAIC). Because of the stochastic variation introduced by the resampling algorithm, we bootstrapped the resampling procedure and the best model for 300 iterations, recording the model coefficients (slope) at each iteration.

We subsequently tested whether topographic complexity and water flow could be generating the distinct relationships between pelagic subsidies and total productivity among zones. We defined a piecewise Structural Equation Model (Lefcheck, 2016) that simultaneously considered the direct effects of water flow and topographic complexity on pelagic subsidies and on the remaining fish productivity (defined as the productivity of all other pathways excluding reef and off-reef water column). Pelagic subsidies in this analysis were considered to be the productivity, in mass units, of off-reef and reef water column pathways, and not their proportion relative to total productivity. The model also included an indirect effect of water flow on topographic complexity and a correlated error term between pelagic

subsidies and all other fish productivity. We started by running preliminary piecewise SEMs with standard linear models using the reported reef zone-level average net water flow values (Fulton & Bellwood, 2005). No independence claims were included. We checked whether including interaction terms between water flow and topographic complexity, and whether including a random intercept for each site improved our model by comparing models using the AIC and wAIC. The most parsimonious model did neither include interaction terms nor a random intercept for site, and was structured as:

$$Prod_{pel} = \alpha_{pel} + \left(\beta_{pel_1} \times WatFlow\right) + \left(\beta_{pel_2} \times TopComp\right) + \varepsilon_{pel} \quad (12)$$

$$Prod_{oth} = \alpha_{oth} + \left(\beta_{oth_1} \times WatFlow\right) + \left(\beta_{oth_2} \times TopComp\right) + \varepsilon_{oth} \quad (13)$$

$$TopComp = \alpha_{tc} + (\beta_{tc} \times WatFlow) + \varepsilon_{tc} \quad (14)$$

$$\varepsilon_{pel} \propto \varepsilon_{oth} \quad (15)$$

Where α indicates intercepts, β slopes and ε error terms, and the subscripts relate the coefficients to the response variable on each case. **Table D2** provides a summary of the final piecewise SEM with the average net water flow values. However, this model assumes that water flow is constant throughout its average values. We, thus, devised a random sampling procedure that incorporated the variability around the mean net water flow at each reef zone by generating a sample water flow intensity value that could be used at the survey-scale in our model. This procedure involved, for each transect, drawing a random value from the normal distribution defined by the reported average and standard deviation net water flow. Then, we ran the structural equation model and recorded all the model coefficients, as well as if the relationships they represented were statistically significant at the $\alpha = 0.05$ threshold or not. The random sampling of water flow values was done 200 times within each of the 200 resampling iterations. This resulted in a final dataset that comprised of 4,000 sets of bootstrapped standardised piecewise SEM coefficients. We used the distributions of these coefficients, in association to the proportion of them that were significant at $\alpha = 0.05$ to determine each variable importance in the piecewise SEM model.

Validation of productivity estimates and sensitivity analyses

We validated our measure of productivity by assessing the accuracy of the estimates of K_{max}, and the productivity calculated from it, in a sensitivity analysis composed of two procedures. First, we implemented an accuracy analysis for the 56 species in our study that had empirical VBGM parameters available. This is an extension of the accuracy analysis in **Chapter 2** and (Morais & Bellwood, 2018b), using the same machine learning technique. However, because we were only concerned about the ability of the model to predict the present set of growth parameters, we included all available curves to improve prediction (i.e. no division of the data in training and testing portions). Second, we used the accuracy analysis above to perform a sensitivity test on our estimates of productivity (**Appendix D**). We replaced the predicted K_{max} by the empirical K_{max} values for the 56 species mentioned above. For the remaining species, we simulated a random bias in the K_{max} prediction by drawing from a distribution defined by the mean bias and standard deviation of the 56 species with empirical data. We then reran all resampling and bootstrapping procedures and the three main analysis of our manuscript, that is: 1) the proportional productivity represented by each trophic pathway; 2) the relationship between proportion of pelagic subsidies and total productivity for different reef zones; and 3) the relationship of topography and water flow with pelagic and non-pelagic productivity (**Appendix D**).

A second sensitivity analysis was performed to that test if the initial size structure of the fish assemblage we surveyed was dictating some of our results (**Appendix D**). Size structure effects could potentially occur, for example, if we sampled before or after the recruitment period. We first evaluated the proportion of the population size range (i.e. the maximum size of an individual ever observed in the population minus a generalised settlement size of 1 cm TL) encompassed by each of the species surveyed. Then, we evaluated the possibility that oversampling of highly productive size classes of planktivores was affecting our results. Following this reasoning, species whose size structure was mostly represented by earlier ontogenetic stages could potentially dominate the productivity because of their maximised investment in growth. If that was the case, we should observe productivity concentrated in the smaller sizes of all or most species. To evaluate this possibility, we looked at how the productivity of each species was divided among the different sizes sampled. Finally, to formally test this potential

impact, in addition to the aforementioned analyses, we performed a sensitivity analysis excluding the smallest individuals of each species. Thus, we explicitly examined the effect of recruits and small juveniles on productivity. These small individuals are the part of fish size structures that tend to exhibit the largest temporal fluctuations and that demonstrate, at the same time, the largest relative growth. We excluded the bottom 25% of the size structure, i.e. individuals smaller than 25% of the maximum size observed in our dataset and, again, reran all resampling and bootstrapping procedures and the three main analysis as described above (**Appendix D**).

Results and Discussion

Fish productivity across reef zones and trophic pathways

Across all reef zones, average fish productivity was 4.7 kg ha^{-1} day^{-1}. The reef slope had the highest productivity (6.86 kg ha^{-1} day^{-1}, **Figure D1**A), followed by the back reef (5.21 kg ha^{-1} day^{-1}) and crest (4.78 kg ha^{-1} day^{-1}). The shallow reef flat had the lowest fish productivity (2.02 kg ha^{-1} day^{-1}). Water column trophic pathways supported 1.93 kg ha^{-1} day^{-1} of fish productivity (**Figure 12**), of which 1.13 kg ha^{-1} day^{-1} was supported by reef planktivores, and 0.8 kg ha^{-1} day^{-1} by off-reef planktivores and their predators (*e.g.* fusiliers, jacks, **Figure 12**, **Figure D1**B). The epibenthic trophic pathway, i.e. fishes that feed on benthic organisms on the reef surface (*e.g.* grazing herbivores, sessile invertivores), was the second most important pathway with 1.37 kg ha^{-1} day^{-1}. The cryptobenthic pathway (*e.g.* gobies, blennies and predators of cryptic invertebrates), off-reef sediment feeders supported intermediate productivities (0.64 and 0.51 kg ha^{-1} day^{-1} respectively). Generalised predation contributed only (0.24 kg ha^{-1} day^{-1}). Overall, these results identify the primacy of water column trophic pathways for sustaining fish productivity, followed closely by epibenthic pathways.

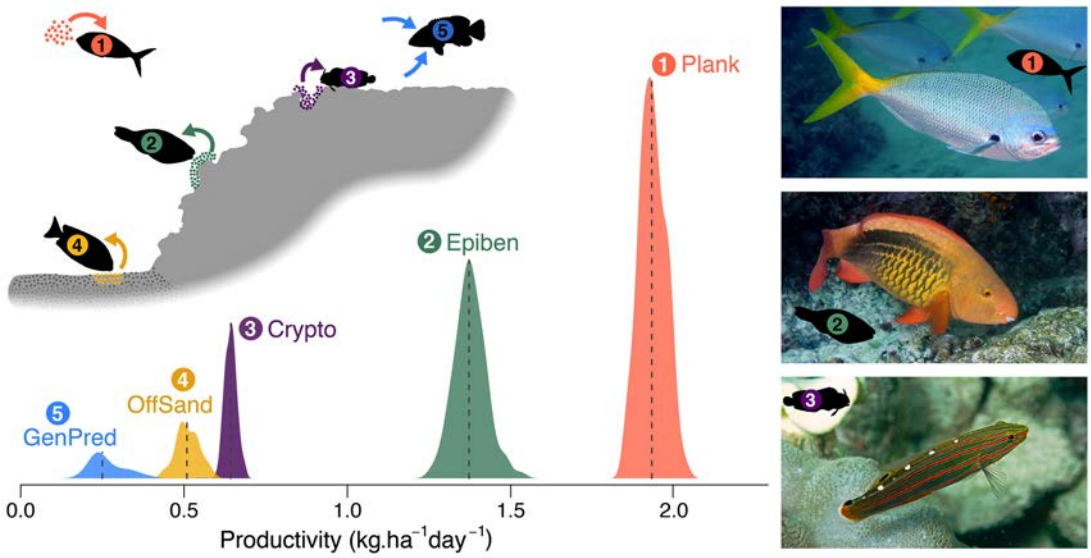

Figure 12: *The fish productivity of a windward reef in the Great Barrier Reef is dominated by water column (Plank) and epibenthic pathways (Epiben). Cryptobenthic feeders (Crypto) and the off-reef sand pathway (OffSand) also represent important contributions to total fish productivity, while generalised predation contributes less. Dashed lines represent median productivity and the density curves are resampling distributions (see Methods) with area scaled proportionally to the x-axis. See also* ***Figure D1*** *in* ***Appendix D****. Right upper and middle photographs: JP Krajewski.*

Traditionally, the high benthic primary productivity of coral reefs is considered to dominate food chains, with planktonic production assigned to a minor role (Glynn, 1973; Hatcher, 1988; Lewis, 1977). Planktonic productivity in surface waters around coral reefs is considered insufficient to support reef community metabolism (Glynn, 1973; Lewis, 1977). However, detailed mapping of water movements and plankton abundance have revealed that oceanic plankton is primarily transported to the windward side of coral reefs in subsurface waters (Hamner et al., 1988). Various physical transport mechanisms (e.g. currents, tidal-forcing) interact with the submerged reef topography, driving vertical transport of plankton that is orders of magnitude more abundant than in surface waters (Gove et al., 2016; Hamner et al., 1988). We found that approximately 41% of total fish productivity originates from water column pathways, rising to 57% for fishes on the forereef slope. As a windward reef, the predominant particle transport is assumed to take place from the open ocean to the reef (e.g. Hamner et al., 1988), and we

thus consider water column pathways to represent potential pelagic energetic subsidies. The high contribution of these pathways to the productivity identified here highlights the potential importance of pelagic subsidies to coral reef food webs.

Recently, considerable attention has focused on inverted biomass pyramids (IBPs) on coral reefs (McCauley et al., 2018; Mourier et al., 2016; Woodson, Schramski, & Joye, 2018). Allochthonous energetic inputs and low trophic-level feeding by large-sized consumers have been invoked to explain IBPs (McCauley et al., 2018; Mourier et al., 2016; Woodson et al., 2018), with inter-habitat predator mobility and spawning-prey aggregations offered as mechanisms providing allochthonous inputs to reef consumers (McCauley et al., 2018; Mourier et al., 2016). We show that pelagic energetic subsidies to fishes can also provide abundant allochthonous inputs to coral reefs. This has important consequences for coral reef fish productivity and fisheries yields. For example, in many parts of the Indo-Pacific, pelagic energy via off-reef planktivores can support significant subsistence and commercial fisheries (Dalzell, 1996; Russ et al., 2017). While some systems may have reef-ocean feedbacks (Gove et al., 2016), our results suggest that these fisheries can be relatively independent of reef production, especially on windward reefs.

Contrasting fish biomass and productivity

Biomass was a poor predictor of the contribution of different trophic pathways to coral reef fish productivity. Neither the importance of pelagic subsidies, which include reef and off-reef water column pathways, nor that of cryptobenthic-derived productivity are apparent from their standing biomass. Indeed, reef planktivores and cryptobenthic feeders composed only a minor portion of fish biomass, despite their major contribution to productivity (**Figure 13**). Body size is probably why these pathways were underrepresented by biomass. Water column pathways are dominated by damselfishes (Pomacentridae), while small wrasses (Labridae) and cryptobenthic reef fishes are the main components of the cryptobenthic pathway. These fishes are predominantly smaller than 10 cm, and contribute little to standing biomass (Ackerman & Bellwood, 2000; Depczynski et al., 2007). However, they are among the most abundant coral reef fishes (Ackerman & Bellwood, 2000; Depczynski et al., 2007), and can produce biomass at rates as high as fishes orders of magnitude larger (Depczynski et al., 2007). We

show that water column and cryptobenthic pathways, together, exceeded 1.77 kg ha^{-1} day^{-1}, approximately 38% of total productivity. Most of this production would be disregarded if considering biomass alone.

While the perceived importance of some pathways changed between biomass and productivity, both variables unveiled similar among-zone patterns (**Figure 13**). The epibenthic, cryptobenthic and off-reef sand pathways, had relatively consistent productivity across zones. By contrast, reef and off-reef water column pathways had high productivity on the slope and crest, dropping to almost zero on the flat. Thus, while some pathways were relatively important in all habitats, pelagic subsidies were mostly confined to exposed forereef zones. This highlights the potential for pelagic subsidies to shape reef-zone differences in productivity.

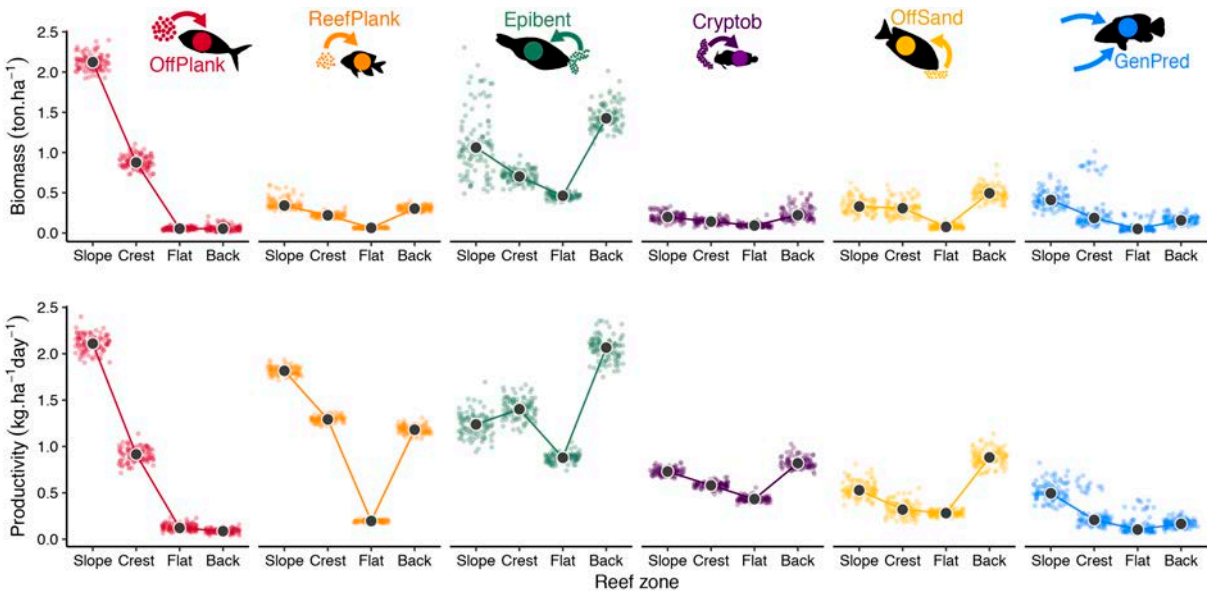

Figure 13: *Standing biomass and productivity of different trophic pathways vary considerably in importance across reef zones in a windward section of a coral reef in the northern Great Barrier Reef, Australia. Each coloured dot is a combined subsample of multiple transect areas and enclosed clove oil stations and dark dots are median values. The water column pathway from* ***Figure 12*** *is divided into two components: off-reef planktivores (OffPlank) and reef planktivores (ReefPlank). Epibent = epibenthic feeders; Cryptob = cryptobenthic feeders; OffSand = off-reef sand feeders; Mixed = multiple trophic pathway feeders.*

Pelagic pathways as drivers of coral reef fish productivity

Given the large disparities in pelagic subsidies among habitats (**Figure 13**), we tested the potential effect of these subsidies in driving total productivity. We found a strong positive relationship between productivity and the proportion of pelagic subsidies (**Figure 14**A) that was driven by reef zone (Figure 3B). Reef slopes had the highest pelagic subsidies and productivity, back reefs and reef crests had intermediate values, and reef flats the lowest values (**Figure 14**B, **Table D1**). A tight and steep coupled increase in productivity and proportional pelagic subsidies was observed on the slope and crest, but not on the back or flat reef zones (**Figure 14**B; **Table D1**). Forereef zones had not only a higher contribution of pelagic subsidies, compared to reef flats and back reefs, but also a higher proportion of subsidies, underpinning their exceptional fish productivity.

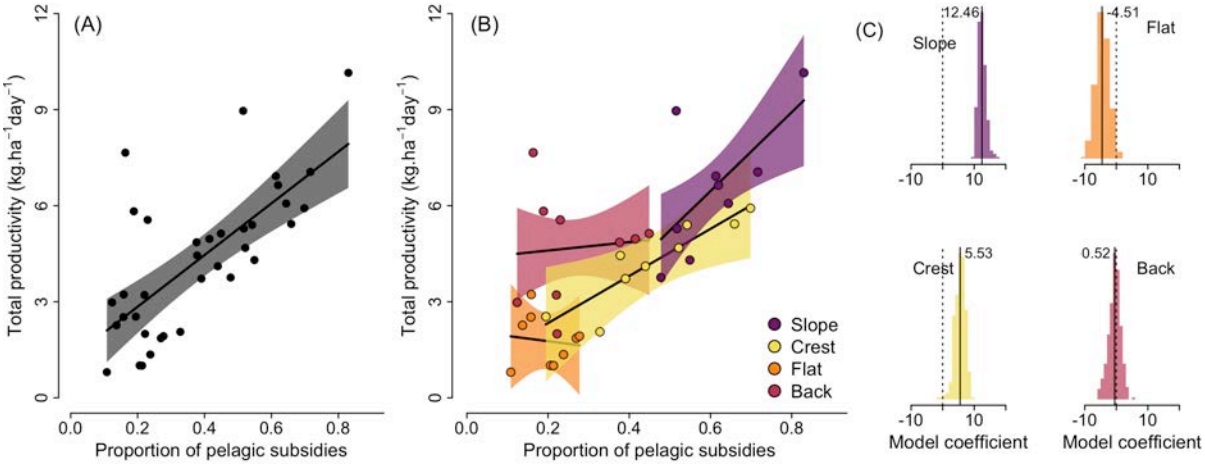

Figure 14: *The strong positive relationship between pelagic subsidies and total fish productivity on a windward reef in the Great Barrier Reef* ***(A)*** *is driven by reef zone* ***(B)****. The model in* ***(B)*** *including an interaction between subsidies and reef zones had better support than the one in* ***(A)****: AIC model* ***(B)*** *= 123.5, wAIC = 1; AIC model* ***(A)*** *= 142.8, wAIC = 0. Whereas pelagic subsidies were not or only weakly related to total productivity in back or flat reef zones, these variables were strongly and tightly related in crests and, especially, reef slopes.* ***(A)*** *and* ***(B)*** *depict one resampling iteration, where dots are resampled visual surveys (see Methods), and lines and bands are, respectively, model predictions and 95% confidence intervals (LMMs, see also* ***Table D1****). The histograms in* ***(C)*** *show the bootstrapped distributions of model coefficients (slope) for the proportion of pelagic subsidies for each reef zone. Although coefficients for the flat were most*

*often negative, they almost invariably had 95% confidence intervals overlapping with zero (not shown, example on **Table D1**)*

Our data suggests that there are two main components of coral reef fish productivity: an internal component, that relies mainly on reef-based productivity; and pelagic subsidies, accessed by fishes, either off or on the reef, that consistently boost the productivity of exposed forereef zones (**Figure 15**). Feeding on these pelagic energetic sources is limited on sheltered back reefs and, especially, on the reef flat (**Figure 15**A). The internal productivity component depends on both algal production and recycling, and operates mainly through epibenthic and cryptobenthic energetic pathways. It is important across all reef zones. There is also a slightly smaller and more variable contribution from photosynthesis (i.e. from microalgae in the biofilm layer; Hatcher, 1988) and detritus to fish feeding over adjacent sediment areas (**Figure 15**B).

Previous research has reported large differences in water flow and topographic complexity between reef zones, with marked effects on fish assemblages (Darling et al., 2017; Fulton & Bellwood, 2005; Fulton, Bellwood, & Wainwright, 2005). Reef complexity has also been identified as an important driver of fish productivity (Rogers et al., 2014; Rogers, Blanchard, Newman, et al., 2018). We therefore asked if these physical features could explain differences in pelagic subsidies and total productivity between zones. Although water transports particles (*e.g.* zooplankton) to windward reefs (Hamner et al., 1988), maintaining water column position in high flows requires fast swimming that is energetically costly (Fulton & Bellwood, 2005; Fulton et al., 2005). Topographic complexity provides fishes with refuges against both water flow (Johansen, Bellwood, & Fulton, 2008) and predators (Hixon & Beets, 1993). Water flow and topography also tend to be correlated, as water motion affects, for example, coral growth that subsequently shapes topography (Darling et al., 2017). We therefore used a piecewise structural equation model (Lefcheck, 2016) to disentangle the relationships of both productivity from pelagic subsidies and other pathways, with water-flow speed and topographic complexity (see Methods).

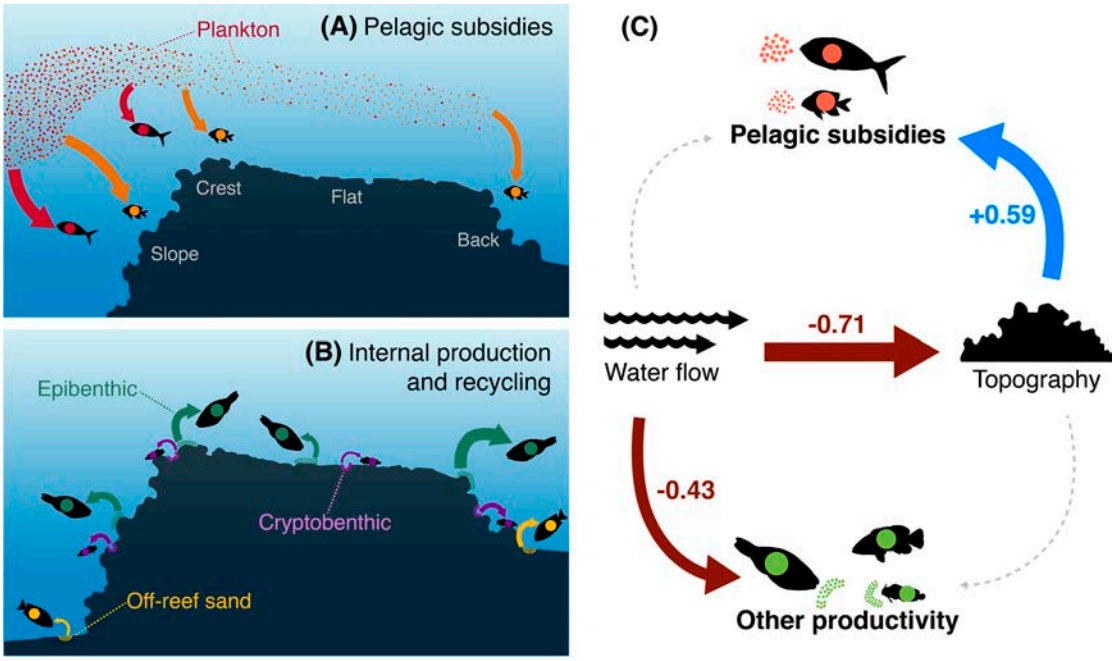

Figure 15: *Schematic representation of the main trophic pathways leading to coral reef fish productivity on the windward section of a coral reef, from the upper slope to the back reef. Width of the arrows is proportional to the raw fish productivity.* ***(A)*** *Pelagic subsidies accessed by fish, either off the reef or on the reef, boost the productivity of exposed forereef zones such as the upper reef slope and the reef crest.* ***(B)*** *Internal production and recycling operate mainly through epibenthic and cryptobenthic energetic pathways, which are relatively consistent across all reef zones, with additional contribution from adjacent sediment areas. Colours follow* ***Figure 13****.* ***(C)*** *The piecewise structural equation model, relating both the productivity of pelagic subsidies and the productivity from all other pathways with water flow speed and topographic complexity. Numbers are bootstrapped standardised coefficients, colours depict whether an effect is positive (blue) or negative (dark red), and the width of the arrow is proportional to the magnitude of the coefficient. Dashed lines represent potential relationships that were not significant at* $\alpha = 0.05$*. See* ***Table D2*** *and* ***Figure D2*** *for more details.*

Model fits were heterogeneous, with 42% and 27% of the variation in pelagic productivity and the remaining productivity, respectively, explained by the predictors (**Table D2**). Pelagic subsidies and the remaining productivity were predicted by different variables (**Figure 15**C, **Table D2**). Whereas water flow had no direct influence on pelagic subsidies, it had a persistent negative effect on the remaining productivity. By contrast, topography had a strong positive effect on pelagic subsidies, but

no effect on the remaining productivity. Water flow had a strong negative effect on topographic complexity, explaining 52% of its variation, and thus exerting a strong indirect negative effect on pelagic subsidies. Despite considerable unexplained variability, we interpret these results as evidence that, at the scales investigated herein, topography mediates the capacity of water column fishes to intercept plankton transport, providing an important link between pelagic primary productivity and coral reefs. The mechanism behind this link is unclear, but probably involves increased provision of refuges against water flow and/or predation (Hixon & Beets, 1993; Johansen et al., 2008). In essence, to benefit from pelagic subsidies, reefs need topographic complexity.

We also detected a moderate correlation between pelagic subsidies and the remaining productivity. This correlation may be driven by multiple possible links between the external and internal sources of productivity in coral reefs, including the sponge and coral-mucus loops (de Goeij et al., 2013; Wild et al., 2004), near-reef plankton blooms (Gove et al., 2016), detritus-enhancement from dead plankton or fish faeces (Wilson et al., 2003), or emerging resident plankton (Hobson & Chess, 1978). Other, unquantified, aspects of structural complexity (e.g. refuge abundance) and hydrodynamics (e.g. wave action), as well as predator abundance and activity are likely to contribute to the unexplained model variation.

Fish productivity on transitioning coral reefs

The reefs at Lizard Island have recently suffered multiple disturbance events, including crown-of-thorns starfish outbreaks (Pratchett, 2010), cyclones (Ceccarelli, Emslie, & Richards, 2016), and widespread coral bleaching (Wismer et al., 2019). In particular, category 5 cyclone Ita, in April 2014, caused coral cover in our study area to decline by ~55% on the forereef slope, and up to ~70% in shallower zones (Ceccarelli et al., 2016). Four years later, non-encrusting coral cover ranged from 1.7% on the reef flat to 6% on the slope (**Figure 11**). Cyclones and other severe storms destroy mechanically-vulnerable corals (Madin & Connolly, 2006), eroding structural complexity (Pratchett et al., 2008) that is critical for small body-sized fishes (Nash, Graham, Wilson, & Bellwood, 2013). This coral loss causes disproportional population declines in small fishes, especially planktivores (Ceccarelli et al., 2016; Pratchett et al., 2008). Even larger off-reef planktivorous fusiliers, presumably less reliant on the reef

structure, may decline following coral loss (Russ et al., 2017). Thus, it would be expected that the trophic pathways used by these planktivores would have diminished in importance in structurally-degraded systems. However, we observed a consistently high contribution of pelagic inputs to the fish productivity of this degraded reef, averaging 41% of the total. This indicates some degree of resilience of planktivorous fish productivity despite coral loss.

This raises the question: what were pre-disturbance reefs like? The total fish productivity of this degraded coral reef does not appear to differ markedly from estimates of other coral reef systems. For example, the productivity of our windward slope (6.86 kg ha^{-1} day^{-1}) is superficially similar to values for a section of fringing reef in French Polynesia (6.85 kg ha^{-1} day^{-1} (Arias-González et al., 1997)). Unfortunately, most previous reef fish productivity estimates used non-comparable methods (Arias-González, Galzin, Nielson, Mahon, & Aiken, 1994), encompassing different spatial scales (Arias-González et al., 1994), and often including adjacent ecosystems (e.g. Polovina, 1984). Our method for estimating fish productivity based on somatic growth and mortality applied to underwater surveys provides a means to easily address productivity at the reef scale. Further studies using comparable methods on other reefs will be critical to understand if and, if so, how coral degradation affects coral reef fish productivity.

Caveats and future research

Our productivity model enabled us to disentangle the relative importance of trophic pathways to total fish productivity on a degraded coral reef. Although our study offers a snapshot of this fish assemblage, our productivity measures are accurate and robust to variations in growth parameters or initial size structure (**Appendix D Sensitivity Analyses**). Future research may explore the link between structural complexity, refuge availability and survivorship (Hixon, 1991; Rogers, Blanchard, Newman, et al., 2018). For example, including a dependence of natural mortality on complexity would likely reveal even stronger pelagic subsidies due to enhanced survivorship of small planktivorous fishes that dominate productivity on high complexity areas.

Our results provide the first empirical estimate of total fish productivity incorporating the full size range of fishes on coral reefs, including pelagic off-reef-feeding taxa (Ackerman et al., 2004;

Depczynski et al., 2007). However, our study location encompasses only a small subset of the conditions that coral reefs experience. Most coral reefs are not contained within a large continental lagoon, with limited wave energy and material transport from oceanic waters (Hamner et al., 1988). Many coral reefs are closer to oceanic waters than the reef studied herein, and thus have a larger potential to receive pelagic subsidies from deep-water upwelling and internal waves (Gove et al., 2016; Hamner et al., 1988; G. J. Williams et al., 2018). It is highly likely that pelagic subsidies will represent a much larger part of total fish productivity in these oceanic coral reef systems.

Furthermore, the interplay between seascape configuration, water flow, and topographic complexity will likely determine the relative extent of pelagic vs. benthic pathways. Larger topographic complexity in shallow reef areas, for example, should increase the chances of strong pelagic coupling of reef food webs. Conversely, the loss of complexity may have significant impacts on pelagic subsidies if corals and three-dimensional structure are the key to accessing pelagic resources. Coral loss is often linked to decreasing fish abundances (Pratchett et al., 2008; Wilson, Graham, Pratchett, Jones, & Polunin, 2006), with likely effects on the ability of coral reefs to retain pelagic inputs. However, recent evidence has suggested that this is not always the case, with sustained productivity reported from reefs after extensive coral mortality (Robinson, Wilson, Robinson, et al., 2019). With coral cover of less than 6% and substantial pelagic productivity, our study supports this view, offering additional hope for sustained pelagic coupling and subsidies even in low-coral systems.

In summary, although reef epibenthic pathways are often assumed to dominate coral reef trophodynamics, we show that pelagic subsidies can make a substantial contribution to total fish productivity. As exemplified by our study system, these subsidies can remain and boost fish productivity even in the context of substantial local coral loss. Our findings suggest that the energetic functioning of coral reefs might show some resilience even after coral loss.

Chapter 5: Severe coral loss and the energetic dynamics of a coral reef

Published as: Morais, R.A., Depczynski, M., Fulton, C., Marnane, M., Narvaez, P., Huertas, V., Brandl, S.J., & Bellwood, D.R. Severe coral loss shifts energetic dynamics on a coral reef. *Functional Ecology*, *34*(7), 1507–1518.

Introduction

The unprecedented, worldwide coral bleaching events of 2015-2017 sparked a re-evaluation of coral reef research, conservation goals and the role of corals in underpinning the services provided by coral reefs (Bellwood, Pratchett, et al., 2019; Bruno et al., 2019; Hughes, Barnes, et al., 2017; G. J. Williams et al., 2019). There have been calls to accept this new low-coral state as an inevitable long-term situation, strengthened by ongoing coral degradation events (Bellwood, Pratchett, et al., 2019; Hughes, Barnes, et al., 2017). If we are to embrace this new reality, we need to understand the biological and ecological attributes of these new coral reef ecosystems (Bellwood, Streit, et al., 2019; Graham, Jennings, MacNeil, Mouillot, & Wilson, 2015). For example, how will new reef configurations affect the energetic dynamics of coral reefs, and can they maintain their capacity to provide food resources for people?

Reduced coral cover and loss of structural complexity are the most widely reported contemporary changes in coral reef ecosystems (Alvarez-Filip, Dulvy, Gill, Côté, & Watkinson, 2009; Graham et al., 2015; Hughes, Kerry, et al., 2017). Such degradation is often exacerbated by other ecosystem stressors, such as increased benthic sediment loads (Tebbett, Streit, & Bellwood, 2020) and reduced water quality (MacNeil et al., 2019). The effect of these synergistic stressors on associated biota are often showcased by the responses of coral reef fishes (e.g. Pratchett, Thompson, Hoey, Cowman, & Wilson, 2018; Stuart-Smith et al., 2018) because of the critical services fishes provide in tropical ecosystems (e.g. fisheries resources, aesthetical value, N. Marshall et al., 2018) and their potential role in mediating coral reef resilience (Bruno et al., 2019; Hughes et al., 2010, 2007).

Reef fish responses to coral reef degradation are often species-specific, depending on body size and the degree of dependence on live coral (Ceccarelli et al., 2016; Cheal, MacNeil, Emslie, &

Sweatman, 2017; Graham et al., 2007; Stuart-Smith et al., 2018). Corallivorous, planktivorous, and coral-dwelling fishes are reported to be particularly susceptible to coral loss while herbivores appear relatively resilient (Gilmour, Smith, Heyward, Baird, & Pratchett, 2013; Graham et al., 2006; Pratchett et al., 2018; Stuart-Smith et al., 2018). Because many of the species investigated initially respond negatively to coral loss (Bellwood, Hoey, Ackerman, & Depczynski, 2006; Wilson et al., 2006), it is generally expected that assemblage-level fish responses would also be negative. However, species-level responses to coral loss are neither linear nor additive at the ecosystem level, with evidence suggesting that post-coral loss stability in coarse fish assemblage metrics, such as abundance or biomass, is possible (Bellwood et al., 2006; Ceccarelli et al., 2016). This apparent community stability may, however, overshadow major changes in species composition that result in alternate ecosystem states (Bellwood, Streit, et al., 2019; Graham, Cinner, Norström, & Nyström, 2014; Hughes, Barnes, et al., 2017).

The energetic consequences of assemblage level responses to coral loss for fishes have relied predominantly on a single metric, standing biomass (e.g. Ceccarelli et al., 2016; Pratchett et al., 2018; Robinson, Wilson, Jennings, & Graham, 2019; Stuart-Smith et al., 2018). However, ecosystem functions operate through time and are, thus, more accurately assessed using dynamic, flow-based rates (Bellwood, Pratchett, et al., 2019; Brandl, Tornabene, et al., 2019; Hooper et al., 2005). Indeed, reef fish biomass and the underlying rate of biomass production often show only limited correlation. For example, small planktivores that comprise a small standing biomass are often important drivers of total biomass productivity (**Chapter 4**; Morais & Bellwood, 2019). Similarly, small cryptobenthic fishes contribute disproportionally to the biomass consumed by predators despite a negligible standing biomass, a result of their fast-paced lifestyle (i.e. short lifespan and high mortality rates, Brandl, Tornabene, et al., 2019). This suggests that different ecosystem functions are likely to respond to coral reef degradation in fundamentally different ways (cf. Rogers, Blanchard, & Mumby, 2018).

Here, we focus on the impacts of coral loss on four metrics of energy flow and storage, which underpin consumer biomass production and thus, coral reef ecosystem functioning (Brandl, Rasher, et al., 2019). We exploit a recently expanded approach to estimate fisheries-independent fish productivity, and other ecosystem functions, in high diversity communities such as coral reefs (see **Chapters 3 and 4**, also: Brandl, Tornabene, et al., 2019; Depczynski et al., 2007; Morais & Bellwood, 2019). Because

this approach is applied for each individual, it provides an ideal interface with underwater fish counts, the universal reef fish censusing method. By simultaneously quantifying multiple aspects of a key ecological process, we reinforce a pluralistic, process-oriented view of ecosystem research needed to decipher and better manage contemporary reef systems (Bellwood, Pratchett, et al., 2019; Brandl, Rasher, et al., 2019; Fulton et al., 2019; Hughes, Barnes, et al., 2017).

Methods

Study locality and survey design

We carried out fish and benthic surveys at Lizard Island, on Australia's Great Barrier Reef (GBR, **Figure 16**), in 2003-2004, and 14-15 years later, in 2018. Benthic surveys were used to quantify live coral and turf cover using point-intercepts and photoquadrats along transects in 2003/04 and 2018, respectively. We randomly subsampled points to ensure a similar precision and to be able to compare among these survey methods. In both 2003/04 and 2018, we surveyed 13 common reef fish families using visual surveys (belt transects) and enclosed clove oil stations. A detailed description of the field procedures is available in the Supplemental Methods (**Appendix E**). To combine the different fish survey methods into a single unit containing all surveyed fish families, we applied the resampling procedure described in **Chapter 4**.

From 2014 to 2017, the reefs around the Lizard Island group were affected by four major coral degradation events which included two severe (category 5 & 4) cyclones in 2014 and 2015, closely followed by two major coral bleaching events in 2016 and 2017. These cumulative events resulted in up to 80% decline in coral cover throughout the island group, particularly at exposed sites (Ceccarelli et al., 2016; Madin et al., 2018). Our fish and benthic surveys were located in the southeast windward reef stretch between South Island and Bird Islet (**Figure 16**) following Depczynski et al. (2007), and encompassed a spectrum of reef habitat zones: upper slope (7-9 m depth), forereef crest (3-4 m depth), flat (1-2 m depth) and lagoonal back reefs (2-3 m). We used satellite images to map each of these reef zones and estimate their area (**Figure 16**, see Supplemental Methods, **Appendix E** for details).

Metrics of energy flow and storage

The procedures to obtain the four metrics used to evaluate energy flow and storage in this study followed (Brandl, Tornabene, et al., 2019), and are described in detail in the Supplemental Methods, **Appendix E**. In brief, growth trajectories are predicted at the species/genus level based on traits and water temperature (Chapter 2 and Morais & Bellwood, 2018b). Then, the expected somatic growth, in g day^{-1}, is estimated by placing each individual in their predicted growth trajectory (**Chapter 3**). Daily mortality rates are obtained by combining species/genus mortality coefficients estimated from growth trajectories and water temperature with an exponential negative relationship with individual body size (see **Chapter 3**; Supplemental Methods, **Appendix E**). These daily mortality rates are multiplied by the individual body mass to generate an 'expected per capita loss of biomass' due to mortality.

The total standing biomass and productivity of each resampled fish assemblage was derived from the combined weights and expected growth of all individuals, respectively. Because productivity was estimated from the expected somatic productivity, it should be considered as a metric of potential productivity. The term 'consumed biomass' is hereafter used broadly to indicate expected losses from standing biomass due to mortality, including losses that are not directly a result of predation (i.e. decomposition). These expected losses were estimated for each individual based on their likely mortality probabilities (see **Appendix E**). While standing biomass measures an ecosystem pool of stored heterotrophic energy (scaled to t ha^{-1}), productivity and consumed biomass are dynamic ecosystem flow metrics (scaled to kg ha^{-1} day^{-1}) (Hooper et al., 2005).

We also calculated two derived rate measures: total turnover (% $year^{-1}$) and an instant biomass change metric (unitless). Turnover is classically defined as the ratio of production to biomass (K. R. Allen, 1971; Odum & Odum, 1955; Waters, 1969). We expand on this concept by defining total turnover as the sum of net turnover (the quotient of productivity and standing biomass) and consumption turnover (the quotient of consumed and standing biomass, Brandl, Tornabene, et al., 2019). Total turnover could be understood as the rate at which particles flow across the system, i.e. are either incorporated into the food chain or released from it. Our instant biomass change metric was obtained by dividing consumed biomass by (net) productivity. This metric positions the fish assemblage along a

gradient of immediate biomass response, from biomass erosion (values > 1, when consumption exceeds production) to biomass accumulation (values < 1, when production exceeds consumption).

To provide a system-level analysis of potential changes in the main reef habitat zones, we calculated the weighted average of the reef zone-specific standing biomass, productivity, consumed biomass and turnover. We used the area of each reef zone as obtained from satellite-based habitat mapping (see full description in the **Appendix E**) as the averaging weights for all descriptors.

Data analyses

All data analyses were performed in R (R Core Team, 2019). To evaluate family-level abundance and biomass patterns across reef zones, as well as potential changes from 2003/04 to 2018, we used 100 bootstrap iterations of resampled fish assemblages. These assemblages were aggregated by family and visualised in two dimensions using a non-metric multidimensional scaling (nMDS) ordination based on Bray-Curtis similarity of the square-root transformed community matrix. Because bootstrapped assemblages do not constitute replicates, instead of individualising samples with dots, we depict their bi-dimensional variability using polygons. The magnitude of potential changes in each family was calculated as the $\log_{10}$ of the ratio of abundance (or biomass) in 2018 and 2003. We used the probability of an effect (decrease or increase) to guide interpretation of these potential changes.

We used a Bayesian analytical framework to test for differences in coral cover and ecosystem functioning metrics (fish standing biomass, productivity, consumed biomass and turnover) between sampling years for the different reef zones. We implemented MCMC chains using the No-U-Turn sampler algorithm in the Stan language with the *rstanarm* interface to R (Goodrich *et al.* 2018; Stan Development Team 2018). The full procedures, priors and model specifications can be found in the Supplemental Methods, **Appendix E**.

Results

Between 2003/04 and 2018, live coral cover declined from 27.0% to 7.3% on the forereef slope (72% decline, high posterior density interval (HPD) = 61-82%) and from 41.6% to 5.7% on the reef crest (83% decline, HPD = 77-90%; **Figure 16**). There was no evidence of changing coral cover over the same time period in either the reef flat or back reef, with both HPDs including 1. The reef flat and back reef had low coral cover in 2003/04 and remained unchanged in 2018 (**Figure 16**). By contrast, turf cover increased substantially in the slope and crest (96% and 100% increase, respectively, HPD = 68-127% and 75-130%; **Figure 16**), but less so in the reef flat and back reef (18% and 29% increase, respectively, HPD = 8-25% and 13-45%; **Figure 16**). Turf cover had zone-specific minimum values of ~30% in 2003/04, but did not comprise less than 60% in any zone in 2018.

There was a clear spatial mismatch between coral cover decline and the response of fish assemblages. While coral loss was greatest in exposed forereef habitats, fish assemblage structure changed markedly across all reef zones (**Figure 17**). The direction of these changes was generally consistent among zones and was marked in terms of both abundance and biomass. Fish assemblages tended to move towards the origin of the abundance ordination, due in particular to family-level decreases in the Epinephelidae, Pomacanthidae and Chaetodontidae. A major shift towards positive MDS1 scores was largely driven by increases in Acanthuridae, Siganidae, Tripterygiidae and Pseudochromidae biomass.

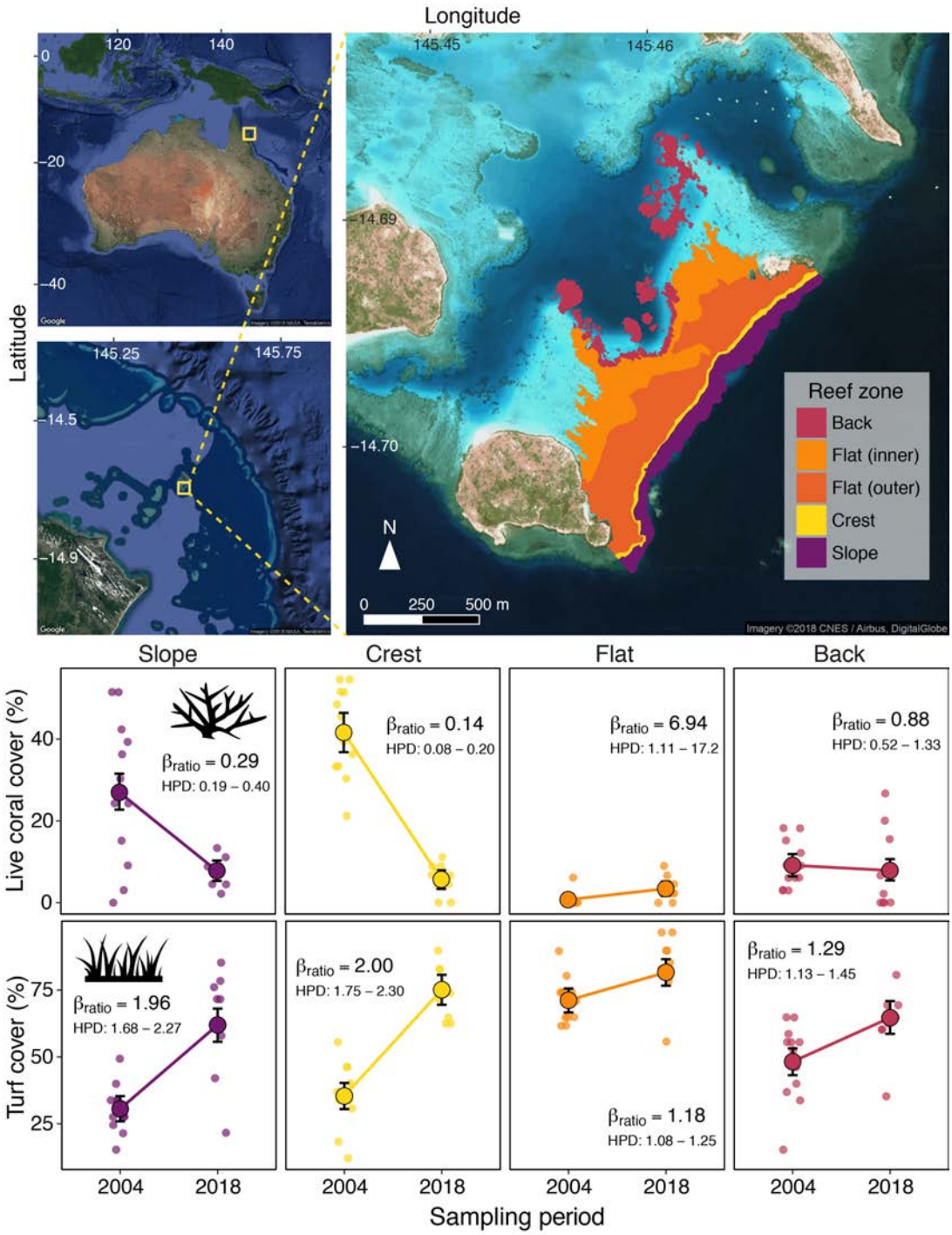

Figure 16: *The studied windward reef at Lizard Island, Great Barrier Reef. Coloured areas in the upper right panel represent the five mapped reef zones. Scatterplots show transect-level proportional live coral cover (upper panels) and turf cover (lower panels) in 2004 and 2018 (individual dots), model estimated median (larger dots) and 95% credibility interval (whiskers) for each reef zone. The inner and outer reef flats have been combined, together comprising the broader 'reef flat' zone.* β_{ratio} *is the ratio between the estimates in 2018 and 2004, HPD is the high posterior density interval of* β_{ratio}.

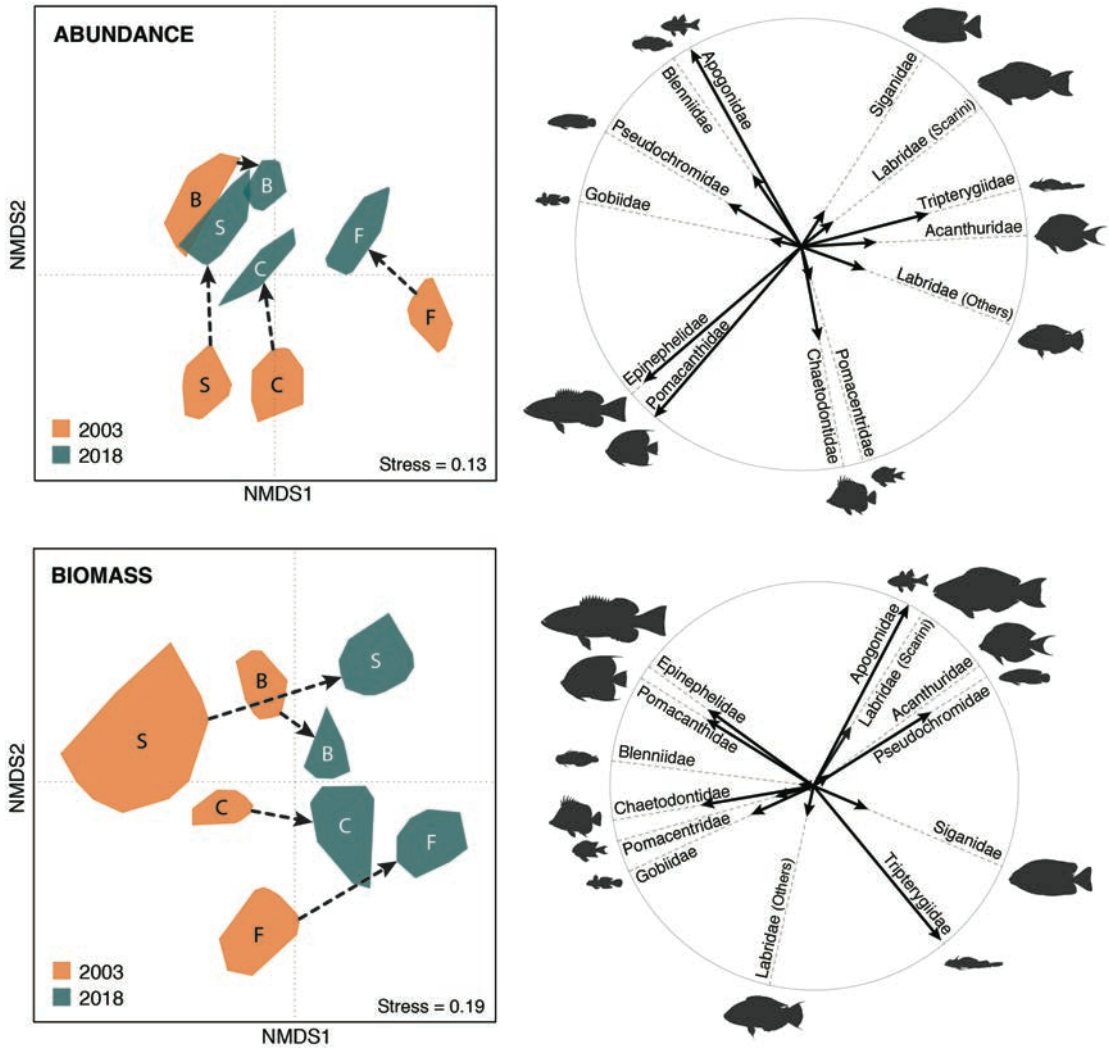

Figure 17: *Patterns in the abundance and biomass of reef fish families among reef zones at Lizard Island in 2003 and 2018. Polygons on the left panels represent the space occupied by 100 resampling iterations of the fish assemblages for each reef zone on each nMDS, while arrows link reef zones in 2003 and 2018. Right panels exhibit the family vectors. S = slope, C = crest, F = flat, B = back reef.*

Changes in fish families showed a degree of consistency among habitat zones (**Figures E1** and **E2**, **Appendix E**). When family-level changes were normalised by the area of each reef zone, it became clear that the changes observed on **Figure 17** were due to a combination of increases and decreases in the abundance and biomass of specific families (**Figure 18**). The Chaetodontidae declined in both abundance and biomass, while the Pomacanthidae and Acanthuridae declined in abundance, but not in biomass. By contrast, the Gobiidae and Blenniidae declined in biomass, but not in abundance, whereas

the Epinephelidae showed no clear reef-level change. However, most families increased in both abundance and biomass following coral loss. This includes mostly small-sized fishes, such the Apogonidae and Pseudochromidae, but also larger body-sized groups, such as the Siganidae and parrotfishes (Labridae, Scarini). The Pomacentridae increased in both abundance and biomass, although these increases were small in magnitude (**Figure 18**).

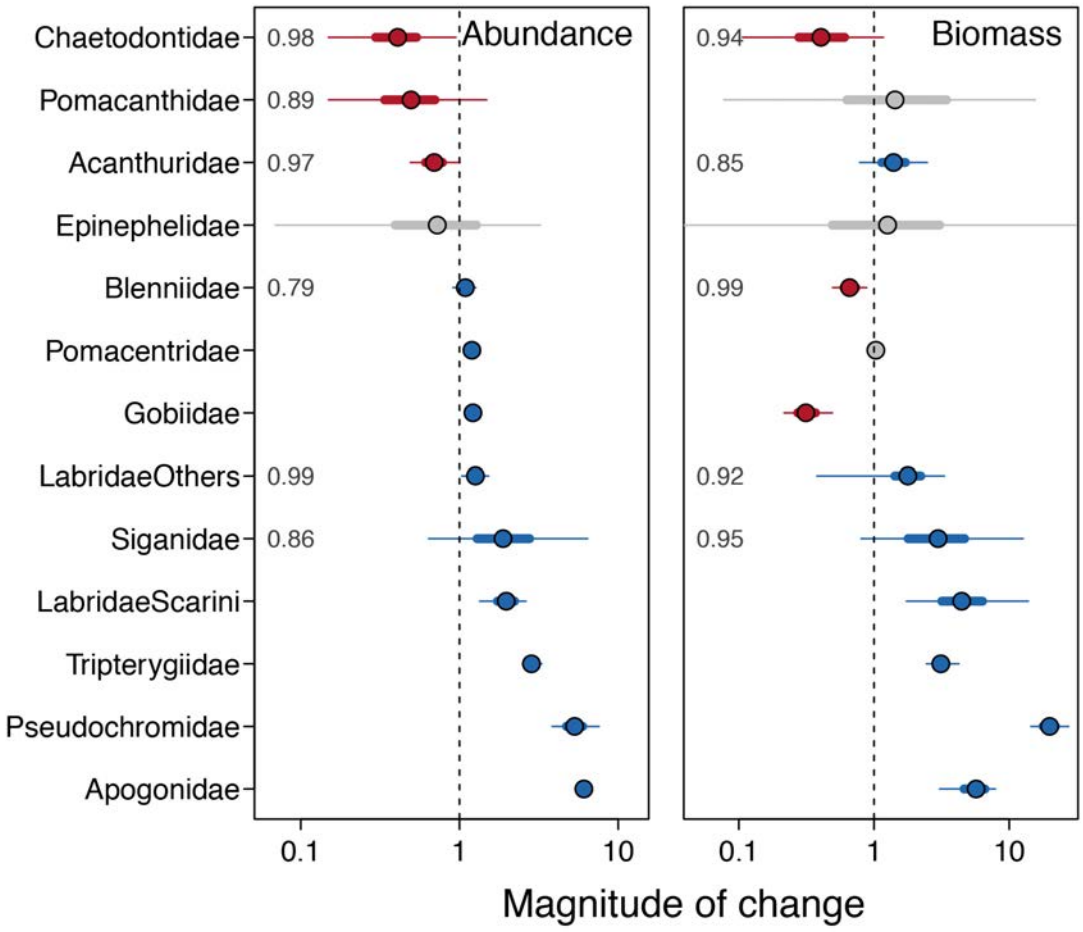

Figure 18: *Magnitude of change in the abundance and biomass of fish families on the studied windward reef at Lizard Island between 2003 and 2018. Circles represent medians across resampling iterations, wide bars the interquartile range, and whiskers the 95% quantile range. Colours are proportional to the probability of an effect: grey = < 70% probability of change; red > 70% probability of a decline; and blue > 70% probability of an increase. Numbers are the probabilities for all families with > 70% and < 100% probability (100% probabilities omitted).*

Evaluating these reef-scale fish assemblage changes from an energetic standpoint revealed that total standing biomass and productivity increased by 71% (HPD = 64-77%) and 41% (HPD = 39-42%), respectively, while consumed biomass increased about 37% (HPD = 35-38%) (**Figure 19**A,B,C). This increase in standing biomass was driven by increases in parrotfishes, which were ranked fourth overall in 2003 and became second in 2018 (**Figure E3**, **Appendix E**), but also by surgeonfishes and rabbitfishes. These three families had higher abundance of moderately large individuals (100-1000g of body mass) and a lower abundance of relatively small individuals (with 10-100g) in 2018 compared to 2003 (**Figure E4**, **Appendix E**). The increase in productivity in 2018 was mainly driven by surgeonfishes, parrotfishes and cardinalfishes and, to a lesser degree, rabbitfishes (**Figure E3**, **Appendix E**). Consumed biomass showed similar family-level changes to productivity (**Figure E3**, **Appendix E**).

By contrast, the total turnover of this reef fish assemblage diminished by 19% (HPD = 17-21%) between 2003/04 and 2018 (**Figure 19**D). This happened irrespective of increased total abundance (from 1275 to 1817 individuals per $100m^2$), and of increased turnover in some small body-sized fish families (**Figure E3**, **Appendix E**). A closer look at the size structure of the fish assemblage in the two survey periods reveals that changes in biomass, productivity and consumed biomass followed similar size-related patterns (**Figure E5**, **Appendix E**). These three metrics clearly increased in the smallest sizes (from 0.1 to 1g), and in moderately large sizes (~1000g, **Figure E5**, **Appendix E**). By contrast, the three showed similar values or even a small decline in the median size range (10-100g) and very high variability in the largest sizes (>1000g).

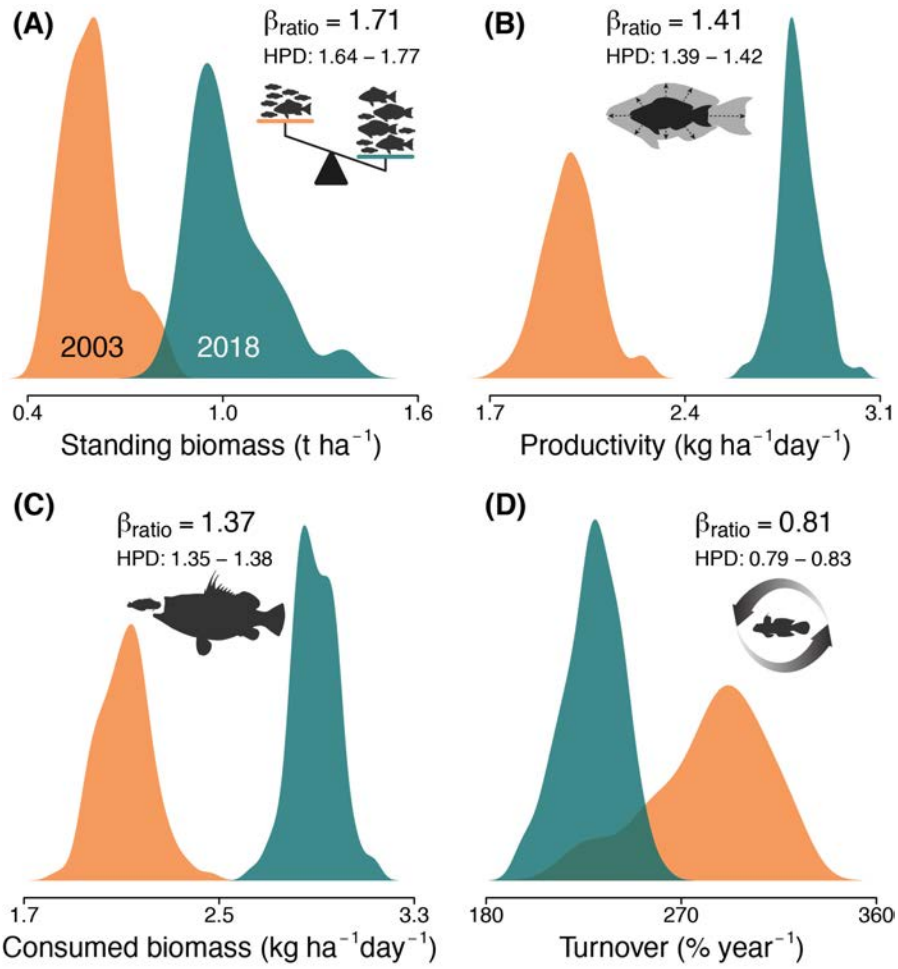

Figure 19: *Differences in standing biomass* ***(A)****, productivity* ***(B)****, consumed biomass* ***(C)*** *and total turnover* ***(D)*** *of 13 reef fish families on a windward reef at Lizard Island between 2003 and 2018. Density curves are based on bootstrapped fish assemblages for each sampling year over 500 iterations.* β_{ratio} *is the ratio between the estimates in 2018 and 2003, HPD is the high posterior density interval of* β_{ratio}.

Produced and consumed biomass increased at similar rates from 2003/04 to 2018 in this fish assemblage (41% for produced and 37% for consumed biomass, **Figure 19** and **Figure 20**). Consequently, there was only a small shift in the instant biomass change, i.e. the ratio of consumed to produced biomass, of this assemblage in 2018 to about 96% relative to its value in 2003 (HPD = 96-97%). In both cases, the total consumed biomass slightly exceeded the amount of produced biomass (change > 1, **Figure 20**), and thus the magnitude of the instant biomass change was similar in both periods.

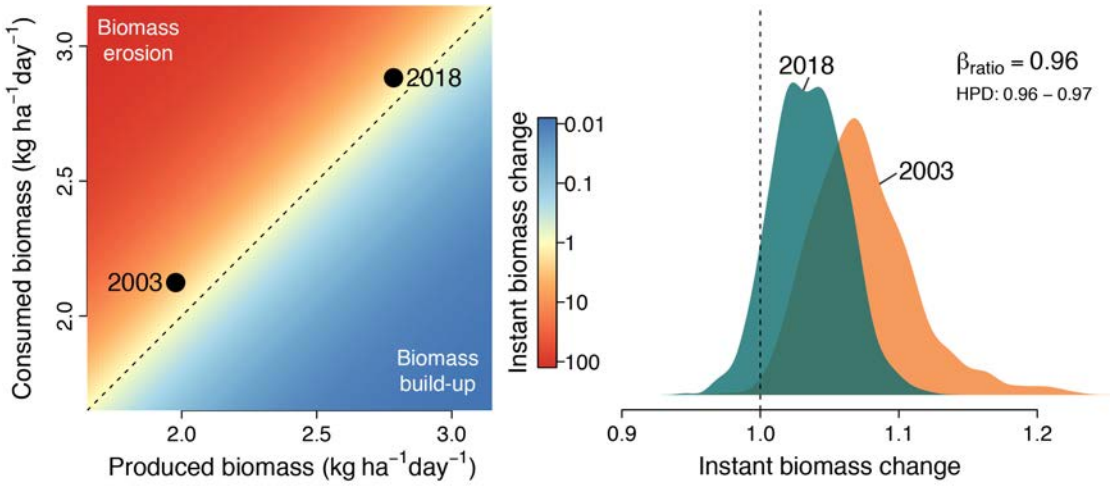

Figure 20: *The relationship between consumed and produced biomass on a windward coral reef at Lizard Island, northern GBR. The instant biomass change is the ratio of biomass consumption to production, with values > 1 meaning biomass erosion, and values < 1 meaning biomass accumulation.* β_{ratio} *is the ratio between the instant biomass change estimates in 2018 and 2003/04, and HPD is the high posterior density interval of* β_{ratio}.

Discussion

While the responses of coral reef fishes to coral reef degradation have attracted considerable attention (reviewed in Pratchett et al., 2008, 2018), most research to date has focused on species and family-level responses and static aggregate metrics such as abundance, diversity and biomass. By estimating multiple dynamic metrics that portray consumer biomass production, a key component of ecosystem functioning, we reveal thus far overlooked ecosystem effects of coral loss that help explain previously documented assemblage responses. Most strikingly, coral loss was associated with substantial increases in total fish biomass, productivity and consumed biomass, but with decreased turnover. These findings imply a more productive but slower-paced reef fish assemblage following severe live coral loss.

Family-specific responses to coral degradation

Family-level responses were largely consistent with the literature. For example, chaetodontids exhibited the most extensive declines in abundance and biomass, a pattern repeatedly reported

previously (e.g. Cheal et al., 2017; Stuart-Smith et al., 2018; Wilson, Graham, & Pratchett, 2013). Similarly, although we did not observe a net decline of pomacentrids, most planktivorous damselfishes exhibited a strong decline on the reef crest (**Figure E6**, **Appendix E**) following an 86% coral loss in this zone. Such declines of planktivorous damselfishes are among the most widely reported responses of fishes after coral loss (Pratchett et al., 2008, 2018; Wilson et al., 2006), potentially due to their reliance on branching coral structures for refuge (Wilson, Burgess, et al., 2008; but see Wismer et al., 2019).

Positive responses were also consistent with previous studies, including increasing biomass of nominally herbivorous fishes (mainly Siganidae, Labridae – Scarini and Acanthuridae) (**Figure 17**). The vast majority of studies evaluating the responses of multiple coral reef fishes to coral degradation have found nominally herbivorous fishes to respond positively with increases in abundance and/or biomass (Adam et al., 2011; Ceccarelli et al., 2016; Cheal et al., 2017; Pratchett et al., 2008, 2018; Robinson, Wilson, Jennings, et al., 2019; Russ, Questel, Rizzari, & Alcala, 2015; Wilson et al., 2006). However, the families that displayed the strongest responses over the 15-year span of our study were small cryptobenthic reef fishes (sensu Brandl et al., 2018). Pseudochromids, tripterygiids and apogonids all displayed over ten-fold increase in abundance and/or biomass (**Figure 18**, **Figures E1** and **E2** in **Appendix E**), although the same pattern did not hold for gobies or blennies. Only one study has documented the response of cryptobenthic reef fishes to coral loss, likewise reporting increased abundance and a markedly different species composition following coral bleaching (Bellwood, Baird, et al., 2012; Bellwood et al., 2006). It is possible that, because of their short generation times (Depczynski & Bellwood, 2006), cryptobenthic fishes are more responsive to changes over medium-term timeframes than larger species.

Potential explanations for the observed energetic shifts

Our study, therefore, revealed responses of reef fishes to coral loss that reflect previous research, thus implying a typical assemblage-level response. The novelty of our findings, however, stems from an understanding of how these responses integrate with key elements of ecosystem function (Bellwood, Streit, et al., 2019; Brandl, Rasher, et al., 2019). The simultaneous increases in reef fish biomass,

productivity and consumed biomass, alongside a decrease in turnover, imply higher productivity but slower-paced energetic flow in the fish assemblage of this new low-coral cover reef state. Although our study was restricted to a single locality, our results have broader implications for coral reefs because many of the key components of change (e.g. increases of nominally-herbivorous fishes from the families Acanthuridae, Siganidae and Labridae - Scarini) are congruent with prior studies across the Indo-Pacific (see above).

Trophic models have suggested that reef fish productivity would follow a parabolic trajectory after coral loss (Rogers, Blanchard, & Mumby, 2018; Rogers, Blanchard, Newman, et al., 2018). Reduced live coral cover would initially trigger increased resource availability, favouring herbivores and invertivores; but the subsequent erosion of the reef structure would reduce the availability of predator refuges (Rogers, Blanchard, Newman, et al., 2018). In our study, despite extensive reduction in structural complexity (as indicated by severe loss of branching corals, Wismer et al., 2019), we found no evidence of declining fish productivity. Rather, our results seem to corroborate long-term catch data that reported maintained, but increasingly variable, reef fishery yields in coral-degraded reefs that underwent phase shifts to dominance of structurally-complex benthic macroalgae (Robinson, Wilson, Robinson, et al., 2019). However, no macroalgae-dominance shifts occurred in our site, suggesting that different mechanisms have underpinned this sustained productivity. Potential explanations for the observed ecosystem function responses in our study can be divided into two classes: 1) reduced resource limitation due to increased abundance, quality or accessibility of benthic resources; and 2) predator-release mechanisms, implying increased fish survivorship. These mechanisms are not mutually exclusive and may reinforce one another.

Nominally-herbivorous fishes have been hypothesised to be resource-limited on coral reefs (Carpenter, 1990; Hart, Klumpp, & Russ, 1996; Hart & Russ, 1996). Their major feeding substratum, algal turfs (Adam et al., 2018; Bellwood & Choat, 1990; Brandl & Bellwood, 2014), is an important colonist of dead coral skeletons and is likely to increase in abundance following coral mortality (e.g. Diaz-Pulido & McCook, 2002). Increased resource availability has been assumed to cause the strong correlation found between changes in coral and turf cover, and the abundance of nominally-herbivorous fishes (Adam et al., 2011; Hart et al., 1996; Hart & Russ, 1996; Russ et al., 2015). Indeed, in our study,

we detected algal turf cover increases of 18-100%, depending on the reef zone, from an estimated cover of 32-70% during 2003/04 to 64-83% in 2018. Although some of this turf increase can be due to 'canopy-effects' from previously undetected turfs underneath structurally-complex corals (Goatley & Bellwood, 2011), increased energy yield of algal turfs to herbivores after coral loss is possible, even if turf abundance remains unchanged, if their accessibility or nutritional quality have improved. Increased accessibility can occur if larger herbivores become able to exploit algal turfs previously underneath branching corals (i.e., due to size constraints, Bennett, Vergés, & Bellwood, 2010; Steneck, Arnold, & Mumby, 2014) or vigorously defended by territorial damselfishes and surgeonfishes (Choat & Bellwood, 1985; Robertson & Polunin, 1981). Although territorial damselfishes, in particular, have been observed to decline following storm-induced coral loss (Ceccarelli et al., 2016; Emslie et al., 2012), these fishes were scarce in the forereef zones of our reef even before coral loss and showed no clear declining trend (**Figure E6**, **Appendix E**).

Improved nutritional quality of algal turfs, can arise though multiple mechanisms. For example, increased light irradiance from reduced coral canopy overshading or reduced sediment loads due to changes in water movements can result in more productive turfs (Carpenter, 1985; Goatley & Bellwood, 2013; Tebbett, Bellwood, & Purcell, 2018). Additionally, other nutritious components of the epilithic algal matrix can be boosted under these circumstances (Clements, German, Piché, Tribollet, & Choat, 2017; Kramer, Bellwood, & Bellwood, 2013). Increases in turf abundance, accessibility, or nutritional quality, in isolation or combination, could provide a causal explanation for the strong herbivore effect observed in our productivity metrics.

Finally, reduced predation could, in theory, contribute to the observed biomass and productivity increases through enhanced survivorship of juveniles settling from the pelagic realm or of adults migrating to forereef areas. It is unlikely that settlers would face decreased predation because of the substantial increases in the abundance of key mesopredators of juvenile reef fishes, such as labrids and pseudochromids (e.g. Connell, 1998; Goatley, González-Cabello, & Bellwood, 2017). However, large juveniles or adult reef fishes migrating to the area could face decreased predation risk from ambush predators that benefit from tabular coral structures for hunting (e.g. epinephelids such as *Plectropomus leopardus*, Kerry & Bellwood, 2012; Samoilys, 1997). Support for this hypothesis is limited. Although

there was a trend of decreasing epinephelid abundance in the exposed forereef habitats (72% chance of a negative effect in the slope and crest, Figure S1), we did not detect clear reef-level responses of epinephelids to coral loss.

Temporal-stability and implications of energetic shifts for ecosystem functioning

Our findings suggest that cumulative coral loss can drive energetic shifts on coral reefs toward biomass accumulation. However, we did not detect a clear and consistent shift in the energetic balance (i.e. produced minus consumed biomass) of these fish assemblages between 2003/04 and 2018, mainly because productivity and consumed biomass increased at similar rates (41% and 37% respectively). Nevertheless, the 71% increase in standing biomass during this period requires some mechanism of biomass accumulation. Two explanations appear plausible: either our two snapshot assessments obscured shifts in the balance between consumed and produced biomass that happened in between sampling periods, or the very small shift towards biomass accumulation (4%, depicted in **Figure 20**) was sufficient over the 15-year time period to generate the observed biomass build-up. As noted above, the elements underpinning the observed energetic shift (i.e. increasing abundance and biomass of herbivores) are shared with other coral reefs, suggesting this may become a common feature of degraded coral reef systems. But what are the potential ecosystem consequences of the observed energetic shifts?

Superficially, the observed biomass accumulation may seem like a positive outcome of coral loss from a human perspective. The increase in fish productivity on our reef reinforces observations of stable reef fish catches after coral loss (Robinson, Wilson, Robinson, et al., 2019), and suggests that the livelihoods of people that rely on food production on degraded coral reefs could be maintained. However, this superficial analysis conceals an important implication of another key finding of the present study: that the turnover of the fish assemblage decreased substantially despite the increased biomass and productivity.

On coral reefs, turnover has been shown to be dominated by small, fast-lived cryptobenthic reef fishes (Brandl, Tornabene, et al., 2019; Depczynski & Bellwood, 2006; Depczynski et al., 2007) suggesting declines in this group could provide a primary driver for assemblage turnover. However, we observed increases in most families of cryptobenthic reef fishes including the highly abundant gobies

(**Figure E3**, **Appendix E**). By contrast, we found evidence for reductions in the turnover of larger fish families (e.g. Labridae, Acanthuridae). Thus, it appears that the decline in turnover is due to a disproportional increase in the biomass relative to productivity or consumed biomass, for larger reef fishes. This is supported by a shift in the size structure of the three main nominally-herbivorous fish families from 2003/04 to 2018 (**Figures E4** and **E7, Appendix E**) that was not associated with an increase in overall abundance (see **Figure E3**, **Appendix E**). This size shift involved reduced biomass in small sizes (5-50g) and increased in moderately large sizes (> 500g) for Acanthuridae and Labridae – Scarini, although these were less marked for the Siganidae (**Figures E4** and **E7, Appendix E**).

Decreased turnover, thus, indicates that the system is currently unable to replace biomass at the same rates as new biomass is generated. This suggests that, regardless of what mechanism underpinned the observed biomass accumulation, the enhanced productivity might be due to storage effects from the somatic growth of individuals previously present (e.g. Hart et al., 1996; Russ et al., 2015). The somatic growth of individual herbivorous fishes has recently been found to increase after acute coral loss (Taylor et al., 2019), further providing support for the role of storage effects in the enhanced productivity. Similar dynamics involving an initial increase of herbivore biomass following abrupt coral loss have been found to result in population crashes after recovery of coral cover (e.g. Gilmour et al., 2013; Russ et al., 2015). Even in the absence of coral recovery, sustained herbivore productivity would theoretically require sustained recruitment. However, so far, the recruitment dynamics of fishes on degraded coral reefs remain largely unknown. Finally, although our results are not entirely consistent with previous models forecasting declining fish productivity after the erosion of structural complexity (e.g. due to refuge loss, Pratchett *et al.* 2018; Rogers, Blanchard & Mumby 2018), it is not impossible that a low complexity threshold exists, which was not reached in our study. In this scenario, if complexity continues to decline past this 'refuge-threshold', fish populations would crash, and productivity would be bound to decline. Altogether, our findings warrant caution in interpreting the newly amassed biomass as temporally stable over extended timescales, especially where harvesting occurs.

Conclusion

Overall, our ecosystem-based functional evaluation of a coral reef fish assemblage after 15 years of cumulative coral loss provides evidence for nuanced but important shifts in the energetic pathways that underpin reef fish assemblages. Measuring, modelling or estimating functional attributes is gaining momentum in coral reef ecology, and can reveal key insights into the components that make or break these diverse marine ecosystems (Longo, Hay, Ferreira, & Floeter, 2019; McWilliam, Chase, & Hoogenboom, 2018; Morais & Bellwood, 2019; Ruttenberg, Adam, Duran, & Burkepile, 2019; Streit, Cumming, & Bellwood, 2019; Tebbett et al., 2020). Our findings further underscore the utility of this approach and emphasize the need to investigate multiple metrics of ecosystem functioning simultaneously to reveal the complexity of functional shifts that can occur after major ecosystem shocks (Brandl, Rasher, et al., 2019). For example, considering only standing biomass and productivity would not in itself reveal the full extent of the altered demographic dynamics unveiled by examining the turnover of this reef fish assemblage. Our results provide evidence that coral reefs facing extensive and cumulative coral loss likely undertake a number of energetic shifts. Furthermore, they suggest that, although some of these changes might be initially perceived as positive, their temporal stability is questionable.

Chapter 6: Human exploitation and productivity-biomass relationships on coral reefs

Published as: Morais, R.A., Connolly, S.R., & Bellwood, D.R. (2020) Human exploitation shapes productivity-biomass relationships on coral reefs. *Global Change Biology, 26(3),* 1295–1305.

Introduction

Understanding the relationship between human harvesting of coral reef resources and resource availability is challenging. Of all indicators used to explore this relationship, fish standing biomass is one of the most widely and successfully employed (Cinner et al., 2018; Nash & Graham, 2016). Standing biomass is conveniently estimated from field data, such as underwater counts of fishes. Further, it responds negatively to multiple proxies of human impacts, such as human population density (Bellwood, Hoey, & Hughes, 2012; Dulvy et al., 2004), distance from markets (Cinner, Graham, Huchery, & Macneil, 2013; Robinson et al., 2017), accessibility (Cinner et al., 2018; Maire et al., 2016) and fishing effort (Jennings & Lock, 1996; Jennings & Polunin, 1996). Standing biomass has also been linked to multiple ecosystem processes, and is often used as a measure of ecosystem functioning and resource production (Bellwood, Hoey, et al., 2012; Duffy et al., 2016; Graham et al., 2015; Mora et al., 2011; M. I. O'Connor et al., 2017). Standing biomass is, above all, an intuitive representation of resource availability: more biomass equals to more fish.

However, standing biomass is a static measure that results from production accumulated over an unknown time frame, whereas resource productivity is a rate associated to how energy or material flow within a system (A. P. Allen & Gillooly, 2009; Jenkins, 2015; Odum & Odum, 1959). Although critical, the relationship between community-level resource productivity and standing stock biomass has rarely been explicitly tested (Jenkins, 2015). For instance, theory predicts that community biomass should not scale proportionally to its underlying rates (e.g. biomass production). Instead of constant, the ratio between productivity and biomass (i.e. biomass turnover) is predicted to scale with body mass at an exponent of -0.25 (A. P. Allen & Gillooly, 2009; Brown et al., 2004; Jennings & Mackinson, 2003; Trebilco et al., 2013). In essence, this means that more biomass per unit productivity is expected as

standing biomass increases. This non-proportionality between community standing biomass and production rates has been observed in empirical data from several terrestrial and aquatic systems (Jenkins, 2015), but remains under-investigated for coral reefs.

Large-scale assessments of coral reef fish assemblages have repeatedly demonstrated depleted biomass in locations with large human populations or easy access (e.g. Cinner et al., 2018; Edgar et al., 2014; Maire et al., 2016; Mora et al., 2011; I. D. Williams et al., 2015). However, even biomass-depleted coral reef fish assemblages can still support socially significant harvesting (Condy et al., 2015; Newton et al., 2007). Human adaptability may help to explain this ongoing food provisioning despite biomass depletion (e.g. use of destructive fishing or exploiting previously ignored grounds or stocks, Berkes et al., 2006; Pauly et al., 2002; Pauly & Zeller, 2014). However, compensatory ecological mechanisms permitting the coexistence of low coral reef fish biomass and relatively high somatic productivity may also be involved. Compensatory dynamics are at the heart of fisheries theory, which considers that fishing mortality drives standing biomass below the carrying capacity and, in doing so, stimulate increased 'surplus' productivity (Beverton & Holt, 1957; Hilborn & Walters, 1992; Schnute & Richards, 2002). These compensatory ecological mechanisms, however, have not commonly been investigated on reef systems, potentially due to logistic constraints and methodological challenges in quantifying coral reef fish productivity and parameterizing multispecies surplus production models (Appeldoorn, 1996; Hollowed et al., 2000). When biomass and fisheries yields were independently estimated and correlated with fishing intensity on coral reefs, diverging relationships were observed (Jennings & Polunin, 1996). Thus, it is possible that human exploitation affects large-scale patterns of coral reef productivity and biomass, yet this hypothesis remains untested.

Here, we base on a recent framework for generating fisheries-independent estimates of fish productivity (**Chapter 3**; Brandl, Tornabene, et al., 2019; Morais & Bellwood, 2019), to evaluate if standing biomass can reliably predict the productivity of coral reef fishes. Specifically, we test whether standing biomass and productivity co-vary proportionally across a large spatial scale dataset spanning 15,000 km from the Western Indian Ocean to the Central Pacific. We first focus on a heavily targeted reef fish group, parrotfishes (Hamilton et al., 2016; Taylor, Lindfield, & Choat, 2015), from uninhabited and near-pristine, to densely populated and highly-exploited locations. We then evaluate the impacts of

human exploitation on the biomass and productivity of coral reef fish assemblages using a model that integrates size-spectrum theory, somatic growth trajectories, and stochastic simulations. Finally, we test predictions from this model by using high-definition datasets of entire coral reef fish assemblages from two of the world's most diverse marine regions, the Coral Triangle and the Great Barrier Reef.

Materials and Methods

Individual body mass and growth, assemblage biomass and production

Standing biomass and biomass production are obtained from fish assemblage data, e.g. underwater surveys, and geometric and life-history traits. The body mass M_i of individual fish i can be obtained from its length, L_i, through:

$$M_i = a_i({L_i}^{b_i}) \tag{12}$$

where a_i and b_i are species-specific power-law parameters with geometric properties, often referred to as length-weight parameters (Froese, 2006). The cumulative sum of n individual fish masses in an assemblage, i.e. the total biomass of the assemblage, can be obtained by:

$$B = \sum_{i=1}^{n} M_i \tag{13}$$

The expected growth, in mass units, of each individual i over a period of m days is obtained from equation (12) by using L_{t_i}, the length of the fish at time t (e.g. at the time of the survey), and L_{t+m_i}, its length after m days. L_{t+m_i} can be calculated in the context of the Von Bertalanffy Growth Model (VBGM, e.g. **Chapters 2, 3**). VBGM coefficients K and L_∞ are highly correlated on the log-scale (Chapter 2; Morais & Bellwood, 2018b; Pauly, 1998), and can be standardised on a single parameter, K_{max}, following the procedures described in **Chapter 2**. The size of individual i in time $t + m$, L_{t+m_i}, is given by the function:

$$L_{t+m_i} = L_{max_i}\left(1 - e^{-K_{max_i}(a_{t+m_i} - a_{0_i})}\right) \tag{14}$$

where L_{max_i} is the maximum species size for individual i; a_{t+m_i} is its age, in years, at time $t + m$; and a_{0_i} is its theoretical age at size = 0 (t_0 in the VBGM). We estimated a_{0_i} from the regression model provided by Pauly (1980) and rescaled the output values between the maximum value obtained and a minimum value of -0.5 to avoid unrealistically low values of a_0 for coral reef fishes (Choat & Robertson, 2002; Grandcourt, 2002). The age of individual i at time $t + m$ (Depczynski et al., 2007) can be estimated from:

$$a_{t+m_i} = \left(\frac{1}{K_{max_i}}\right)\ln\left\{\frac{\left(L_{max_i} - L_{0_i}\right)}{\left[\left(1 - \left(\frac{L_{t_i}}{L_{max_i}}\right)\right)L_{max_i}\right]}\right\} + \left(\frac{m}{365}\right) \tag{15}$$

where L_{t_i} is the size of a fish at time t; and L_{0_i} is its theoretical length at time $t = 0$, calculated by:

$$L_{0_i} = L_{max_i}\left(1 - e^{K_{max_i} a_{0_i}}\right) \tag{16}$$

The total growth in mass units of each individual over m days is thus:

$$G_{m_i} = M_{t+m_i} - M_{t_i} = \left[a_i\left({L_{t+m_i}}^{b_i}\right)\right] - \left[a_i\left({L_{t_i}}^{b_i}\right)\right] \tag{17}$$

and the assemblage-level total biomass production over m days is given by:

$$P = \sum_{i=1}^{n} G_{m_i} \tag{18}$$

Empirical productivity-biomass relationships

We evaluated whether standing biomass can predict the productivity of fish assemblages using a dataset of parrotfishes (Labridae, Scarini) comprising 313 transect counts in 19 locations and 10 regions across the Indo-Pacific realm (**Figure 21**, **Table F5** in the **Appendix F**). At each location, four coral reef habitat zones were surveyed: back, flat, crest and slope, with 4.3 ± 0.8 transects per habitat (mean ± SD). We used Bayesian length-weight parameters (Froese & Pauly, 2018; Froese et al., 2014) and von Bertalanffy Growth Model (VBGM) coefficients to estimate total parrotfish standing biomass (kg m^{-2}) and biomass productivity (g m^{-2} day^{-1}) per transect across our study regions following the procedures described on **Chapters 3** and **4**. We then aggregated both biomass and productivity at each region by averaging among transects.

We tested for productivity-biomass relationships in parrotfish assemblages among and within regions using Generalized Linear Models (GLM), with gamma and Gaussian error distributions, respectively (**Appendix F**). Within-regions, productivity was modelled as a function of region and reef habitat, in addition to biomass, following a model selection procedure that evaluated alternative candidate models (**Appendix F**). Hence, the final model had the form of:

$$\log P_{i,h,r} = (\log \alpha_0 + \log \alpha_h + \log \alpha_r) + (\beta_0 + \beta_r) \log B_{i,h,r} + \varepsilon_{i,h,r} \quad (19)$$

where log denotes $\log_{10}$-transformation, $P_{i,h,r}$ is the total productivity of transect i in habitat h of region r; α_0 is a fixed intercept for all samples, α_h is an intercept for each reef habitat, and α_r is an intercept for each region; β_0 is a fixed slope for all samples, β_r is a slope for each region, $B_{i,h,r}$ is the total standing biomass of transect i in habitat h of region r; and $\varepsilon_{i,h,r}$ is the unexplained residual variation of each transect.

We then evaluated if human population density could explain regional-level patterns in parrotfish biomass, body length and productivity using GLMs with gamma (biomass and productivity) and Gaussian (body length) error distributions. Detailed methods can be found in the **Appendix F**, including the procedures for obtaining human population density data.

Modelling a coral reef fish assemblage and simulating coral reef fisheries impacts

To further explore potential mechanisms relating productivity-biomass relationships with human population density, we developed a modelling framework to simulate size-selective fishing. We started by using size-spectrum theory to derive theoretical expectations on the size structure of fish assemblages in our model (Andersen & Beyer, 2006; Edwards, Robinson, Plank, Baum, & Blanchard, 2017; Jennings & Dulvy, 2005). Size-spectrum expectations have been shown to accurately reflect the empirical size structure of coral reef fish assemblages (Dulvy et al., 2004; Graham, Dulvy, Jennings, & Polunin, 2005; Robinson et al., 2017; Wilson et al., 2010). Thus, we used the principles laid out by Edwards et al. (2017) to guide our model building. Assemblage size distributions were characterized by a power-law distribution bounded by a minimum and a maximum size (Edwards et al., 2017), which we constrained to be between 5 cm total length (TL) and 100 cm TL. The procedures and parameter values employed to define the size-spectra, as well as to obtain length-weight parameters and to estimate VBGM parameters are described in detail in the **Appendix F**.

The next step was to simulate exploitation of our modelled fish assemblages, i.e. coral reef fisheries. We did so by simulating the effect of different capture levels using a size-dependent fishing probability function (**Appendix F**). We defined an arbitrary threshold species maximum size, 20 cm TL (total length), for a fish species to be considered as "fishable" or target for fisheries. Thus, any individuals from species capable of attaining 20 cm TL or more, were considered as targeted. We formulated a size-dependent fishing function to describe how the probability of being captured varied with individual body size for those fishes that satisfied the species target-size criterion above. This fishing function took the form of a mixed Power and Gompertz curve (**Appendix F**). We then simulated fishing impacts by randomly withdrawing a proportion of the target individuals in our assemblage with a probability vector given by the size-dependent fishing probability function (**Appendix F**). Fishing simulations were independently repeated for incremental capture rates (200 iterations for each capture level), up to a previously defined maximum capture rate that resulted in biomass depletion. The procedures and parameter values employed to define the fishing function, incremental capture rates, and to execute fishing simulations are described in detail in the **Appendix F**.

Simulating the impact of coral reef fisheries on empirical fish assemblages

To understand if the observed 'buffering productivity' (see Results) can arise from the size-selective exploitation of empirical coral reef fish assemblages, we used two high-resolution datasets from the Great Barrier Reef (Lizard Island) and the Coral Triangle (Raja Ampat, Indonesia). In both locations, surveys were undertaken primarily within no-take zones of Marine Protected Areas (in the Great Barrier Reef Marine Park and the Misool Private Marine Reserve, respectively). Apart from limited poaching, there is virtually no fishing extraction in both locations, making them ideal for simulating the effects of fishing on reef fish assemblages. We first asked if the same responses of productivity and biomass to overexploitation in the model simulations could be generated by simulating fishing using these empirical datasets. Then, we evaluated features of the initial assemblage size structure likely to affect the shape and intensity of these responses.

The Great Barrier Reef (GBR) dataset encompassed fish counts from Lizard Island, northern GBR (from **Chapter 4**), distributed between the outer slope, crest, flat and back reef. The Coral Triangle dataset was collected in the southern Raja Ampat, Indonesia, and encompassed counts from the crest/slope of fringing reefs (**Appendix F**). These datasets were filtered to include the same size range encompassed by our modelled assemblages (individuals with 5-100 cm TL, with $L_{max} \geq 6\ cm$). Bayesian length-weight parameters and VBGM coefficients were obtained for each species using the procedures and methods used for parrotfish dataset (see **Appendix F**).

We also carried out two sets of fishing simulations using the whole fish assemblage datasets from the GBR and Coral Triangle. First, to evaluate if decoupled responses from productivity and biomass to widespread exploitation occurred at the regional scale, we combined samples within each dataset into one large assemblage, and then simulated fishing on each of these regional assemblages. Second, to compare buffering responses between modelled and empirical fish assemblage submitted to increased local exploitation, we simulated fishing on each of the transect-level fish assemblages. In both cases, the target assemblages were subjected to iterated fishing over a range of capture rates following procedures similar to the modelled assemblages and described in the **Appendix F**.

Comparing modelled and empirical buffering responses to exploitation

We used the transect-level set of fishing simulations above to compare features of buffering responses to fishing between empirical and modelled fish assemblages. Specifically, we examined the extent of peak 'buffering productivity', i.e. the maximum average 'buffering productivity' over iterated fishing simulations (see Results and **Appendix F**), triggered by different size structures of the target component of unfished assemblages. We used four size structure indicators of unfished assemblages as potential predictors of peak buffering responses: the size spectrum exponent, mean individual body size, mean individual growth and biomass turnover rates of unfished assemblages as indicators of size structure (**Appendix F**). Due to extensive collinearity among variables, peak buffering productivity from empirical assemblages was modelled separately by each size structure indicator using Generalized Additive Models (GAMs, **Appendix F**) with the form:

$$PeBuf_i = \alpha_0 + f(V_i) + \varepsilon_i \quad (20)$$

where $PeBuf_{si}$ is the peak buffering productivity for transect i; α_0 is a fixed intercept for all samples; $f(V_i)$ is the spline function applied to each of the size structure indicators V_i listed above; and ε_i is the unexplained residual variation of each transect.

For the modelled assemblages, we simply varied the initial size spectrum exponent over the same interval observed in the empirical assemblages and plotted the peak buffering response against each of the four indicators above. Empirical- and modelled-peak buffering productivity responses to each indicator were compared visually (**Appendix F**).

Results

Across the Indo-Pacific, average parrotfish standing biomass ranged from 73 kg ha^{-1} to 406 kg ha^{-1}, while average productivity varied from 217 to 615 g ha^{-1} day^{-1}. However, this variation in productivity did not mirror spatial patterns in standing biomass (**Figure 21**, **Figure F1** in the **Appendix**

F). Regions with low biomass encompassed as much, or even more, variability in productivity than in high biomass regions. Indeed, the highest productivity values were in regions with some of the lowest biomass. As a result, standing biomass was a poor predictor of large-scale productivity variation in parrotfishes, with an estimated slope that was very close to, and did not differ significantly from, zero (**Figure 22**, **Figure F2** in the **Appendix F**).

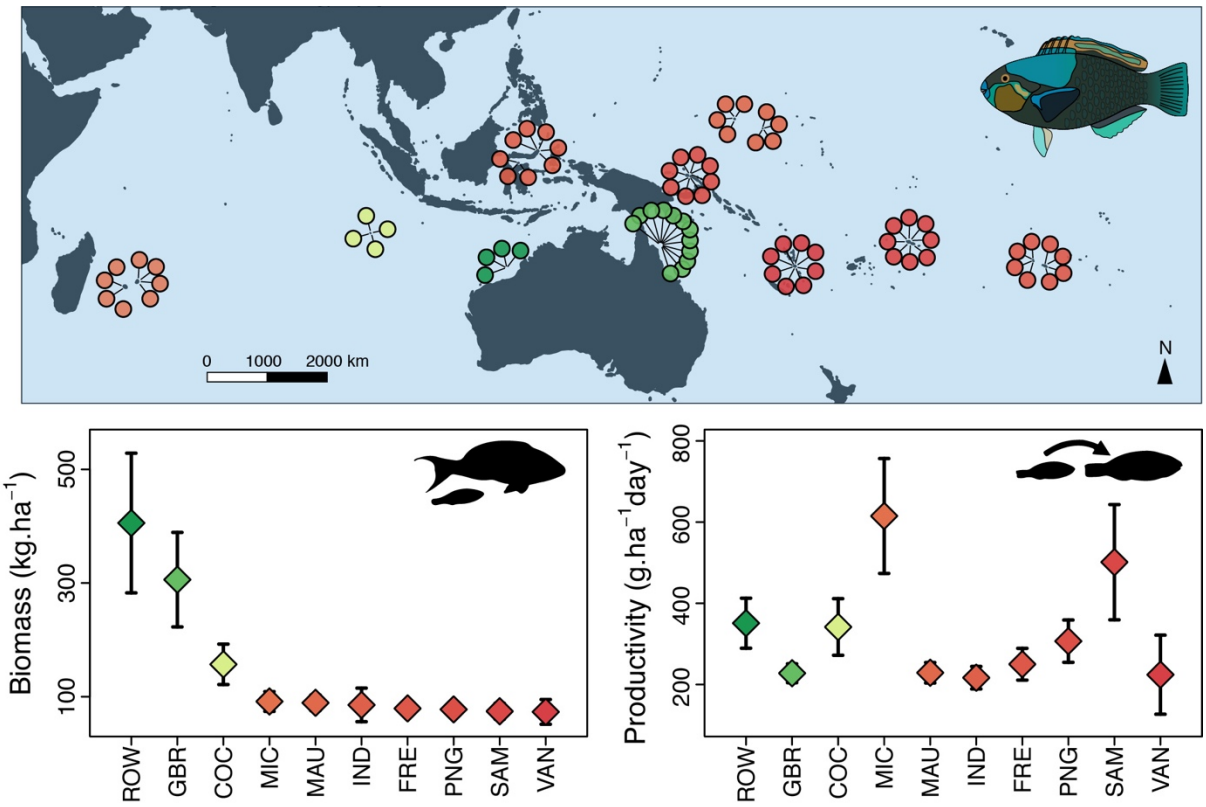

Figure 21: *The mismatch between biomass and productivity in parrotfish assemblages across the Indo-Pacific. Colours on the map and panels and are proportional to the regional-level average biomass (lower-left panel). Error bars represent the standard error of the mean. Individual sample points can be viewed on Figure F1. ROW = Rowley Shoals; GBR = Great Barrier Reef; COC = Cocos (Keeling) Islands; MIC = Micronesia; MAU = Mauritius; IND = Indonesia; FRE = French Polynesia; PNG = Papua New Guinea; SAM = Samoa; VAN = Vanuatu.*

Focusing on the relationship between productivity and standing biomass at the local scale revealed substantially different relationships (**Figure 22**, **Figure F3** in the **Appendix F**). Productivity and biomass were positively associated among transects, but the magnitude of this relationship exhibited considerable variation among regions that were explained neither by habitat nor by

biogeography (**Tables F1** and **F2** in the **Appendix F**). Instead, strength of the local biomass-productivity relationship was strongly correlated with regional average standing biomass (**Tables F1** and **F2**; **Figure 22**, **Figure F3**). In particular, low-biomass regions had steeper local productivity-biomass relationships compared to high biomass regions (**Figure 22**; **Table F2**). These steeper slopes in the productivity-biomass relationships are linked to, and probably caused by, reduced average body sizes in low biomass regions (**Figure 23**A). Hence, parrotfish assemblages with predominantly smaller individuals had increased productivity per unit biomass, i.e. higher biomass turnover (**Figure 23**A).

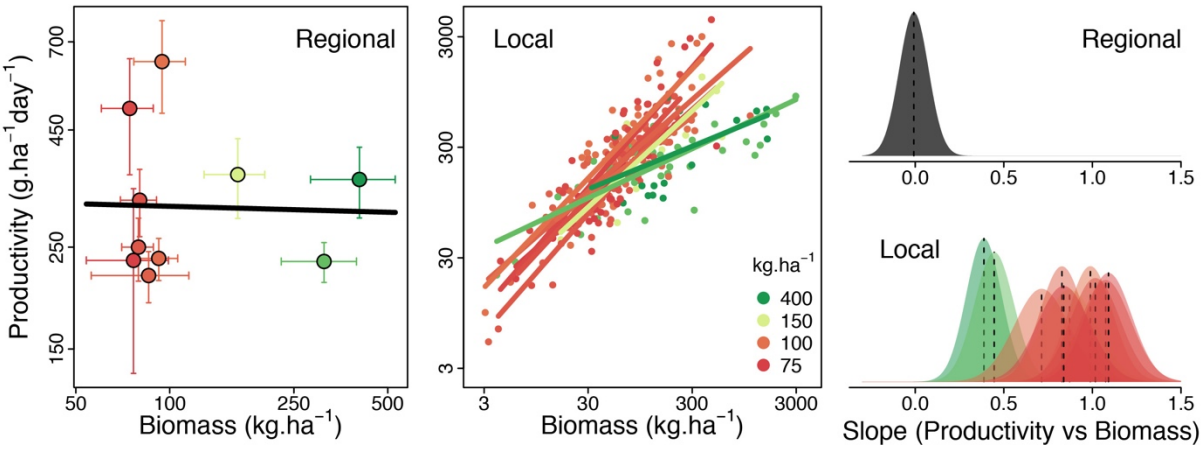

Figure 22: *Regional and local productivity-biomass relationships for parrotfishes exhibit remarkably distinctive scaling. Whereas there is no clear association between productivity and biomass at the regional scale (slope does not differ from zero, left and top-right panels, see also* ***Figure F2*** *in the* ***Appendix F****), relationships at the local scale are all positive and vary according to the regional average standing biomass (mid and bottom-right panels). Low biomass regions (red tones) display steeper slopes compared to high biomass regions (green colours). Error bars (left panel) represent the standard error of the means. Density curves are normal distributions of the model coefficients (slope) from log-scale relationships, with the dashed line indicating the model estimate (****Figure F2****,* ***Table F2*** *in the* ***Appendix F****).*

We observed a strong negative relationship between human population density and both parrotfish biomass and average body length, but not productivity (**Figure 23**B, **Table F3** in the **Appendix F**). Productivity was independent of human population, at least in the range of human population densities examined herein. This indicated that biomass-depleted parrotfish assemblages

underwent size structure changes that culminated in increased turnover rates. Increased turnover, in turn, partially offsets the exploitation-induced productivity depletion.

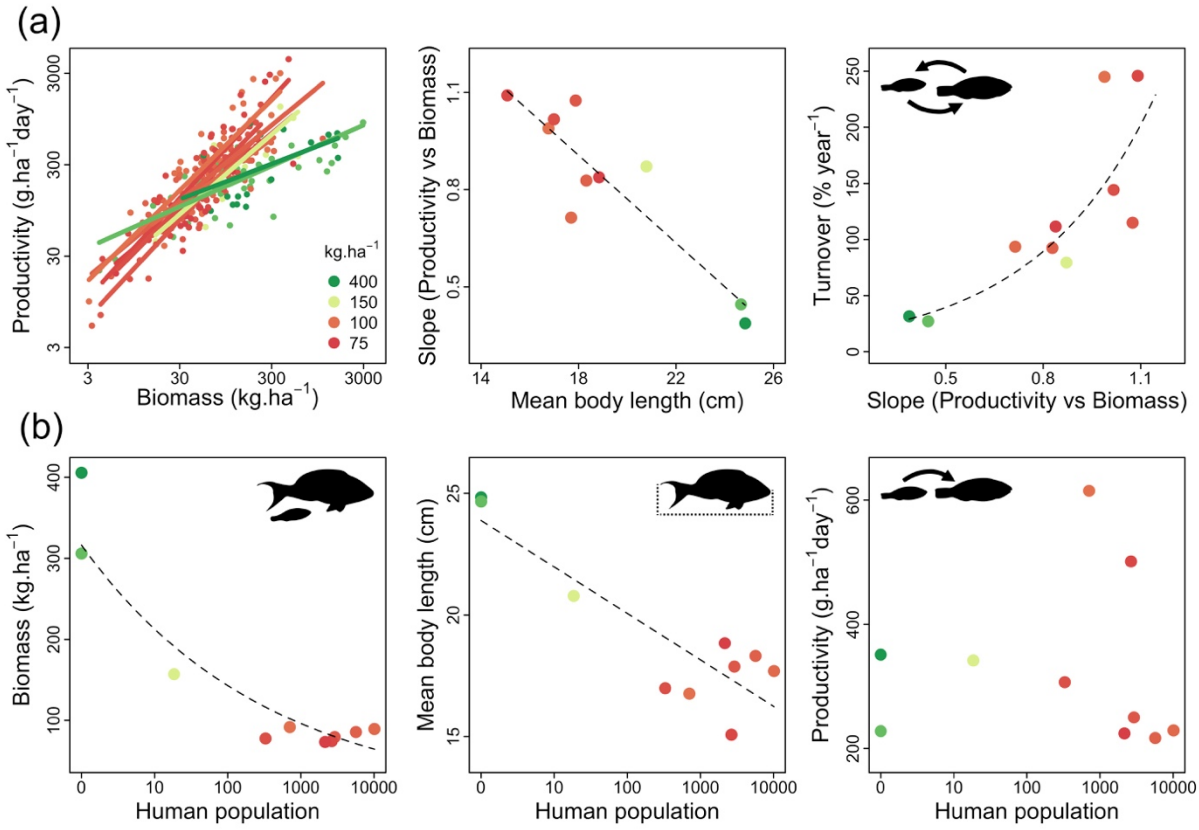

Figure 23: *Distinctive local-scale productivity-biomass relationships for parrotfishes are characterised by reduced body size and increase turnover, which relate to increased human population density.* ***(A)*** *Low biomass regions (red tones, left) with steeper productivity-biomass slopes have also smaller parrotfishes (mid) and higher turnover (right) compared to high biomass regions (green colours, left).* ***(B)*** *Both parrotfish biomass (left) and mean body length (centre) decrease with human population density. In contrast, there is no decrease in productivity (right). Dashed lines represent the linear model fits. For details on the models, see Appendix F. Regions are colour-coded according to the regional-scale average biomass.*

To explore the potential mechanistic basis of the different responses of biomass and productivity to human exploitation, we developed a modelling framework to simulate size-selective fishing. This involved expanding the group-focused taxonomic scope of the study (parrotfishes) to an entire fish assemblage. First, we integrated size-spectrum theory predictions and somatic growth models to

estimate the assemblage-level fish productivity of coral reefs. We then simulated size-selective fishing, over a range of capture rates, and evaluated the impacts on both the standing biomass and productivity of target fishes. We show that with increasing exploitation, fish productivity declines more slowly than standing biomass (**Figure 24**). This is due to a sharp increase in biomass turnover rates (P/B ratio, **Figure F4** in the **Appendix F**) that happened alongside a steepening of the size-spectrum exponent with increasing exploitation (**Figure F5** in the **Appendix F**). We propose the term 'buffering productivity' to describe the community level decoupled response of productivity relative to biomass as exploitation rates increase. We define 'buffering productivity' as the difference between the proportion of initial productivity and the proportion of initial biomass that remains after any degree of exploitation (**Figure 24**). Buffering productivity encompasses the surplus production from multiple populations/species that vary in body size and that, when subjected to similar size-selective fisheries, are driven to different parts of their exploitation axis (see **Appendix F**). The buffering nature of productivity was unveiled both when considering all fishes or only target species (**Figure F4** in the **Appendix F**), and was robust to varying model assumptions such as the initial exponent of the size-spectrum, minimum fishable size, and the form of the size-specific fishing function (**Figures F6-F11**, **Appendix F**).

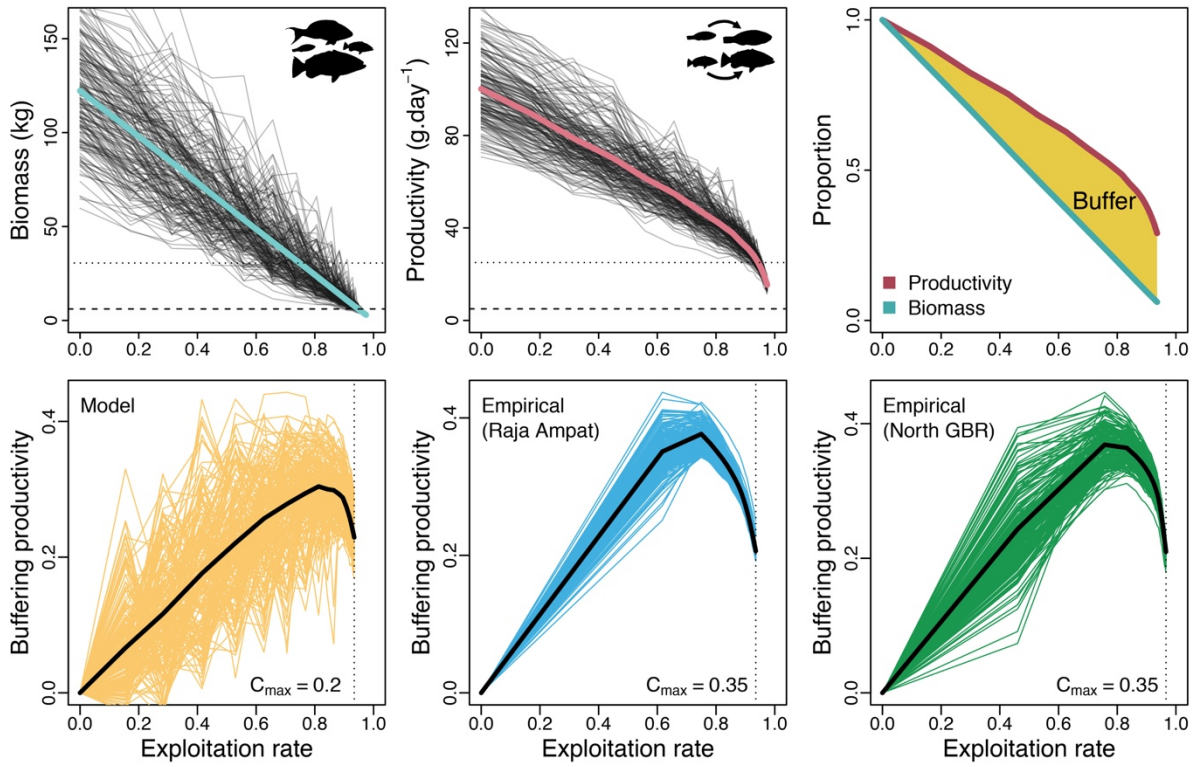

Figure 24: *Buffering productivity is triggered by decoupled responses of productivity and biomass with increasing exploitation in both modelled and empirical coral reef fish assemblages. (Top row) At high exploitation, modelled coral reef fish biomass approaches zero (left), yet productivity consistently remains higher (centre), resulting in a buffer zone (right), the 'buffering productivity'. Black lines denote the output of each fishing simulation, and coloured lines represent their average. The dotted and dashed horizontal lines represent, respectively, the 25% and 5% values of the unfished assemblage biomass or productivity. (Bottom row) Buffering productivity increases with exploitation until it reaches a peak value, and shows the same features in modelled and empirical fish assemblages (see also* ***Figure F13*** *in the* ***Appendix F****). C_{max} is the maximum capture level as a proportion of initial abundance (see* ***Appendix F****). Coloured lines denote the output of each fishing simulation, and black lines represent their average. The dotted vertical line denotes the maximum exploitation under the C_{max}.*

To evaluate if buffering productivity can also arise from the size-selective exploitation of natural fish assemblages, we simulated fishing using datasets from the highly diverse Coral Triangle (Raja Ampat, Indonesia) and Great Barrier Reef (Lizard Island). These datasets provide a comprehensive snapshot of fish assemblages from two of the world's most diverse coral reef regions, encompassing

the full size-range of non-cryptobenthic fishes and including all groups, from strictly benthic, to pelagic reef fishes. Similar to our modelled assemblages, increasing the intensity of exploitation of these natural reef fish assemblages generated consistent, decoupled declines in biomass and productivity, as well as increased turnover rates (**Figure F12** in the **Appendix F**). As a result, increased exploitation induced strong buffering productivity responses in both the Coral Triangle and the GBR fish assemblages (**Figure 24**; **Figure F13**).

Buffering productivity increased with exploitation rates up to a peak value, and then either stabilised or started to decline, both in our modelled assemblages and in the empirical dataset (**Figure 24**). This peak buffering productivity varied with features of the assemblage before the simulations (**Figures F14** and **F15** in the **Appendix F**). For example, unfished assemblages with steeper size spectrum (i.e. a more negative exponent) were characterized by fish with small average body weight and growth, and large turnover rates (**Figures F14** and **F15**). In both model and empirical data, increasing the steepness of the size spectrum resulted in larger peak buffering productivity (**Figure F16**, **Table F4**, in the **Appendix F**).

Discussion

In this study, we integrated large-scale empirical data analysis and robust modelling approaches to unveil the effects of exploitation on the relationship between reef fish productivity and standing biomass. Using parrotfishes as a case study, we first showed that productivity and biomass did not relate at the regional scale. This was due to diverging local relationships, with low-biomass regions having steeper local productivity-biomass relationships, and thus higher productivity per unit biomass (turnover), than high-biomass regions. We also found that, although both parrotfish biomass and average size strongly declined as human population increased, productivity did not respond to human population. Human population density is widely used as a surrogate for fishing pressure (Duffy et al., 2016; Jennings & Polunin, 1996; Mora et al., 2011; Robinson et al., 2017), and changes in fish assemblage biomass or size structure are common indicators of the impacts of fishing on coral reefs (Dulvy et al., 2004; Graham et al., 2005; Nash & Graham, 2016; Robinson et al., 2017). Thus, the

differential relationship of parrotfish size, biomass and productivity to human population suggested a potential compensatory response of productivity to overexploitation.

Size-selective fishing simulations on both modelled and empirical whole fish assemblages (i.e. all non-cryptobenthic groups) showed that increased exploitation rates drove slower declines in fish productivity compared to standing biomass (**Figure 24**). This was paralleled by a sharp increase in biomass turnover rates (**Figure F4** in the **Appendix F**) and a steepening of the size-spectrum exponent, as seen elsewhere (Blanchard et al., 2009; Dulvy et al., 2004; Graham et al., 2005; Jennings & Blanchard, 2004; Robinson et al., 2017). Increased exploitation rates in both modelled and empirical coral reef fish assemblages triggered a buffering productivity that is consistent with previous theory and empirical data (Jennings & Blanchard, 2004; McCann et al., 2016). The intensity of the buffering responses to exploitation depended on the pre-exploitation size structure of the fish assemblages, highlighting its compensatory nature: as exploitation increased, fisheries operating under the worst ecological situations (i.e. in assemblages with a low abundance of large fishes) got the most intense buffering responses. Thus, buffering productivity is likely to contribute to the remaining fisheries productivity of some severely depleted coral reef regions (MacNeil et al., 2015; Newton et al., 2007).

Non-equivalence between biomass and productivity has also been implied by recent coral reef research showing that fish productivity does not necessarily decrease following structural complexity loss (Robinson, Wilson, Robinson, et al., 2019; Rogers, Blanchard, Newman, et al., 2018). Although these observations arise in a different context (i.e. habitat changes leading to the expansion of algal resources and loss of prey refuges), they reveal another mechanism that can potentially decouple large-scale community productivity from biomass. Because habitat changes can occur simultaneously with overexploitation, they may potentially obscure the detection of these ecosystem responses (Wilson, Fisher, et al., 2008), this reinforces the need to tease apart both effects. Our study offers the ideal ground for this because all regions in our large-scale parrotfish dataset had intact coral communities when surveyed, with previous analyses of ecosystem functions consistently detecting a negative effect of human impacts (Bellwood, Hoey, & Choat, 2003; Bellwood, Hoey, et al., 2012).

Although diverging responses of biomass and yields to increasing exploitation have been observed previously on coral reefs (Jennings & Polunin, 1996), our study is the first to integrate large-

scale empirical data analysis and modelling to unveil the effects of exploitation on reef fish production and turnover. The compensatory community responses observed here are paralleled by widely appreciated compensatory population dynamics in the fisheries literature (e.g. Beverton & Holt, 1957; Hilborn & Walters, 1992; but see Keith & Hutchings, 2012), yet have rarely been explored in coral reef settings (Dulvy et al., 2004). By drawing from a longstanding body of work in fisheries science, we demonstrate a clear mechanistic connection between size-selective fishing and the differential depletion trajectories of reef fish biomass and productivity. In doing so, we cast new light on the relationship between structure and function in coral reef ecology.

Buffering productivity, as defined here, only describes the somatic component of productivity in response to exploitation. By using it as a proxy for overall productivity, we implicitly assume that somatic productivity varies more strongly with assemblage biomass than recruitment does. This can happen if assemblage-scale density-dependence operates more strongly on recruitment than on somatic growth, consistent with the fact that incoming recruits tend to be particularly vulnerable to negative species interactions, such as predation and competition (Caley et al., 1996; White & Kendall, 2007). Indeed, even at the single species level, evidence suggests that recruitment saturates or peaks at low to intermediate biomass, with further increases in biomass yielding no recruitment gains or even decreases in recruitment (Beverton & Holt, 1957; Hilborn & Walters, 1992; Subbey, Devine, Schaarschmidt, & Nash, 2014). Three circumstantial lines of evidence suggest that this may be the case for reef fishes.

First, although the impacts of fishing on reproductive-biomass and -energy output are often strong (Barneche, Robertson, White, & Marshall, 2018; Hixon et al., 2014; Scott, Marteinsdottir, & Wright, 1999), evidence for strong positive relationships between reproductive biomass and recruitment in marine fishes is weak, suggesting that any such relationships are likely to be small in magnitude (Munch, Giron-Nava, & Sugihara, 2018; Szuwalski et al., 2015). In coral reef fishes, for example, the lack of relationship between spawning biomass and recruitment has been attributed to high density-dependent pelagic mortality of larvae (Doherty, 1991; Meekan et al., 1993; Robertson, 1990), although there is limited direct evidence to evaluate this suggestion. Second, the degree of spawning-recruitment decoupling varies with body size among fish families globally, with larger fishes having low recruitment despite high reproductive output, and smaller fishes the opposite pattern (Brandl,

Tornabene, et al., 2019). This implies that families of larger fishes that are most likely to drive buffering productivity do so despite limited inputs from recruitment. Third, we found much stronger productivity-biomass relationships within regions than among regions (**Figure 22**), suggesting the potential for high reproductive output in high-biomass locations to be exported to low-biomass locations, where they would experience less density-dependent mortality (reflecting Jensen's inequality, Chan, Connolly, & Mapstone, 2012; White & Kendall, 2007). This would further reduce the magnitude of between-region differences in recruitment. Moreover, we hypothesize that density-dependent dampening of the relationship between biomass and productivity will be even more pronounced at the assemblage than at the single species level, given the potential for interspecific predation on recruits (Caley et al., 1996; Hixon & Webster, 2002). Testing this hypothesis would involve currently unavailable empirical quantifications of biomass-recruitment relationships at the assemblage level.

In summary, we present both theoretical and empirical evidence of the decoupling of productivity and biomass in coral reef fish assemblages. This decoupling has important consequences for studies that assume equivalence between fish biomass and coral reef functioning or service provision. Our study significantly expands previous findings of how fish biomass and fisheries yields relate to fishing pressure on coral reefs (Jennings & Polunin, 1996). We show that overexploitation can cause distinct productivity-biomass relationships to emerge in coral reef fish assemblages: as overfishing drives fish biomass down, an increase in biomass turnover ameliorates, to some extent, expected productivity declines. Increased turnover leads to buffering productivity, a mechanism that contributes to averting immediate coral reef fisheries collapse. Buffering productivity appears to be compensatory as initial assemblages with steeper size-spectrum trigger the most intense buffering responses both in our model and empirical datasets.

Two decades ago, the most important questions were if, and how, marine ecosystems were declining, and what were the causes (Myers & Worm, 2003; Pauly et al., 2002). This was followed by a change in focus to what could be done to avoid or avert some of the perceived changes (Bellwood et al., 2004; Hughes et al., 2010; Worm et al., 2009). Moving forward, there is a need to accept degradation as part of the new configuration of Anthropocene coral reef systems. Marine scientists are beginning to explore the functioning of these transitioning ecosystems (Bellwood, Pratchett, et al., 2019; Hughes,

Barnes, et al., 2017; Mellin et al., 2019; Norström et al., 2016). By bridging the gap between ecological and fisheries theory and coral reef empirical research, we point to an ecological mechanism that can potentially explain how, despite widespread depletion, coral reef fisheries continue to sustain the livelihoods of people. This cautions against interpreting coral reef functioning and food production exclusively through the lens of available standing biomass. Furthermore, it offers hope that even biomass depleted reef systems may still be able to partially deliver the goods and services needed during this new transitional period.

Chapter 7: General Discussion

Assessing fish and fisheries productivity on tropical reefs

Productivity lies at the very core of sustained fishing activities: harvesting that continually exceeds natural bounds of stock productivity will, inevitably, crash. Although mechanistic principles to quantify the productivity of fish cohorts were established more than 70 years ago (cf. K. R. Allen, 1971; Beverton & Holt, 1957; Ricker, 1946), fish productivity *per se* is rarely quantified directly. Most often, productivity is estimated from fisheries yields, i.e. rates of biomass harvested by humans, or by standing stock biomass, i.e. the snapshot of 'available' biomass. Fisheries yields are frequently used in the context of classical fisheries stock assessments that hinge on concepts such as Maximum Sustainable Yield and Surplus Production (Hilborn & Walters, 1992). Standing stock biomass, conversely, has had a prominent role in informing resource production estimates in tropical fisheries, facilitated on coral reefs by the advent of visual survey methods to estimate fish populations (V. E. Brock, 1954).

It was recognised over half a century ago, however, that standing stock biomass is only a proxy for resource production (e.g. Bardach, 1959). The development of ecosystem models from early productivity theory offered a way forward. ECOPATH and extensions, provided a way to directly estimate reef fish production rates (K. R. Allen, 1971; Christensen & Pauly, 1992; Polovina, 1984). However, ecosystem models proved to have limited compatibility with the increasingly popular underwater visual surveys. ECOPATH routines, for example, require detailed inputs of trophic relationships to be able to predict biomass and production rates for specific trophic groups, including different guilds of fishes (Christensen & Pauly, 1992; Polovina, 1984). Conversely, underwater survey methods output data from which standing biomass can be estimated directly, but are rarely followed by broad trophic investigations. As a result, although ecosystem models have the theoretical potential to inform the productivity of coral reef resources, bottlenecks in data availability meant that they were rarely used for this end. Meanwhile, standing stock biomass, easily obtained from underwater survey data, continued to figure as the main data source in resource assessments on tropical reefs (e.g. R. E. Brock et al., 1979; Cinner et al., 2018; D'agata et al., 2016; Friedlander & DeMartini, 2002; Friedlander

& Parrish, 1998; McClanahan, Graham, MacNeil, & Cinner, 2014; Morais, Ferreira, & Floeter, 2017; Russ & Alcala, 2010; Russ et al., 2005; Sandin et al., 2008).

The key conceptual breakthrough was that visual survey data, that includes individual sizes and abundance, can be used to estimate somatic productivity if species-specific growth trajectories are known. In essence, this involves determining the 'expected' age of each fish at the moment they are surveyed. This age determination is achieved by positioning each fish in their likely growth trajectory under a Von Bertalanffy Growth Model (VBGM), based on their body length. This approach was first used by Depczynski, Fulton, Marnane, & Bellwood (2007), providing a simple but critical advancement in applying methods traditionally used in fisheries studies to coral reef ecology. This thesis further expands on this approach by: **1)** providing a computational routine that forecasts VBGM growth trajectories from species traits and environmental temperature, allowing predictions not only for data-scarce species, but also for environmentally separated populations of the same species (Chapter 2; Morais & Bellwood, 2018b); **2)** integrating negative exponential natural mortality, in addition to somatic growth, into the framework for estimating fish productivity with both probabilistic and deterministic applications (**Chapters 3, 4** and **5**; Morais & Bellwood, 2019); **3)** formalising a framework to quantify fish productivity from largely available data using intuitive, easy to apply methods (including an R package interface, **Chapter 3**); **4)** using the developed framework to test hypotheses pertaining to the trophodynamics (**Chapter 4**; Morais & Bellwood, 2019), the effects of habitat degradation (**Chapter 5**) and human exploitation (Chapter 6; Morais et al., 2020) on the productivity of coral reef fishes; and, finally, by **5)** pioneering the use of complementary metrics of the contribution of fishes to coral reef functioning and productivity, particularly the expected consumed biomass and total biomass turnover (Chapter 5; Brandl, Tornabene, et al., 2019).

Future developments

While methodological bottlenecks might have curbed the development of simple methods to quantify fish production in the past (Bardach, 1959; Roedel & Saila, 1980), this thesis synthesises principles, procedures and recommendations that help to overcome some of these bottlenecks (**Chapter 3**). Nevertheless, this individual-level productivity framework will benefit from future developments,

particularly those aimed at: **1)** improving estimates of mortality rates; and **2)** incorporating long-term dynamics by explicitly considering recruitment. Initial estimates of natural mortality have been obtained at the individual level from Gislason, Daan, Rice, & Pope (2010)'s empirical relationship, and from a procedure to scale the species level mortality estimates from Pauly (1980)'s empirical relationship by ontogenetic risk declines (see **Chapter 3** and **Appendix C**). Because of the relatively few mortality values from coral reef fishes used to generate both Pauly's and Gislason et al.'s relationships, both methods to estimate natural mortality in **Chapter 3** should be considered cursory. Expanded reef fish natural mortality datasets will be important in developing models capable of accurately predicting mortality coefficients based on species traits and the environment, similarly to the one developed for VBGM coefficients in the **Chapter 2** of this thesis. Such a development would be particularly important to incorporate the effect of mortality rates when deriving ecosystem functioning metrics, such as biomass consumed and turnover of coral reef fish assemblages.

Beyond mortality rates, explicitly incorporating recruitment dynamics to expand on the temporal scale of productivity estimates requires defining the extent of connection between adult and recruit populations. This challenge will involve understanding, and being able to predict, potential stock-recruitment relationships for coral reef fishes. Stock-recruitment relationships assume that the number of recruiting fishes is a function of population spawning biomass or reproductive adults (e.g. Beverton & Holt, 1957; Ricker, 1954). Although stock-recruitment relationships are a cornerstone of fisheries dynamics, there has been much debate on the occurrence and strength of these relationships. Recent meta-analyses, for example, point to the occurrence of relatively weak stock-recruitment relationships in marine fishes (e.g. Munch et al., 2018; Szuwalski et al., 2015). However, coral reef fishes have remained understudied and notoriously underrepresented in stock-recruitment meta-analyses (e.g. Gilbert, 1997; Munch et al., 2018; Myers & Barrowman, 1996; Szuwalski et al., 2015). One possible way of accounting for recruitment in the productivity framework of this thesis that neither assumes density-dependence nor density-independence would be to consider the size-structure of fish assemblages to be constant through time, i.e. enough fish recruit as to make up for the mortality or growth of immediately larger size classes.

The productivity of coral reef fishes

Our understanding of the productivity of coral reef fishes has remained cloudy due to the absence of a universal method allowing data collected in independent studies to be compared. Ecosystem models and fisheries yield monitoring are particularly prone to this issue because their estimates of productivity rely heavily on seascape features of the area considered. Thus, the availability of reef substratum and of different reef habitats can drastically bias productivity estimates, yet this information is not always available or might be difficult to quantify (Arias-González et al., 1994; Bellwood, 1988; Polunin, 1996).

Early attempts to compile existing fisheries yields data, for example, have documented wildly varying yields due to multiple confounding factors (e.g. varying fishing pressure or survey area) (Marten & Polovina, 1982; Munro & Williams, 1985; Russ, 1984). In practice, this rendered unclear results and precluded the identification of general patterns. A later tentative generalisation of fish productivity estimates derived from ECOPATH models suggested that approximately 20 t km^{-2} $year^{-1}$ of wet fish weight are produced on coral reefs (Polunin, 1996). Subsequent ECOPATH studies yielded larger, but highly variable, values, from about 33 t km^{-2} $year^{-1}$ (Bozec, Gascuel, & Kulbicki, 2004) to over 330 t km^{-2} $year^{-1}$ (Arias-González et al., 1997). More recently, a size-spectrum based ecosystem model has also estimated total fish productivity for a Caribbean coral reef at about 330 t km^{-2} $year^{-1}$ (Rogers et al., 2014), with approximately 175 t km^{-2} $year^{-1}$ composed of fisheries target species (>25cm TL). This model was also used to forecast the productivity of fisheries target species on another reef, at about 50 t km^{-2} $year^{-1}$ (Rogers, Blanchard, & Mumby, 2018). Assuming a similar target species composition, this would generate an estimate of about 100 t km^{-2} $year^{-1}$ of total productivity.

In this thesis, using a complete fish assemblage survey scheme, I estimated fish productivities for a coral reef subjected to coral loss, but closed to fishing, that varied from 73 t km^{-2} $year^{-1}$ on the reef flat up to 250 t km^{-2} $year^{-1}$ on the reef slope (**Chapter 4**; Morais & Bellwood, 2019). Due to the generally low abundance of fishes on reef flats (e.g. Bellwood et al., 2018), it is possible that the estimate of 73 t km^{-2} $year^{-1}$ is close to the lower bound of total fish productivity expected for reef habitats not subject to fishing. The productivity of fisheries target species would be expected to comprise a fraction of this value, increasing in proportion to the breadth of the fisheries. Regardless, the individual-level productivity framework presented in this thesis provides a way of effectively obtaining fish productivity

estimates from smaller areas and suggests that previous estimates may have been highly sensitive to reef-habitat type (see below for fish movements and external subsidies).

New avenues for research

Results from this thesis open up new avenues for research on coral reef functioning. **Chapter 4** provided evidence of the importance of external energetic pathways in sustaining fish productivity on coral reefs. This is consistent with recent research quantifying substantial reliance by coral reef fishes on external energetic subsidies (e.g. Barneche et al., 2014; McCauley et al., 2018; K. W. McMahon et al., 2016; Trebilco et al., 2013). Although the role of pelagic plankton in the trophodynamics of reef consumers has been recognised for decades (e.g. Hamner et al., 1988; Hobson & Chess, 1978), their importance for fish productivity and fisheries yields remained poorly investigated. Complementary to the understanding of external pelagic subsidies as a critical resource for reef consumers is the consideration that some reef fishes can acquire a substantial part of their resources from non-reef habitats (e.g. Fox & Bellwood, 2011). Both pelagic subsidies and fish movements can, thus, decouple spatial scales at which survey efforts and energy intake occur in coral reef fish assemblages. This suggests that the trophodynamics of coral reefs might require re-evaluation under a spatially explicit perspective that accounts for: **1)** external (passive) food inputs to reef consumers; and **2)** external (active) food harvesting by mobile reef consumers executing trans-habitat movements. These forms of nutrient and energy subsidies (Polis, Anderson, & Holt, 1997) have been increasingly reported for coral reefs in empirical studies (e.g. McCauley et al., 2012; K. W. McMahon et al., 2016; Mourier et al., 2016) and could be more important as reefs degrade. Therefore, future steps might benefit from an integrative approach considering the relationship between fish mobility and survey design (e.g. Heenan et al., 2019; Ward-Paige et al., 2010). This should ideally involve explicitly measuring/modelling passive and active external food inputs to reef consumers.

This thesis also provides insights into a potential mechanism helping to explain sustained yields in biomass-depleted fisheries. In **Chapter 6**, I found that overexploitation disproportionally depletes the standing biomass compared to the productivity of coral reef fish assemblages. This is due to increased turnover as fish size distributions are constrained in their upper range due to size-selective

fishing, triggering compensatory 'buffering' responses (**Chapter 6**; Morais et al., 2020). While buffering productivity could help to explain the occurrence of simultaneous biomass depletion and sustained fisheries yields, temporal persistence of this mechanism requires recruitment not to be substantially affected by biomass reduction. In essence, this requires stock-recruitment relationships that quickly saturate as adult biomass increases (e.g. Gilbert, 1997). While research has shown how fecundity and the energetic investment in reproduction from large fishes disproportionally outweigh the same indicators in smaller fishes, including reef fishes (Barneche et al., 2018; Birkeland & Dayton, 2005; Hixon et al., 2014; D. J. Marshall, Gaines, Warner, Barneche, & Bode, 2019; Scott et al., 1999), we know comparatively less about how reproductive output translates into fish recruitment onto coral reefs. To date, evidence suggests that large density-dependent mortality in either the pelagic phase or immediately after settling can result in weak stock-recruitment (Caley et al., 1996; Doherty, 1991; Meekan et al., 1993; Robertson, 1990), but a comprehensive analysis of this question with multiple sources of empirical data across multiple families is lacking. In my point of view, the extent to which local populations are sustained by locally-sourced recruits is a key aspect that should be investigated in a range of reef fish species. Would, for example, weak locally-sourced recruitment in fisheries target species mean that 'buffering productivity' could be maintained from external recruitment? Spatially-explicit models incorporating metacommunity dynamics and data collected over large spatial-scales (e.g. Bode et al., 2019; Harrison et al., 2012; Hopf, Jones, Willamson, & Connolly, 2015; Hopf, Jones, Williamson, & Connolly, 2019; D. J. Marshall et al., 2019) will be crucial in determining the importance of compensatory buffering responses as a mechanism underpinning sustained fisheries yields in depleted biomass situations. In this context, methods incorporating dispersal kernels might be ideal to merge biophysical models, dispersal potential, and seascape features in a metacommunity framework within which to further explore buffering responses (e.g. Bode et al., 2019; Bode, Williamson, Harrison, Outram, & Jones, 2018).

A new paradigm for reef resource assessment

In summary, this thesis presents evidence that a non-linear relationship between fish weight and growth constrains our ability to safely infer the production of coral reef fish biomass production from

their standing stock biomass alone (**Chapters 4** and **6**; Morais & Bellwood, 2019; Morais et al., 2020). The same might indeed apply to any high species diversity aquatic environments in which fish are key consumers. At the same time, this thesis provides a simple and accessible method to estimate fish productivity from underwater visual survey data (**Chapter 3**). It therefore offers a tool with the potential to generate a new paradigm for resource assessment in reef systems: one that is process-based, dynamic and that takes into consideration how fast new resource, i.e. fish biomass, is produced, rather than only how much is available at a given time.

References

Ackerman, J. L., & Bellwood, D. R. (2000). Reef fish assemblages: A re-evaluation using enclosed rotenone stations. *Marine Ecology Progress Series*, *206*(1954), 227–237. doi: 10.3354/meps206227

Ackerman, J. L., Bellwood, D. R., & Brown, J. H. (2004). The contribution of small individuals to density-body size relationships: Examination of energetic equivalence in reef fishes. *Oecologia*, *139*(4), 568–571. doi: 10.1007/s00442-004-1536-0

Adam, T. C., Duran, A., Fuchs, C. E., Roycroft, M. V., Rojas, M. C., Ruttenberg, B. I., & Burkepile, D. E. (2018). Comparative analysis of foraging behavior and bite mechanics reveals complex functional diversity among Caribbean parrotfishes. *Marine Ecology Progress Series*, *597*, 207–220. doi: 10.3354/meps12600

Adam, T. C., Schmitt, R. J., Holbrook, S. J., Brooks, A. J., Edmunds, P. J., Carpenter, R. C., & Bernardi, G. (2011). Herbivory, connectivity, and ecosystem resilience: Response of a coral reef to a large-scale perturbation. *PLoS ONE*, *6*(8). doi: 10.1371/journal.pone.0023717

Allen, A. P., & Gillooly, J. F. (2009). Towards an integration of ecological stoichiometry and the metabolic theory of ecology to better understand nutrient cycling. *Ecology Letters*, *12*(5), 369–384. doi: 10.1111/j.1461-0248.2009.01302.x

Allen, K. R. (1971). Relation between Production and Biomass. *Journal of the Fisheries Research Board of Canada*, *28*, 1573–1581.

Allgeier, J. E., Speare, K. E., & Burkepile, D. E. (2018). Estimates of fish and coral larvae as nutrient subsidies to coral reef ecosystems. *Ecosphere*, *9*(6). doi: 10.1002/ecs2.2216

Almany, G. R., Planes, S., Thorrold, S. R., Berumen, M. L., Bode, M., Saenz-Agudelo, P., … Jones, G. P. (2017). Larval fish dispersal in a coral-reef seascape. *Nature Ecology and Evolution*, *1*(6), 1–7. doi: 10.1038/s41559-017-0148

Almany, G. R., & Webster, M. S. (2006). The predation gauntlet: early post-settlement mortality in reef fishes. *Coral Reefs*, *25*(1), 19–22. doi: 10.1007/s00338-005-0044-y

Alvarez-Filip, L., Dulvy, N. K., Gill, J. A., Côté, I. M., & Watkinson, A. R. (2009). Flattening of

Caribbean coral reefs: region-wide declines in architectural complexity. *Proceedings of the Royal Society B: Biological Sciences*, *276*(1669), 3019–3025. doi: 10.1007/s00338-011-0795-6

Andersen, K. H., & Beyer, J. E. (2006). Asymptotic Size Determines Species Abundance in the Marine Size Spectrum. *The American Naturalist*, *168*(1), 54–61. doi: 10.1086/504849

Andrews, J., & Gentien, P. (1982). Upwelling as a Source of Nutrients for the Great Barrier Reef Ecosystems: A Solution to Darwin's Question? *Marine Ecology Progress Series*, *8*, 257–269. doi: 10.3354/meps008257

Appeldoorn, R. S. (1996). Model and method in reef fishery assessment. In *Reef fisheries* (pp. 219–248). Springer.

Arias-González, J. E., Delesalle, B., Salvat, B., & Galzin, R. (1997). Trophic functioning of the Tiahura reef sector, Moorea Island, French Polynesia. *Coral Reefs*, *16*(4), 231–246. doi: 10.1007/s003380050079

Arias-González, J. E., Galzin, R., Nielson, J., Mahon, R., & Aiken, K. (1994). Reference area as a factor affecting the potential yield estimates of coral reef fishes. *Naga, The ICLARM Quarterly*, Vol. 17, pp. 37–40.

Balakrishnan, N., & Nevzorov, V. B. (2003). *A Primer on Statistical Distributions*. doi: 10.1002/0471722227

Barange, M., Merino, G., Blanchard, J. L., Scholtens, J., Harle, J., Allison, E. H., … Jennings, S. (2014). Impacts of climate change on marine ecosystem production in societies dependent on fisheries. *Nature Climate Change*, *4*(3), 211–216. doi: 10.1038/nclimate2119

Bardach, J. E. (1959). The summer standing crop of fish on a shallow Bermuda reef. *Limnology and Oceanography*, *4*(1954), 77–85. doi: 10.4319/lo.1959.4.1.0077

Barneche, D. R., & Allen, A. P. (2018). The energetics of fish growth and how it constrains food-web trophic structure. *Ecology Letters*, *21*(6), 836–844. doi: 10.1111/ele.12947

Barneche, D. R., Kulbicki, M., Floeter, S. R., Friedlander, A. M., Maina, J., & Allen, A. P. (2014). Scaling metabolism from individuals to reef-fish communities at broad spatial scales. *Ecology Letters*, *17*(9), 1067–1076. doi: 10.1111/ele.12309

Barneche, D. R., Robertson, D. R., White, C. R., & Marshall, D. J. (2018). Fish reproductive-energy

output increases disproportionately with body size. *Science*, *360*(6389), 642–645. doi: 10.1126/science.aao6868

Bartoń, K. (2016). *MuMIn: Multi-Model Inference*. R package version 1.15.6.

Begon, M., Townsend, C. R., & Harper, J. L. (2006). *Ecology: from Individuals to Ecosystems* (4th ed.). Malden, Oxford and Carlton: Blackwell Publishing Ltd.

Behrenfeld, M. J., & Falkowski, P. G. (1997). Photosynthetic rates derived from satellite-based chlorophyll concentration. *Limnology and Oceanography*, *42*(1), 1–20. doi: 10.4319/lo.1997.42.1.0001

Bellwood, D. R. (1988). Seasonal changes in the size and composition of the fish yield from reefs around Apo Island, Central Philippines, with notes on methods of yield estimation. *Journal of Fish Biology*, *32*, 881–893. doi: 10.1111/j.1095-8649.1988.tb05431.x

Bellwood, D. R., Baird, A. H., Depczynski, M., González-Cabello, A., Hoey, A. S., Lefèvre, C. D., & Tanner, J. K. (2012). Coral recovery may not herald the return of fishes on damaged coral reefs. *Oecologia*, *170*(2), 567–573. doi: 10.1007/s00442-012-2306-z

Bellwood, D. R., & Choat, J. H. (1990). A functional analysis of grazing in parrotfishes (family Scaridae): the ecological implications. *Enviromental Biology of Fishes*, *28*, 189–214.

Bellwood, D. R., Hoey, A. S., Ackerman, J. L., & Depczynski, M. (2006). Coral bleaching, reef fish community phase shifts and the resilience of coral reefs. *Global Change Biology*, *12*(9), 1587–1594. doi: 10.1111/j.1365-2486.2006.01204.x

Bellwood, D. R., Hoey, A. S., & Choat, J. H. (2003). Limited functional redundancy in high diversity systems: Resilience and ecosystem function on coral reefs. *Ecology Letters*, *6*(4), 281–285. doi: 10.1046/j.1461-0248.2003.00432.x

Bellwood, D. R., Hoey, A. S., & Hughes, T. P. (2012). Human activity selectively impacts the ecosystem roles of parrotfishes on coral reefs. *Proceedings of the Royal Society B: Biological Sciences*, *279*(1733), 1621–1629. doi: 10.1098/rspb.2011.1906

Bellwood, D. R., Hughes, T. P., Folke, C., & Nyström, M. (2004). Confronting the coral reef crisis. *Nature*, *429*(6994), 827–833. doi: 10.1038/nature02691

Bellwood, D. R., Pratchett, M. S., Morrison, T. H., Gurney, G. G., Hughes, T. P., Álvarez-Romero, J.

G., … Cumming, G. S. (2019). Coral reef conservation in the Anthropocene: Confronting spatial mismatches and prioritizing functions. *Biological Conservation*. doi: doi: 10.1016/j.biocon.2019.05.056

Bellwood, D. R., Streit, R. P., Brandl, S. J., & Tebbett, S. B. (2019). The meaning of the term 'function' in ecology: a coral reef perspective. *Functional Ecology*, *33*, 948–961. doi: 10.1111/1365-2435.13265

Bellwood, D. R., Tebbett, S. B., Bellwood, O., Mihalitsis, M., Morais, R. A., Streit, R. P., & Fulton, C. J. (2018). The role of the reef flat in coral reef trophodynamics: Past, present, and future. *Ecology and Evolution*, *8*, 4108–4119. doi: 10.1002/ece3.3967

Bellwood, D. R., & Wainwright, P. C. (2002). The History and Biogeography of Fishes on Coral Reefs. In P. Sale (Ed.), *Coral reef fishes: dynamics and diversity in a complex ecosystem* (pp. 5–32). San Diego: Academic Press.

Benkwitt, C. E., Wilson, S. K., & Graham, N. A. J. (2020). Biodiversity increases ecosystem functions despite multiple stressors on coral reefs. *Nature Ecology & Evolution*, *4*, 919–926. doi: 10.1038/s41559-020-1203-9

Bennett, S., Vergés, A., & Bellwood, D. R. (2010). Branching coral as a macroalgal refuge in a marginal coral reef system. *Coral Reefs*, *29*(2), 471–480. doi: 10.1007/s00338-010-0594-5

Berkes, F., Hughes, T. P., Steneck, R. S., Wilson, J. A., Bellwood, D. R., Crona, B., … Worm, B. (2006). Globalization, roving bandits, and marine resources. *Science*, *311*(5767), 1557–1558. doi: 10.1126/science.1122804

Bertalanffy, L. von. (1938). A Quantitative Theory of Organic Growth (Inquiries on Growth Laws. II). *Human Biology*, *10*(2), 181–213.

Bertalanffy, L. von. (1949). Problems of Organic Growth. *Nature*, *163*, 156–158. doi: 10.1038/163156a0

Bertalanffy, L. von. (1957). Quantitative Laws in Metabolism and Growth. *The Quarterly Review of Biology*, *32*(3), 217–231. doi: 10.1086/401873

Berumen, M. L. (2005). The importance of juveniles in modelling growth: butterflyfish at Lizard Island. *Environmental Biology of Fishes*, *72*(4), 409–413. doi: 10.1007/s10641-004-2595-0

Betancur-R, R., Wiley, E. O., Arratia, G., Acero, A., Bailly, N., Miya, M., … Ortí, G. (2017). Phylogenetic classification of bony fishes. *BMC Evolutionary Biology*, *17*(1), 162. doi: 10.1186/s12862-017-0958-3

Beverton, R. J. H., & Holt, S. J. (1957). On the Dynamics of Exploited Fish Populations. In *Fisheries Investigations Series 2: Sea Fisheries* (Vol. 4). doi: 10.1007/978-94-011-2106-4

Beverton, R. J. H., & Holt, S. J. (1959). A Review of the Lifespans and Mortality Rates of Fish in Nature, and Their Relation to Growth and Other Physiological Characteristics. In G. E. W. Wolstenholme & M. O'Connor (Eds.), *Ciba Foundation Symposium - The Lifespan of Animals (Colloquia on Ageing)* (pp. 142–180). doi: 10.1002/9780470715253.ch10

Birkeland, C., & Dayton, P. (2005). The importance in fishery management of leaving the big ones. *Trends in Ecology & Evolution*, *20*(7), 356–358. doi: 10.1016/j.tree.2005.03.015

Blanchard, J. L., Jennings, S., Holmes, R., Harle, J., Merino, G., Allen, J. I., … Barange, M. (2012). Potential consequences of climate change for primary production and fish production in large marine ecosystems. *Philosophical Transactions of the Royal Society B: Biological Sciences*, *367*(1605), 2979–2989. doi: 10.1098/rstb.2012.0231

Blanchard, J. L., Jennings, S., Law, R., Castle, M. D., McCloghrie, P., Rochet, M. J., & Benoît, E. (2009). How does abundance scale with body size in coupled size-structured food webs? *Journal of Animal Ecology*, *78*(1), 270–280. doi: 10.1111/j.1365-2656.2008.01466.x

Bode, M., Leis, J. M., Mason, L. B., Williamson, D. H., Harrison, H. B., Choukroun, S., & Jones, G. P. (2019). Successful validation of a larval dispersal model using genetic parentage data. *PLoS Biology*, *17*(7), 1–13. doi: 10.1371/journal.pbio.3000380

Bode, M., Williamson, D. H., Harrison, H. B., Outram, N., & Jones, G. P. (2018). Estimating dispersal kernels using genetic parentage data. *Methods in Ecology and Evolution*, *9*(3), 490–501. doi: 10.1111/2041-210X.12922

Bowen, S. H., Lutz, E. V, & Ahlgren, M. O. (1995). Dietary Protein and Energy as Determinants of Food Quality: Trophic Strategies Compared. *Ecology*, *76*(3), 899–907. doi: 10.2307/1939355

Bozec, Y.-M., Gascuel, D., & Kulbicki, M. (2004). Trophic model of lagoonal communities in a large open atoll (Uvea, Loyalty islands, New Caledonia). *Aquatic Living Resources*, *17*(2), 151–162.

doi: 10.1051/alr:2004024

Bozec, Y.-M., O'Farrell, S., Bruggemann, J. H., Luckhurst, B. E., & Mumby, P. J. (2016). Tradeoffs between fisheries harvest and the resilience of coral reefs. *Proceedings of the National Academy of Sciences*, *113*(16), 4536–4541. doi: 10.1073/pnas.1601529113

Brandl, S. J., & Bellwood, D. R. (2014). Individual-based analyses reveal limited functional overlap in a coral reef fish community. *Journal of Animal Ecology*, *83*(3), 661–670. doi: 10.1111/1365-2656.12171

Brandl, S. J., Goatley, C. H. R., Bellwood, D. R., & Tornabene, L. (2018). The hidden half: ecology and evolution of cryptobenthic fishes on coral reefs. *Biological Reviews*, *93*, 1846–1873. doi: 10.1111/brv.12423

Brandl, S. J., Rasher, D. B., Côté, I. M., Casey, J. M., Darling, E. S., Lefcheck, J. S., & Duffy, J. E. (2019). Coral reef ecosystem functioning: eight core processes and the role of biodiversity. *Frontiers in Ecology and the Environment*, *17*(8), 445–454. doi: 10.1002/fee.2088

Brandl, S. J., Tornabene, L., Goatley, C. H. R., Casey, J. M., Morais, R. A., Côté, I. M., … Bellwood, D. R. (2019). Demographic dynamics of the smallest marine vertebrates fuel coral reef ecosystem functioning. *Science*, *364*(6446), 1189–1192. doi: 10.1126/science.aav3384

Brey, T., Müller-Wiegmann, C., Zittier, Z. M. C., & Hagen, W. (2010). Body composition in aquatic organisms - A global data bank of relationships between mass, elemental composition and energy content. *Journal of Sea Research*, *64*(3), 334–340. doi: 10.1016/j.seares.2010.05.002

Brock, R. E., Lewis, C., & Wass, R. C. (1979). Stability and structure of a fish community on a coral patch reef in Hawaii. *Marine Biology*, *54*(3), 281–292. doi: 10.1007/BF00395790

Brock, V. E. (1954). A Preliminary Report on a Method of Estimating Reef Fish Populations. *The Journal of Wildlife Management*, *18*(3), 297–308.

Brown, J. H., Gillooly, J. F., Allen, A. P., Savage, V. M., & West, G. B. (2004). Toward a Metabolic Theory of Ecology. *Ecology*, *85*(7), 1771–1789. doi: 10.1890/03-9000

Bruno, J. F., Côté, I. M., & Toth, L. T. (2019). Climate Change, Coral Loss, and the Curious Case of the Parrotfish Paradigm: Why Don't Marine Protected Areas Improve Reef Resilience? *Annual Review of Marine Science*, *11*(1), 307–334. doi: 10.1146/annurev-marine-010318-095300

Buesa, R. (1987). Growth rate of tropical demersal fishes. *Marine Ecology Progress Series*, *36*(1963), 191–199. doi: 10.3354/meps036191

Bürkner, P.-C. (2017). brms : An R Package for Bayesian Multilevel Models Using Stan. *Journal of Statistical Software*, *80*(1), 1–28. doi: 10.18637/jss.v080.i01

Burnham, K. P., & Anderson, D. R. (2002). *Model Selection and Multimodel Inference A Practical Information-Theoretic Approach* (2nd ed.). New York: Springer-Verlag.

Burns, E., Ifrach, I., Carmeli, S., Pawlik, J. R., & Ilan, M. (2003). Comparison of anti-predatory defenses of Red Sea and Caribbean sponges. I. Chemical defense. *Marine Ecology Progress Series*, *252*(Meylan 1988), 105–114. doi: 10.3354/meps252115

Calder, W. A. (1984). *Size, function and life history*. Cambridge. Massachusetts; London, England: Harvard University Press.

Caley, M. J., Carr, M. H., Hixon, M. A., Hughes, T. P., Jones, G. P., & Menge, B. A. (1996). Recruitment and the local dynamics of open marine populations. *Annual Review of Ecology and Systematics*, *27*, 477–500. doi: 10.1146/annurev.ecolsys.27.1.477

Campana, S. E. (2001). Accuracy, precision and quality control in age determination, including a review of the use and abuse of age validation methods. *Journal of Fish Biology*, *59*(2), 197–242. doi: 10.1111/j.1095-8649.2001.tb00127.x

Carpenter, R. C. (1985). Relationships between primary production and ii radiance in coral reef algal communities. *Limnology and Oceanography*, *30*(4), 784–793. doi: 10.4319/lo.1985.30.4.0784

Carpenter, R. C. (1990). Mass mortality of Diadema antillarum - II. Effects on population densities and grazing intensity of parrotfishes and surgeonfishes. *Marine Biology*, *104*(1), 79–86. doi: 10.1007/BF01313160

Ceccarelli, D. M., Emslie, M. J., & Richards, Z. T. (2016). Post-disturbance stability of fish assemblages measured at coarse taxonomic resolution masks change at finer scales. *PLoS ONE*, *11*(6), e0156232. doi: 10.1371/journal.pone.0156232

Chan, N. C. S., Connolly, S. R., & Mapstone, B. D. (2012). Effects of sex change on the implications of marine reserves for fisheries. *Ecological Applications*, *22*(3), 778–791. doi: 10.1890/11-0036.1

Charnov, E. L., & Gillooly, J. F. (2004). Size and Temperature in the Evolution of Fish Life Histories.

Integrative and Comparative Biology, *44*(6), 494–497. doi: 10.1093/icb/44.6.494

Cheal, A. J., MacNeil, M. A., Emslie, M. J., & Sweatman, H. (2017). The threat to coral reefs from more intense cyclones under climate change. *Global Change Biology*, *23*(4), 1511–1524. doi: 10.1111/gcb.13593

Chen, T., & Guestrin, C. (2016). XGBoost. *Proceedings of the 22nd ACM SIGKDD International Conference on Knowledge Discovery and Data Mining - KDD '16*, 785–794. doi: 10.1145/2939672.2939785

Chen, T., He, T., Benesty, M., Khotilovich, V., & Tang, Y. (2018). *xgboost: Extreme Gradient Boosting*. R package version 0.6.4.1.

Cheung, W. W. L., Lam, V. W. Y., Sarmiento, J. L., Kearney, K., Watson, R., Zeller, D., & Pauly, D. (2010). Large-scale redistribution of maximum fisheries catch potential in the global ocean under climate change. *Global Change Biology*, *16*(1), 24–35. doi: 10.1111/j.1365-2486.2009.01995.x

Choat, J. H., & Axe, L. M. (1996). Growth and longevity in acanthurid fishes; an analysis of otolith increments. *Marine Ecology Progress Series*, *134*(1–3), 15–26. doi: 10.3354/meps134015

Choat, J. H., Axe, L. M., & Lou, D. C. (1996). Growth and longevity in fishes of the family Scaridae. *Marine Ecology Progress Series*, *145*, 33–41. doi: 10.3354/meps145033

Choat, J. H., & Bellwood, D. R. (1985). Interactions amongst herbivorous fishes on a coral reef: influence of spatial variation. *Nature*, (221), 234. doi: 10.1038/164914a0

Choat, J. H., & Clements, K. D. (1998). Vertebrate herbivores in marine and terrestrial environments: A Nutritional Ecology Perspective. *Annual Review of Ecology and Systematics*, *29*(1), 375–403. doi: 10.1146/annurev.ecolsys.29.1.375

Choat, J. H., Clements, K. D., & Robbins, W. D. (2002). The trophic status of herbivorous fishes on coral reefs 1: Dietary analyses. *Marine Biology*, *140*(3), 613–623. doi: 10.1007/s00227-001-0715-3

Choat, J. H., & Robertson, D. R. (2002). Age-Based Studies. In P. F. Sale (Ed.), *Coral reef fishes: dynamics and diversity in a complex ecosystem* (pp. 57–80). Burlington, San Diego, London: Academic Press.

Christensen, V., & Pauly, D. (1992). ECOPATH II - a software for balancing steady-state ecosystem

models and calculating network characteristics. *Ecological Modelling*, *61*(3–4), 169–185. doi: 10.1016/0304-3800(92)90016-8

Cinner, J. E. (2014). Coral reef livelihoods. *Current Opinion in Environmental Sustainability*, *7*, 65–71. doi: 10.1016/j.cosust.2013.11.025

Cinner, J. E., Graham, N. A. J., Huchery, C., & Macneil, M. A. (2013). Global Effects of Local Human Population Density and Distance to Markets on the Condition of Coral Reef Fisheries. *Conservation Biology*, *27*(3), 453–458. doi: 10.1111/j.1523-1739.2012.01933.x

Cinner, J. E., Maire, E., Huchery, C., MacNeil, M. A., Graham, N. A. J., Mora, C., … Mouillot, D. (2018). Gravity of human impacts mediates coral reef conservation gains. *Proceedings of the National Academy of Sciences of the United States of America*, *115*(27), E6116–E6125. doi: 10.1073/pnas.1708001115

Clarke, A. (2019). Energy Flow in Growth and Production. *Trends in Ecology and Evolution*, *34(6)*, 502–509. doi: 10.1016/j.tree.2019.02.003

Clements, K. D., German, D. P., Piché, J., Tribollet, A., & Choat, J. H. (2017). Integrating ecological roles and trophic diversification on coral reefs: Multiple lines of evidence identify parrotfishes as microphages. *Biological Journal of the Linnean Society*, *120*(4), 729–751. doi: 10.1111/bij.12914

Clements, K. D., Raubenheimer, D., & Choat, J. H. (2009). Nutritional ecology of marine herbivorous fishes: Ten years on. *Functional Ecology*, *23*(1), 79–92. doi: 10.1111/j.1365-2435.2008.01524.x

Clifton, K. E. (1995). Asynchronous food availability on neighboring Caribbean coral reefs determines seasonal patterns of growth and reproduction for the herbivorous parrotfish *Scarus iserti*. *Marine Ecology Progress Series*, *116*(1–3), 39–46. doi: 10.3354/meps116039

Condy, M., Cinner, J. E., McClanahan, T. R., & Bellwood, D. R. (2015). Projections of the impacts of gear-modification on the recovery of fish catches and ecosystem function in an impoverished fishery. *Aquatic Conservation: Marine and Freshwater Ecosystems*, *25*(3), 396–410. doi: 10.1002/aqc.2482

Connell, S. D. (1998). Patterns of piscivory by resident predatory reef fish at One Tree Reef, Great Barrier Reef. *Marine and Freshwater Research*, *49*(1), 25–30.

Craig, P., Green, A., & Tuilagi, F. (2008). Subsistence harvest of coral reef resources in the outer islands

of American Samoa: Modern, historic and prehistoric catches. *Fisheries Research*, *89*(3), 230–240. doi: 10.1016/j.fishres.2007.08.018

Crossland, C. J., Hatcher, B. G., & Smith, S. V. (1991). Role of coral reefs in global ocean production. *Coral Reefs*, *10*(2), 55–64. doi: 10.1007/BF00571824

D'agata, S., Mouillot, D., Wantiez, L., Friedlander, A. M., Kulbicki, M., & Vigliola, L. (2016). Marine reserves lag behind wilderness in the conservation of key functional roles. *Nature Communications*, *7*(May), 12000. doi: 10.1038/ncomms12000

Dalzell, P. (1996). Reef Fisheries. In N. V. C. Polunin & C. M. Roberts (Eds.), *Reef Fisheries*. doi: 10.1007/978-94-015-8779-2

Dalzell, P., Adams, T. J. H., & Polunin, N. V. C. (1996). Coastal fisheries in the Pacific Islands. *Oceanography and Marine Biology: An Annual Review.*, *34*, 395–531.

Darling, E. S., Graham, N. A. J., Januchowski-Hartley, F. A., Nash, K. L., Pratchett, M. S., & Wilson, S. K. (2017). Relationships between structural complexity, coral traits, and reef fish assemblages. *Coral Reefs*, *36*(2), 561–575. doi: 10.1007/s00338-017-1539-z

de Goeij, J. M., van Oevelen, D., Vermeij, M. J. A., Osinga, R., Middelburg, J. J., de Goeij, A. F. P. M., & Admiraal, W. (2013). Surviving in a Marine Desert: The Sponge Loop Retains Resources Within Coral Reefs. *Science*, *342*(6154), 108–110. doi: 10.1126/science.1241981

Deines, A. M., Bunnell, D. B., Rogers, M. W., Bennion, D., Woelmer, W., Sayers, M. J., … Beard, T. D. (2017). The contribution of lakes to global inland fisheries harvest. *Frontiers in Ecology and the Environment*, *15*(6), 293–298. doi: 10.1002/fee.1503

Depczynski, M., & Bellwood, D. R. (2006). Extremes, plasticity, and invariance in vertebrate life history traits: insights from coral reef fishes. *Ecology*, *87*(12), 3119–3127. doi: 10.2307/20069341

Depczynski, M., Fulton, C. J., Marnane, M. J., & Bellwood, D. R. (2007). Life history patterns shape energy allocation among fishes on coral reefs. *Oecologia*, *153*(1), 111–120. doi: 10.1007/s00442-007-0714-2

Dickens, L. C., Goatley, C. H. R., Tanner, J. K., & Bellwood, D. R. (2011). Quantifying relative diver effects in underwater visual censuses. *PLoS ONE*, *6(4)*, e18965. doi: 10.1371/journal.pone.0018965

Diaz-Pulido, G., & McCook, L. J. (2002). The fate of bleached corals: patterns and dynamics of algal recruitment. *Marine Ecology Progress Series*, *232*, 115–128.

Doherty, P. J. (1991). Spatial and Temporal Patterns in Recruitment. In P F Sale (Ed.), *The ecology of fishes on coral reefs* (pp. 261–293). San Diego: Academic Press.

Donelson, J. M., Munday, P. L., McCormick, M. I., & Pitcher, C. R. (2012). Rapid transgenerational acclimation of a tropical reef fish to climate change. *Nature Climate Change*, *2*(1), 30–32. doi: 10.1038/nclimate1323

Donelson, J. M., Salinas, S., Munday, P. L., & Shama, L. N. S. (2018). Transgenerational plasticity and climate change experiments: Where do we go from here? *Global Change Biology*, *24*(1), 13–34. doi: 10.1111/gcb.13903

Donner, S. D., & Potere, D. (2007). The Inequity of the Global Threat to Coral Reefs. *BioScience*, *57*(3), 214–215. doi: 10.1641/B570302

Duffy, J. E., Lefcheck, J. S., Stuart-Smith, R. D., Navarrete, S. A., & Edgar, G. J. (2016). Biodiversity enhances reef fish biomass and resistance to climate change. *Proceedings of the National Academy of Sciences of the United States of America*, *113*(22), 6230–6235. doi: 10.1073/pnas.1524465113

Dulvy, N. K., Polunin, N. V. C., Mill, A. C., & Graham, N. A. J. (2004). Size structural change in lightly exploited coral reef fish communities: evidence for weak indirect effects. *Canadian Journal of Fisheries and Aquatic Sciences*, *61*(3), 466–475. doi: 10.1139/f03-169

Edgar, G. J., Stuart-Smith, R. D., Willis, T. J., Kininmonth, S., Baker, S. C., Banks, S., … Thomson, R. J. (2014). Global conservation outcomes depend on marine protected areas with five key features. *Nature*, *506*(7487), 216–220. doi: 10.1038/nature13022

Edwards, A. M., Robinson, J. P. W., Plank, M. J., Baum, J. K., & Blanchard, J. L. (2017). Testing and recommending methods for fitting size spectra to data. *Methods in Ecology and Evolution*, *8*(1), 57–67. doi: 10.1111/2041-210X.12641

Elith, J., Leathwick, J. R., & Hastie, T. (2008). A working guide to boosted regression trees. *Journal of Animal Ecology*, *77*(4), 802–813. doi: 10.1111/j.1365-2656.2008.01390.x

Embke, H. S., Rypel, A. L., Carpenter, S. R., Sass, G. G., Ogle, D., Cichosz, T., Hennessy, J., Essington, T. E., & Jake Vander Zanden, M. (2019). Production dynamics reveal hidden overharvest of inland

recreational fisheries. Proceedings of the National Academy of Sciences of the United States of America, 116(49), 24676–24681. doi: 10.1073/pnas.1913196116

Emery, A. R. (1968). Preliminary observations on coral reef plankton. *Limnology and Oceanography*, *13*(2), 293–303.

Emslie, M. J., Logan, M., Ceccarelli, D. M., Cheal, A. J., Hoey, A. S., Miller, I., & Sweatman, H. P. A. (2012). Regional-scale variation in the distribution and abundance of farming damselfishes on Australia's Great Barrier Reef. *Marine Biology*, *159*(6), 1293–1304. doi: 10.1007/s00227-012-1910-0

Emslie, M. J., Cheal, A. J., MacNeil, M. A., Miller, I. R., & Sweatman, H. P. A. (2018). Reef fish communities are spooked by scuba surveys and may take hours to recover. *PeerJ*, *6*, e4886. doi: 10.7717/peerj.4886

Erlandson, J. M. (2001). The Archaeology of aquatic adaptations: Paradigms for a new millennium. *Journal of Archaeological Research*, *9*(4), 287–350. doi: 10.1023/A:1013062712695

Erlandson, J. M., & Rick, T. C. (2010). Archaeology Meets Marine Ecology: The Antiquity of Maritime Cultures and Human Impacts on Marine Fisheries and Ecosystems. *Annual Review of Marine Science*, *2*(1), 231–251. doi: 10.1146/annurev.marine.010908.163749

Ernest, S. K. M., Enquist, B. J., Brown, J. H., Charnov, E. L., Gillooly, J. F., Savage, V. M., … Tiffney, B. (2003). Thermodynamic and metabolic effects on the scaling of production and population energy use. *Ecology Letters*, *6*(11), 990–995. doi: 10.1046/j.1461-0248.2003.00526.x

Eurich, J. G., Baker, J. K. M. R., & Jones, M. I. M. G. P. (2019). Stable isotope analysis reveals trophic diversity and partitioning in territorial damselfishes on a low-latitude coral reef. *Marine Biology*, 1–14. doi: 10.1007/s00227-018-3463-3

Fox, R. J., & Bellwood, D. R. (2011). Unconstrained by the clock? Plasticity of diel activity rhythm in a tropical reef fish, Siganus lineatus. *Functional Ecology*, *25*(5), 1096–1105. doi: 10.1111/j.1365-2435.2011.01874.x

Francis, R. I. C. C. (1988). Are Growth Parameters Estimated from Tagging and Age–Length Data Comparable? *Canadian Journal of Fisheries and Aquatic Sciences*, *45*(6), 936–942. doi: 10.1139/f88-115

Friedlander, A. M., & DeMartini, E. E. (2002). Contrasts in density, size, and biomass of reef fishes between the northwestern and the main Hawaiian islands: The effects of fishing down apex predators. *Marine Ecology Progress Series*, *230*, 253–264. doi: 10.3354/meps230253

Friedlander, A. M., & Parrish, J. D. (1998). Habitat characteristics affecting fish assemblages on a Hawaiian coral reef. *Journal of Experimental Marine Biology and Ecology*, *224*(1), 1–30. doi: 10.1016/S0022-0981(97)00164-0

Froese, R. (2006). Cube law, condition factor and weight-length relationships: history, meta-analysis and recommendations. *Journal of Applied Ichthyology*, *22*(4), 241–253. doi: 10.1111/j.1439-0426.2006.00805.x

Froese, R., & Binohlan, C. (2003). Simple methods to obtain preliminary growth estimates for fishes. *Journal of Applied Ichthyology*, *19*(6), 376–379. doi: 10.1111/j.1439-0426.2003.00490.x

Froese, R., & Pauly, D. (2018). FishBase. World Wide Web page. http://www.fishbase.org.

Froese, R., Thorson, J. T., & Reyes, R. B. (2014). A Bayesian approach for estimating length-weight relationships in fishes. *Journal of Applied Ichthyology*, *30*(1), 78–85. doi: 10.1111/jai.12299

Fulton, C. J., Abesamis, R. A., Berkström, C., Depczynski, M., Graham, N. A. J., Holmes, T. H., … Wilson, S. K. (2019). Form and function of tropical macroalgal reefs in the Anthropocene. *Functional Ecology*, *33*(6), 989–999. doi: 10.1111/1365-2435.13282

Fulton, C. J., & Bellwood, D. R. (2005). Wave-induced water motion and the functional implications for coral reef fish assemblages. *Limnology and Oceanography*, *50*(1), 255–264. doi: 10.4319/lo.2005.50.1.0255

Fulton, C. J., Bellwood, D. R., & Wainwright, P. C. (2005). Wave energy and swimming performance shape coral reef fish assemblages. *Proceedings of the Royal Society B: Biological Sciences*, *272*(1565), 827–832. doi: 10.1098/rspb.2004.3029

Genin, A. (2004). Bio-physical coupling in the formation of zooplankton and fish aggregations over abrupt topographies. *Journal of Marine Systems*, *50*(1–2), 3–20. doi: 10.1016/j.jmarsys.2003.10.008

Genin, A., Jaffe, J. S., Reef, R., Richter, C., & Franks, P. J. S. (2005). Swimming Against the Flow : A Mechanism of Zooplankton Aggregation. *Science*, *308*, 860–863. doi: 10.3354/meps340001

Gilbert, D. J. (1997). Towards a new recruitment paradigm for fish stocks. *Canadian Journal of Fisheries and Aquatic Sciences*, *54*(4), 969–977. doi: 10.1139/f96-272

Gillooly, J. F., Brown, J. H., West, G. B., Savage, V. M., & Charnov, E. L. (2001). Effects of Size and Temperature on Metabolic Rate. *Science*, *293*(5538), 2248–2251. doi: 10.1126/science.1061967

Gillooly, J. F., Charnov, E. L., West, G. B., Savage, V. M., & Brown, J. H. (2002). Effects of size and temperature on developmental time. *Nature*, *417*, 70–73. doi: 10.1038/417070a

Gilmour, J. P., Smith, L. D., Heyward, A. J., Baird, A. H., & Pratchett, M. S. (2013). Recovery of an isolated coral reef system following severe disturbance. *Science*, *340*(6128), 69–71. doi: 10.1126/science.1232310

Giovas, C. M., Lambrides, A. B. J., Fitzpatrick, S. M., & Kataoka, O. (2017). Reconstructing prehistoric fishing zones in Palau, Micronesia using fish remains: A blind test of inter-analyst correspondence. *Archaeology in Oceania*, *52*(1), 45–61. doi: 10.1002/arco.5119

Gislason, H., Daan, N., Rice, J. C., & Pope, J. G. (2010). Size, growth, temperature and the natural mortality of marine fish. *Fish and Fisheries*, *11*(2), 149–158. doi: 10.1111/j.1467-2979.2009.00350.x

Glynn, P. W. (1973). Ecology of a Caribbean coral reef. The Porites reef-flat biotope: Part II. Plankton community with evidence for depletion. *Marine Biology*, *22*(1), 1–21. doi: 10.1007/BF00388905

Goatley, C. H. R., & Bellwood, D. R. (2011). The roles of dimensionality, canopies and complexity in ecosystem monitoring. *PLoS ONE*, *6*(11). doi: 10.1371/journal.pone.0027307

Goatley, C. H. R., & Bellwood, D. R. (2013). Ecological Consequences of Sediment on High-Energy Coral Reefs. *PLoS ONE*, *8*(10), 1–7. doi: 10.1371/journal.pone.0077737

Goatley, C. H. R., & Bellwood, D. R. (2016). Body size and mortality rates in coral reef fishes : a three-phase relationship. *Proceedings of the Royal Society B: Biological Sciences*, *283*, 20161858. doi: 10.1098/rspb.2016.1858

Goatley, C. H. R., González-Cabello, A., & Bellwood, D. R. (2017). Small cryptopredators contribute to high predation rates on coral reefs. *Coral Reefs*, *36*(1), 207–212. doi: 10.1007/s00338-016-1521-1

Gove, J. M., McManus, M. A., Neuheimer, A. B., Polovina, J. J., Drazen, J. C., Smith, C. R., …

Williams, G. J. (2016). Near-island biological hotspots in barren ocean basins. *Nature Communications*, *7*, 10581. doi: 10.1038/ncomms10581

Grafen, A. (1989). The phylogenetic regression. *Philosophical Transactions of the Royal Society B: Biological Sciences*, *326*, 119–157.

Graham, N. A. J., Cinner, J. E., Norström, A. V., & Nyström, M. (2014). Coral reefs as novel ecosystems: embracing new futures. *Current Opinion in Environmental Sustainability*, *7*, 9–14. doi: 10.1016/j.cosust.2013.11.023

Graham, N. A. J., Dulvy, N., Jennings, S., & Polunin, N. (2005). Size-spectra as indicators of the effects of fishing on coral reef fish assemblages. *Coral Reefs*, *24*(1), 118–124. doi: 10.1007/s00338-004-0466-y

Graham, N. A. J., Jennings, S., MacNeil, M. A., Mouillot, D., & Wilson, S. K. (2015). Predicting climate-driven regime shifts versus rebound potential in coral reefs. *Nature*, *518*(7537), 94–97. doi: 10.1038/nature14140

Graham, N. A. J., & Nash, K. L. (2013). The importance of structural complexity in coral reef ecosystems. *Coral Reefs*, *32*(2), 315–326. doi: 10.1007/s00338-012-0984-y

Graham, N. A. J., Wilson, S. K., Jennings, S., Polunin, N. V. C., Bijoux, J. P., & Robinson, J. (2006). Dynamic fragility of oceanic coral reef ecosystems. *Proceedings of the National Academy of Sciences of the United States of America*, *103*(22), 8425–8429. doi: 10.1073/pnas.0600693103

Graham, N. A. J., Wilson, S. K., Jennings, S., Polunin, N. V. C., Robinson, J., Bijoux, J. P., & Daw, T. M. (2007). Lag effects in the impacts of mass coral bleaching on coral reef fish, fisheries, and ecosystems. *Conservation Biology*, *21*(5), 1291–1300. doi: 10.1111/j.1523-1739.2007.00754.x

Grandcourt, E. M. (2002). Demographic characteristics of a selection of exploited reef fish from the Seychelles: preliminary study. *Marine and Freshwater Research*, *53*(2), 123. doi: 10.1071/MF01123

Gust, N., Choat, J. H., & Ackerman, J. L. (2002). Demographic plasticity in tropical reef fishes. *Marine Biology*, *140*(5), 1039–1051. doi: 10.1007/s00227-001-0773-6

Halpern, B. S. (2003). The impact of marine reserves: Do reserves work and does reserve size matter? *Ecological Applications*, *13*(1 SUPPL.). doi: 10.1890/1051-0761(2003)013[0117:tiomrd]2.0.co;2

Hamilton, R. J., Almany, G. R., Stevens, D., Bode, M., Pita, J., Peterson, N. A., & Choat, J. H. (2016). Hyperstability masks declines in bumphead parrotfish (*Bolbometopon muricatum*) populations. *Coral Reefs*, *35*(3), 751–763. doi: 10.1007/s00338-016-1441-0

Hamner, W. M., & Hauri, I. R. (1981). Effects of island mass: Water flow and plankton pattern around a reef in the Great Barrier Reef lagoon, Australia1. *Limnology and Oceanography*, *26*(6), 1084–1102. doi: 10.4319/lo.1981.26.6.1084

Hamner, W. M., Jones, M. S., Carleton, J. H., Hauri, I. R., & Williams, D. M. B. (1988). Zooplankton, planktivorous fish, and water currents on a windward reef face: Great Barrier Reef, Australia. *Bulletin of Marine Science*, *42*(3), 459–479.

Harmelin-Vivien, M. L. (2002). Energetics and Fish Diversity on Coral Reefs. In P. Sale (Ed.), *Coral reef fishes: dynamics and diversity in a complex ecosystem* (pp. 265–274). Burlington, San Diego, London: Academic Press.

Harrison, H. B., Williamson, D. H., Evans, R. D., Almany, G. R., Thorrold, S. R., Russ, G. R., … Jones, G. P. (2012). Larval export from marine reserves and the recruitment benefit for fish and fisheries. *Current Biology*, *22*(11), 1023–1028. doi: 10.1016/j.cub.2012.04.008

Hart, A. M., Klumpp, D. W., & Russ, G. R. (1996). Response of herbivorous fishes to crown-of-thorns starfish Acanthaster planci outbreaks. II. Density and biomass of selected species of herbivorous fish and fish-habitat correlations. *Marine Ecology Progress Series*, *132*(1–3), 21–30. doi: 10.3354/meps132021

Hart, A. M., & Russ, G. R. (1996). Response of herbivorous fishes to crown-of-thorns starfish Acanthaster planci outbreaks. III. Age, growth, mortality and maturity indices of Acanthurus nigrofuscus. *Marine Ecology Progress Series*, *136*, 25–35.

Harvey, E., Fletcher, D., & Shortis, M. (2002). Estimation of reef fish length by divers and by stereo-video. *Fisheries Research*, *57(3)*, 255–265. doi: 10.1016/s0165-7836(01)00356-3

Hatcher, B. G. (1988). Coral reef primary productivity: A beggar's banquet. *Trends in Ecology & Evolution*, *3*(5), 106–111. doi: 10.1016/0169-5347(88)90117-6

Hay, M. E. (1991). Fish–seaweed interactions on coral reefs: effects of herbivorous fishes and adaptations of their prey. In P. Sale (Ed.), *The ecology of fishes on coral reefs* (pp. 96–119). San

Diengo: Academic Press.

Heenan, A., Williams, G. J., & Williams, I. D. (2019). Natural variation in coral reef trophic structure across environmental gradients. *Frontiers in Ecology and the Environment*, 1–7. doi: 10.1002/fee.2144

Hemingson, C. R., & Bellwood, D. R. (2018). Biogeographic patterns in major marine realms: function not taxonomy unites fish assemblages in reef, seagrass and mangrove systems. *Ecography*, *41*(1), 174–182. doi: 10.1111/ecog.03010

Hiatt, R. W., & Strasburg, D. W. (1960). Ecological Relationships of the Fish Fauna on Coral Reefs of the Marshall Islands. *Ecological Monographs*, *30*(1), 65–127. doi: 10.2307/1942181

Hilborn, R., & Walters, C. J. (1992). *Quantitative Fisheries Stock Assessment*. doi: 10.1007/978-1-4615-3598-0

Hinchliff, C. E., Smith, S. A., Allman, J. F., Burleigh, J. G., Chaudhary, R., Coghill, L. M., … Cranston, K. A. (2015). Synthesis of phylogeny and taxonomy into a comprehensive tree of life. *Proceedings of the National Academy of Sciences of the United States of America*, *112*(41), 12764–12769. doi: 10.1073/pnas.1423041112

Hixon, M. A. (1991). Predation as a process structuring coral reef fish communities. In P. Sale (Ed.), *The ecology of fishes on coral reefs* (pp. 475–508). San Diego: Academic Press.

Hixon, M. A., & Beets, J. P. . (1993). Predation, Prey Refuges, and the Structure of Coral-Reef Fish Assemblages. *Ecological Monographs*, *63*(1), 77–101.

Hixon, M. A., Johnson, D. W., & Sogard, S. M. (2014). BOFFFFs: on the importance of conserving old-growth age structure in fishery populations. *ICES Journal of Marine Science*, *71*(8), 2171–2185. doi: 10.1093/icesjms/fst200

Hixon, M. A., & Webster, M. S. (2002). Density dependence in reef fish populations. In P. Sale (Ed.), *Coral reef fishes: dynamics and diversity in a complex ecosystem* (pp. 303–325). Burlington, San Diego, London: Academic Press.

Hobson, E. S. (1991). Trophic relationships of fishes specialized to feed on zooplankters above coral reefs. In P F Sale (Ed.), *The ecology of fishes on coral reefs* (pp. 69–95). San Diego: Academic Press.

Hobson, E. S., & Chess, J. R. (1978). Trophic Relationships Among Fishes and plankton in the lagoon at Enewetak Atoll, Marshall Islands. *Fishery Bulletin*, *76*(1), 133–153.

Hollowed, A. B., Bax, N., Beamish, R., Collie, J., Fogarty, M., Livingston, P., … Rice, J. C. (2000). Are multispecies models an improvement on single-species models for measuring fishing impacts on marine ecosystems? *ICES Journal of Marine Science*, *57*(3), 707–719. doi: 10.1006/jmsc.2000.0734

Hooper, D. U., III, F. S. C., Ewel, J. J., Hector, A., Inchausti, P., Lavorel, S., … Wardle, D. A. (2005). Effects of biodiversity on ecosystem functioning: a consensus of current knowledge. *Ecological Monographs*, *75*(July 2004), 3–35. doi: 10.1890/04-0922

Hopf, J. K., Jones, G. P., Willamson, D. H., & Connolly, S. R. (2015). Fishery consequences of marine reserves: short-term pain for longer-term gain. *Ecological Applications*, *26*(3), 150825143423007. doi: 10.1890/15-0348.1

Hopf, J. K., Jones, G. P., Williamson, D. H., & Connolly, S. R. (2019). Marine reserves stabilize fish populations and fisheries yields in disturbed coral reef systems. *Ecological Applications*, *29*(5), 1–13. doi: 10.1002/eap.1905

Horn, M. (1989). Biology of marine herbivorous fishes. *Oceanography and Marine Biology: An Annual Review*, *27*, 167–272.

Hughes, T. P., Anderson, K. D., Connolly, S. R., Heron, S. F., Kerry, J. T., Lough, J. M., … Wilson, S. K. (2018). Spatial and temporal patterns of mass bleaching of corals in the Anthropocene. *Science*, *359*(6371), 80–83. doi: 10.1126/science.aan8048

Hughes, T. P., Barnes, M. L., Bellwood, D. R., Cinner, J. E., Cumming, G. S., Jackson, J. B. C., … Scheffer, M. (2017). Coral reefs in the Anthropocene. *Nature*, *546*(7656), 82–90. doi: 10.1038/nature22901

Hughes, T. P., Graham, N. A. J., Jackson, J. B. C., Mumby, P. J., & Steneck, R. S. (2010). Rising to the challenge of sustaining coral reef resilience. *Trends in Ecology and Evolution*, *25*(11), 633–642. doi: 10.1016/j.tree.2010.07.011

Hughes, T. P., Kerry, J. T., Álvarez-Noriega, M., Álvarez-Romero, J. G., Anderson, K. D., Baird, A. H., … Wilson, S. K. (2017). Global warming and recurrent mass bleaching of corals. *Nature*,

543(7645), 373–377. doi: 10.1038/nature21707

Hughes, T. P., Kerry, J. T., Baird, A. H., Connolly, S. R., Chase, T. J., Dietzel, A., … Woods, R. M. (2019). Global warming impairs stock–recruitment dynamics of corals. *Nature*, *568*(7752), 387–390. doi: 10.1038/s41586-019-1081-y

Hughes, T. P., Kerry, J. T., Baird, A. H., Connolly, S. R., Dietzel, A., Eakin, C. M., … Torda, G. (2018). Global warming transforms coral reef assemblages. *Nature*, *556*(7702), 492–496. doi: 10.1038/s41586-018-0041-2

Hughes, T. P., Rodrigues, M. J., Bellwood, D. R., Ceccarelli, D., Hoegh-Guldberg, O., McCook, L., … Willis, B. (2007). Phase Shifts, Herbivory, and the Resilience of Coral Reefs to Climate Change. *Current Biology*, *17*(4), 360–365. doi: 10.1016/j.cub.2006.12.049

Jackson, J. B. C., Kirby, M. X., Berger, W. H., Bjorndal, K. A., Louis W. Botsford, Bourque, B. J., … Warner, R. R. (2001). Historical Overfishing and the Recent Collapse of Coastal Ecosystems. *Science*, *293*(5530), 629–637. doi: 10.1126/science.1059199

Jacobsen, N. S., Gislason, H., & Andersen, K. H. (2014). The consequences of balanced harvesting of fish communities. *Proceedings of the Royal Society B: Biological Sciences*, *281(1775)*, 20132701. doi: 10.1098/rspb.2013.2701

Jenkins, D. G. (2015). Estimating ecological production from biomass. *Ecosphere*, *6*(4), art49. doi: 10.1890/ES14-00409.1

Jennings, S., & Blanchard, J. L. (2004). Fish abundance with no fishing: predictions based on macroecological theory. *Journal of Animal Ecology*, *73*(4), 632–642. doi: 10.1111/j.0021-8790.2004.00839.x

Jennings, S., & Collingridge, K. (2015). Predicting consumer biomass, size-structure, production, catch potential, responses to fishing and associated uncertainties in the world's marine ecosystems. *PLoS ONE*, *10*(7), 1–28. doi: 10.1371/journal.pone.0133794

Jennings, S., & Dulvy, N. K. (2005). Reference points and reference directions for size-based indicators of community structure. *ICES Journal of Marine Science*, *62*(3), 397–404.

Jennings, S., & Kaiser, M. J. (1998). The Effects of Fishing on Marine Ecosystems. In P. A. T. J.H.S. Blaxter, A.J. Southward (Ed.), *Advances in Marine Biology* (Vol. 34, pp. 201–352). doi:

10.1016/S0065-2881(08)60212-6

Jennings, S., & Lock, J. M. (1996). Population and ecosystem effects of reef fishing. In *Reef fisheries* (pp. 193–218). Springer.

Jennings, S., & Mackinson, S. (2003). Abundance-body mass relationships in size-structured food webs. *Ecology Letters*, *6*(11), 971–974. doi: 10.1046/j.1461-0248.2003.00529.x

Jennings, S., & Polunin, N. V. C. (1996). Effects of Fishing Effort and Catch Rate Upon the Structure and Biomass of Fijian Reef Fish Communities. *The Journal of Applied Ecology*, *33*(2), 400. doi: 10.2307/2404761

Johansen, J. L., Bellwood, D. R., & Fulton, C. J. (2008). Coral reef fishes exploit flow refuges in high-flow habitats. *Marine Ecology Progress Series*, *360*, 219–226. doi: 10.3354/meps07482

Jørgensen, C., & Holt, R. E. (2013). Natural mortality: its ecology, how it shapes fish life histories, and why it may be increased by fishing. *Journal of Sea Research*, *75*, 8–18.

Kavanagh, K. D., & Olney, J. E. (2006). Ecological correlates of population density and behavior in the circumtropical black triggerfish *Melichthys niger* (Balistidae). *Environmental Biology of Fishes*, *76*(2–4), 387–398. doi: 10.1007/s10641-006-9044-1

Keith, D. M., & Hutchings, J. A. (2012). Population dynamics of marine fishes at low abundance. *Canadian Journal of Fisheries and Aquatic Sciences*, *69*(10), 1722–1722. doi: 10.1139/f2012-100

Kerry, J. T., & Bellwood, D. R. (2012). The effect of coral morphology on shelter selection by coral reef fishes. *Coral Reefs*, *31*(2), 415–424. doi: 10.1007/s00338-011-0859-7

Kingsford, M. J. (1992). Spatial and temporal variation in predation on reef fishes by coral trout (*Plectropomus leopardus*, Serranidae). *Coral Reefs*, *11*, 193–198.

Kingsford, M. J., O'Callaghan, M. D., Liggins, L., & Gerlach, G. (2017). The short-lived neon damsel Pomacentrus coelestis: Implications for population dynamics. *Journal of Fish Biology*, *90(5)*, 2041–2059. doi: 10.1111/jfb.13288

Kinsey, D. W. (1985). Metabolism, calcification and carbon production: 1 Systems level studies. *Proceedings of the Fifth International Coral Reef Congress*, Vol. 4, pp. 505–526.

Kramer, M. J., Bellwood, O., & Bellwood, D. R. (2013). The trophic importance of algal turfs for coral reef fishes: the crustacean link. *Coral Reefs*, *32*(2), 575–583. doi: 10.1007/s00338-013-1009-1

Kritzer, J. P. (2002). Stock structure, mortality and growth of the decorated goby, *Istigobius decoratus* (Gobiidae), at Lizard Island, Great Barrier Reef. *Environmental Biology of Fishes*, *63*(2), 211–216. doi: 10.1023/A:1014278319097

Kritzer, J. P., Davies, C. R., & Mapstone, B. D. (2001). Characterizing fish populations: effects of sample size and population structure on the precision of demographic parameter estimates. *Canadian Journal of Fisheries and Aquatic Sciences*, *58*(8), 1557–1568. doi: 10.1139/cjfas-58-8-1557

Kulbicki, M., Parravicini, V., Bellwood, D. R., Arias-Gonzàlez, E., Chabanet, P., Floeter, S. R., … Mouillot, D. (2013). Global biogeography of reef fishes: A hierarchical quantitative delineation of regions. *PLoS ONE*, *8*(12), e81847. doi: 10.1371/journal.pone.0081847

Kuparinen, A., & Merilä, J. (2007). Detecting and managing fisheries-induced evolution. *Trends in Ecology and Evolution*, *22*(12), 652–659. doi: 10.1016/j.tree.2007.08.011

Lefcheck, J. S. (2016). piecewiseSEM: Piecewise structural equation modelling in R for ecology, evolution, and systematics. *Methods in Ecology and Evolution*, *7*(5), 573–579. doi: 10.1111/2041-210X.12512

Lewis, J. B. (1977). Processes of organic production on coral reefs. *Biological Reviews*, *52*(3), 305–347.

Lobato, F. L., Barneche, D. R., Siqueira, A. C., Liedke, A. M. R., Lindner, A., Pie, M. R., … Floeter, S. R. (2014). Diet and Diversification in the Evolution of Coral Reef Fishes. *PLoS ONE*, *9*(7), e102094. doi: 10.1371/journal.pone.0102094

Longenecker, K., Chan, Y. L., Toonen, R. J., Carlon, D. B., Hunt, T. L., Friedlander, A. M., & Demartini, E. E. (2014). Archaeological evidence of validity of fish populations on unexploited reefs as proxy targets for modern populations. *Conservation Biology*, *28*(5), 1322–1330. doi: 10.1111/cobi.12287

Longo, G. O., Hay, M. E., Ferreira, C. E. L., & Floeter, S. R. (2019). Trophic interactions across 61 degrees of latitude in the Western Atlantic. *Global Ecology and Biogeography*, *28*(2), 107–117.

Lotze, H. K., Tittensor, D. P., Bryndum-Buchholz, A., Eddy, T. D., Cheung, W. W. L., Galbraith, E. D., … Worm, B. (2019). Global ensemble projections reveal trophic amplification of ocean

biomass declines with climate change. *Proceedings of the National Academy of Sciences of the United States of America*, *116*(26), 12907–12912. doi: 10.1073/pnas.1900194116

Lynch, A. J., Cooke, S. J., Deines, A. M., Bower, S. D., Bunnell, D. B., Cowx, I. G., … Beard, T. D. (2016). The social, economic, and environmental importance of inland fish and fisheries. *Environmental Reviews*, *24*(2), 115–121. doi: 10.1139/er-2015-0064

MacNeil, M. A., Graham, N. A. J., Cinner, J. E., Wilson, S. K., Williams, I. D., Maina, J., … McClanahan, T. R. (2015). Recovery potential of the world's coral reef fishes. *Nature*, *520*(7547), 341–344. doi: 10.1038/nature14358

MacNeil, M. A., Mellin, C., Matthews, S., Wolff, N. H., McClanahan, T. R., Devlin, M., … Graham, N. A. J. (2019). Water quality mediates resilience on the Great Barrier Reef. *Nature Ecology & Evolution*, *3*(4), 620–627. doi: 10.1038/s41559-019-0832-3

Madin, J. S., Baird, A. H., Bridge, T. C. L., Connolly, S. R., Zawada, K. J. A., & Dornelas, M. (2018). Cumulative effects of cyclones and bleaching on coral cover and species richness at Lizard Island. *Marine Ecology Progress Series*, *604*, 263–268. doi: 10.3354/meps12735

Madin, J. S., & Connolly, S. R. (2006). Ecological consequences of major hydrodynamic disturbances on coral reefs. *Nature*, *444*(7118), 477–480. doi: 10.1038/nature05328

Maire, E., Cinner, J., Velez, L., Huchery, C., Mora, C., Dagata, S., … Mouillot, D. (2016). How accessible are coral reefs to people? A global assessment based on travel time. *Ecology Letters*, *19*(4), 351–360. doi: 10.1111/ele.12577

Marshall, D. J., Gaines, S., Warner, R., Barneche, D. R., & Bode, M. (2019). Underestimating the benefits of marine protected areas for the replenishment of fished populations. *Frontiers in Ecology and the Environment*, *17*(7), 407–413. doi: 10.1002/fee.2075

Marshall, N., Barnes, M. L., Birtles, A., Brown, K., Cinner, J., Curnock, M., … Tobin, R. (2018). Measuring what matters in the Great Barrier Reef. *Frontiers in Ecology and the Environment*, *16*(5), 271–277. doi: 10.1002/fee.1808

Marten, G. G., & Polovina, J. J. (1982). A Comparative Study of fish Yields from Various Tropical Ecosystems. In *Theory and management of tropical fisheries* (pp. 255–289).

McCann, K. S., Gellner, G., McMeans, B. C., Deenik, T., Holtgrieve, G., Rooney, N., … Nam, S.

(2016). Food webs and the sustainability of indiscriminate fisheries. *Canadian Journal of Fisheries and Aquatic Sciences*, *73*(4), 656–665. doi: 10.1139/cjfas-2015-0044

McCauley, D. J., Gellner, G., Martinez, N. D., Williams, R. J., Sandin, S. A., Micheli, F., … McCann, K. S. (2018). On the prevalence and dynamics of inverted trophic pyramids and otherwise top-heavy communities. *Ecology Letters*, *21*(3), 439–454. doi: 10.1111/ele.12900

McCauley, D. J., Young, H. S., Dunbar, R. B., Estes, J. A., Semmens, B. X., & Micheli, F. (2012). Assessing the effects of large mobile predators on ecosystem connectivity. *Ecological Applications*, *22*(6), 1711–1717. doi: 10.1890/11-1653.1

McClanahan, T. R., Graham, N. A. J., MacNeil, M. A., & Cinner, J. E. (2014). Biomass-based targets and the management of multispecies coral reef fisheries. *Conservation Biology*, *29*(2), 409–417. doi: 10.1111/cobi.12430

McClanahan, T. R. (2018). Community biomass and life history benchmarks for coral reef fisheries. *Fish and Fisheries*, *19*(3), 471–488. doi: 10.1111/faf.12268

McClanahan, T. R., Darling, E. S., Maina, J. M., Muthiga, N. A., 'agata, S. D., Jupiter, S. D., … Leblond, J. (2019). Temperature patterns and mechanisms influencing coral bleaching during the 2016 El Niño. *Nature Climate Change*, *9*(11), 845–851. doi: 10.1038/s41558-019-0576-8

McClanahan, T. R., Graham, N. A. J., MacNeil, M. A., Muthiga, N. A., Cinner, J. E., Bruggemann, J. H., & Wilson, S. K. (2011). Critical thresholds and tangible targets for ecosystem-based management of coral reef fisheries. *Proceedings of the National Academy of Sciences of the United States of America*, *108*(41), 17230–17233. doi: 10.1073/pnas.1106861108

McMahon, K. W., Thorrold, S. R., Houghton, L. A., & Berumen, M. L. (2016). Tracing carbon flow through coral reef food webs using a compound-specific stable isotope approach. *Oecologia*, *180*(3), 809–821. doi: 10.1007/s00442-015-3475-3

McMahon, T. A., & Bonner, J. T. (1983). *On size and life*. New York: Scientific American Library.

McWilliam, M., Chase, T. J., & Hoogenboom, M. O. (2018). Neighbor Diversity Regulates the Productivity of Coral Assemblages. *Current Biology*, *28*(22), 3634-3639.e3. doi: 10.1016/j.cub.2018.09.025

Meekan, M., Milicich, M., & Doherty, P. (1993). Larval production drives temporal patterns of larval

supply and recruitment of a coral reef damselfish. *Marine Ecology Progress Series*, *93*(17), 217–225. doi: 10.3354/meps093217

Mellin, C., Matthews, S., Anthony, K. R. N., Brown, S. C., Caley, M. J., Johns, K. A., … MacNeil, M. A. (2019). Spatial resilience of the Great Barrier Reef under cumulative disturbance impacts. *Global Change Biology*, *25*(7), 2431–2445. doi: 10.1111/gcb.14625

Michonneau, F., Brown, J. W., & Winter, D. J. (2016). rotl: an R package to interact with the Open Tree of Life data. *Methods in Ecology and Evolution*, *7*(12), 1476–1481. doi: 10.1111/2041-210X.12593

Mitchell, R., & Frank, E. (2017). Accelerating the XGBoost algorithm using GPU computing. *PeerJ Computer Science*, *3*(7), e127. doi: 10.7717/peerj-cs.127

Moberg, F., & Folke, C. (1999). Ecological goods and services of coral reef ecosystems. *Ecological Economics*, *29*(2), 215–233. doi: 10.1016/S0921-8009(99)00009-9

Mora, C., Aburto-Oropeza, O., Ayala-Bocos, A., Ayotte, P. M., Banks, S., Bauman, A. G., … Zapata, F. a. (2011). Global human footprint on the linkage between biodiversity and ecosystem functioning in reef fishes. *PLoS Biology*, *9*(4), e1000606. doi: 10.1371/journal.pbio.1000606

Mora, C., Andréfouët, S., Costello, M. J., Kranenburg, C., Rollo, A., Veron, J., … Myers, R. A. (2006). Coral reefs and the global network of marine protected areas. *Science*, *312*(5781), 1750–1751. doi: 10.1126/science.1125295

Morais, R. A., & Bellwood, D. R. (2018a). Data from 'Global drivers of reef fish growth.' doi: 10.4225/28/5ae8f3cc790f9

Morais, R. A., & Bellwood, D. R. (2018b). Global drivers of reef fish growth. *Fish and Fisheries*, *19*(5), 874–889. doi: 10.1111/faf.12297

Morais, R. A., & Bellwood, D. R. (2019). Pelagic subsidies underpin fish productivity on a degraded coral reef. *Current Biology*, *29*(9), 1521–1527. doi: 10.1016/j.cub.2019.03.044

Morais, R. A., Connolly, S. R., & Bellwood, D. R. (2020). Human exploitation shapes productivity-biomass relationships on coral reefs. *Global Change Biology 26*(3), 1295–1305. doi: 10.1111/gcb.14941.

Morais, R. A., Ferreira, C. E. L., & Floeter, S. R. (2017). Spatial patterns of fish standing biomass

across Brazilian reefs. *Journal of Fish Biology*, *91*(6), 1642–1667. doi: 10.1111/jfb.13482

Morales-Nin, B. (1989). Growth determination of tropical marine fishes by means of otolith interpretation and length frequency analysis. *Aquatic Living Resources*, *2*(4), 241–253. doi: 10.1051/alr:1989029

Mouillot, D., Villeger, S., Parravicini, V., Kulbicki, M., Arias-Gonzalez, J. E., Bender, M., … Bellwood, D. R. (2014). Functional over-redundancy and high functional vulnerability in global fish faunas on tropical reefs. *Proceedings of the National Academy of Sciences of the United States of America*, *111*(38), 13757–13762. doi: 10.1073/pnas.1317625111

Mourier, J., Maynard, J., Parravicini, V., Ballesta, L., Clua, E., Domeier, M. L., & Planes, S. (2016). Extreme Inverted Trophic Pyramid of Reef Sharks Supported by Spawning Groupers. *Current Biology*, *26*(15), 2011–2016. doi: 10.1016/j.cub.2016.05.058

Mumby, P. J., Dahlgren, C. P., Harborne, A. R., Kappel, C. V., Micheli, F., Brumbaugh, D. R., … Gill, A. B. (2006). Fishing, Trophic Cascades, and the Process of Grazing on Coral Reefs. *Science*, *311*(5757), 98–101. doi: 10.1126/science.1121129

Mumby, P. J., & Steneck, R. S. (2018). Paradigm lost: Dynamic nutrients and missing detritus on coral reefs. *BioScience*, *68*(7), 487–495. doi: 10.1093/biosci/biy055

Munch, S. B., Giron-Nava, A., & Sugihara, G. (2018). Nonlinear dynamics and noise in fisheries recruitment: A global meta-analysis. *Fish and Fisheries*, *19*(6), 964–973. doi: 10.1111/faf.12304

Munro, J. L., & Pauly, D. (1983). A Simple Method for Comparing the Growth of Fishes and Invertebrates. *Fishbyte*, *1*(1), 5–6.

Munro, J. L., & Williams, D. M. (1985). Assessment and managements of coral reef fishes: biological, environmental and socio-economic aspects. *Proceedings of the Fifth International Coral Reef Symposium*, *4*, 544–581.

Myers, R. A., & Barrowman, N. J. (1996). Is fish recruitment related to spawner abundance? *Fishery Bulletin*, *94*(4), 707–724.

Myers, R. A., & Worm, B. (2003). Rapid worldwide depletion of predatory fish communities. *Nature*, *423*(6937), 280–283. doi: 10.1038/nature01610

Nash, K. L., & Graham, N. A. J. (2016). Ecological indicators for coral reef fisheries management. *Fish*

and Fisheries, *17*(4), 1029–1054. doi: 10.1111/faf.12157

Nash, K. L., Graham, N. A. J., Wilson, S. K., & Bellwood, D. R. (2013). Cross-scale Habitat Structure Drives Fish Body Size Distributions on Coral Reefs. *Ecosystems*, *16*(3), 478–490. doi: 10.1007/s10021-012-9625-0

Newton, K., Côté, I. M., Pilling, G. M., Jennings, S., & Dulvy, N. K. (2007). Current and Future Sustainability of Island Coral Reef Fisheries. *Current Biology*, *17*(7), 655–658. doi: 10.1016/j.cub.2007.02.054

Norström, A. V., Nyström, M., Jouffray, J. B., Folke, C., Graham, N. A. J., Moberg, F., … Williams, G. J. (2016). Guiding coral reef futures in the Anthropocene. *Frontiers in Ecology and the Environment*, *14*(9), 490–498. doi: 10.1002/fee.1427

Nunes, L. T., Morais, R. A., Longo, O., Sabino, J., & Floeter, S. R. (2020). Habitat and community structure modulate fish interactions in a neotropical clearwater river. *Neotropical Ichthyology*, *18(1)*, 1–20. doi: 10.1590/1982-0224-2019-0127

O'Connor, M. I., Gonzalez, A., Byrnes, J. E. K., Cardinale, B. J., Duffy, J. E., Gamfeldt, L., … Dolan, K. L. (2017). A general biodiversity-function relationship is mediated by trophic level. *Oikos*, *126*(1), 18–31. doi: 10.1111/oik.03652

O'Connor, S., Ono, R., & Clarkson, C. (2011). Pelagic Fishing at 42,000 Years Before the Present and the Maritime Skills of Modern Humans. *Science*, *334*(6059), 1117–1121. doi: 10.1126/science.1207703

Odum, H. T., & Odum, E. P. (1955). Trophic Structure and Productivity of a Windward Coral Reef Community on Eniwetok Atoll. *Ecological Monographs*, *25*(3), 291–320. doi: 10.2307/1943285

Odum, H. T., & Odum, E. P. (1959). Principles and concepts pertaining to energy in ecological systems. In E. P. Odum (Ed.), *Fundamentals of Ecology* (2nd ed., pp. 43–87). Philadelphia and London: W. B. Saunders Company.

Opitz, S. (1996). Trophic Interactions in Caribbean Coral Reefs L. In *ICLARM Techinical Report* (Vol. 43). Manila, Philippines: International Center for Living Aquatic Resources Management.

Paradis, E., Claude, J., & Strimmer, K. (2004). APE: analyses of phylogenetics and evolution in R language. *Bioinformatics*, *20*, 289–290. doi: 10.1093/bioinformatics/btg412

Parravicini, V., Kulbicki, M., Bellwood, D. R., Friedlander, A. M., Arias-Gonzalez, J. E., Chabanet, P., … Mouillot, D. (2013). Global patterns and predictors of tropical reef fish species richness. *Ecography*, *36*(12), 1254–1262. doi: 10.1111/j.1600-0587.2013.00291.x

Parravicini, Valeriano, Villéger, S., McClanahan, T. R., Arias-González, J. E., Bellwood, D. R., Belmaker, J., … Mouillot, D. (2014). Global mismatch between species richness and vulnerability of reef fish assemblages. *Ecology Letters*, *17*(9), 1101–1110. doi: 10.1111/ele.12316

Pauly, D. (1979). Gill size and temperature as governing factors in fish growth: a generalization of von Bertalanffy´s growth formula. *Berichte Aus Dem Institut Für Meereskunde Kiel*, Vol. 63, pp. 1–156.

Pauly, D. (1980a). A new methodology for rapidly acquiring basic information on tropical fish stocks: growth, mortality and stock-recruitment relationships. In P. M. Roedel & S. B. Saila (Eds.), *Stock assessment for tropical small-scale fisheries* (pp. 154–172). Kingston, Rhode Island, USA: International Center for Marine Resource Development.

Pauly, D. (1980b). On the Interrelationships between Natural Mortality, Growth Parameters, and Mean Environmental Temparature in 175 Fish Stocks. *ICES Journal of Marine Science*, *39*(2), 175–192.

Pauly, D. (1998). Tropical fishes: patterns and propensities. *Journal of Fish Biology*, *53*, 1–17. doi: 10.1006/jfbi.1998.0810

Pauly, D., Christensen, V., Guénette, S., Pitcher, T. J., Sumaila, U. R., Walters, C. J., … Zeller, D. (2002). Towards sustainability in world fisheries. *Nature*, *418*(6898), 689–695. doi: 10.1038/nature01017

Pauly, D., & Morgan, G. R. (1987). *Length-Based Methods in Fisheries Research*. Manila, Philippines: International Center for Living Aquatic Resources Management.

Pauly, D., & Zeller, D. (2014). Accurate catches and the sustainability of coral reef fisheries. *Current Opinion in Environmental Sustainability*, *7*, 44–51. doi: 10.1016/j.cosust.2013.11.027

Pella, J. J., & Tomlinson, P. K. (1969). A generalized stock production model. *IATTC Bulletin*, Vol. 13, p. 83.

Pinheiro, J., Bates, D., DebRoy, S., Sarkar, D., & R Core Team. (2017). *nlme: Linear and Nonlinear Mixed Effects Models*. R package version 3.1-131

Polis, G. A., Anderson, W. B., & Holt, R. D. (1997). Toward an Integration of Landscape and Food Web Ecology: The Dynamics of Spatially Subsidized Food Webs. *Annual Review of Ecology and Systematics*, *28*(1), 289–316. doi: 10.1146/annurev.ecolsys.28.1.289

Pollom, R. A., & Rose, G. A. (2016). A global review of the spatial, taxonomic, and temporal scope of freshwater fisheries hydroacoustics research. *Environmental Reviews*, *24*(3), 333–347. doi: 10.1139/er-2016-0017

Polovina, J. J. (1984). Coral Reefs Model of a Coral Reef Ecosystem. *Coral Reefs*, *3*, 1–11. doi: 10.1007/bf00306135

Polunin, N. V. C. (1996). Trophodynamics of reef fisheries productivity. In N. V. C. Polunin & C. M. Roberts (Eds.), *Reef Fisheries* (Vol. 20, pp. 113–135). doi: 10.1007/978-94-015-8779-2_5

Pratchett, M. S. (2010). Changes in coral assemblages during an outbreak of Acanthaster planci at Lizard Island, northern Great Barrier Reef (1995-1999). *Coral Reefs*, *29*(3), 717–725. doi: 10.1007/s00338-010-0602-9

Pratchett, M. S., Munday, P., Wilson, S., Graham, N., Cinner, J., Bellwood, D., … Mcclanahan, T. R. (2008). Effects Of Climate-Induced Coral Bleaching On Coral-Reef Fishes – Ecological And Economic Consequences. *Oceanography and Marine Biology: An Annual Review*, *46*, 251–296. doi: 10.1201/9781420065756.ch6

Pratchett, M. S., Thompson, C. A., Hoey, A. S., Cowman, P. F., & Wilson, S. K. (2018). Effects of coral bleaching and coral loss on the structure and function of reef fish assemblages. In *Coral Bleaching* (pp. 265–293). Springer.

R Core Team. (2019). *R: A language and environment for statistical computing*. Retrieved from http://www.r-project.org/

Randall, J. E. (1967). Food habits of reef fishes of the West Indies. *Studies of Tropical Oceanography*, *5*, 665–847.

Randall, J. E. (1997). *Fishes of the Great Barrier Reef and Coral Sea* (2nd ed.). University of Hawai'i Press.

Revell, L. J. (2012). phytools: An R package for phylogenetic comparative biology (and other things). *Methods in Ecology and Evolution*, *3*(2), 217–223. doi: 10.1111/j.2041-210X.2011.00169.x

Richardson, L. E., Graham, N. A. J., Pratchett, M. S., Eurich, J. G., & Hoey, A. S. (2018). Mass coral bleaching causes biotic homogenization of reef fish assemblages. *Global Change Biology*, *24*(7), 3117–3129. doi: 10.1111/gcb.14119

Richter, C., Wunsch, M., Rasheed, M., Kötter, I., & Badran, M. I. (2001). Endoscopic exploration of Red Sea coral reefs reveals dense populations of cavity-dwelling sponges. *Nature*, *413*(6857), 726–730. doi: 10.1038/35099547

Ricker, W. E. . (1946). Production and Utilization of Fish Populations. *Ecological Monographs*, *16*(4), 373–391.

Ricker, W. E. (1954). Stock and Recruitment. *Journal of the Fisheries Research Board of Canada*, *11*(5), 559–623.

Ricker, W. E. (1979). Growth Rates and Models. In W. S. Hoar, D. J. Randall, & J. R. Brett (Eds.), *Fish Physiology: Bioenergetics and Growth* (Vol. 8, pp. 677–743). doi: 10.1016/S1546-5098(08)60034-5

Robertson, D. R. (1982). Fish Feces as Fish Food on a Pacific Coral Reef. *Marine Ecology Progress Series*, *7*, 253–265. doi: 10.3354/meps007253

Robertson, D. R. (1990). Differences in the seasonalities of spawning and recruitment of some small neotropical reef fishes. *Journal of Experimental Marine Biology and Ecology*, *144*(1), 49–62.

Robertson, D. R. (2008). Global biogeographical data bases on marine fishes: Caveat emptor. *Diversity and Distributions*, *14(6)*, 891–892. doi: 10.1111/j.1472-4642.2008.00519.x

Robertson, D. R., & Polunin, N. V. C. (1981). Coexistence: Symbiotic sharing of feeding territories and algal food by some coral reef fishes from the Western Indian Ocean. *Marine Biology*, *62*(2–3), 185–195. doi: 10.1007/BF00388182

Robinson, J. P. W., Williams, I. D., Edwards, A. M., McPherson, J., Yeager, L., Vigliola, L., … Baum, J. K. (2017). Fishing degrades size structure of coral reef fish communities. *Global Change Biology*, *23*(3), 1009–1022. doi: 10.1111/gcb.13482

Robinson, J. P. W., Wilson, S. K., Jennings, S., & Graham, N. A. J. (2019). Thermal stress induces persistently altered coral reef fish assemblages. *Global Change Biology*, *25*(8), 2739–2750. doi: 10.1111/gcb.14704

Robinson, J. P. W., Wilson, S. K., Robinson, J., Gerry, C., Lucas, J., Assan, C., … Graham, N. A. J. (2019). Productive instability of coral reef fisheries after climate-driven regime shifts. *Nature Ecology and Evolution*, *3*(2), 183–190. doi: 10.1038/s41559-018-0715-z

Roedel, P. M., & Saila, S. B. (Eds.). (1980). *Stock assessment for tropical small-scale fisheries*. Kingston, Rhode Island, USA: International Center for Marine Resource Development.

Roff, D. A. (1992). *The Evolution of Life Histories: Theory and Analysis*. London: Chapman & Hall.

Rogers, A., Blanchard, J. L., & Mumby, P. J. (2014). Vulnerability of coral reef fisheries to a loss of structural complexity. *Current Biology*, *24*(9), 1000–1005. doi: 10.1016/j.cub.2014.03.026

Rogers, A., Blanchard, J. L., & Mumby, P. J. (2018). Fisheries productivity under progressive coral reef degradation. *Journal of Applied Ecology*, *55*(3), 1041–1049. doi: 10.1111/1365-2664.13051

Rogers, A., Blanchard, J. L., Newman, S. P., Dryden, C. S., & Mumby, P. J. (2018). High refuge availability on coral reefs increases the vulnerability of reef-associated predators to overexploitation. *Ecology*, *99*(2), 450–463. doi: 10.1002/ecy.2103

Rougerie, F., & Wauthy, B. (1993). The endo-upwelling concept: from geothermal convection to reef construction. *Coral Reefs*, *12*(1), 19–30. doi: 10.1007/BF00303781

Rummer, J. L., Couturier, C. S., Stecyk, J. A. W., Gardiner, N. M., Kinch, J. P., Nilsson, G. E., & Munday, P. L. (2014). Life on the edge: thermal optima for aerobic scope of equatorial reef fishes are close to current day temperatures. *Global Change Biology*, *20*(4), 1055–1066. doi: 10.1111/gcb.12455

Russ, G. R. (1984). A Review of Coral Reef Fisheries. *UNESCO Reports in Marine Science*, *27*, 74–92.

Russ, G. R., & Alcala, A. C. (2003). Marine reserves: rates and patterns of recovery and decline of predatory fish, 1983–2000. *Ecological Applications*, *13*(6), 1553–1565. doi: 10.1890/01-5341

Russ, G. R., & Alcala, A. C. (2010). Decadal-scale rebuilding of predator biomass in Philippine marine reserves. *Oecologia*, *163*(4), 1103–1106. doi: 10.1007/s00442-010-1692-3

Russ, G. R., Aller-Rojas, O. D., Rizzari, J. R., & Alcala, A. C. (2017). Off-reef planktivorous reef fishes respond positively to decadal-scale no-take marine reserve protection and negatively to benthic habitat change. *Marine Ecology*, *38*(3), 1–14. doi: 10.1111/maec.12442

Russ, G. R., Questel, S. L. A., Rizzari, J. R., & Alcala, A. C. (2015). The parrotfish–coral relationship: refuting the ubiquity of a prevailing paradigm. *Marine Biology*, *162*(10), 2029–2045. doi: 10.1007/s00227-015-2728-3

Russ, G. R., Stockwell, B., & Alcala, A. C. (2005). Inferring versus measuring rates of recovery in no-take marine reserves. *Marine Ecology Progress Series*, *292*, 1–12. doi: 10.3354/meps292001

Ruttenberg, B. I., Adam, T. C., Duran, A., & Burkepile, D. E. (2019). Identity of coral reef herbivores drives variation in ecological processes over multiple spatial scales. *Ecological Applications*, *29*(4), e01893.

Sale, Peter F., Cowen, R. K., Danilowicz, B. S., Jones, G. P., Kritzer, J. P., Lindeman, K. C., … Steneck, R. S. (2005). Critical science gaps impede use of no-take fishery reserves. *Trends in Ecology and Evolution*, *20*(2), 74–80. doi: 10.1016/j.tree.2004.11.007

Samoilys, M. A. (1997). Movement in a large predatory fish: coral trout, *Plectropomus leopardus* (Pisces: Serranidae), on Heron Reef, Australia. *Coral Reefs*, *16*(3), 151–158.

Sandin, S. A., Smith, J. E., DeMartini, E. E., Dinsdale, E. A., Donner, S. D., Friedlander, A. M., … Sala, E. (2008). Baselines and degradation of coral reefs in the Northern Line Islands. *PLoS ONE*, *3*(2), e1548. doi: 10.1371/journal.pone.0001548

Sargent, M. C., & Austin, T. S. (1954). Biologic Economy of Coral Reefs. In *Bikini and Nearby Atolls, Marshall Islands. Geological Survey Professional Paper 260-E* (pp. 293–300).

Savage, V. M., Gillooly, J. F., Brown, J. H., West, G. B., & Charnov, E. L. (2004). Effects of Body Size and Temperature on Population Growth. *The American Naturalist*, *163*(3), 429–441. doi: doi: 10.1086/381872

Savage, V. M., Gillooly, J. F., Woodruff, W. H., West, G. B., Allen, A. P., Enquist, B. J., & Brown, J. H. (2004). The predominance of quarter-power scaling in biology. *Functional Ecology*, *18*(2), 257–282. doi: 10.1111/j.0269-8463.2004.00856.x

Schmidt-Nielsen, K. (1984). *Scaling: why is animal size so important?* Cambridge: Cambridge University Press.

Schnute, J. T., & Richards, L. (2002). Surplus production models. In P. H. & J. Reynolds (Ed.), *Handbook of Fish Biology & Fisheries* (pp. 105–126). Blackwell Publishing Ltd.

Schwamborn, S. H. L., & Ferreira, B. P. (2002). Age structure and growth of the dusky damselfish, *Stegastes fuscus*, from Tamandaré reefs, Pernambuco, Brazil. *Environmental Biology of Fishes*, *63*(1), 79–88. doi: 10.1023/A:1013851532298

Scott, B., Marteinsdottir, G., & Wright, P. (1999). Potential effects of maternal factors on spawning stock–recruitment relationships under varying fishing pressure. *Canadian Journal of Fisheries and Aquatic Sciences*, *56*(10), 1882–1890. doi: 10.1139/f99-125

Steneck, R. S., Arnold, S. N., & Mumby, P. J. (2014). Experiment mimics fishing on parrotfish: insights on coral reef recovery and alternative attractors. *Marine Ecology Progress Series*, *506*, 115–127.

Streit, R. P., Cumming, G. S., & Bellwood, D. R. (2019). Patchy delivery of functions undermines functional redundancy in a high diversity system. *Functional Ecology*, *33*(6), 1144–1155. doi: 10.1111/1365-2435.13322

Stuart-Smith, R. D., Brown, C. J., Ceccarelli, D. M., & Edgar, G. J. (2018). Ecosystem restructuring along the Great Barrier Reef following mass coral bleaching. *Nature*, *560*(7716), 92–96. doi: 10.1038/s41586-018-0359-9

Stuart-Smith, R. D., Edgar, G. J., & Bates, A. E. (2017). Thermal limits to the geographic distributions of shallow-water marine species. *Nature Ecology and Evolution*, *1*(12), 1846–1852. doi: 10.1038/s41559-017-0353-x

Subbey, S., Devine, J. A., Schaarschmidt, U., & Nash, R. D. M. (2014). Modelling and forecasting stock-recruitment: current and future perspectives. *ICES Journal of Marine Science*, *71*(8), 2307–2322. doi: 10.1093/icesjms/fsu148

Symonds, M. R. E., & Blomberg, S. P. (2014). A Primer on Phylogenetic Generalised Least Squares. In L. Z. Garamszegi (Ed.), *Modern Phylogenetic Comparative Methods and their Application in Evolutionary Biology* (pp. 105–130). doi: 10.1007/978-3-662-43550-2

Szuwalski, C. S., Vert-Pre, K. A., Punt, A. E., Branch, T. A., & Hilborn, R. (2015). Examining common assumptions about recruitment: a meta-analysis of recruitment dynamics for worldwide marine fisheries. *Fish and Fisheries*, *16*(4), 633–648. doi: 10.1111/faf.12083

Takeuchi, Y., Ochi, H., Kohda, M., Sinyinza, D., & Hori, M. (2010). A 20-year census of a rocky littoral fish community in Lake Tanganyika. *Ecology of Freshwater Fish*, *19*(2), 239–248. doi:

10.1111/j.1600-0633.2010.00408.x

Taylor, B. M., Lindfield, S. J., & Choat, J. H. (2015). Hierarchical and scale-dependent effects of fishing pressure and environment on the structure and size distribution of parrotfish communities. *Ecography*, *38*(5), 520–530. doi: 10.1111/ecog.01093

Taylor, B.M., Benkwitt, C.E., Choat, H., Clements, K., Graham, N.A.J., & Meekan, M.G. (2020) Synchronous biological feedbacks in parrotfishes associated with pantropical coral bleaching. *Global Change Biology, 26*, 1285–1294. doi: 10.1111/gcb.14909

Tebbett, S. B., Bellwood, D. R., & Purcell, S. W. (2018). Sediment addition drives declines in algal turf yield to herbivorous coral reef fishes: implications for reefs and reef fisheries. *Coral Reefs*, *37*(3), 929–937. doi: 10.1007/s00338-018-1718-6

Tebbett, S. B., Streit, R. P., & Bellwood, D. R. (2020). A 3D perspective on sediment accumulation in algal turfs: Implications of coral reef flattening. *Journal of Ecology*, *108*(1), 70–80. doi: 10.1111/1365-2745.13235

Teh, L. S. L., Teh, L. C. L., & Sumaila, U. R. (2013). A Global Estimate of the Number of Coral Reef Fishers. *PLoS ONE*, *8*(6). doi: 10.1371/journal.pone.0065397

Teresa, F. B., Romero, R. D. M., Casatti, L., & Sabino, J. (2011). Fish as indicators of disturbance in streams used for snorkeling activities in a tourist region. *Environmental Management*, *47*(5), 960–968. doi: 10.1007/s00267-011-9641-4

Tewksbury, J. J., Huey, R. B., & Deutsch, C. A. (2008). Putting the Heat on Tropical Animals. *Science*, *320*(5881), 1296–1297. doi: 10.1126/science.1159328

Thiault, L., Mora, C., Cinner, J. E., Cheung, W. W. L., Graham, N. A. J., Januchowski-hartley, F. A., … Claudet, J. (2019). Escaping the perfect storm of simultaneous climate change impacts on agriculture and marine fisheries. *Science Advances*, *5*(11), 1–10. doi: 10.1126/sciadv.aaw9976

Thillainath, E. C., McIlwain, J. L., Wilson, S. K., & Depczynski, M. (2016). Estimating the role of three mesopredatory fishes in coral reef food webs at Ningaloo Reef, Western Australia. *Coral Reefs*, *35*(1), 261–269. doi: 10.1007/s00338-015-1367-y

Thompson, A. A., & Mapstone, B. D. (1997). Observer effects and training in underwater visual surveys of reef fishes. *Marine Ecology Progress Series*, *154*, 53–63. doi: 10.3354/meps154053

Thorson, J. T., Cope, J. M., & Patrick, W. S. (2014). Assessing the quality of life history information in publicly available databases. *Ecological Applications*, *24(1),* 217–226. doi: 10.1890/12-1855.1

Thorson, J. T., Munch, S. B., Cope, J. M., & Gao, J. (2017). Predicting life history parameters for all fishes worldwide. *Ecological Applications*, *27*(8), 2262–2276. doi: 10.1002/eap.1606

Trebilco, R., Baum, J. K., Salomon, A. K., & Dulvy, N. K. (2013). Ecosystem ecology: Size-based constraints on the pyramids of life. *Trends in Ecology and Evolution*, *28*(7), 423–431. doi: 10.1016/j.tree.2013.03.008

Trip, E. L., Choat, J. H., Wilson, D. T., & Robertson, D. R. (2008). Inter-oceanic analysis of demographic variation in a widely distributed Indo-Pacific coral reef fish. *Marine Ecology Progress Series*, *373*, 97–109. doi: 10.3354/meps07755

Trip, E. L., Raubenheimer, D., Clements, K. D., & Choat, J. H. (2011). Reproductive demography of a temperate protogynous and herbivorous fish, *Odax pullus* (Labridae, Odacini). *Marine and Freshwater Research*, *62*(2), 176–186. doi: 10.1071/MF10238

Truong, L., Suthers, I. M., Cruz, D. O., & Smith, J. A. (2017). Plankton supports the majority of fish biomass on temperate rocky reefs. *Marine Biology*, *164*(4), 73. doi: 10.1007/s00227-017-3101-5

Tyberghein, L., Verbruggen, H., Pauly, K., Troupin, C., Mineur, F., & De Clerck, O. (2012). Bio-ORACLE: a global environmental dataset for marine species distribution modelling. *Global Ecology and Biogeography*, *21*(2), 272–281. doi: 10.1111/j.1466-8238.2011.00656.x

Wainwright, P. C., & Bellwood, D. R. (2002). Ecomorphology of feeding in coral reef fishes. In P F Sale (Ed.), *Coral reef fishes: dynamics and diversity in a complex ecosystem* (pp. 33–55). San Diego: Academic Press.

Waldock, C., Stuart-Smith, R. D., Edgar, G. J., Bird, T. J., & Bates, A. E. (2019). The shape of abundance distributions across temperature gradients in reef fishes. *Ecology Letters*, *22*(4), 685–696. doi: 10.1111/ele.13222

Ward-Paige, C., Flemming, J. M., & Lotze, H. K. (2010). Overestimating fish counts by non-instantaneous visual censuses: Consequences for population and community descriptions. *PLoS ONE*, *5*(7), e11722. doi: 10.1371/journal.pone.0011722

Waters, T. F. . (1969). The Turnover Ratio in Production Ecology of Freshwater Invertebrates. *Ecology*,

103(930), 173–185.

West, G. B., Brown, J. H., & Enquist, B. J. (1997). General Model for the Origin of Allometric Scaling Laws in Biology. *Science*, *276*, 122–126. doi: 10.1126/science.276.5309.122

West, G. B., Brown, J. H., & Enquist, B. J. (2001). A general model for ontogenetic growth. *Nature*, *413*(6856), 628–631. doi: 10.1038/35098076

White, C., & Kendall, B. E. (2007). A reassessment of equivalence in yield from marine reserves and traditional fisheries managament. *Oikos*, *116*(12), 2039–2043. doi: 10.1111/j.2007.0030-1299.16167.x

Wickler, S., & Spriggs, M. (1988). Pleistocene human occupation of the Solomon Islands, Melanesia. *Antiquity*, *62*, 703–706.

Wild, C., Huettel, M., Klueter, A., Kremb, S. G., Rasheed, M. Y. M., & Jørgensen, B. B. (2004). Coral mucus functions as an energy carrier and particle trap in the reef ecosystem. *Nature*, *428*(6978), 66–70. doi: 10.1038/nature02344

Williams, G. J., Graham, N. A. J., Jouffray, J.-B., Norström, A. V, Nyström, M., Gove, J. M., … Wedding, L. M. (2019). Coral reef ecology in the Anthropocene. *Functional Ecology*, *33*(6), 1014–1022. doi: 10.1111/1365-2435.13290

Williams, G. J., Sandin, S. A., Zgliczynski, B. J., Fox, M. D., Gove, J. M., Rogers, J. S., … Smith, J. E. (2018). Biophysical drivers of coral trophic depth zonation. *Marine Biology*, *165*(4), 60. doi: 10.1007/s00227-018-3314-2

Williams, I. D., Baum, J. K., Heenan, A., Hanson, K. M., Nadon, M. O., & Brainard, R. E. (2015). Human, Oceanographic and Habitat Drivers of Central and Western Pacific Coral Reef Fish Assemblages. *PLoS ONE*, *10*(4), e0120516. doi: 10.1371/journal.pone.0120516

Wilson, S. K., Bellwood, D. R., Choat, J. H., & Furnas, M. J. (2003). Detritus in the epilithic algal matrix and its use by coral reef fishes. *Oceanography and Marine Biology: An Annual Review*, *41*, 279–309.

Wilson, S. K., Burgess, S. C., Cheal, A. J., Emslie, M., Fisher, R., Miller, I., … Sweatman, H. P. A. (2008). Habitat utilization by coral reef fish: implications for specialists vs. generalists in a changing environment. *Journal of Animal Ecology*, *77*(2), 220–228. doi: 10.1111/j.1365-

2656.2007.01341.x

Wilson, S. K., Fisher, R., Pratchett, M. S., Graham, N. A. J., Dulvy, N. K., Turner, R. A., … Polunin, N. V. C. (2010). Habitat degradation and fishing effects on the size structure of coral reef fish communities. *Ecological Applications*, *20*(2), 442–451. doi: 10.1890/08-2205.1

Wilson, S. K., Fisher, R., Pratchett, M. S., Graham, N. A. J., Dulvy, N. K., Turner, R. A., … Rushton, S. P. (2008). Exploitation and habitat degradation as agents of change within coral reef fish communities. *Global Change Biology*, *14*(12), 2796–2809. doi: 10.1111/j.1365-2486.2008.01696.x

Wilson, S. K., Graham, N. A. J., & Polunin, N. V. C. (2007). Appraisal of visual assessments of habitat complexity and benthic composition on coral reefs. *Marine Biology*, *151*(3), 1069–1076. doi: 10.1007/s00227-006-0538-3

Wilson, S. K., Graham, N. A. J., & Pratchett, M. S. (2013). Susceptibility of butterflyfish to habitat disturbance: do 'chaets' ever prosper. In M. S. Pratchett, M. L. Berumen, & B. . Kapoor (Eds.), *Biology of Butterflyfishes* (pp. 226–245). Boca Raton, FL: CRC Press.

Wilson, S. K., Graham, N. A. J., Pratchett, M. S., Jones, G. P., & Polunin, N. V. C. (2006). Multiple disturbances and the global degradation of coral reefs: Are reef fishes at risk or resilient? *Global Change Biology*, *12*(11), 2220–2234. doi: 10.1111/j.1365-2486.2006.01252.x

Winterbottom, R., Alofs, K. M., & Marseu, A. (2011). Life span, growth and mortality in the western Pacific goby *Trimma benjamini*, and comparisons with *T. nasa*. *Environmental Biology of Fishes*, *91*(3), 295–301. doi: 10.1007/s10641-011-9782-6

Winterbottom, R., & Southcott, L. (2008). Short lifespan and high mortality in the western Pacific coral reef goby *Trimma nasa*. *Marine Ecology Progress Series*, *366*, 203–208. doi: 10.3354/meps07517

Wismer, S., Tebbett, S. B., Streit, R. P., & Bellwood, D. R. (2019). Spatial mismatch in fish and coral loss following 2016 mass coral bleaching. *Science of The Total Environment*, *650*, 1487–1498. doi: 10.1016/j.scitotenv.2018.09.114

Woodson, C. B., Schramski, J. R., & Joye, S. B. (2018). A unifying theory for top-heavy ecosystem structure in the ocean. *Nature Communications*, *9*(1), 23. doi: 10.1038/s41467-017-02450-y

Worm, B., Hilborn, R., Baum, J. K., Branch, T. A., Collie, J. S., Costello, C., … Zeller, D. (2009).

Rebuilding Global Fisheries. *Science*, *325*(5940), 578–585. doi: 10.1126/science.1173146

Wyatt, A. S. J., Lowe, R. J., Humphries, S., & Waite, A. M. (2010). Particulate nutrient fluxes over a fringing coral reef: Relevant scales of phytoplankton Production and mechanisms of supply. *Marine Ecology Progress Series*, *405*(Hatcher 1997), 113–130. doi: 10.3354/meps08508

Wyatt, A. S. J., Waite, A. M., & Humphries, S. (2012). Stable isotope analysis reveals community-level variation in fish trophodynamics across a fringing coral reef. *Coral Reefs*, *31*(4), 1029–1044. doi: 10.1007/s00338-012-0923-y

Yvon-Durocher, G., & Allen, A. P. (2012). Linking community size structure and ecosystem functioning using metabolic theory. *Philosophical Transactions of the Royal Society B: Biological Sciences*, *367(1605)*, 2998–3007. doi: 10.1098/rstb.2012.0246

Zottoli, J., Collie, J., & Fogarty, M. (2020). Measuring the balance between fisheries catch and fish production. *Marine Ecology Progress Series*, 643, 145–158. doi: 10.3354/meps13316

Zuur, A. F., Ieno, E. N., Walker, N. J., Saveliev, A. A., & Smith, G. M. (2009). *Mixed Effects Models and Extensions in Ecology with R*. New York, NY: Springer, New York.

Appendix A: The elusive ‘Darwin’s Paradox’

The outstanding productivity of coral reefs, deeply nested within desert tropical oceans, has captured scientists’ minds. This energetic and nutrient paradox has repeatedly been attributed to Charles Darwin in his 1842 book entitled “*The structure and distribution of coral reefs*” (e.g. de Goeij et al., 2013; McMahon, Thorrold, Houghton, & Berumen, 2016; Mumby & Steneck, 2018; Richter, Wunsch, Rasheed, Kötter, & Badran, 2001; Sammarco, Risk, Schwarcz, & Heikoop, 1999). Indeed, judging from the number of times it has been used in recent years, media articles claiming scientists have ‘solved’ the ‘Darwin’s Paradox’ have become a successful strategy to draw attention to the topic (e.g. Fitch, 2016; Johnson, 2016; Nowak, 2002; Pennisi, 2019). But have we actually solved the ‘Darwin’s Paradox’? Do we even know what it means? Answering these questions requires tracing the origin of the term and clearly defining what ‘the Darwin’s Paradox’ is and what it is not. This is what this appendix endeavours.

In its most recent common form, the ‘Darwin’s Paradox’ is defined as the counterintuitive high productivity, abundance and/or diversity of organisms on coral reefs despite them being situated in nutrient-poor, oligotrophic tropical oceans (e.g. Mumby & Steneck, 2018; Richter et al., 2001). However, Darwin’s “*The structure and distribution of coral reefs”,* the most often cited source of the paradox, is very narrowly focused on the geological origins and features of coral reefs. Geology appeared to be, indeed, Darwin’s main interest before boarding the Beagle, and the geographical distribution of coral reefs appeared to provide data in support of his hypothesis on seamount subsidence and the formation of the different types of reefs. The few explicit ecological excerpts in the book offer little evidence that Darwin was explicitly curious about the ecological productivity of coral reefs. Subsequent mentions of a ‘Coral Reef Problem’ (Davis, 1928) refer to the competing theories attempting to explain the geological origins of coral reefs (of which Darwin’s appeared to be favoured), and also do not appear to address their paradoxical productivity patterns.

The first traceable, explicit mention to the term ‘Darwin’s Paradox’ in the coral reef ecological literature appears relatively recently, in the work of Andrews & Gentien (1982). These authors refer to ‘the Darwin’s question’ when quoting Darwin's (1842) conclusion that “(…) the polypifers in their turn

must prey on some other organic beings; the decrease of which from any cause, would cause a proportionate destruction of the living coral". The fragment quoted by Andrews & Gentien (1982) is one of the few in which Darwin indeed considers patterns and mechanisms other than geological ones. However, even in that case the goal was clearly to explain a geographical pattern: why are coral reefs common in some tropical areas (Indian and Pacific Oceans), but absent from others (East and South Atlantic) (Darwin, 1842). It is also worth noting that Darwin's conjecture above is restricted to the nutrition of corals (or, in his words, 'polypifers'), with no evidence that he was generalising this conjecture to other organisms or to coral reefs as a whole.

Andrews & Gentien (1982) did not specify to which 'Darwin's question' in the quoted excerpt they were referring to. Because their study demonstrated a new upwelling source of nitrogen to corals, they presumably referred to Darwin's conjecture on coral nutrition. Andrews and Gentien's study was subsequently cited by Rougerie & Wauthy (1993) as providing a "solution to Darwin's question concerning functioning", although 'functioning' is not defined. The word 'paradox' is first mentioned (i.e. as 'Old Paradox') in Rougerie & Wauthy (1988), defined as the "huge production/calcification of coral communities surrounded by clear oligotrophic waters". These authors, however, neither attribute the pioneering of this paradox to Darwin, nor to anybody else. Hence, it appears that Sammarco et al. (1999) were the first to explicitly put together the term 'Darwin's Paradox', defining it as "the apparent health of coral reefs in nutrient-poor waters" while attributing it to Darwin (1842). Besides Darwin, Sammarco et al. (1999) cited Andrews & Gentien (1982) and Rougerie & Wauthy (1993) but no other studies in this excerpt. The subsequent work of Richter et al. (2001) repeats the term "Darwin's Paradox" but only references Darwin (1842).

In their seminal study of the trophic structure of coral reef communities from Eniwetok Atoll, Odum & Odum (1955) offer the first account on the apparent contradictory nature of high diversity/low food sources on coral reefs. The authors write that "The coral reef communities of the world are tremendously varied associations of plants and animals growing luxuriantly in tropical waters of impoverished plankton content". Their detailed quantification of the energetics of a coral reef alongside Sargent & Austin (1954) measurements of coral reef photosynthesis provided the basis for the view that coral reefs are steady-state, closed, systems, with very limited energetic or nutrient connections to

adjacent ecosystems (e.g. Lewis, 1977). Furthermore, this perspective highlights the vast photosynthesis gradient existing between coral reefs and the adjacent open ocean (Stoddart, 1969). Stoddart (1969) offered one of the first numerical comparisons of gross productivity rates between coral reefs and the adjacent open ocean, highlighting the perceived productivity gradient, but noting that plankton inputs were largely unknown. The perspective of coral reefs as energetically auto-sufficient was posteriorly emphasised by Emery (1968) and Glynn (1973)'s collections of plankton, both authors concluding that the quantity of plankton flushed through coral reefs on a daily basis was insufficient to respond for the metabolism of coral reef consumers. Although this view of plankton insufficiency has later been challenged by studies such as those of Hamner & Hauri (1981), Andrews & Gentien (1982), Hamner, Jones, Carleton, Hauri, & Williams (1988) and others, as showed in the first paragraph of this appendix, the idea of an unexplained paradoxical productivity on coral reefs still remains. It is also clear, however, that the closed-system perspective of coral reefs and, particularly, the idea of photosynthesis gradients between coral reefs and the open ocean, introduced by Odum & Odum (1955), matches more closely the core idea expressed by the 'Darwin's paradox', i.e. high diversity/productivity on nutrient-poor coral reefs, than Darwin's original, geologically-focused contribution. Therefore, I propose that the term 'Darwin's paradox' should be reserved to Darwin's 1842 conjecture on the then enigmatic nutrition of corals and the distribution of coral reefs, and that what is nowadays referred to as the 'Darwin's paradox' would be most adequately termed the 'Odunian paradox'.

Appendix A References

Andrews, J., & Gentien, P. (1982). Upwelling as a Source of Nutrients for the Great Barrier Reef Ecosystems: A Solution to Darwin's Question? *Marine Ecology Progress Series*, *8*, 257–269. doi: 10.3354/meps008257

Darwin, C. R. . L. S. E. and C. (1842). *The structure and distribution of coral reefs. Being the first part of the geology of the voyage of the Beagle, under the command of Capt. Fitzroy, R.N. during the years 1832 to 1836.* New York: Appleton.

Davis, W. M. (1928). *The coral reef problem*. New York, New York, USA: American Geographical Society.

de Goeij, J. M., van Oevelen, D., Vermeij, M. J. A., Osinga, R., Middelburg, J. J., de Goeij, A. F. P. M., & Admiraal, W. (2013). Surviving in a Marine Desert: The Sponge Loop Retains Resources Within Coral Reefs. *Science*, *342*(6154), 108–110. doi: 10.1126/science.1241981

Emery, A. R. (1968). Preliminary observations on coral reef plankton. *Limnology and Oceanography*, *13*(2), 293–303.

Fitch, C. (2016). Solving "Darwin's Paradox." *Geographical*. Retrieved from: https://geographical.co.uk/nature/oceans/item/1605-solving-darwin-s-paradox

Glynn, P. W. (1973). Ecology of a Caribbean coral reef. The Porites reef-flat biotope: Part II. Plankton community with evidence for depletion. *Marine Biology*, *22*(1), 1–21. doi: 10.1007/BF00388905

Hamner, W. M., & Hauri, I. R. (1981). Effects of island mass: Water flow and plankton pattern around a reef in the Great Barrier Reef lagoon, Australia1. *Limnology and Oceanography*, *26*(6), 1084–1102. doi: 10.4319/lo.1981.26.6.1084

Hamner, W. M., Jones, M. S., Carleton, J. H., Hauri, I. R., & Williams, D. M. B. (1988). Zooplankton, planktivorous fish, and water currents on a windward reef face: Great Barrier Reef, Australia. *Bulletin of Marine Science*, *42*(3), 459–479.

Johnson, A. F. (2016). Solving 'Darwin' s Paradox': why coral island hotspots exist in an oceanic desert. *The Conversation*. Retrieved from: http://theconversation.com/solving-darwins-paradox-why-coral-island-hotspots-exist-in-an-oceanic-desert-54719

Lewis, J. B. (1977). Processes of organic production on coral reefs. *Biological Reviews*, *52*(3), 305–347.

McMahon, K. W., Thorrold, S. R., Houghton, L. A., & Berumen, M. L. (2016). Tracing carbon flow through coral reef food webs using a compound-specific stable isotope approach. *Oecologia*, *180*(3), 809–821. doi: 10.1007/s00442-015-3475-3

Mumby, P. J., & Steneck, R. S. (2018). Paradigm lost: Dynamic nutrients and missing detritus on coral reefs. *BioScience*, *68*(7), 487–495. doi: 10.1093/biosci/biy055

Nowak, R. (2002). Corals play rough over Darwin's paradox. Retrieved from: http://www.newscientist.com/article/mg17523612.100-corals-play-rough-over-darwins-paradox.html

Odum, H. T., & Odum, E. P. (1955). Trophic Structure and Productivity of a Windward Coral Reef Community on Eniwetok Atoll. *Ecological Monographs*, *25*(3), 291–320. doi: 10.2307/1943285

Pennisi, E. (2019). These tiny, mysterious fish may be key to solving coral reef 'paradox.' doi: 10.1126/science.aay1453

Richter, C., Wunsch, M., Rasheed, M., Kötter, I., & Badran, M. I. (2001). Endoscopic exploration of Red Sea coral reefs reveals dense populations of cavity-dwelling sponges. *Nature*, *413*(6857), 726–730. doi: 10.1038/35099547

Rougerie, F., & Wauthy, B. (1988). The Endo-Upwelling Concept: a New Paradigm for Solving an Old Paradox. *Proceedings of the 6th International Coral Reef Symposium, Australia*, *3*, 21–26.

Rougerie, F., & Wauthy, B. (1993). The endo-upwelling concept: from geothermal convection to reef construction. *Coral Reefs*, *12*(1), 19–30. doi: 10.1007/BF00303781

Sammarco, P. W., Risk, M. J., Schwarcz, H. P., & Heikoop, J. M. (1999). Cross-continental shelf trends in coral δ15N on the Great Barrier Reef: Further consideration of the reef nutrient paradox. *Marine Ecology Progress Series*, *180*, 131–138. doi: 10.3354/meps180131

Sargent, M. C., & Austin, T. S. (1954). Biologic Economy of Coral Reefs. In *Bikini and Nearby Atolls, Marshall Islands. Geological Survey Professional Paper 260-E* (pp. 293–300). Retrieved from http://dx.plos.org/10.1371/journal.pone.0102094

Stoddart, D. R. (1969). Ecology and Morphology of Recent Coral Reefs. *Biological Reviews*, *44*(4), 433–498. doi: 10.1111/j.1469-185x.1969.tb00609.x

Appendix B: Supporting Information for Chapter 2

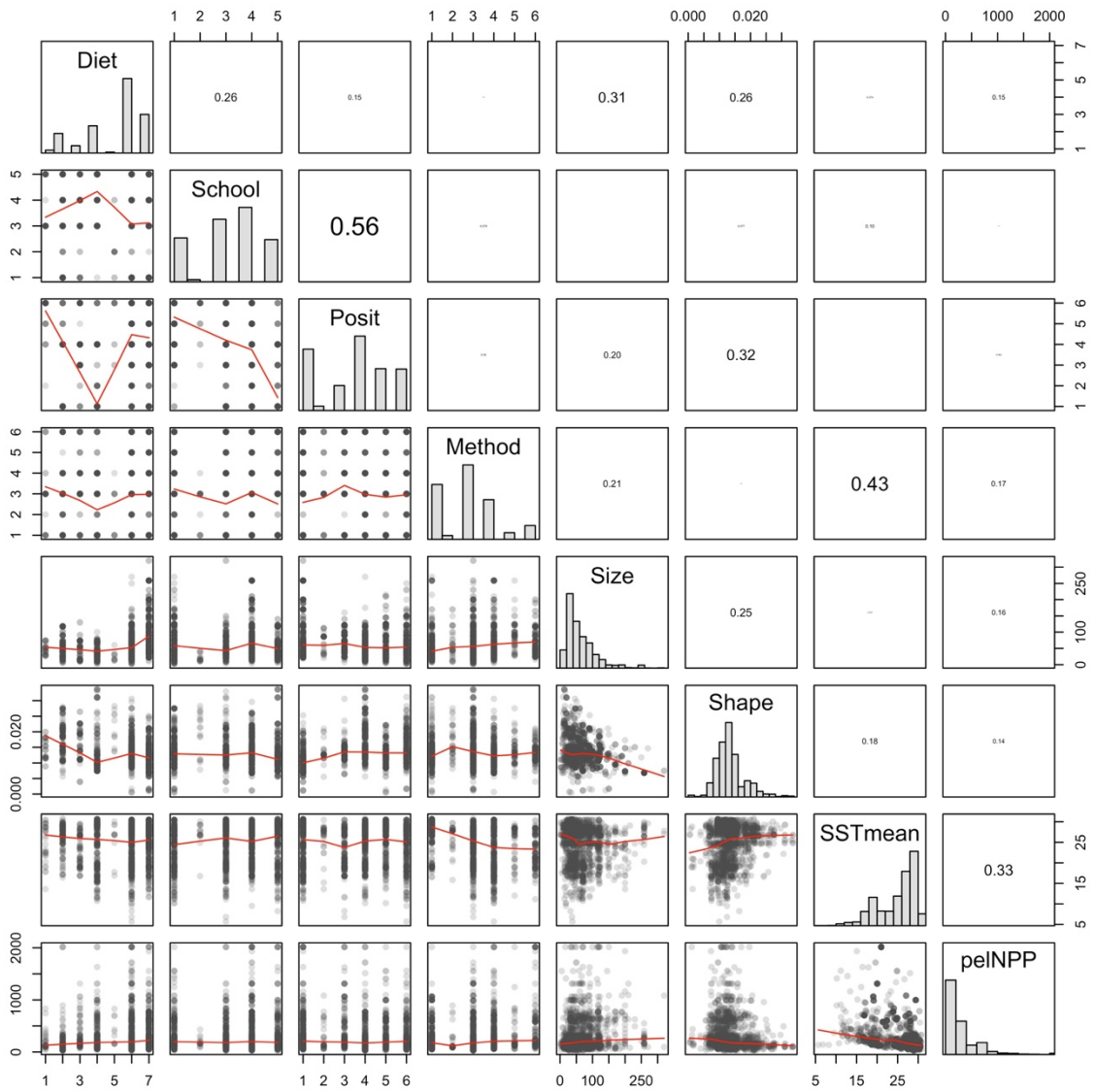

Figure B1: *Pearson's correlation (upper right panels) and relationship (lower left panels) among potential correlates of reef fish growth. The diagonal panels show histograms of each variable. Trend lines are LOWESS smoothers. Diet, from 1 to 7: herbivores/macroalgivores, herbivores/detritivores, omnivores, planktivores, sessile invertivores, mobile invertivores, and fish and cephalopod predators; School = schooling behaviour, from 1 to 5: solitary, pair, small groups, medium groups and large groups; Posit = position relative to the reef, from 1 to 6: pelagic associated, pelagic dwelling, bentho-pelagic associated, bentho-pelagic dwelling, benthic associated and benthic dwelling; Method, from 1 to 6: length-frequency, mark-recapture, otolith rings, unknown, other rings and scale rings; Shape = body form shape; SSTmean = average sea surface temperature; pelNPP = average pelagic net primary productivity.*

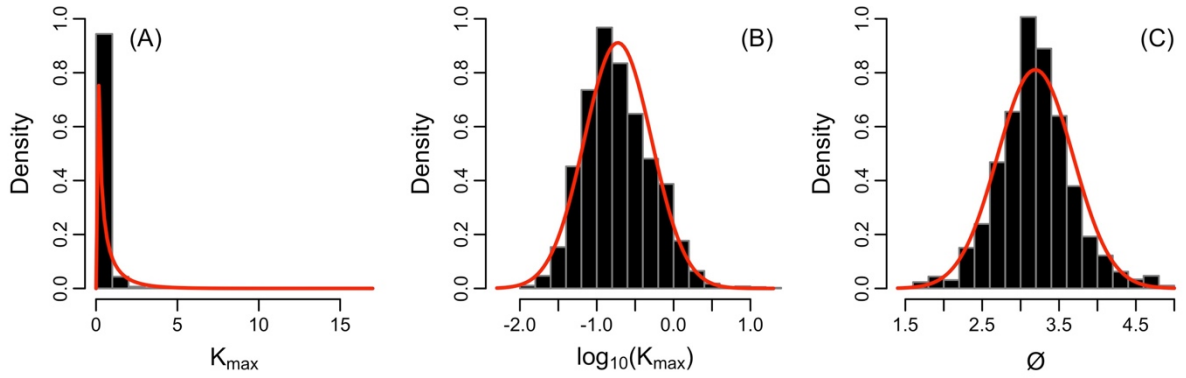

Figure B2: *Histograms and approximate distribution of standardized reef fish growth coefficients.* ***(A)*** K_{max} *is approximately Gamma distributed, whereas* $log_{10}(K_{max})$ ***(B)*** *and* **Ø** ***(C)*** *are approximately Gaussian distributed.*

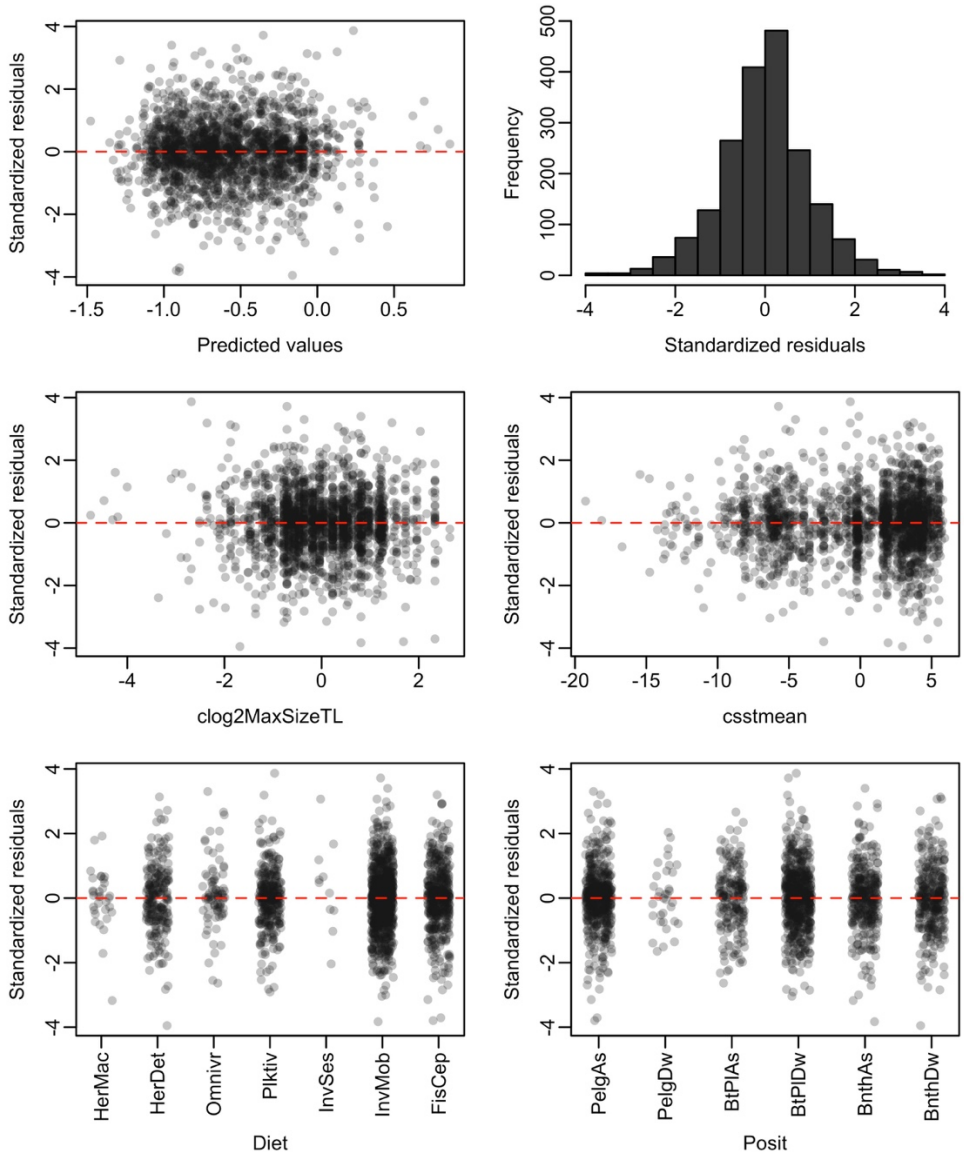

Figure B3: *Model validation procedures for the final PGLS with K_{max} as the response variable. Steps are as described by (Zuur, Ieno, Walker, Saveliev, & Smith, 2009) and include checking for patterns: (upper row) in the standardized residuals against the predicted values and in the distribution of the residuals; and (middle and bottom rows) in the residuals by explanatory variables. No residual patterns were detected in any of these steps. clog2MaxSizeTL = centred log2 of maximum body size; csstmean = entered mean sea surface temperature; HerMac = herbivores/macroalgivores; HerDet = herbivores/detritivores; Omnivr = omnivores; InvSes = sessile invertivores; InvMob = mobile invertivores; FisCep = fish and cephalopod predators; PelgAs = pelagic reef associated; PelgDw = pelagic reef dwelling; BtPlAs = bentho-pelagic reef associated; BtPlDw = bento-pelagic reef dwelling; BnthAs = benthic reef associated; BnthDw = benthic reef dwelling.*

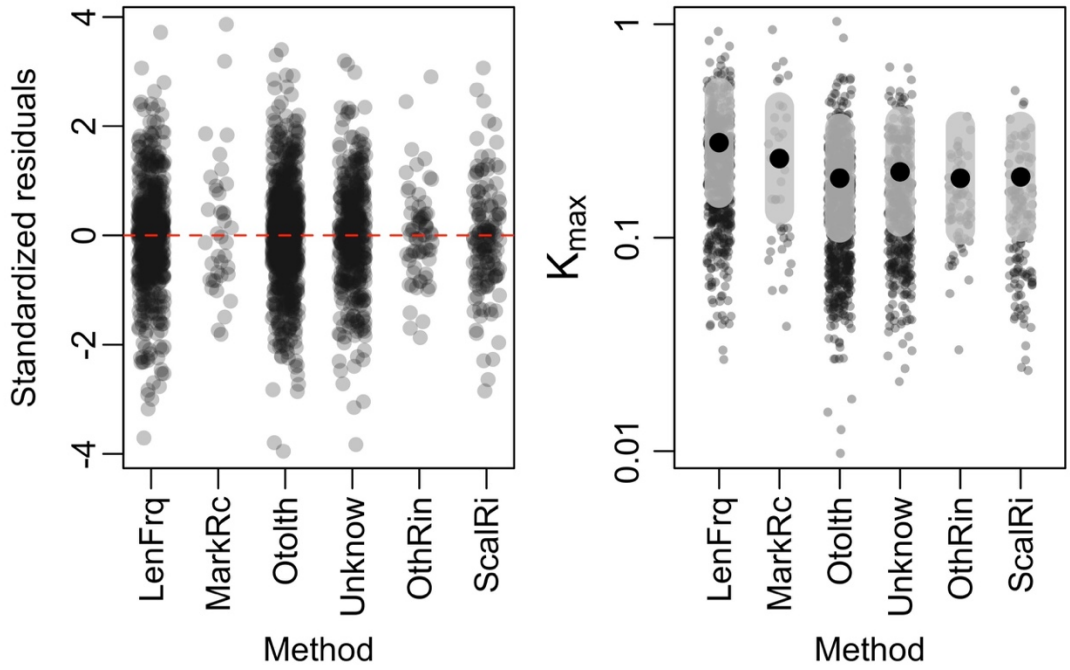

Figure B4: *Standardized residuals from the final PGLS with K_{max} as the response variable, plotted against the explanatory variable method used to derive growth curves (left, continuation of model validation step in* ***Figure B3****); plus the relationship between K_{max} and the method (right). In the right panel the large black dots indicate model predictions (accounting for phylogenetic structure) and the grey bands the 95% confidence intervals of model predictions calculated from model standard errors. The small grey dots are the partial residuals, that is, the raw data after accounting for the effect of method.*

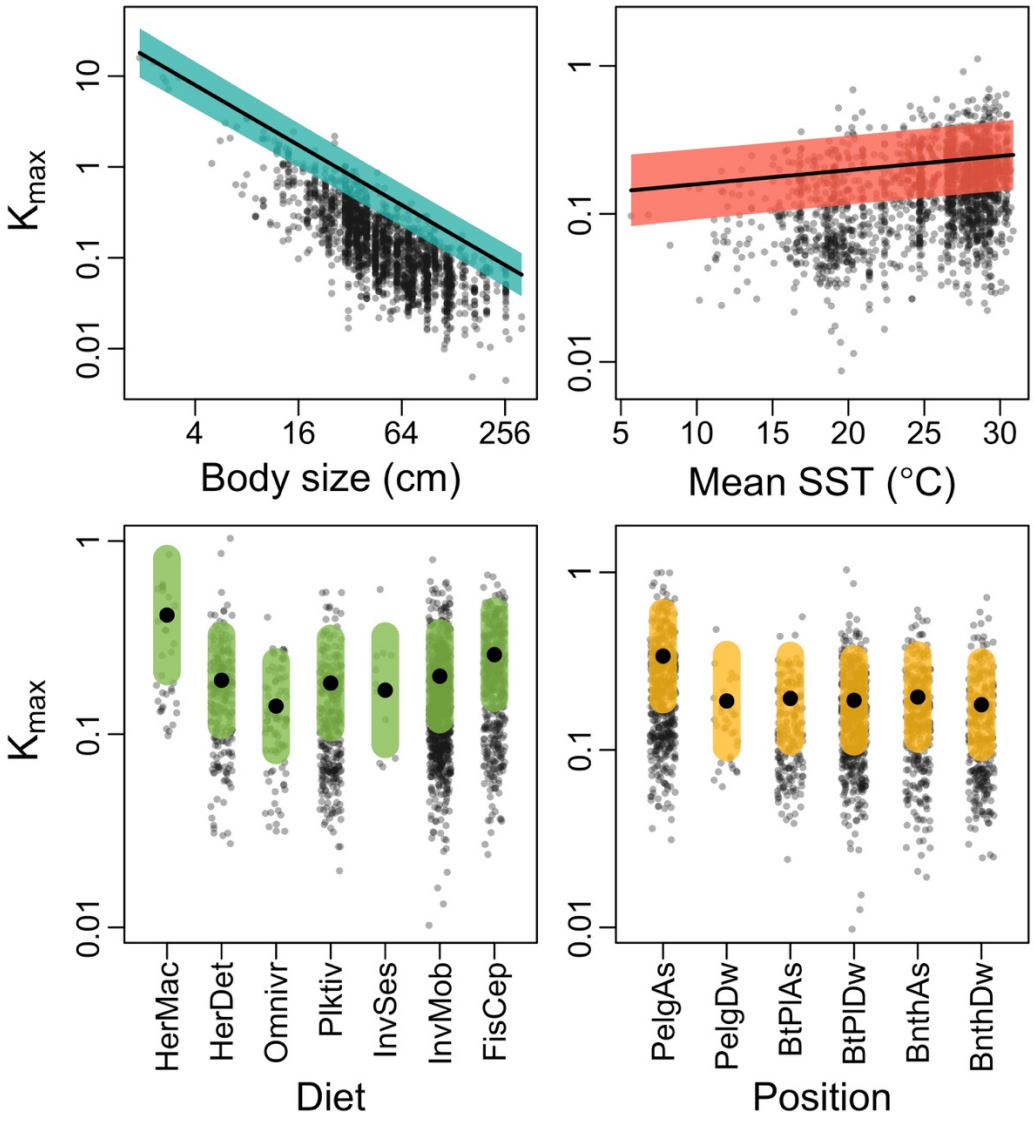

Figure B5: *Relationship between K_{max} and body size, sea surface temperature, diet and position relative to the reef in the final PGLS with data points. Black lines and black dots indicate model predictions (accounting for phylogenetic structure), and coloured bands the 95% confidence intervals of model predictions calculated from model standard errors. The small grey dots are the partial residuals, that is, the raw data after accounting for the effect of the variable in the plot. HerMac = herbivores/macroalgivores; HerDet = herbivores/detritivores; Omnivr = omnivores; InvSes = sessile invertivores; InvMob = mobile invertivores; FisCep = fish and cephalopod predators; PelgAs = pelagic reef associated; PelgDw = pelagic reef dwelling; BtPlAs = bentho-pelagic reef associated; BtPlDw = bento-pelagic reef dwelling; BnthAs = benthic reef associated; BnthDw = benthic reef dwelling.*

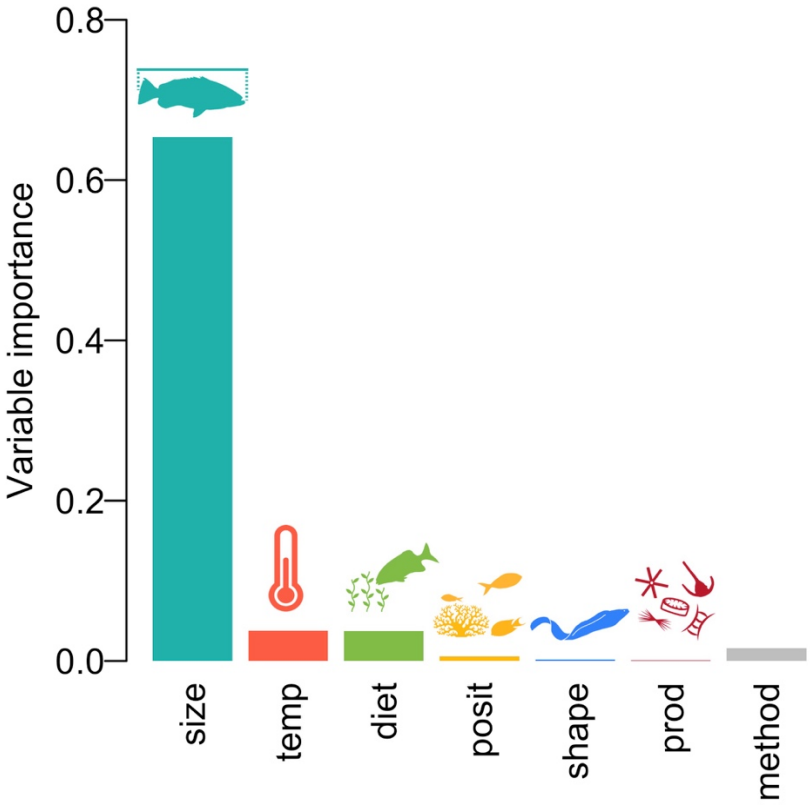

Figure B6: *The importance of each variable in our full model of Ø using a global dataset of reef fish growth. This metric represents, for each variable, the proportion of total variability explained. size = body size, temp = mean sea surface temperature, posit = position relative to the reef, shape = body shape factor, prod = mean pelagic net primary productivity, method = method used to derive the growth curves.*

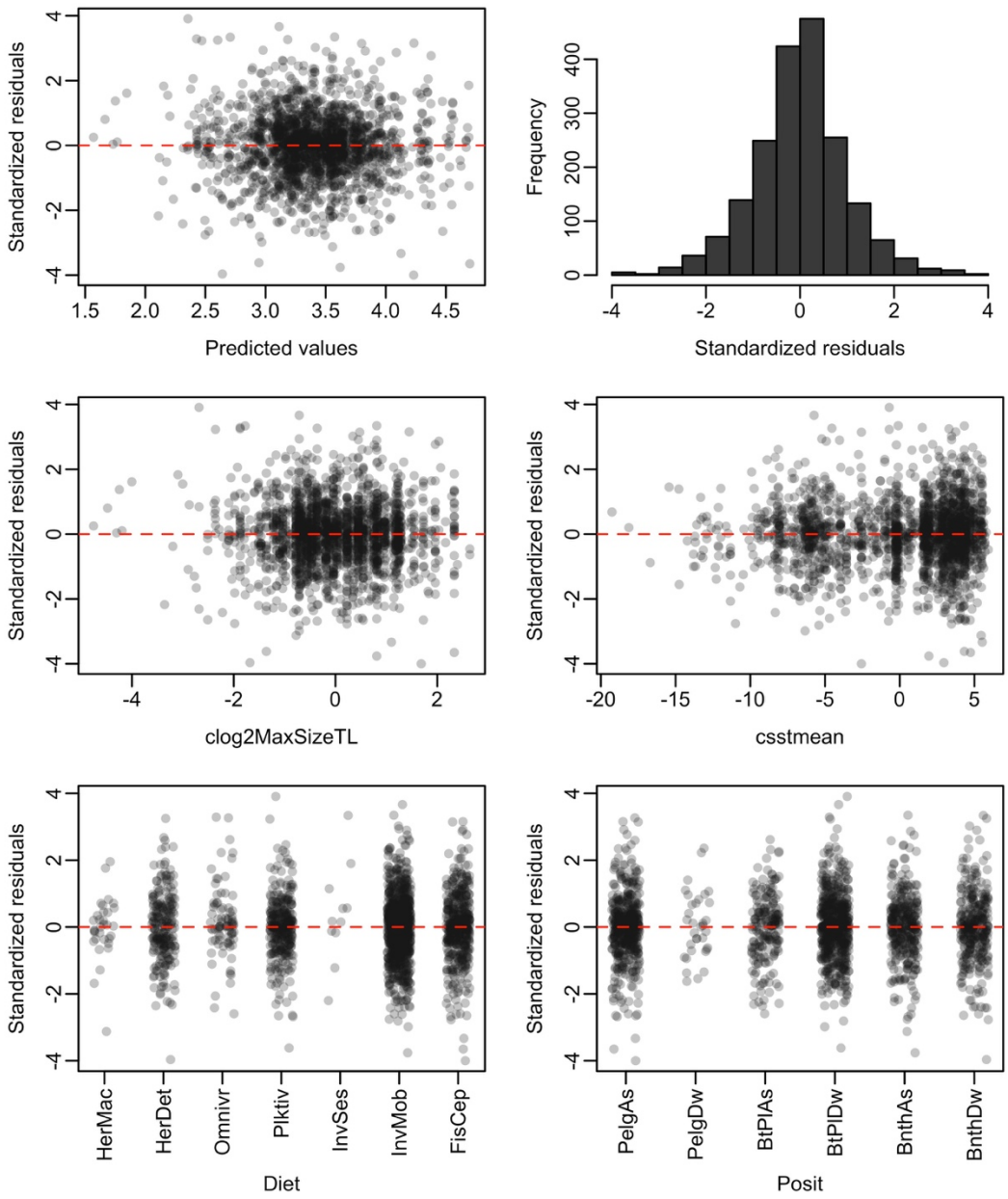

Figure B7: *Model validation procedures for the final PGLS with Ø as the response variable. Steps are as described by* (Zuur et al., 2009) *and include checking for patterns: (upper row) in the standardized residuals against the predicted values and in the distribution of the residuals; and (middle and bottom rows) in the residuals by explanatory variables. No residual patterns were detected in any of these steps. clog2MaxSizeTL = centred $\log_2$ of maximum body size; csstmean = centred mean sea surface temperature; HerMac = herbivores/macroalgivores; HerDet = herbivores/detritivores; Omnivr = omnivores; InvSes = sessile invertivores; InvMob = mobile invertivores; FisCep = fish and cephalopod predators; PelgAs = pelagic reef associated; PelgDw = pelagic reef dwelling; BtPlAs = bentho-pelagic reef associated; BtPlDw = bento-pelagic reef dwelling; BnthAs = benthic reef associated; BnthDw = benthic reef dwelling.*

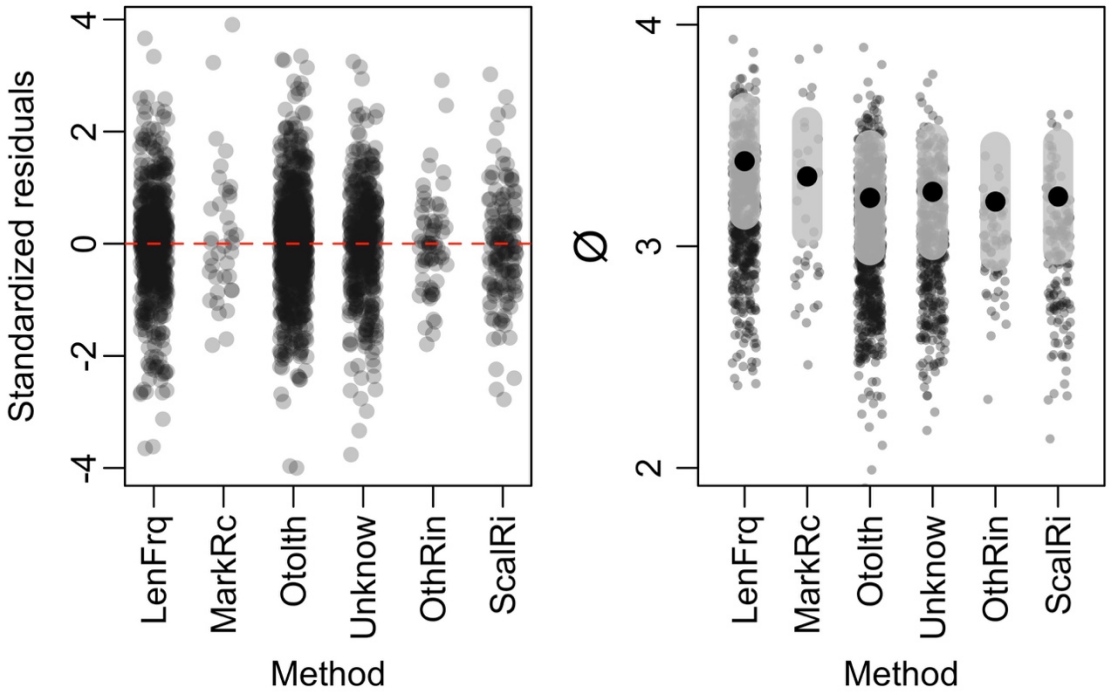

Figure B8: *Standardized residuals from the final PGLS with Ø as the response variable, plotted against the explanatory variable method used to derive growth curves (left, continuation of model validation step in* ***Figure B3****); plus the relationship between Ø and the method (right). In the right panel the large black dots indicate model predictions (accounting for phylogenetic structure) and the grey bands the 95% confidence intervals of model predictions calculated from model standard errors. The small grey dots are the partial residuals, that is, the raw data after accounting for the effect of method.*

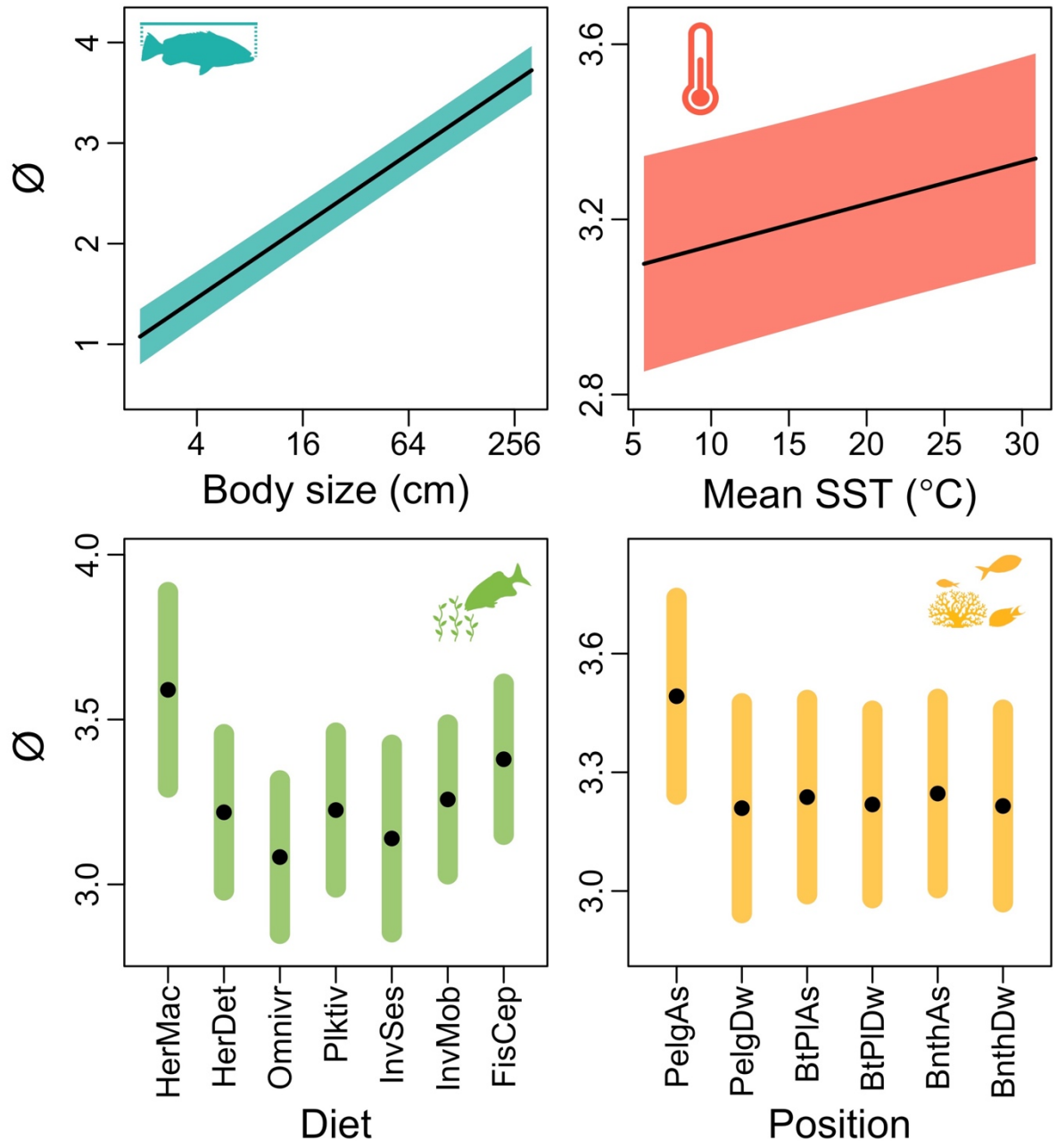

Figure B9: *Relationship between Ø and body size, temperature, diet and position relative to the reef for reef fishes in a PGLS using a global dataset of growth. Note the different y-axis scales. Black lines and black dots indicate model predictions, and coloured bands the 95% confidence intervals of model predictions calculated from model standard errors. HerMac = herbivores/macroalgivores; HerDet = herbivores/detritivores; Omnivr = omnivores; InvSes = sessile invertivores; InvMob = mobile invertivores; FisCep = fish and cephalopod predators; PelgAs = pelagic reef associated; PelgDw = pelagic reef dwelling; BtPlAs = bentho-pelagic reef associated; BtPlDw = bento-pelagic reef dwelling; BnthAs = benthic reef associated; BnthDw = benthic reef dwelling.*

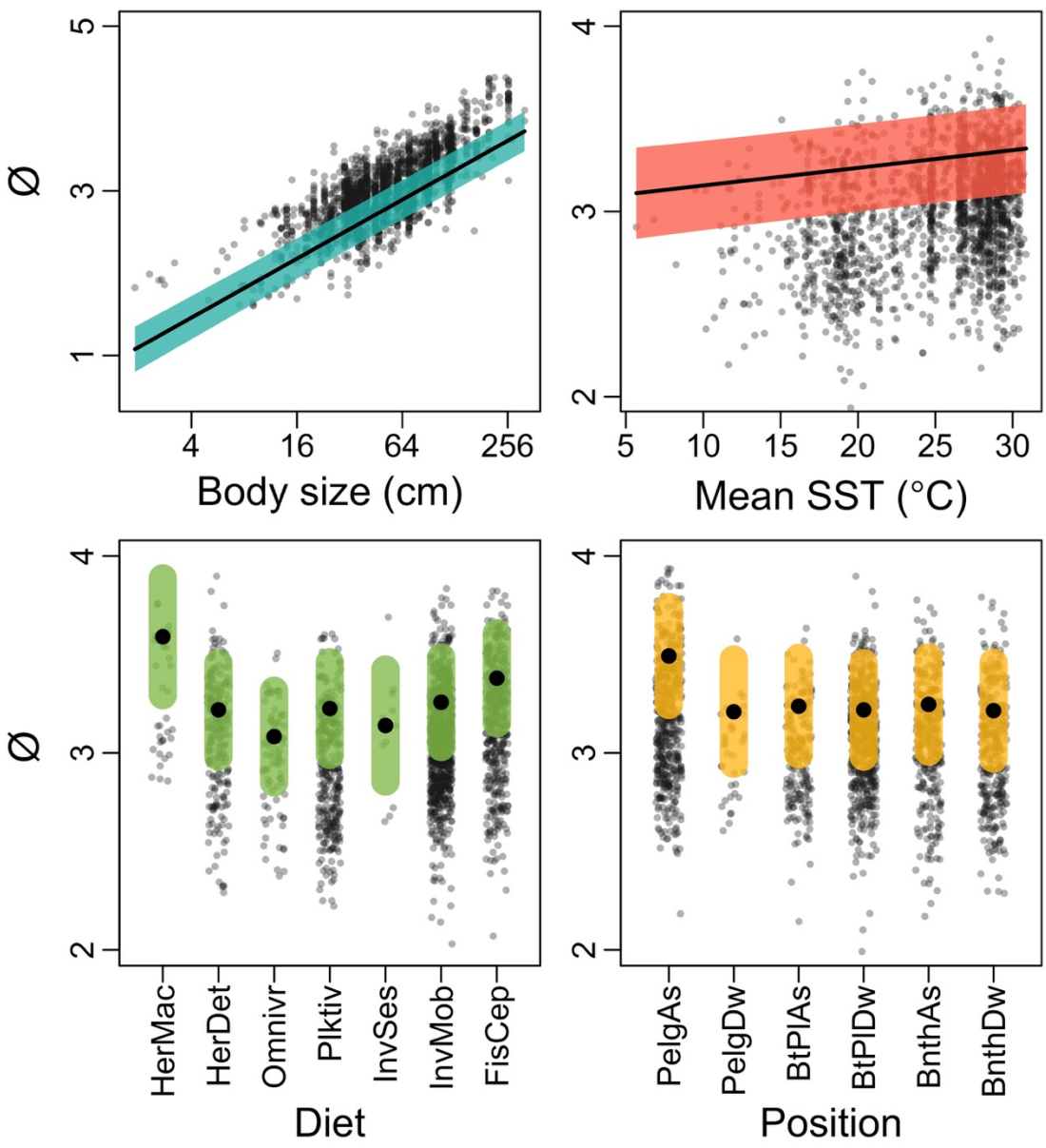

Figure B10: *Relationship between Ø and body size, sea surface temperature, diet and position relative to the reef in the final PGLS with data points. Black lines and black dots indicate model predictions (accounting for phylogenetic structure), and coloured bands the 95% confidence intervals of model predictions calculated from model standard errors. The small grey dots are the partial residuals, that is, the raw data after accounting for the effect of the variable in the plot. HerMac = herbivores/macroalgivores; HerDet = herbivores/detritivores; Omnivr = omnivores; InvSes = sessile invertivores; InvMob = mobile invertivores; FisCep = fish and cephalopod predators; PelgAs = pelagic reef associated; PelgDw = pelagic reef dwelling; BtPlAs = bentho-pelagic reef associated; BtPlDw = bento-pelagic reef dwelling; BnthAs = benthic reef associated; BnthDw = benthic reef dwelling.*

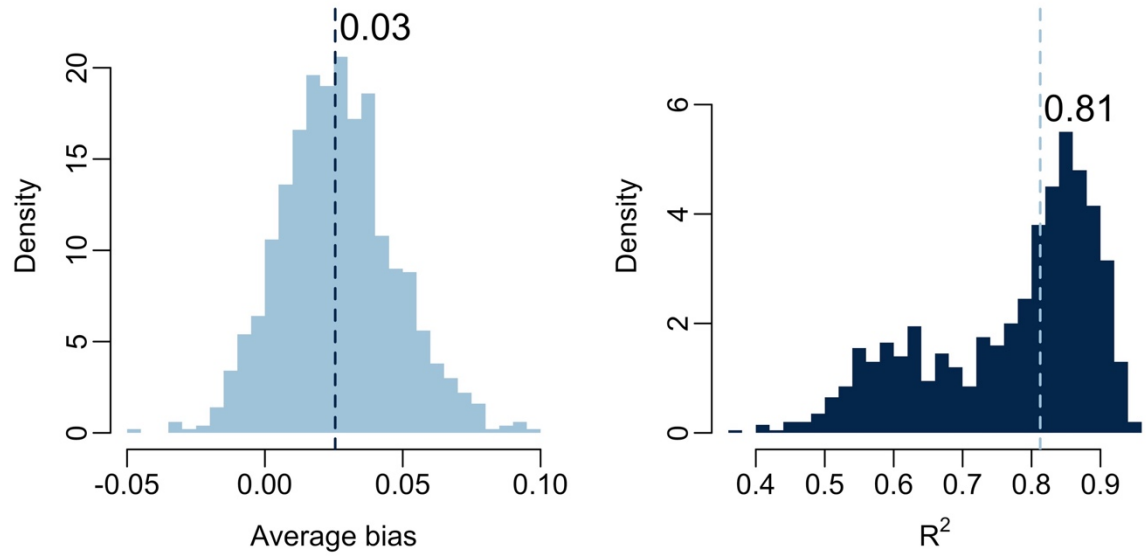

Figure B11: *Cross-validation of XGBoost predictions of growth coefficients K_{max} for reef fishes using a global dataset. Histograms summarize densities of 1,000 cross-validation iterations, each one comprehending (left) the average bias among all data points in the testing datasets and (right) the predicted R2 of the model. The bias metric used was, for each data point, the K_{max} value minus the XGBoost predicted K_{max} and is, thus, in K_{max} units. Dashed vertical lines represent median values across iterations.*

Table B1: *Model selection table of nested submodels of the PGLS used to model K_{max} in reef fishes. Drop models indicate which variables were dropped. Shap = shape factor; Size = Body size; Prod = Primary Productivity; Temp = Sea surface temperature; Method = Method used to obtain the growth curve; Posi = Position relative to the reef.*

Model	Interc.	Shap	Size	Prod	Temp	Diet	Meth	Posi	df	ΔAIC	wAIC
drop.prod	0.018	-4.368	-0.331	-	0.010	+	+	+	21	0.00	0.48
full	0.018	-4.450	-0.331	0.005	0.010	+	+	+	22	1.33	0.25
drop.shape.prod	0.032	-	-0.330	-	0.010	+	+	+	20	1.93	0.18
drop.shape	0.032	-	-0.330	0.004	0.010	+	+	+	21	3.40	0.09
drop.posit	-0.166	-6.410	-0.313	0.006	0.011	+	+	-	17	15.49	0.00
drop.temp	0.066	-3.455	-0.338	-0.003	-	+	+	+	21	20.75	0.00
drop.diet	-0.252	-6.522	-0.310	0.004	0.011	-	+	+	16	29.64	0.00
drop.method	-0.107	-6.416	-0.330	0.009	0.017	+	-	+	17	101.69	0.00
drop.size	-0.290	-1.823	-	0.005	0.017	+	+	+	21	592.82	0.00

Table B2: *Model selection table of nested submodels of the PGLS used to model Ø in reef fishes. Drop models indicate which variables were dropped. Shap = shape factor; Size = Body size; Prod = Primary Productivity; Temp = Sea surface temperature; Method = Method used to obtain the growth curve; Posi = Position relative to the reef.*

Model	Inte	Shap	Size	Prod	Temp	Diet	Meth	Posi	df	ΔAIC	wAIC
drop.shape.prod	4.029	-	0.358	-	0.010	+	+	+	20	0.00	0.41
drop.prod	4.021	-2.538	0.357	-	0.010	+	+	+	21	0.75	0.28
drop.shape	4.029	-	0.358	0.003	0.010	+	+	+	21	1.64	0.18
full	4.021	-2.605	0.357	0.004	0.010	+	+	+	22	2.32	0.13
drop.posit	3.818	-4.828	0.378	0.006	0.011	+	+	-	17	20.02	0.00
drop.temp	4.068	-1.631	0.351	-0.004	-	+	+	+	21	20.21	0.00
drop.diet	3.739	-5.047	0.382	0.003	0.011	-	+	+	16	40.56	0.00
drop.method	3.899	-4.605	0.358	0.008	0.017	+	-	+	17	103.30	0.00
drop.size	4.353	-5.438	-	0.004	0.003	+	+	+	21	657.36	0.00

Table B3: *Model coefficients of the final PGLS used to model the growth coefficient Ø in reef fishes with a global dataset.*

Variable	Level	Estimate	St. Error	t-value	p-value
Intercept	-	4.029	0.155	26.07	<0.0001
Body size	-	0.358	0.013	27.92	<0.0001
Sea surface temperature	-	0.010	0.002	4.37	<0.0001
Diet	Herbivores/detritivores	-0.371	0.103	-3.61	0.0003
	Omnivores	-0.507	0.105	-4.85	<0.0001
	Planktivores	-0.365	0.103	-3.53	0.0004
	Invertivores sessile	-0.451	0.125	-3.61	0.0003
	Invertivores mobile	-0.332	0.100	-3.34	0.0009
	Fish/cephalopod predators	-0.211	0.101	-2.08	0.0379
Position	Pelagic reef dwelling	-0.283	0.075	-3.78	0.0002
	Bentho-pelagic reef associated	-0.255	0.056	-4.57	<0.0001
	Bentho-pelagic reef dwelling	-0.274	0.053	-5.18	<0.0001
	Benthic reef dwelling	-0.246	0.057	-4.31	<0.0001
	Benthic reef associated	-0.277	0.054	-5.12	<0.0001
Method	Mark-recapture	-0.069	0.038	-1.80	0.0716
	Otoliths rings	-0.165	0.016	-10.01	<0.0001
	Unknown	-0.138	0.018	-7.84	<0.0001
	Other rings	-0.182	0.033	-5.58	<0.0001
	Scale rings	-0.160	0.024	-6.57	<0.0001

Appendix B Datasets

Dataset 1

This metadata refers to the dataset 'Supporting Information - DS1.csv' permanently available from the Tropical Data Hub (Morais & Bellwood, 2018), which contains a global dataset of Von Bertalanffy growth parameters, morphological and behavioural traits, and length-weight regression coefficients for reef fishes. The variables included in this dataset are:

Family: Taxonomic family.

Species: Species name.

SpecCode: Species code from FishBase.

MaxSizeTL: Maximum recorded size for the species, referring to Total Length in cm

Diet: Dietary category, in seven levels (see **Chapter 2** for explanation).

Schooling: Schooling behaviour or gregariousness, in six levels (see **Chapter 2** for explanation).

Position: Position relative to the reef, combining horizontal and vertical components, in six levels (see **Chapter 2** for explanation).

a: Length-weight regression parameter 'a', estimated from the Bayesian Hierarchical Model from (Froese, Thorson, & Reyes, 2014) and FishBase.

b: Length-weight regression parameter 'b', estimated from the Bayesian Hierarchical Model from (Froese et al., 2014) and FishBase.

FormFactor: Body shape factor (as Form Factor in Froese, 2006) measuring the extent to which a fish is elongated or deep-bodied. It can be perceived as the 'a' parameter value a fish species should have if its b = 3.

Linf: Population asymptotic length in cm as reported by the growth study.

LinfType: Type of measure used to derive Linf. SL = Standard Length; FL = Fork Length; TL = Total Length; NG = Not Given (conservatively assumed to be TL).

LinfTL: Population asymptotic length in cm, converted to total length if Linf was reported in a measure other than this (see LinfType).

K: The Von Bertalanffy Growth coefficient K, as reported by the growth study.

Kmax: The standardized growth coefficient Kmax (see **Chapter 2** for explanation).

O: The standardized growth coefficient Ø, also termed Growth Performance Index (see **Chapter 2** for explanation).

lon: Longitudinal geographic coordinate of the population studied (see article for its derivation).

lat: Latitudinal geographic coordinate of the population studied (see **Chapter 2** for its derivation).

sstmean: Mean sea surface temperature from the geographic coordinate of the population studied, obtained from Bio-ORACLE (Tyberghein et al., 2012).

pelnpp: Mean pelagic net primary productivity from the geographic coordinate of the population studied, modelled from chlorophyll concentration and photosynthetic active radiation data obtained from Bio-ORACLE (see **Chapter 2** for explanation; Tyberghein et al., 2012).

Method: Method used to derive the growth curve, also referred to as the ageing method, in six levels (see **Chapter 2** for explanation).

Country: Country of the population studied.

Locality: Locality of the population studied, when available.

GrowthRef: Reference of the growth study that includes the referred growth curve. When a number, it matches the reference number from FishBase (Froese & Pauly, 2018).

Dataset 2

This metadata refers to the dataset 'Supporting Information – DS2.csv' permanently available from the Tropical Data Hub (Morais & Bellwood, 2018), which contains predictions of the standardized growth coefficient Kmax (derived from the Von Bertalanffy growth parameters K and Linf) for combinations of morphological and behavioural traits, and sea surface temperature. The variables included in this dataset are:

MaxSizeTL: Maximum recorded size for the species for which growth is being predicted. It refers to Total Length in cm.

sstmean: Mean sea surface temperature from the geographic coordinates of the population for which growth is being predicted (see **Chapter 2** for explanation).

Diet: Dietary category of the species for which growth is being predicted, in seven levels (see **Chapter 2** for explanation).

Position: Position relative to the reef of the species for which growth is being predicted, combining horizontal and vertical components, in six levels (see **Chapter 2** for explanation).

Kmax: The predicted standardized growth coefficient Kmax. It is the median of 1,000 bootstrap estimates (see **Chapter 2** for explanation).

Kmax_lowqt: The lower quantile (2.5%) of the standardized growth coefficient Kmax predictions across 1,000 bootstrapping iterations (see **Chapter 2** for explanation).

Kmax_upqt: The upper quantile (97.5%) of the standardized growth coefficient Kmax predictions across 1,000 bootstrapping iterations (see **Chapter 2** for explanation).

Appendix B References

Froese, R. (2006). Cube law, condition factor and weight-length relationships: history, meta-analysis and recommendations. *Journal of Applied Ichthyology*, *22*(4), 241–253. doi: 10.1111/j.1439-0426.2006.00805.x

Froese, R., & Pauly, D. (2018). FishBase. World Wide Web page. http://www.fishbase.org.

Froese, R., Thorson, J. T., & Reyes, R. B. (2014). A Bayesian approach for estimating length-weight relationships in fishes. *Journal of Applied Ichthyology*, *30*(1), 78–85. doi: 10.1111/jai.12299

Morais, R. A., & Bellwood, D. R. (2018). Data from 'Global drivers of reef fish growth.' doi: 10.4225/28/5ae8f3cc790f9

Tyberghein, L., Verbruggen, H., Pauly, K., Troupin, C., Mineur, F., & De Clerck, O. (2012). Bio-ORACLE: a global environmental dataset for marine species distribution modelling. *Global Ecology and Biogeography*, *21*(2), 272–281. doi: 10.1111/j.1466-8238.2011.00656.x

Zuur, A. F., Ieno, E. N., Walker, N. J., Saveliev, A. A., & Smith, G. M. (2009). *Mixed Effects Models and Extensions in Ecology with R*. New York, NY: Springer, New York.

Appendix C: Supporting Information for Chapter 3

Calculating individual body mass, growth and natural mortality, and assemblage biomass and production from field data

Standing biomass and biomass production can be obtained by applying geometric and growth functions to fish assemblage data, e.g. from underwater surveys. Because length is the primary data obtained in the field, we start with L_{t_i}, representing the length of any individual fish i at time t (e.g. at the time of the survey). Its body mass can be obtained by:

$$M_{t_i} = a_i({L_{t_i}}^{b_i}) \quad \text{(C1)}$$

where a_i and b_i are species-specific power-law parameters with geometric properties, often referred to as length-weight parameters (Froese, 2006). The cumulative sum of n individual fish masses in an assemblage, i.e. the total biomass of the assemblage, can be obtained by:

$$B_t = \sum_{i=1}^{n} M_{t_i} \quad \text{(C2)}$$

The expected growth, in mass units, of each individual i over a period of m days can be obtained from equation (C1) from $L_{t_i}$and L_{t+m_i}, the length values at the time of the survey and after m days, respectively. L_{t+m_i} can be calculated in the context of the Von Bertalanffy Growth Model (VBGM) (Depczynski, Fulton, Marnane, & Bellwood, 2007; Morais & Bellwood, 2019). VBGM coefficients K (the rate at which fish in a population, on average, approaches its population asymptotic body size) and L_∞ (the population asymptotic body length of a fish) are highly correlated on the log-scale (Beverton & Holt, 1959; Kozlowski, 1996; Pauly, 1998; **Chapter 2**). In **Chapter 2** it was shown how this relationship can be used to standardise Von Bertalanffy growth coefficients for a reef fish population at L_{max}, the maximum species size, instead of L_∞, obtaining K_{max}. Predictions of K_{max} for reef fishes

based on species maximum body size, water temperature, trophic group, and the position relative to the reef were also provided (Morais & Bellwood, 2018a). Thus, the size of individual i in time $t + m$, L_{t+m_i}, is given by the function:

$$L_{t+m_i} = L_{max_i}\left(1 - e^{-K_{max_i}(a_{t+m_i} - a_{0_i})}\right) \quad \text{(C3)}$$

where L_{max_i} is the maximum species size for individual i; a_{t+m_i} is its age, in years, at time $t + m$; and a_{0_i} is its theoretical age at size = 0 (most commonly referred to as t_0 in the VBGM). We estimated a_{0_i} from the regression model provided by Pauly (1979, 1980a) and rescaled the output values between the maximum value obtained and a minimum value of -0.5. This was done to avoid very low values of a_0 that are unrealistic for coral reef fishes (Choat & Robertson, 2002; Grandcourt, 2002). The next step hinges on the 'operational' age of individual i at time $t + m$, a_{t+m_i}. Because fishes and, particularly, reef fishes can live for many years after reaching their population asymptotic size (Choat & Robertson, 2002), it is impossible to estimate the real age of a fish based solely on its size. Instead, the operational age represents the expected age of a fish relative to its species maximum size, L_{max_i}. a_{t+m_i} can be estimated from:

$$a_{t+m_i} = \left(\frac{1}{K_{max_i}}\right) \ln\left\{\frac{\left(L_{max_i} - L_{0_i}\right)}{\left[\left(1 - \left(\frac{L_{t_i}}{L_{max_i}}\right)\right)L_{max_i}\right]}\right\} + \left(\frac{m}{365}\right) \quad \text{(C4)}$$

where L_{t_i} is the size of a fish at time t; and L_{0_i} is its theoretical length at age $a_i = 0$, calculated by:

$$L_{0_i} = L_{max_i}\left(1 - e^{K_{max_i} a_{0_i}}\right) \quad \text{(C5)}$$

When $L_{t_i} = L_{max_i}$, that is, when the fish has reached its species maximum size, the denominator

within the ln function in (C4) becomes 0, and $a_{t+m_i} = \infty$, that is, no further growth is expected. This is not an issue for Equation (C3), because $e^{-\infty} = 0$ and, thus, $L_{t+m_i} = L_{max_i}$. With L_{t+m_i}, the expected growth of each individual, in mass units, over m days can be calculated as:

$$G_{m_i} = M_{t+m_i} - M_{t_i} = \left[a_i\left({L_{t+m_i}}^{b_i}\right)\right] - \left[a_i\left({L_{t_i}}^{b_i}\right)\right] \quad \text{(C6)}$$

Natural mortality can be accounted for deterministically or stochastically. Both cases require the input of an instant mortality rate parameter, which can be obtained from field data or using empirical relationships (see below *Estimating exponential natural mortality*, also, Gislason, Daan, Rice, & Pope, 2010). Total mortality (M in the fisheries literature) is the sum of two components: Z, the natural mortality, and F the fisheries mortality. Because Z_i, the natural mortality of individual fish i, is normally estimated over a year, it should be rescaled using:

$$Z_{m_i} = Z_i\left(\frac{m}{365}\right) \quad \text{(C7)}$$

The probability of survival after m days is then obtained from:

$$s_{m_i} = e^{-Z_{m_i}} \quad \text{(C8)}$$

Deterministically accounting for natural mortality is useful when one wishes to calculate per capita losses of biomass. It involves multiplying the body mass of individual i on time t, M_{t_i}, by its probability of survival on time $t + m$:

$$D_{m_i} = s_{m_i} M_{t_i} \quad \text{(C9)}$$

where D_{m_i} is the per capita expected loss due to mortality for individual i. In this context, the

assemblage-level standing biomass $t + m$ and total biomass production over m days are given by:

$$B_{t+m} = \sum_{i=1}^{n} M_{t_i} + G_{m_i} - D_{m_i} \quad \text{(C10)}$$

and

$$P_m = \sum_{i=1}^{n} G_{m_i} - D_{m_i} \quad \text{(C11)}$$

Stochastically accounting for mortality is useful when one wants to trace the fate of the individuals on a population instead of calculating per capita losses. In this case, the fate of each individual after m days is judged based on a Bernoulli distribution with $p = s_{m_i}$, $F_i \sim Bernoulli\ (s_{m_i})$. Following this, B_{t+m} and P_m become, respectively, the sum of the body masses and of growth increments of the surviving individuals. Table C1 summarises the parameters estimated from the equations C1 to C11.

Table C1: *Model selection Relevant parameters estimated from the equations of the individual age framework (see main text), including their notation, equations in which they are referred and definition.*

Parameter	Equation(s)	Definition
M_{t_i}	1.1, 1.2, 5, 6.3, 7.1	The body mass of any individual fish i at time t
B_t	1.2	The total biomass of an assemblage
L_{t+m_i}	2, 5	The size of an individual i in time $t + m$, in which m is the defined time interval (days) over which growth is forecasted
a_{t+m_i}	2, 3	The operational age of a fish i, *i.e.* its expected age relative to its species maximum size, L_{max_i}
L_{0_i}	3, 4	The theoretical length of a fish i at age $a_i = 0$
G_{m_i}	5, 7.1, 7.2	The expected growth of a fish i, in mass units, over m days
Z_{m_i}	6.1, 6.2	The instantaneous natural mortality of individual fish i, rescaled m days
s_{m_i}	6.1, 6.2, 6.3	The probability of fish i surviving after m days
D_{m_i}	6.3, 7.1, 7.2	The expected loss of biomass of fish i after m days due to mortality (deterministic)
B_{t+m}	7.1	The assemblage-level standing biomass at time $t + m$
P_m	7.2	The assemblage-level total biomass production over m days

Methods to derive life-history parameters for reef fishes

Estimating von Bertalanffy Growth Model parameters

Somatic growth for each individual is modelled from expected growth trajectories in the Von Bertalanffy Growth Model (VBGM) as in **Chapter 2**. The original VBGM uses population asymptotic length, L_∞, and a shape parameter, K, to estimate growth in length (Bertalanffy, 1949, 1957; Pauly, 1979). There is substantial intra and interspecific variation in both L_∞ and K, but a correlation between these parameters precludes direct evaluation of both simultaneously. To solve this, Pauly (1979) and Munro and Pauly (1983) suggested using the intercept of the log-log relationship between L_∞ and K as a standardised growth parameter. Developing on this, in **Chapter 2** it was suggested that projecting this relationship to the maximum size reported for a species, L_{max}, would yield an easily interpretable, standardised parameter that could be used in the VBGM formula along with L_{max}. This parameter, K_{max}, is the shape parameter describing the expected growth trajectory of a fish with the determined values of L_∞ and K if it was supposed to reach its species maximum size, L_{max}.

In **Chapter 2**, an extreme gradient boosting modelling framework was used to predict K_{max} at the species level using L_{max} ('body size'), sea surface temperature, and two broad categorical traits: trophic group (in seven levels) and relationship with the reef (in six levels). To this end, a database of VBGM parameters was compiled from the literature, consisting in 1,921 curves and 588 species. This model showed highly accurate and precise predictions (see **Chapters 2** and **4**, and **Appendices B** and **D**; also Morais & Bellwood, 2018b, 2019). A table with K_{max} predictions for a non-exhaustive range of combinations of predictors was also provided in (see **Appendix B**; Morais & Bellwood, 2018a). We now provide an interface to the boosting model itself in the package *rfishprod*, allowing the user to predict K_{max} for any combinations of the predictors. This includes the possibility of expanding the input dataset to improve predictions even further or of specifying a different model structure. The model is executed by the function '*predKmax*'. K_{max} predictions are then incorporated in the formulas (C1) to (C11) above within *rfishprod* to generate the growth trajectories and expected somatic growth. A beta

version of the package *rfishprod* is available from http://github.com/renatoamorais/rfishprod.

Estimating exponential natural mortality

Total mortality is often described in the fisheries literature in terms of the instantaneous mortality rate parameter, M. This is composed by natural mortality, Z, and fisheries mortality, F (Beverton & Holt, 1957, 1959; Hilborn & Walters, 1992; Pauly, 1980b). In the absence of fishing mortality, $M = Z$. Although Z describes the exponential mortality rate experienced by a cohort of individuals from a population, it is also generally acknowledged that the mortality risk of a fish declines exponentially with its body size (Andersen & Beyer, 2006, 2015; Gislason et al., 2010; Goatley & Bellwood, 2016; Jørgensen & Holt, 2013).

We implement two methods to estimate Z_i, the instantaneous natural mortality rate of individual fish i. Because of obvious logistical constraints in obtaining field estimates of natural mortality, predictions of M based on empirical relationships are often used (Brown, Gillooly, Allen, Savage, & West, 2004; Gislason et al., 2010; Pauly, 1980b). Widely used methods, such as Pauly's and Hoenig's empirical relationships (Hoenig, 1983; Pauly, 1980b), generate predictions of mortality coefficients at the species/population level. These methods do not consider known declines in natural mortality risk due to body size increases along the ontogeny of a species (Gislason et al., 2010; Jørgensen & Holt, 2013). That drove Gislason et al. (2010) to revisit Pauly's empirical relationship, further including age-specific, or size-specific, values of Z for as many species as available. We implement Gislason et al.'s empirical relationship as the first method to estimate Z_i in the *rfishprod* package. Although these authors applied high-quality filters to isolate the most trustable data points, they recognised limitations in some of their methodological assumptions to incorporate individual body size-specific values of Z (Gislason et al., 2010).

Natural mortality is expected to scale with individual body mass within a species according to an exponent of approximately 0.25 (Andersen & Beyer, 2006, 2015; Brown et al., 2004; Jørgensen & Holt, 2013). Rescaling that to body length, instead of mass, yields an exponent of 0.75 (Jørgensen & Holt, 2013). Hence, another potential approach to account for intraspecific mortality risk would be to apply

a function of individual body size to species-level estimates of Z. A similar reasoning was used by Bozec et al. (2016), although these authors used optimization routines to find functional parameters. Instead, one could use the theoretical scaling of 0.75 along with a ratio R_s, a scaling parameter that describes how Z is expressed relative to a fixed (at the population/species level) size proportion p, so that

$$Z_i = R_s Z^{0.75} \tag{C12}$$

where Z_i is the instantaneous natural mortality of individual i, M is a population level average instantaneous mortality rate as measured or estimated from empirical relationships (such as Pauly's). R_s is then defined as

$$R_s = \left(\frac{L_i - L_r}{L_p}\right) \tag{C13}$$

where L_i is the length of individual i, L_r is the length at recruitment (e.g. settlement from the pelagic realm for reef fishes) and L_p is the length at p. An intuitive value for p could be, for example, 0.5, which would indicate that $Z_i = Z$ for fishes at the mid point of their body size range (i.e. between their size at settlement and their maximum species size). In the package *rfishprod*, this functional relationship is used alongside Pauly's empirical relationship to generate the second method to predict Z_i. A comparison of mortality rates and daily survival probabilities estimated using the two methods for the same dataset composed of three reef fish species can be seen in **Figure C1**. Also represented is the population-level estimate from Pauly (1980b). Although the trajectory from the size-specific function appears visually to resemble more closely the empirical relationship provided by Goatley and Bellwood (2016) for reef fishes, it is not in the scope of this work to evaluate which approach would

generate more adequate mortality estimates.

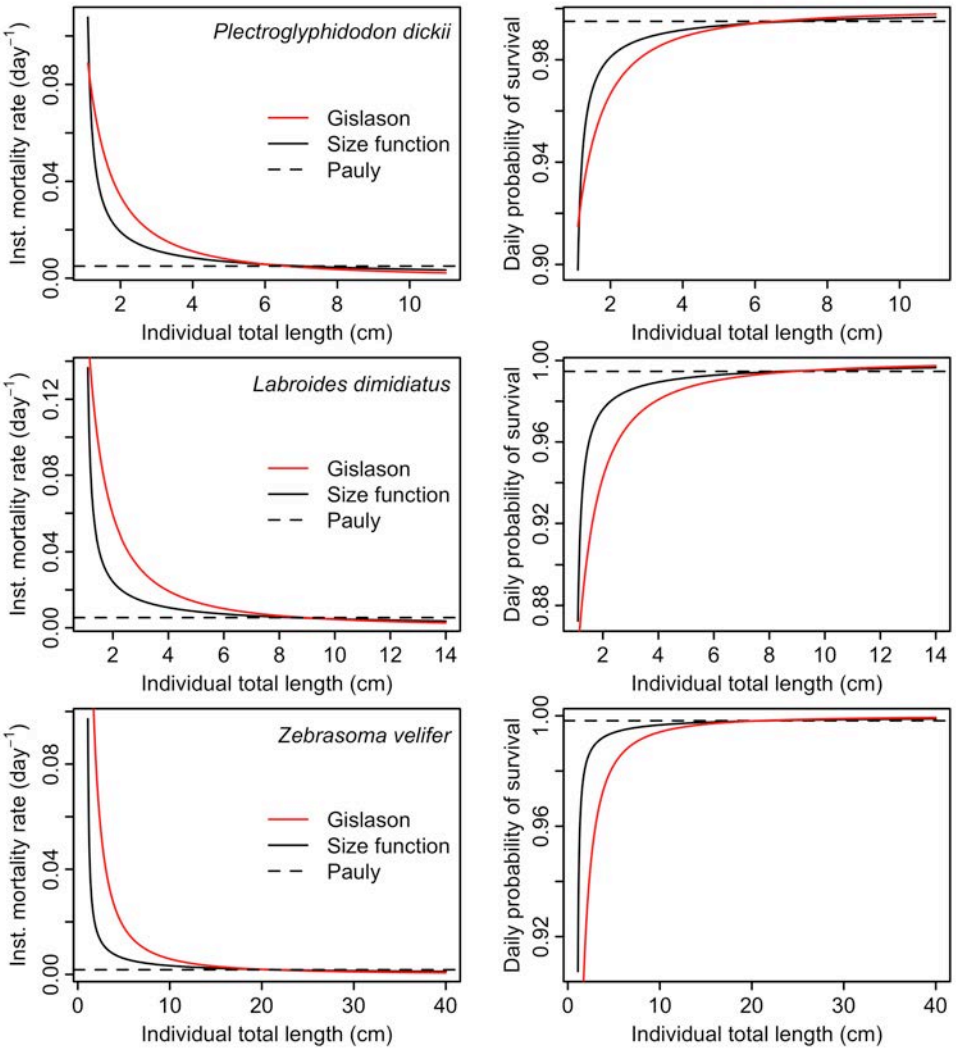

Figure C1: *A comparison of two methods to estimate size-specific mortality rates (Z, left panels) and survival probabilities (right panels). Depicted are three reef fish species. 'Gislason' is the empirical equation from Gislason et al. (2010), 'Size function' is the second method presented in the main text, which combines a functional relationship with body size with population-level estimates of Z, such as the one from Pauly (1980b).*

Table C2 below summarises the parameters cited above to derive life-history parameters (both growth and mortality) for reef fishes.

Table C1: *Parameters from the methods used to derive life-history parameters for use in the individual age framework (see main text) for reef fishes, including its notation, method to which this parameter pertains and definition*

Parameter	Method	Definition
L_∞	Growth	The population asymptotic body length of a fish
K	Growth	The rate at which fish in a population, on average, approaches its population asymptotic body size
L_{max}	Growth	The maximum reported size for a species
K_{max}	Growth	A standardised Von Bertalanffy Growth Parameter (related to the shape, or K). The rate at which a fish with the specific values of L_∞ and K would approach its species L_{max}, if it could grow to L_{max} (see Morais and Bellwood 2018).
M, Z and F	Mortality	The traditional notation for the total instantaneous mortality rate parameter (M), the instantaneous natural mortality (Z) and the instantaneous fishing-induced mortality (F) at the **population-level**. M is avoided herein, both to avoid confusion with individual body mass (represented as M_{t_i} see Table S1) and because the individual age framework is most directly concerned with natural mortality, Z. Also, in the absence of fishing ($F = 0$), $M = Z$.
Z_i	Mortality	The instantaneous natural mortality rate parameter, Z, of an individual fish i
R_s	Mortality	A scaling ratio parameter that describes how Z is expressed relative to a fixed size proportion p
p	Mortality	The portion of the body size range of a fish species in which $Z_i = Z$, that is, the individual mortality risk equals the instantaneous population mortality rate

Appendix C References

Andersen, K. H., & Beyer, J. E. (2006). Asymptotic Size Determines Species Abundance in the Marine Size Spectrum. *The American Naturalist*, *168*(1), 54–61. doi: 10.1086/504849

Andersen, K. H., & Beyer, J. E. (2015). Size structure, not metabolic scaling rules, determines fisheries reference points. *Fish and Fisheries*, *16*(1), 1–22. doi: 10.1111/faf.12042

Bertalanffy, L. von. (1949). Problems of Organic Growth. *Nature*, *163*, 156–158. doi: 10.1038/163156a0

Bertalanffy, L. von. (1957). Quantitative Laws in Metabolism and Growth. *The Quarterly Review of Biology*, *32*(3), 217–231. doi: 10.1086/401873

Beverton, R. J. H., & Holt, S. J. (1957). On the Dynamics of Exploited Fish Populations. In *Fisheries*

Investigations Series 2: Sea Fisheries (Vol. 4). doi: 10.1007/978-94-011-2106-4

Beverton, R. J. H., & Holt, S. J. (1959). A Review of the Lifespans and Mortality Rates of Fish in Nature, and Their Relation to Growth and Other Physiological Characteristics. In G. E. W. Wolstenholme & M. O'Connor (Eds.), *Ciba Foundation Symposium - The Lifespan of Animals (Colloquia on Ageing)* (pp. 142–180). doi: 10.1002/9780470715253.ch10

Bozec, Y.-M., O'Farrell, S., Bruggemann, J. H., Luckhurst, B. E., & Mumby, P. J. (2016). Tradeoffs between fisheries harvest and the resilience of coral reefs. *Proceedings of the National Academy of Sciences of the United States of America*, *113*(16), 4536–4541. doi: 10.1073/pnas.1601529113

Brown, J. H., Gillooly, J. F., Allen, A. P., Savage, V. M., & West, G. B. (2004). Toward a Metabolic Theory of Ecology. *Ecology*, *85*(7), 1771–1789. doi: 10.1890/03-9000

Choat, J. H., & Robertson, D. R. (2002). Age-Based Studies. In P. F. Sale (Ed.), *Coral reef fishes: dynamics and diversity in a complex ecosystem* (pp. 57–80). Burlington, San Diego, London: Academic Press.

Depczynski, M., Fulton, C. J., Marnane, M. J., & Bellwood, D. R. (2007). Life history patterns shape energy allocation among fishes on coral reefs. *Oecologia*, *153*(1), 111–120. doi: 10.1007/s00442-007-0714-2

Froese, R. (2006). Cube law, condition factor and weight-length relationships: history, meta-analysis and recommendations. *Journal of Applied Ichthyology*, *22*(4), 241–253. doi: 10.1111/j.1439-0426.2006.00805.x

Gislason, H., Daan, N., Rice, J. C., & Pope, J. G. (2010). Size, growth, temperature and the natural mortality of marine fish. *Fish and Fisheries*, *11*(2), 149–158. doi: 10.1111/j.1467-2979.2009.00350.x

Goatley, C. H. R., & Bellwood, D. R. (2016). Body size and mortality rates in coral reef fishes : a three-phase relationship. *Proceedings of the Royal Society B: Biological Sciences*, *283*, 20161858. doi: 10.1098/rspb.2016.1858

Grandcourt, E. M. (2002). Demographic characteristics of a selection of exploited reef fish from the Seychelles: preliminary study. *Marine and Freshwater Research*, *53*(2), 123. doi: 10.1071/MF01123

Hilborn, R., & Walters, C. J. (1992). *Quantitative Fisheries Stock Assessment*. Boston: Springer US. doi: 10.1007/978-1-4615-3598-0

Hoenig, J. M. (1983). Emprical use of Longevity Data to Estimate Mortality Rates Mortality Rates. *Fishery Bulletin*, *81*(4), 898–905.

Jørgensen, C., & Holt, R. E. (2013). Natural mortality: its ecology, how it shapes fish life histories, and why it may be increased by fishing. *Journal of Sea Research*, *75*, 8–18.

Kozlowski, J. (1996). Optimal allocation of resources explains interspecific life-history patterns in animals with indeterminate growth. *Proceedings of the Royal Society B: Biological Sciences*, *263(1370)*, 559–566. doi: 10.1098/rspb.1996.0084

Morais, R. A., & Bellwood, D. R. (2018a). Data from 'Global drivers of reef fish growth.' doi: 10.4225/28/5ae8f3cc790f9

Morais, R. A., & Bellwood, D. R. (2018b). Global drivers of reef fish growth. *Fish and Fisheries*, *19*(5), 874–889. doi: 10.1111/faf.12297

Morais, R. A., & Bellwood, D. R. (2019). Pelagic subsidies underpin fish productivity on a degraded coral reef. *Current Biology*, *29*(9), 1521–1527. doi: 10.1016/j.cub.2019.03.044

Munro, J. L., & Pauly, D. (1983). A Simple Method for Comparing the Growth of Fishes and Invertebrates. *Fishbyte*, *1*(1), 5–6.

Pauly, D. (1979). Gill size and temperature as governing factors in fish growth: a generalization of von Bertalanffy´s growth formula. *Berichte Aus Dem Institut Für Meereskunde Kiel*, Vol. 63, pp. 1–156.

Pauly, D. (1980a). A new methodology for rapidly acquiring basic information on tropical fish stocks: growth, mortality and stock-recruitment relationships. In P. M. Roedel & S. B. Saila (Eds.), *Stock assessment for tropical small-scale fisheries* (pp. 154–172). Kingston, Rhode Island, USA: International Center for Marine Resource Development.

Pauly, D. (1980b). On the Interrelationships between Natural Mortality, Growth Parameters, and Mean Environmental Temparature in 175 Fish Stocks. *ICES Journal of Marine Science*, *39*(2), 175–192.

Pauly, D. (1998). Tropical fishes: patterns and propensities. *Journal of Fish Biology*, *53*, 1–17. doi: 10.1006/jfbi.1998.0810

Appendix D: Supporting Information for Chapter 4

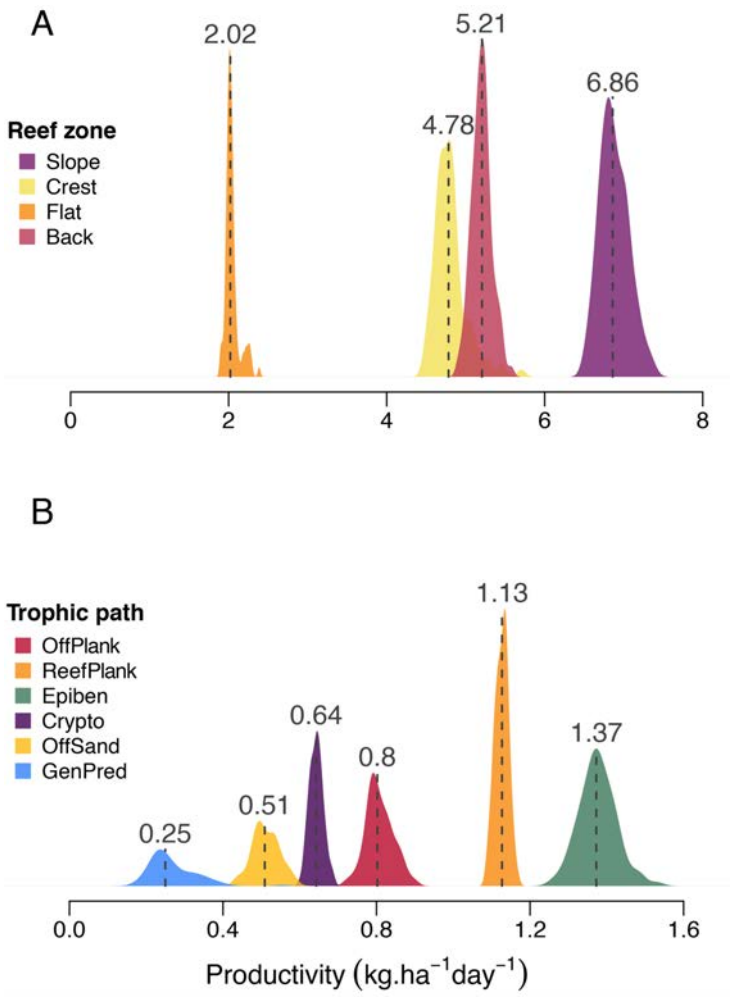

Figure D1: *Components of the fish productivity of a windward reef on the northern Great Barrier Reef.* ***(A)*** *Total per unit area fish productivity by reef zone;* ***(B)*** *per unit area fish productivity by trophic pathway, averaged among reef zones. This panel uses the same data from* ***Figure 12****, however, here the water column pathway (Plank in* ***Figure 12****) is decomposed in its proportion explored from the reef (ReefPlank) and its proportion explored off the reef (OffPlank). Epiben = epibenthic feeders; Crypto = cryptobenthic feeders; OffSand = off-reef sand pathway; GenPred = generalised predation pathway. Numbers above distributions represent the median productivity.*

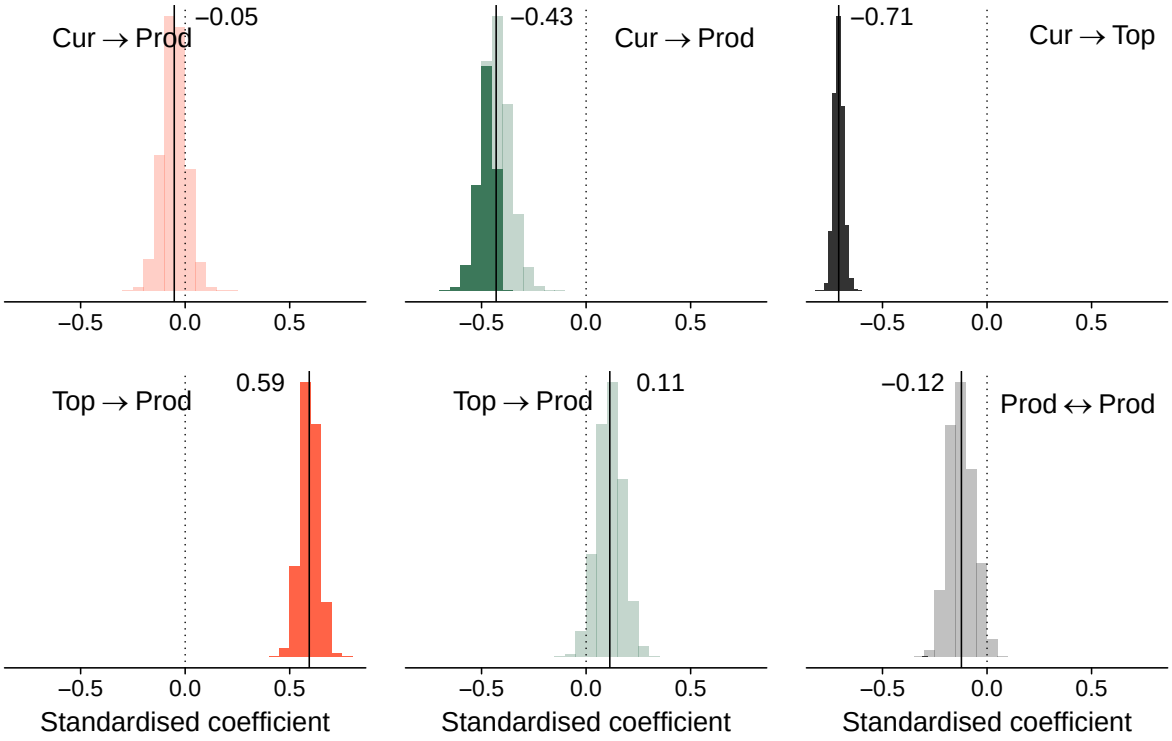

Figure D2: *Bootstrapped coefficients of the piecewise structural equation model relating both the productivity of pelagic subsidies and the productivity from the other pathways with water flow speed and topographic complexity at a windward reef on the Great Barrier Reef. Left panels are the coefficients for pelagic productivity as the response variable (Cur = water flow, Top = topographic complexity), mid panels are the coefficients for all other sources of productivity as the response variable, and right panels depict the relationship between water flow and topographic complexity (Cur → Top), and the correlated errors of pelagic and other sources of productivity (Prod ←→ Prod). Opaque histograms summarise significant coefficients (with α=0.05), whereas transparent histograms summarise non-significant coefficients.*

Table D1: *Linear Mixed Model used to test the relationship between pelagic subsidies and total productivity on a windward reef in the Great Barrier Reef. This model includes an interaction term with reef zone and a random intercept for site. This table illustrates one iteration of the bootstrapped model; a full distribution of the coefficients (slopes) for each habitat can be found on Figure 3. Random effect (Site) intercept = 0.0000565, residual variance = 1.334.*

Fixed effects	**Value**	**Std. Error**	**DF**	**t-value**	**p-value**
(Intercept)	-0.927	2.612	26	-0.355	0.7255
Pelagic Subsidies	12.309	4.226	26	2.913	0.0073
Reef Zone - Crest	1.789	2.975	26	0.601	0.5528
Reef Zone - Flat	3.024	3.074	26	0.984	0.3342
Reef Zone - Back	5.264	2.857	26	1.842	0.0769
Pelagic Subsidies x Reef Zone - Crest	-4.951	5.143	26	-0.963	0.3446
Pelagic Subsidies x Reef Zone - Flat	-13.955	8.989	26	-1.552	0.1327
Pelagic Subsidies x Reef Zone - Back	-10.993	5.835	26	-1.884	0.0708

Table D2: *Piecewise Structural Equation Model relating both the productivity of pelagic subsidies and the productivity from the other pathways with water flow speed and topographic complexity at a windward reef on the Great Barrier Reef, related to Figure 4. PelProd = productivity of pelagic subsidies; NonPelProd = productivity from other pathways; WatFlow = water flow speed; TopComp = topographic complexity. The '~~' symbols indicates correlation, but no causational hypothesis is included (no response and predictor in this case). Coef and Std Coef = coefficient and standardised coefficient, respectively; St Error = standard error; DF = degrees of freedom, Crit Val = critical value.*

Response	Predictor	Coef	R^2	St Error	DF	Crit Val	p-value	Std Coef	
PelProd	WatFlow	-0.110	0.42	0.340	33	-0.322	0.9895	-0.062	
PelProd	TopComp	1.066		0.340	33	3.131	0.0041	0.600	**
NonPelProd	WatFlow	-0.325	0.27	0.239	33	-2.156	0.0185	-0.464	*
NonPelProd	TopComp	-0.066		0.239	33	0.328	0.6202	0.070	
TopComp	WatFlow	-0.722	0.52	0.119	34	-6.088	<0.0001	-0.722	***
~~PelProd	~~NonPelProd	-0.118	-	-	36	-2.048	0.0243	-0.118	

Appendix D Sensitivity Analyses

Accuracy test of VBGF parameters, the K_{max} parameter

VBGF parameters estimated from otolith ageing were available for 56 of the 309 species of this study, totalling 136 growth curves. These growth curves were predicted with 98.7% of accuracy, as indicated by the relationship between measured and predicted values. Mean bias across all curves was of only 0.01 units of K_{max} or, on average, 8.7%. A linear model showed that this bias could neither be predicted by body size, nor by diet or position relative to the reef (all variables $p > 0.3$; $R^2 = 0.066$), and the intercept did not differ from 0 (-0.15 ± 0.31 SE). In other words, there were no distinguishable patterns in the bias of VBGF predictions among species traits that mediate trophic interactions. This suggested that the small bias detected was mostly based on random deviations, and that it would not affect the importance of the different pathways to productivity.

Sensitivity test of productivity estimates

The main features of this sensitivity analysis are included in **Table D3**. Overall, quantitative changes to any set of results were small (10% or less) and no qualitative changes were observed in any of the three analyses. Therefore, we can confidently conclude that the growth parameters used in our study and the productivity measures estimated from them are accurate, and the minor heterogeneous bias in some of them insufficient to affect our main findings.

Table D3: *Sensitivity of the three main analyses of the manuscript to bias in estimating K_{max}, the standardised growth parameter. Percentages and the absolute productivity values in the first analysis are median from bootstrapped distributions. In analyses 2 and 3, the coefficient is the median from bootstrapped distributions and the square brackets depict the 95% bootstrapped quantile interval.*

Analysis	Variable	Indicator	Before	Sens. Analysis	Evaluation	Conclusions
1) Proportional productivity among trophic pathways	Relative productivity	OffWaCol	17.06%	16.67%	Minor change	Unchanged
		ReefWaCol	24%	23.75%	Minor change	
		ReefEpib	29.38%	30.11%	Minor change	
		ReefCryp	13.65%	13.37%	Minor change	
		OffSand	10.71%	10.30%	Minor change	
		GenPred	5.24%	5.79%	Minor change	
	Total productivity	Total	4.71 $kg.ha^{-1}.day^{-1}$	4.48 $kg.ha^{-1}.day^{-1}$	Minor change	
2) Proportional pelagic subsidies driving total productivity among reef zones	Slope of linear relationships	Reef zone, slope	12.46 [10.48, 15.22]	11.29 [9.68, 13.61]	Remained strongly positive	Unchanged
		Reef zone, crest	5.53 [2.10, 8.42]	5.79 [2.38, 8.62]	Remained positive	
		Reef zone, flat	-4.51 [-9.00, -0.45]	-5.32 [-12.5, -1.18]	Remained negative/neutral	
		Reef zone, back	-0.52 [-4.50, 2.93]	0.78 [-2.77, 4.02]	Remained neutral	
3) Topography and water flow effects on pelagic and non-pelagic productivity	Standardised SEM coefficients	TotNonPel~~TotPel	-0.13 [0.00, -0.23]	-0.13 [0.00, -0.23]	No change	Unchanged
		NetFlow->TopComp	-0.71 [-0.66, -0.75]	-0.71 [-0.66, -0.75]	No change	
		NetFlow->TotNonPel	-0.43 [-0.29, -0.55]	-0.39 [-0.22, -0.53]	Minor change	
		TopComp->TotNonPel	0.11 [-0.01, 0.23]	0.11 [-0.01, 0.27]	Insignificant change	
		NetFlow->TotPel	-0.05 [-0.16, 0.06]	-0.05 [-0.17, 0.06]	Insignificant change	
		TopComp->TotPel	0.59 [0.51, 0.67]	0.59 [0.50, 0.68]	Insignificant change	

Evaluating the initial size structure of the dataset

Since planktivores are the most likely to affect our results (which depend on their productivity), we first thoroughly analysed the size distributions of these species from two different perspectives. We used insights from these size distributions to address the broader issue using a size-based sensitivity analysis. We started by selecting all planktivores among the species that summed > 90% of the total productivity. This resulted in 21 focal species (**Table D4**) that also accounted for 97% of the planktivore productivity, and over 36% of the total productivity in our study. One species, representing 3% of the planktivore productivity had to be excluded because only one size has been observed. The remaining species had on average 64 ± 23% (mean ± SD) of their population size range (i.e. the maximum size of an individual ever observed in the population minus a generalised settlement size of 1 cm TL) sampled (see table below with size indicators for the planktivores). This is a conservative measure since many of these species recruit at a size larger than 1cm TL. Furthermore, the five most abundant of these species (accounting for 64% of planktivore productivity) had between 79% and 92% of their population size range sampled. This strongly suggests that, for the species that contribute most to pelagic subsidies, the limited temporal scope of the sampling did not appear to result in a biased size structure.

To evaluate the possibility that oversampling of highly productive size classes of planktivores was affecting our results possibility, we looked at how the productivity of each species was divided among the different sizes sampled (**Figure D3**). Species with size structure mostly represented by earlier ontogenetic stages could potentially dominate productivity because of their maximised investment in growth. If that was the case, we should observe productivity concentrated in the smaller sizes of all or most species. The figure below shows that, for most of the 20 species investigated this is not the case. Indeed, only one species showed clearly higher productivity in the smallest size class compared to the others, *Pterocaesio digramma*. The other species depicted the opposite pattern (i.e. highest productivity in the largest sizes, e.g. *Caesio cuning*, *Chromis* sp., *C. viridis*, and *Ostorhinchus neotes*), showed uniform distribution (e.g. *Naso hexacanthus*, *Pomacentus brachialis*), concentration in both smallest and largest sizes (e.g. *Caesio caerulaurea*, *Ostorhinchus cyanosoma*), or depicted varying levels of concentration in the middle classes (e.g. all other species). These patterns in size structure

offer further evidence that there is no consistent concentration of planktivore productivity in early ontogenetic phases with exacerbated relative growth rates. This, again, supports the conclusion that the snapshot nature of our sampling is not a major factor affecting our analyses.

Table D4: *The 21 most abundant planktivorous fish species in the study. minObs = minimum size observed; maxObs = maximum size observed; PopMaxSize = maximum size expected for this population; PropSizeRange = the size range observed relative to the population size range; CumProd = cumulative planktivore productivity.*

Species	minObs	maxObs	PopMaxSize	PropSizeRange	CumProd
Caesio cuning	3	30	33	0.84	0.22
Neopomacentrus azysron	1	7	7.5	0.92	0.35
Pomacentrus lepidogenys	1	8	8.8	0.9	0.48
Acanthochromis polyacanthus	1	12	13.2	0.9	0.58
Caesio caerulaurea	4	25	27.5	0.79	0.64
Naso brevirostris	10	30	38.5	0.53	0.69
Pomacentrus brachialis	1	9	9.4	0.95	0.74
Ostorhinchus cyanosoma	2	4	4.4	0.59	0.79
Naso hexacanthus	20	40	44	0.47	0.82
*Taeniamia fucata**	4	4	10	0	0.85
Pomacentrus nagasakiensis	2	8	8.8	0.77	0.87
Pterocaesio digramma	5	25	27.5	0.75	0.9
Chromis sp.	4	5	8	0.14	0.92
Chromis atripectoralis	3	8	8.8	0.64	0.93
Ostorhinchus neotes	1	3	4	0.67	0.94
Chrysiptera rollandi	2	5	5.5	0.67	0.94
Abudefduf whitleyi	5	12	16.5	0.45	0.95
Thalassoma amblycephalum	3	12	13.2	0.74	0.96
Nectamia fusca	3.25	4.54	11.2	0.13	0.96
Zoramia viridiventer	2	4	5.5	0.44	0.97
Chromis viridis	2	6	8	0.57	0.97

*All individuals from this species sampled had the same size and were, thus, excluded from the analyses.

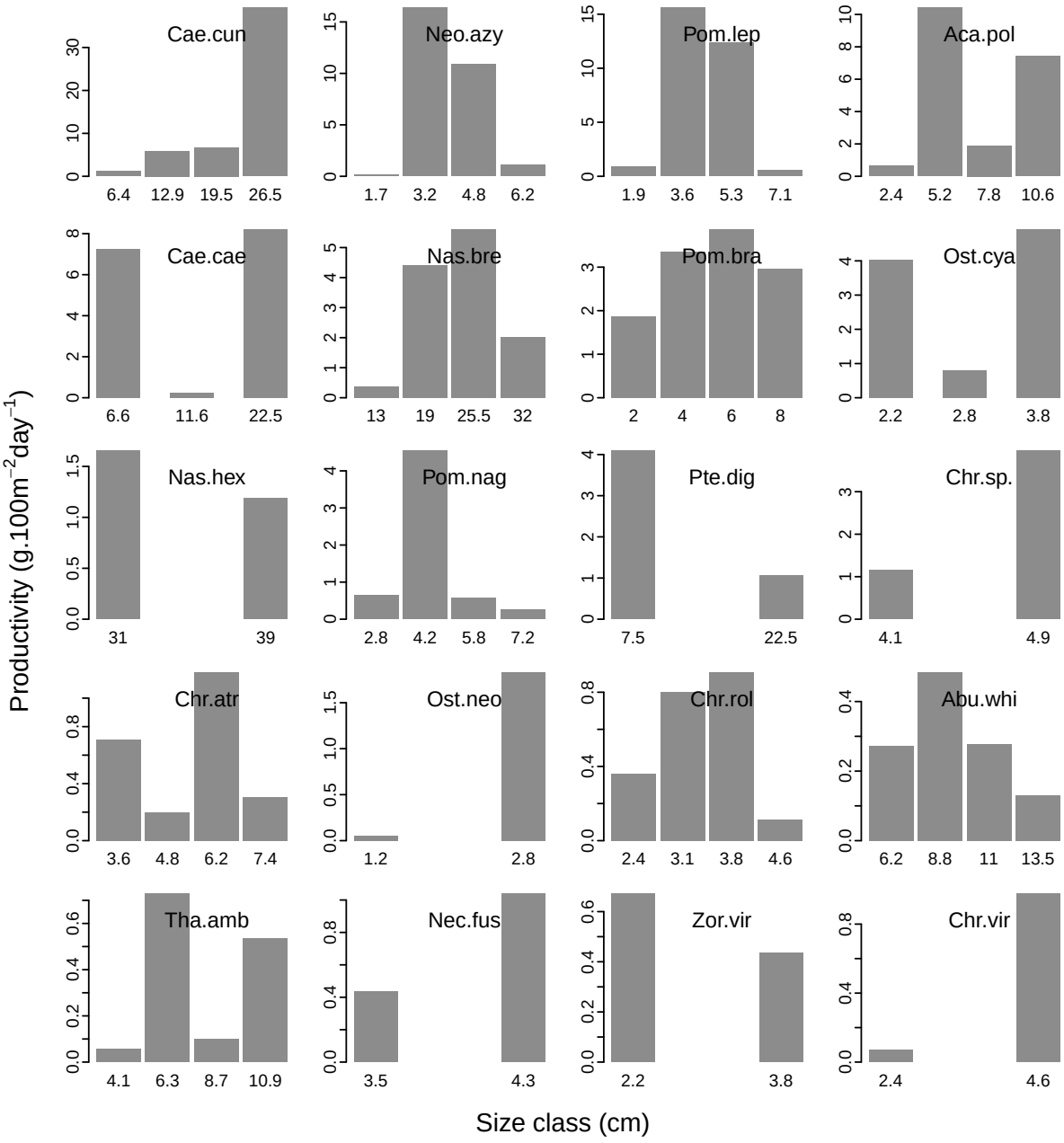

Figure D3: *Size-specific productivity of the 20 most abundant planktivorous fishes. Numbers under the bar are the mid-point of the size class, in cm. Labels are the abbreviations of species names in the Table above, following the same order from left to right, from top to bottom.*

Sensitivity test of removing recruits

The main features of this sensitivity analysis are included in **Table D5**. Overall, quantitative changes to any set of results were small and no qualitative changes were observed in analyses 1) or 3) (see **Chapter 4**). In analysis 2) the slope of the relationship between the proportion of pelagic subsidies and total productivity of the reef crest changed from being unequivocally positive originally (i.e. the bootstrapped interval never intercepted zero) to being mainly positive in the sensitivity analysis (i.e. the bootstrapped interval intercepted zero, although the vast majority of values are still positive). We interpret this as evidence that recruits had a complementary and important role in providing pelagic subsidies to the reef crest. However, even excluding all recruits changed this relationship in only a small proportion of iterations, indicating that adults are still more important than juveniles in accessing pelagic subsidies in the reef crest. These results offer additional support to our conclusions in the paragraphs above that the snapshot nature of our sampling does not significantly affect our conclusions.

Table D5: *Sensitivity of the three main analyses of the manuscript to the effects of excluding the smallest size class (25% of known size range) for all reef fish species. Percentages and the absolute productivity values in the first analysis are median from bootstrapped distributions. In analyses 2 and 3, the coefficient is the median from bootstrapped distributions and the square brackets depict the 95% bootstrapped quantile interval.*

Analysis	Variable	Indicator	Before	Sens. Analysis	Evaluation	Conclusions
1) Proportional productivity among trophic pathways	Relative productivity	OffWaCol	17.06%	16.35%	Small change	Unchanged
		ReefWaCol	24%	25.04%	Small change	
		ReefEpib	29.38%	29.79%	Minor change	
		ReefCryp	13.65%	12.78%	Small change	
		OffSand	10.71%	11.04%	Minor change	
		GenPred	5.24%	5.00%	Minor change	
	Total productivity	Total	4.71 $kg.ha^{-1}.day^{-1}$	4.04 $kg.ha^{-1}.day^{-1}$	Expected change, small	
2) Proportional pelagic subsidies driving total productivity among reef zones	Slope of linear relationships	Reef zone, slope	12.46 [10.48, 15.22]	12.24 [10.16, 14.60]	Remained strongly positive	Affected by recruits in the crest and back reefs
		Reef zone, crest	5.53 [2.10, 8.42]	2.95 [-0.85, 5.83]	No longer definitely positive	
		Reef zone, flat	-4.51 [-9.00, -0.45]	-6.65 [-10.59, -2.76]	Became more strongly negative	
		Reef zone, back	-0.52 [-4.50, 2.93]	-3.24 [-6.39, 0.05]	Almost negative	
3) Topography and water flow effects on pelagic and non-pelagic productivity	Standardised SEM coefficients	TotNonPel~~TotPel	-0.13 [-0.23, 0.00]	-0.09 [-0.22, 0.04]	Minor change	Unchanged
		NetFlow->TopComp	-0.71 [-0.75, -0.66]	-0.71 [-0.75, -0.66]	No change	
		NetFlow->TotNonPel	-0.43 [-0.55, -0.29]	-0.37 [-0.50, -0.24]	Minor change	
		TopComp->TotNonPel	0.11 [-0.01, 0.23]	0.14 [0.02, 0.25]	Insignificant change	
		NetFlow->TotPel	-0.05 [-0.16, 0.06]	-0.04 [-0.15, 0.08]	Insignificant change	
		TopComp->TotPel	0.59 [0.51, 0.67]	0.59 [0.51, 0.68]	Insignificant change	

Appendix E: Supporting Information for Chapter 5

Supplemental Methods

Study locality and survey design

Lizard Island is a mid-shelf island group in the northern Great Barrier Reef, offshore from a low-populated coastline and away from major sources of coastal runoff and intensive agricultural activities (Bainbridge et al., 2018). Human population at Lizard Island is minimal and restricted to small-scale tourism and scientific research. Most of Lizard Island's marine environments are part of no-take areas of the Great Barrier Reef Marine Park, with all forms of recreational and commercial fishing strictly prohibited (GBRMPA, 2016). Thus, apart from relatively small crown-of-thorns starfish outbreaks that caused localised damage (Pratchett, 2010), the reefs we surveyed around Lizard Island remained largely intact in 2003-2004.

Detailed survey procedures and resampling algorithms

Benthic surveys to quantify live coral and turf cover were conducted using point-intercept and photoquadrats along transects in 2003/4 and 2018, respectively. In 2004, 12 x 10 m-long transects were surveyed at each of the four reef zones, totalling 33 points per transect and 396 points per reef zone. In 2018, five 1 m^2 photoquadrats were obtained from each of nine replicated 30 m long transects. From a total of 50 randomly distributed points per photoquadrat (Morais & Bellwood, 2019b), we randomly subsampled nine, totalling 45 points per transect and 405 points per reef zone. Subsampling followed by bootstrapping ensured that a similar number of point-intercepts and, hence, a similar precision in coral and turf cover estimates were used in 2003/4 and 2018. Detailed description of the field procedures is available in Wismer, Hoey, & Bellwood (2009) and **Chapter 4** for the surveys in 2003/04 and 2018, respectively.

In both 2003/04 and 2018, we used an array of visual surveys (belt transects) and enclosed clove oil stations to generate a comprehensive sampling of 13 common reef fish families. Visual surveys encompassed the families Acanthuridae, Apogonidae, Chaetodontidae, Epinephelidae, Labridae, Pomacanthidae, Pomacentridae and Siganidae, and clove oil collection methods the families

Blenniidae, Gobiidae, Pseudochromidae and Tripterygiidae. We subsequently split the family Labridae into Scarini and non-Scarini subgroups. To combine the different survey methods into a single unit containing all surveyed fish families, we applied the resampling procedure described in **Chapter 2** (Morais & Bellwood, 2019b). In brief, individual fishes are randomly sampled within each census at each zone and each year, proportionally to their density. The final fish assemblage for each year/zone combination was based on an arbitrary resampling area unit of 100 m^2. The resampling procedure was bootstrapped for 100 or 500 iterations to create distributions of parameters of interest (see main text for the ordination methods and below for the Bayesian analytical approach).

In 2003/4, visual surveys were family-targeted and divided into three blocks: Block 1 targeted parrotfishes (Labridae: Scarini) covering an area of approximately 587 m^2 per transect (four transects per zone); Block 2 targeted cardinalfishes (Apogonidae) covering an area of 400 m^2 per transect (nine transects per zone, except for the back reef, with 18 transects); Block 3 targeted Acanthuridae, Chaetodontidae, Epinephelidae, Labridae, Pomacanthidae, Pomacentridae and Siganidae on an area of 250 m^2 per transect (six transects per zone). In 2018, visual surveys were size and behaviour-targeted, and were also divided into three blocks: Block 1 targeted large (> 25 cm total length, TL), water-column located or quick swimming fishes, covering 250 m^2 per transect (nine transects per zone); Block 2 targeted smaller (< 25 cm TL), quick-swimming or water column-positioned fishes, covering 150 m^2 per transect (nine transects per zone); and Block 3 targeted small, non-cryptic, site-attached fishes found typically within 1 m from the benthic substrate, covering 30 m^2 per transect (nine transects per zone). Because these surveys were not taxonomically-driven, they initially included all detected fish families following **Chapter 4**. Families not surveyed in 2003/4 were subsequently excluded to keep consistency. Cryptobenthic reef fish families (Blenniidae, Gobiidae, Pseudochromidae and Tripterygiidae) were surveyed in both 2003/4 and 2018 using enclosed clove oil stations. Small (0.4 m^2 per station), approximately circular reef areas were enclosed with a fine-mesh mosquito net weighted with a steel chain and sprayed with an ethanol:clove oil solution. In 2003, 24 stations were haphazardly laid in the dominant substrate types within each reef zone (Depczynski & Bellwood, 2005). In 2018, eight stations were laid systematically along three 14 m-long transects (totalling 24 stations per reef zone).

Identification was done at the species level for the enclosed clove oil collections in both time periods, for all visual survey blocks in 2018, and for block 1 in 2003/4. However, blocks 2 and 3 were surveyed at the genus-level in 2003/4. To ensure comparability between all blocks and years, we downgraded species-level identification to the genus resolution. All fishes surveyed visually were size-tallied in the same size bins (in total length, TL), with 2.5 cm precision up to 20 cm TL (e.g. 0-2.5 cm, 2.6-5 cm, etc.) and 5 cm thereafter. Cryptobenthic fishes collected with clove oil were measured to the nearest 0.1 mm, but were binned in the same size classes to keep consistency with small fishes from other families. Detailed description of the field procedures is available in (Depczynski & Bellwood, 2005; Depczynski, Fulton, Marnane, & Bellwood, 2007; Fulton & Bellwood, 2005) and in **Chapter 4** for the surveys in 2004 and 2018, respectively.

We used a series of procedures to ensure that visual estimates of reef fish abundance and sizes were accurate and precise and consistent between surveys. First, all three surveyors (CJF, MM and RAM) had extensive previous experience in doing fish counts at the time of the surveys, ranging from over a hundred to over a thousand counts per person. This also included 20-100 hours identifying and estimating fish sizes previously to the surveys in the same specific field site. Fish sizes were also constantly calibrated against objects with known sizes, particularly the tape measurement markings and the annotation slates. Finally, to avoid unconscious bias in either abundance or size estimates, the surveyor in 2018 had no previous access to the data from 2003/04. This ensured that size estimates from 2018 were kept independent from 2003/04.

Mapping reef zones

To provide a system-level analysis of potential changes in the main reef habitat zones, we calculated the weighted average of the reef zone-specific standing biomass, productivity, consumed biomass and turnover. We used the area of each reef zone obtained from satellite-based habitat mapping as the averaging weights for all descriptors. We started by mapping and subsequently measuring the area of the distinct reef zones of this windward reef stretch (Fulton & Bellwood, 2005). We used similar procedures to Bellwood et al. (2018) when distinguishing among reef zones from satellite images. Initially, the crest was defined and visually identified as the pale outer margin of the windward edge of

the reef. The crest was connected to the slope, characterised by a darker blue colour due to deeper waters. Leeward from the crest, a dark brown colour indicated the exposed outer flat, and a gradual transition lighter brown tone indicated the inner flat. The back reef was located immediately after the inner flat toward the lagoon and was identified by a blue colour tone due to increasing bottom depth. The back reef presented a disconnect between its north-eastern and southwestern parts and was flanked by small isolated patch reefs amidst sand. These patch reefs were not included on the mapping.

All mapping procedures were undertaken with Google Earth Pro, and the polygons were read and processed in R (R Core Team, 2019) using the package *rgdal* (Bivand, Keitt, & Rowlingson, 2019). The total planar area of each reef zone, in km^2, was obtained using the package *geosphere* (Hijmans, 2019). We used the Pythagoras' theorem to obtain the real area of the slope from its planar area and its maximum depth (about 20 m). We constrained the mapping to the boundaries of the area surveyed, except for the inner reef flat. Although we did not directly survey the inner reef flat, we included it alongside the outer flat for two reasons. First, although the inner flat is composed of reef pavement interspersed with sand, its reef fish assemblage was qualitatively similar to the outer flat (authors pers. obs.). Second, not accounting for the inner flat would result in an overestimate of the contribution of other, more structurally complex zones, to the energetics of this windward reef system, particularly the slope and back reef (Bellwood et al., 2018). Because the inner flat is structurally and biologically more similar to the outer reef flat than to any of these other reef zones, aggregating it alongside the outer flat was the most parsimonious and conservative procedure.

Obtaining and aggregating metrics of energy flow and storage

We used the trait dataset from **Chapter 4** (Morais & Bellwood, 2019a) to obtain genus-level maximum length, length-weight, growth and mortality coefficients. This was done by averaging these traits across the different species of each genus in that dataset, a procedure that assumes species composition at the reef scale has not undergone extensive changes between the survey years, i.e. changes were mainly in terms of abundance. Although this procedure could generate biased genus-level estimates of traits if local extinctions were common, there is ample evidence that, even after extensive coral mortality, local extinctions are a rare phenomenon largely restricted to very specialized

corallivorous species (Brooker, Munday, Brandl, & Jones, 2014; Munday, 2004; Pratchett, Wilson, & Baird, 2006). Combined with the naturally low abundance of corallivores relative to other feeding guilds (e.g. Bellwood, Hughes, Folke, & Nyström, 2004), it is unlikely that this small potential bias would affect our system-level energetic analyses.

Length-weight power coefficients were used to convert individual lengths as obtained from counts to individual weight (Froese, 2006). Genus-averaged maximum species length and growth coefficients (K_{max}) were used to estimate the expected size of each fish after a one-day period of growth under a Von Bertalanffy Growth Model (VBGM) trajectory (Morais & Bellwood, 2018, 2019b). Expected growth, in weight, was then obtained by subtracting the weight of the fish during the survey from the weight of the same fish after a one-day following its expected growth trajectory. Daily mortality rates were estimated in a two-step procedure. First, we obtained instantaneous mortality coefficients for each genus using Pauly's empirical equation, which considers VBGM parameters and water temperature (Pauly, 1980). These mortality coefficients were then used to delineate a negative exponential relationship between mortality rates and individual body size (see Bozec, O'Farrell, Bruggemann, Luckhurst, & Mumby, 2016), reproducing the reported empirical decline in mortality risk as individuals age and grow (Gislason, Daan, Rice, & Pope, 2010; Goatley & Bellwood, 2016; Jørgensen & Holt, 2013). This provided daily probabilities of survival for each individual in the dataset, which were subsequently multiplied by the individual body mass to generate an 'expected per capita loss of biomass' due to mortality. The total standing biomass, productivity and consumed biomass of resampled fish assemblages were the combined weights, growth, and expected loss of biomass from all individuals, respectively.

Bayesian data analysis procedures

We combined bootstrapping and a Bayesian analytical framework to test for differences in coral and turf cover, and ecosystem functioning metrics (fish standing biomass, productivity, consumed biomass and turnover) between sampling years. For coral and turf cover, we tested for differences between years for each reef zone, whereas for the function metrics we used the reef-level values calculated from weight averaging zone-specific values (see above *Mapping reef zones*). All models

used the No-U-Turn sampler algorithm to sample MCMC chains, and were implemented using the Stan language with the *rstanarm* interface to R (Goodrich, Gabry, Ali, & Brilleman, 2018; Stan Development Team, 2018). For all model sets, we inspected the MCMC chains for convergence and efficiency by using the number of effectives and the Gelman-Rubin statistic (Rhat).

Because of the subsampling procedure employed to keep benthic surveys consistent among sampling years (see *Detailed survey procedures and resampling algorithms*), we ran one Bayesian model for each of the 500 subsampling bootstrap iterations. These models included number of coral/turf points per subsample as the response variable, and sampling period and reef zone as predictors. We used a binomial error distribution with logit link, and normally distributed priors with mean = 0 and standard deviation = 3 for both intercept and slopes. Each model had three chains of 1,000 steps, with a 50% burn-in and no thinning, yielding a final composite of chains summing 750,000 steps. We calculated the effect sizes of sampling year by dividing the estimated parameter value (coral or turf cover) for 2018 by the 2003/4 value for each step of the composite of chains. We then used the high posterior density interval (HPD, 95% credibility interval) of the effect sizes to guide statistical inference.

For the fish component, we bootstrapped the ecosystem functioning metrics (standing biomass, productivity, consumed biomass, turnover and instant biomass change) calculated from the resampled fish assemblages for 500 iterations (see *Detailed survey procedures and resampling algorithms*). We used these 500 bootstrapped observations of each metric as the response dataset and sampling period as predictor. Following histogram inspection of the bootstrap distributions, we used gaussian error distributions for the standing biomass, productivity and instant biomass change models, and gamma error distributions with log link for the consumed biomass and turnover models. Each model was run for three chains of 3,000 steps with a 50% burn-in and a thinning of one in every two steps per model. We used normally distributed priors with mean = 0 and standard deviation = 10 and 100, respectively, for intercept and slopes; as well as Cauchy distributed auxiliary priors with mean = 0 and standard deviation = 5. Similar to the benthic data analysis, we calculated the effect sizes of sampling year by dividing the estimated parameter values of each metric for 2018 by the 2003/4 values for each MCMC step and HPD of the effect sizes to guide statistical inference.

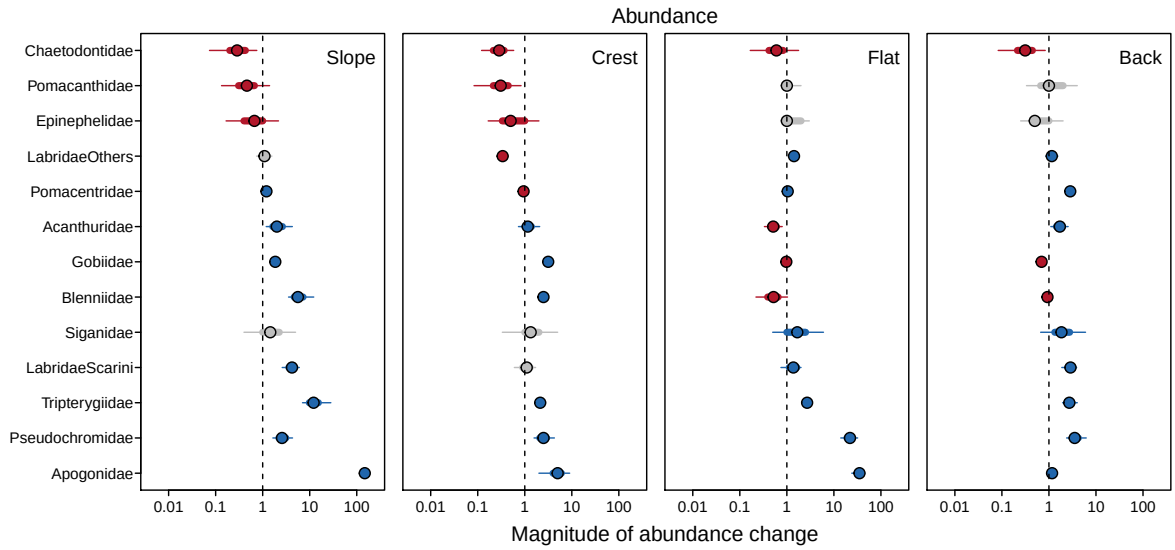

Figure E1: *Magnitude of change in the abundance of fish families in different reef zones on a windward reef at Lizard Island, northern GBR, between 2003 and 2018. Circles are the median across resampling iterations, wide bars represent the interquartile range, and whiskers the 95% quantile range. Colours are proportional to the probability of an effect: grey = < 70% probability of change; red > 70% probability of a decline; and blue > 70% probability of an increase.*

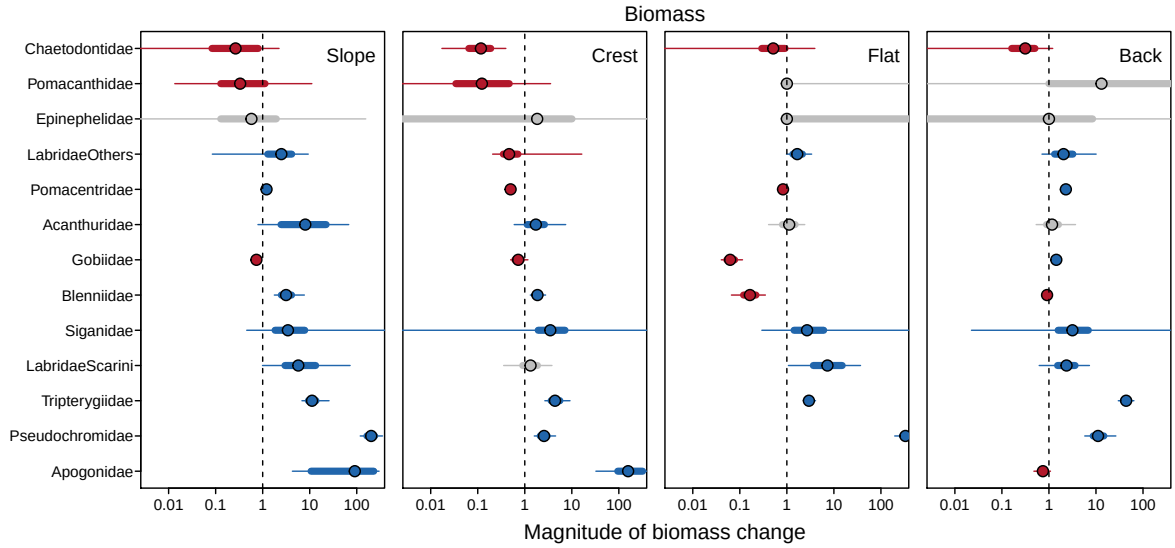

Figure E2: *Magnitude of change in the standing biomass of fish families in different reef zones on a windward reef at Lizard Island, northern GBR, between 2003 and 2018. Circles are the median across resampling iterations, wide bars represent the interquartile range, and whiskers the 95% quantile range. Colours are proportional to the probability of an effect: grey = < 70% probability of change; red > 70% probability of a decline; and blue > 70% probability of an increase.*

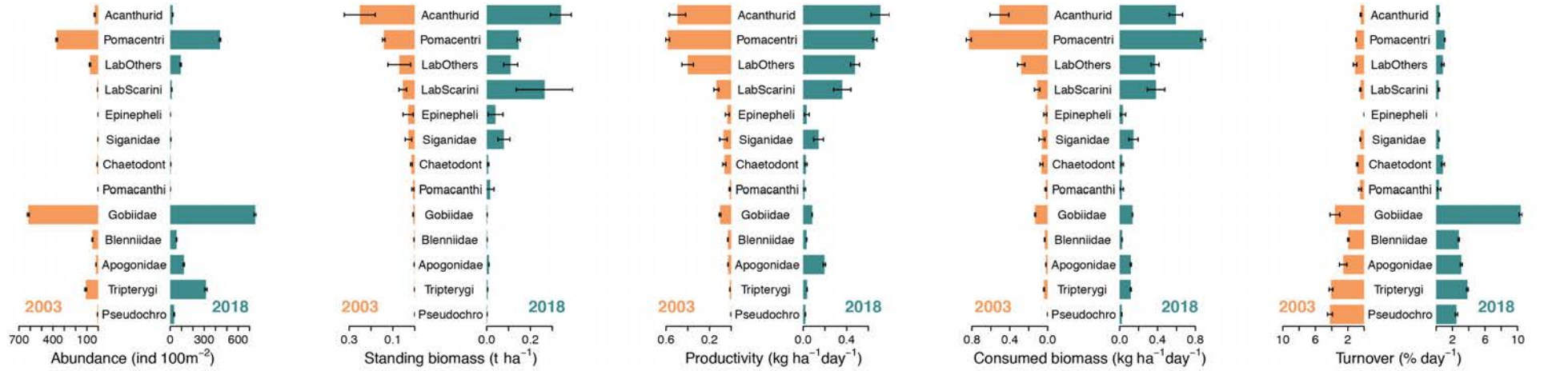

Figure E3: *Family-level abundance, standing biomass, productivity, consumed biomass and total turnover on a windward reef at Lizard Island, northern GBR, in 2003 and 2018. Error bars represent the standard deviation of resampling distributions. Acanthurid = Acanthuridae, Pomacentri = Pomacentridae, LabOthers = Labridae excluding Scarini, LabScarini = Labridae, Scarini, Epinepheli = Epinephelidae, Chaetodont = Chaetodontidae, Pomacanthi = Pomacanthidae, Tripterygi = Tripterygiidae, Pseudochro = Pseudochromidae.*

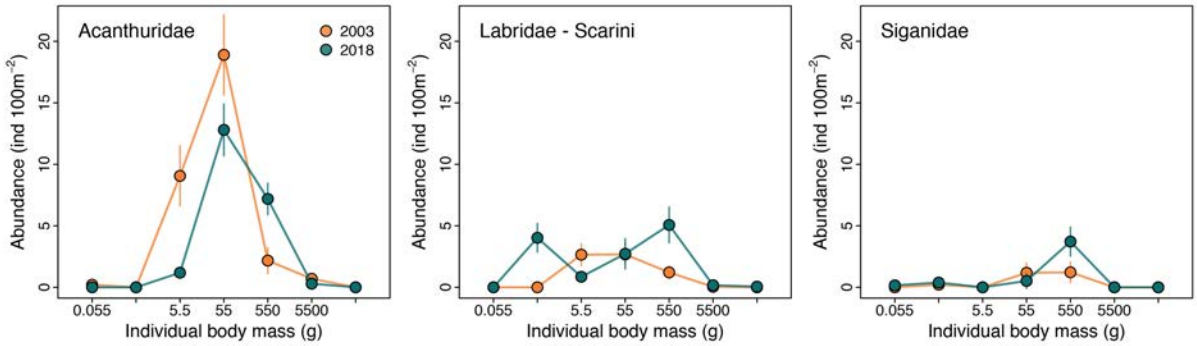

Figure E4: *Size distribution of the studied reef fish assemblage at Lizard Island, northern GBR, in 2003 and 2018. Lines and dots describe the mean abundance of each family aggregated in log10 body mass bins across 500 resampling iterations, with intervals representing standard deviations.*

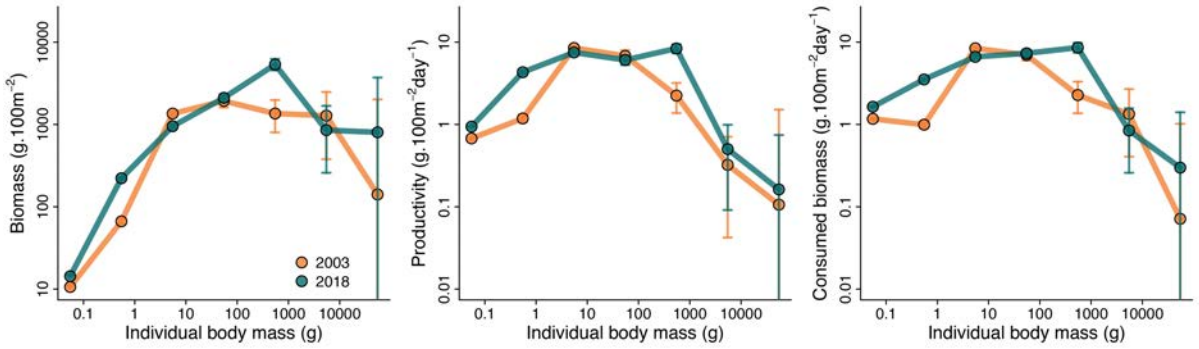

Figure E5: *Biomass, productivity and consumed biomass size spectra of the studied reef fish assemblage at Lizard Island, northern GBR, in 2003 and 2018. Lines and dots describe the mean value of each metric, aggregated in log_{10} body mass bins, across 500 resampling iterations. Intervals define the 90% quantile interval. Note log_{10} scale in the y-axis implying that differences among sampling periods are larger than perceived.*

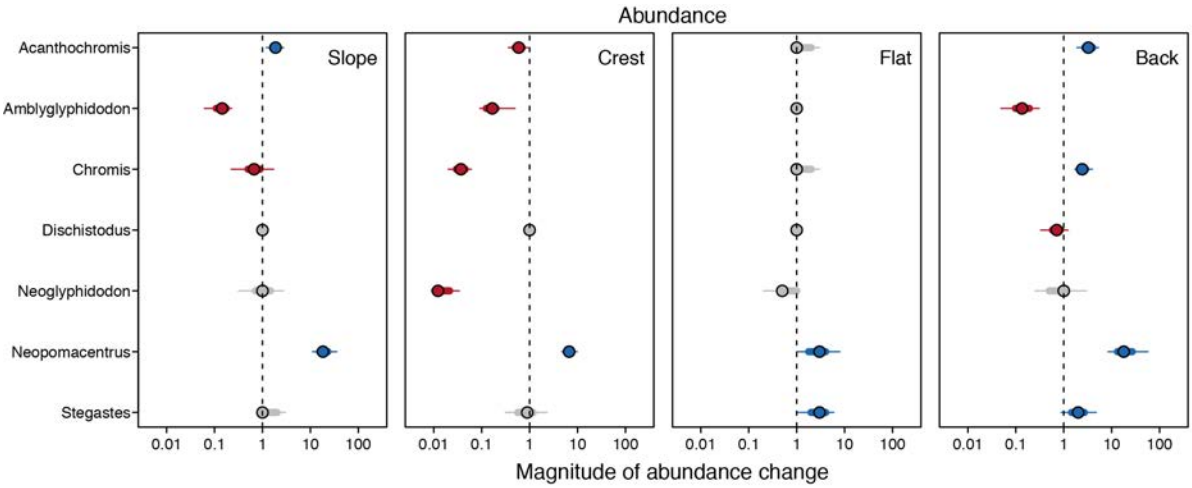

Figure E6: *Magnitude of change in the abundance of the main genera of planktivorous (*Acanthochromis*,* Amblyglyphidodon*,* Chromis*,* Neoglyphidodon *and* Neopomacentrus*) and territorial herbivorous (*Dischistodus *and* Stegastes*) damselfishes (Pomacentridae) in different reef zones on a windward reef at Lizard Island, northern GBR, between 2003 and 2018. Circles are the median across resampling iterations, wide bars represent the interquartile range, and whiskers the 95% quantile range. Colours are proportional to the probability of an effect: grey = < 70% probability of change; red > 70% probability of a decline; and blue > 70% probability of an increase.*

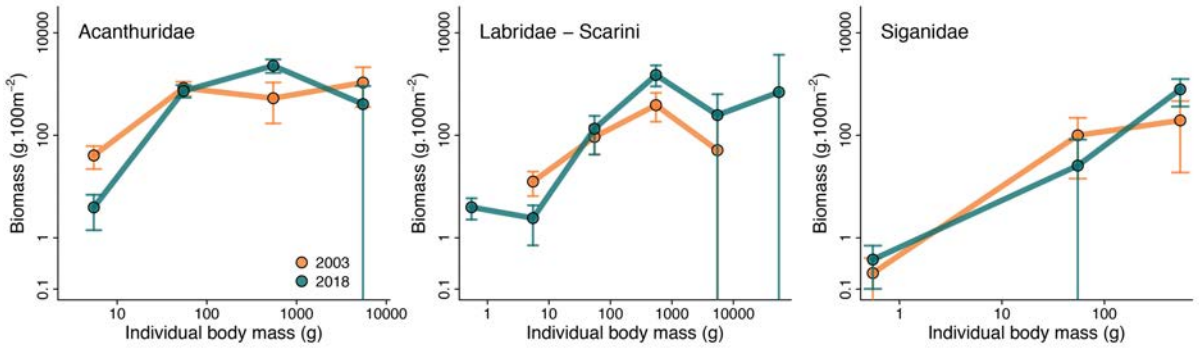

Figure E7: *Biomass size structure of the three main nominally-herbivorous fish families at Lizard Island, northern GBR, in 2003 and 2018. Lines and dots describe the pattern of standing biomass for a family, aggregated in log_{10} body mass bins, across 500 resampling iterations. Intervals define the 90% quantile interval. Note log_{10} scale in the y-axis implying that differences among sampling periods are larger than perceived.*

On the relationship between individual weight and somatic growth

Growth, as a proportion of the body size of a fish tends to exponentially decline over time as the individual gets larger. Growth in mass units, on the other hand, can be high for a relatively large period in the life of a fish, and, thus, fish with different body sizes can sustain raw growths of similar magnitude. This implies that the increased productivity observed simultaneously to increased biomass, as observed in our study, is not necessarily paradoxical.

This reasoning can be exemplified if we consider a hypothetical growth curve of a reef fish as in **Figure E8** (following a VBGM trajectory with K = 0.2, L_{inf} = 30 cm and t_0 = -0.2; and average length-weight regression parameters a = 0.015 and b = 3.01). Growth as a proportion of the asymptotic body weight shows an asymmetric, dome-shaped trajectory, in which maximum growth potential occurs relatively early in the ontogeny, but at a relatively large size (in that case, ~30% of W_{inf}, the asymptotic body weight). The asymmetric nature of the curve implies that the growth deceleration that follows peak growth is less pronounced than the growth acceleration that led to the peak growth. Take, for example, an arbitrary growth rate of 70% of the maximum growth relative to the asymptotic weight (y-axis, **Figure E8**). This magnitude of growth can occur in two moments of the ontogeny of this fish, highlighted with two green circles linked by a line (**Figure E8**). These two moments correspond to an order of magnitude difference in body weight (numbers 1 and 2), from ~6% to ~65% of the asymptotic weight. Thus, in a simplified scenario, a fish assemblage composed of individuals with size 1, can increase in both biomass and productivity if these individuals grow to any size between sizes 1 and 2. This observation implies that the size structure of a fish assemblage is critical in determining its productivity.

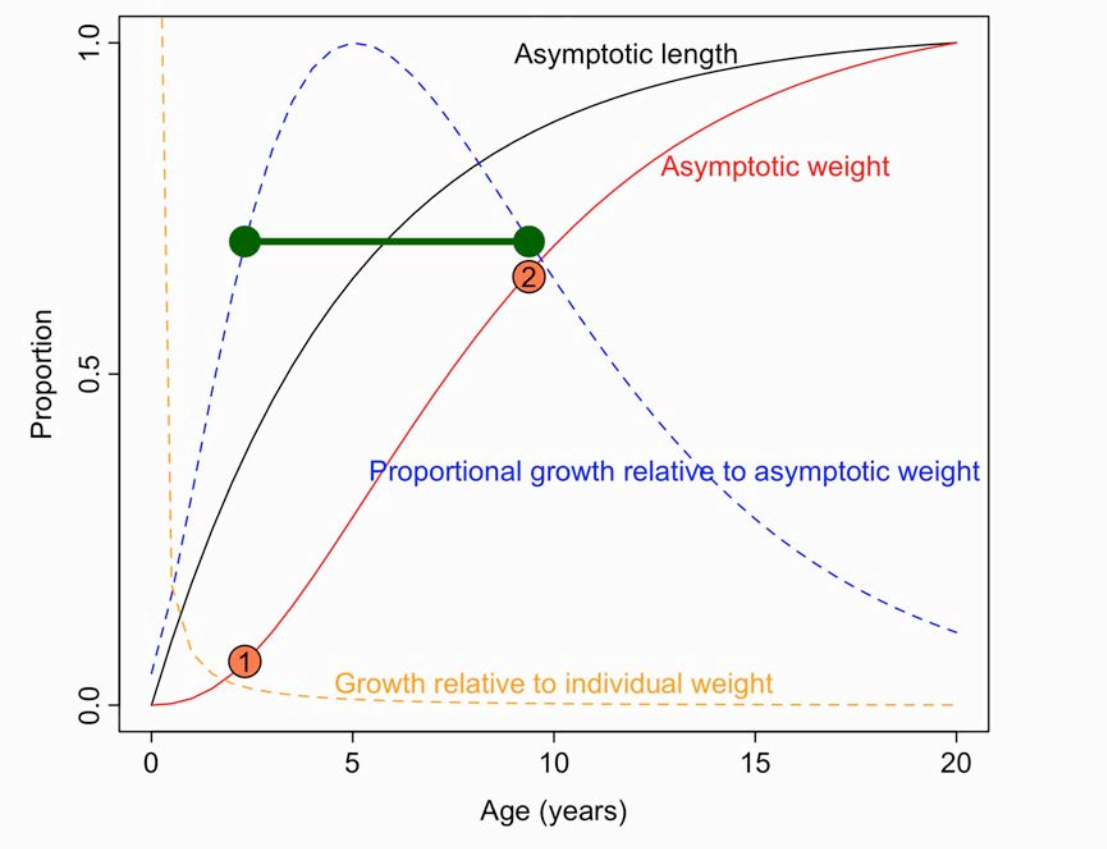

Figure E8: *Relative length, weight, growth rate relative to individual weight and proportional growth rate relative to asymptotic weight for a hypothetical fish (VBGM coefficients: K = 0.2; L_{inf} = 20 cm; t_0 = -0.2; Length-weight parameters: a = 0.015; b = 3.01). Green circles linked by a green line represent 70% of the maximum growth rate, which occurs at two points in the ontogeny of this fish, coincident with body weights of an order of magnitude difference (1 and 2).*

Appendix E References

Bainbridge, Z., Lewis, S., Bartley, R., Fabricius, K., Collier, C., Waterhouse, J., … Brodie, J. (2018). Fine sediment and particulate organic matter: A review and case study on ridge-to-reef transport, transformations, fates, and impacts on marine ecosystems. *Marine Pollution Bulletin*, *135*, 1205–1220. doi: 10.1016/j.marpolbul.2018.08.002

Bellwood, D. R., Hughes, T. P., Folke, C., & Nyström, M. (2004). Confronting the coral reef crisis. *Nature*, *429*(6994), 827–833. doi: 10.1038/nature02691

Bellwood, D. R., Tebbett, S. B., Bellwood, O., Mihalitsis, M., Morais, R. A., Streit, R. P., & Fulton, C. J. (2018). The role of the reef flat in coral reef trophodynamics: Past, present, and future. *Ecology and Evolution*, *8*, 4108–4119. doi: 10.1002/ece3.3967

Bivand, R., Keitt, T., & Rowlingson, B. (2019). *rgdal: Bindings for the "Geospatial" Data Abstraction Library.* R package version 1.4-4.

Bozec, Y.-M., O'Farrell, S., Bruggemann, J. H., Luckhurst, B. E., & Mumby, P. J. (2016). Tradeoffs between fisheries harvest and the resilience of coral reefs. *Proceedings of the National Academy of Sciences of the United States of America*, *113*(16), 4536–4541. doi: 10.1073/pnas.1601529113

Brooker, R. M., Munday, P. L., Brandl, S. J., & Jones, G. P. (2014). Local extinction of a coral reef fish explained by inflexible prey choice. *Coral Reefs*, *33*(4), 891–896.

Depczynski, M., & Bellwood, D. R. (2005). Wave energy and spatial variability in community structure of small cryptic coral reef fishes. *Marine Ecology-Progress Series*, *303*, 283–293. doi: 10.3354/meps303283

Depczynski, M., Fulton, C. J., Marnane, M. J., & Bellwood, D. R. (2007). Life history patterns shape energy allocation among fishes on coral reefs. *Oecologia*, *153*(1), 111–120. doi: 10.1007/s00442-007-0714-2

Froese, R. (2006). Cube law, condition factor and weight-length relationships: history, meta-analysis and recommendations. *Journal of Applied Ichthyology*, *22*(4), 241–253. doi: 10.1111/j.1439-0426.2006.00805.x

Fulton, C. J., & Bellwood, D. R. (2005). Wave-induced water motion and the functional implications for coral reef fish assemblages. *Limnology and Oceanography*, *50*(1), 255–264. doi:

10.4319/lo.2005.50.1.0255

GBRMPA. (2016). *Great Barrier Reef Marine Parks Zoning Map 4 - Cooktown.* Great Barrier Reef Marine Park Authority.

Gislason, H., Daan, N., Rice, J. C., & Pope, J. G. (2010). Size, growth, temperature and the natural mortality of marine fish. *Fish and Fisheries*, *11*(2), 149–158.

Goatley, C. H. R., & Bellwood, D. R. (2016). Body size and mortality rates in coral reef fishes : a three-phase relationship. *Proceedings of the Royal Society B: Biological Sciences*, *283*, 20161858. doi: 10.1098/rspb.2016.1858

Goodrich, B., Gabry, J., Ali, I., & Brilleman, S. (2018). *rstanarm: Bayesian applied regression modeling via Stan*. R package version 2.17.4.

Hijmans, R. J. (2019). *geosphere: Spherical Trigonometry.* R package version 1.5-10.

Jørgensen, C., & Holt, R. E. (2013). Natural mortality: its ecology, how it shapes fish life histories, and why it may be increased by fishing. *Journal of Sea Research*, *75*, 8–18.

Morais, R. A., & Bellwood, D. R. (2018). Global drivers of reef fish growth. *Fish and Fisheries*, *19*(5), 874–889. doi: 10.1111/faf.12297

Morais, R. A., & Bellwood, D. R. (2019a). Data from "Pelagic subsidies underpin fish productivity on a degraded coral reef". doi: 10.25903/5c89c4ebba610

Morais, R. A., & Bellwood, D. R. (2019b). Pelagic subsidies underpin fish productivity on a degraded coral reef. *Current Biology*, *29*(9), 1521–1527. doi: 10.1016/j.cub.2019.03.044

Munday, P. L. (2004). Habitat loss, resource specialization, and extinction on coral reefs. *Global Change Biology*, *10*(10), 1642–1647.

Pauly, D. (1980). On the Interrelationships between Natural Mortality, Growth Parameters, and Mean Environmental Temparature in 175 Fish Stocks. *ICES Journal of Marine Science*, *39*(2), 175–192.

Pratchett, M. S. (2010). Changes in coral assemblages during an outbreak of Acanthaster planci at Lizard Island, northern Great Barrier Reef (1995-1999). *Coral Reefs*, *29*(3), 717–725. doi: 10.1007/s00338-010-0602-9

Pratchett, M. S., Wilson, S. K., & Baird, A. H. (2006). Declines in the abundance of *Chaetodon* butterflyfishes following extensive coral depletion. *Journal of Fish Biology*, *69*(5), 1269–1280.

doi: 10.1111/j.1095-8649.2006.01161.x

R Core Team. (2019). *R: A language and environment for statistical computing*. Retrieved from http://www.r-project.org/

Stan Development Team (2018). *RStan: the R interface to Stan.* R package version 2.18.2.

Wismer, S., Hoey, A. S., & Bellwood, D. R. (2009). Cross-shelf benthic community structure on the Great Barrier Reef: Relationships between macroalgal cover and herbivore biomass. *Marine Ecology Progress Series*, *376*, 45–54. doi: 10.3354/meps07790

Appendix F: Supporting Information for Chapter 6

Supplemental Methods

Productivity-biomass relationships: a large-scale empirical dataset

To evaluate whether standing biomass is able to predict the productivity of fish assemblages, we used a dataset of parrotfish (Labridae, Scarini) counts across the Indo-Pacific realm, from Mauritius, in the Western Indian Ocean, to French Polynesia, in the Central Pacific (Bellwood, Hoey, & Choat, 2003; Bellwood, Hoey, & Hughes, 2012). This spanned 154º of longitude and around 15,000 km of linear distance. Parrotfishes have been repeatedly identified both as key to coral reef functioning (Bellwood, Hughes, Folke, & Nyström, 2004; Bonaldo, Hoey, & Bellwood, 2014; Hoey, Taylor, Hoey, & Fox, 2018) and coral reef fisheries, in studies ranging from local scales to across the whole Indo-Pacific (Bellwood et al., 2012; DeMartini et al., 2017; Hamilton et al., 2016; Houk et al., 2012; Rhodes, Tupper, & Wichilmel, 2008; Taylor, Lindfield, & Choat, 2015). Furthermore, although large parrotfish species can be very susceptible to fishing (Bellwood et al., 2012; Hamilton et al., 2016), small species often exhibit quick life-histories, maturing early and having a relatively short lifespan (Choat, Axe, & Lou, 1996; Choat & Robertson, 2002). Parrotfishes have been shown to play a key role in sustaining fisheries-depleted stocks in developing countries (Condy, Cinner, McClanahan, & Bellwood, 2015; McClanahan, 2018), and are likely to play an even greater role in sustaining coral reef fisheries as longer-lived species are depleted from these systems.

Parrotfishes were counted and had their size estimated (total length, TL, in cm) during timed-swim transects of 20 min duration that covered an average distance of 235 m (Bellwood & Wainwright, 2001). The width of the transects was 5 m for fish larger than 10 cm, and 1 m for fish 10 cm or smaller. Details on the procedures are available in Bellwood & Wainwright (2001). Transects were laid in four coral reef habitat zones: back, flat, crest and slope, with 4.3 ± 0.8 transects per habitat (mean ± SD). The dataset had a total of 313 counts divided in 19 locations and 10 regions (Figure 1, Table S5). Bayesian length-weight parameters a and b (Froese, Thorson, & Reyes, 2014) and species maximum size (L_{max}) for all parrotfish species were obtained from FishBase (Froese & Pauly, 2018). VBGM coefficients were estimated following **Chapter 2**, using mean sea surface temperature data for each

locality extracted from Bio-Oracle (Tyberghein et al., 2012). We used the procedures in equations (12) to (18) in the Methods of **Chapter 6** to estimate total parrotfish standing biomass (kg m^{-2}) and biomass productivity (g m^{-2} day^{-1}) per transect across our study regions, and then aggregated both biomass and productivity by averaging among transects within regions.

We evaluated potential productivity-biomass relationships in parrotfish assemblages in two spatial scales. First, we tested whether standing biomass could predict patterns in productivity among regions using a Generalized Linear Model (GLM) with gamma error distribution. Second, within-regions, we modelled productivity as a linear function of biomass, region, reef habitat, and a biogeographic measure of distance to the centre of the Indo-Australian Archipelago (IAA), using a Gaussian linear model. This distance was calculated in longitudinal degrees from each sampled coordinate towards the longitude of 131º, in Raja Ampat, Indonesia. This region has been showcased as the centre of biodiversity in the Coral Triangle, having the highest recorded coral reef fish species richness in the world (Allen, 2008; Allen & Erdmann, 2009). The distance to the centre of the IAA was intended to account for biogeographic differences in species composition between different regions along the broad longitudinal stretch sampled. Our linear model included interactions between biomass and region, biomass and reef habitat, and biomass and distance to the centre of the IAA. We compared this full model with nested subset models using Akaike Information Criterion and derived measures, as implemented by the R package *MuMIn* (Bartoń, 2016). The two most informative sub models had AICs that differ in less than two units and were, thus, indistinguishable (Burnham & Anderson, 2002). Both models included biomass, region, habitat, and an interaction between biomass and region (**Table F1**), but only one of these models included distance to the centre of the IAA. Since these models were indistinguishable, we opted for the simplest model, which excluded distance to the centre of the IAA (see Methods section on **Chapter 6** for the model equation).

To disentangle some of the drivers of patterns in productivity versus biomass for parrotfish assemblages, we modelled regional-level biomass, body length and productivity as linear functions of human population density and distance to the centre of the IAA. Biomass, productivity and body length were first averaged among individual transects for each habitat, then across habitats in each location, and then between locations, if a region comprised more than one location. Distance to the centre of the

IAA was processed in a similar hierarchical way, although it was obtained for different sites in a location, and most habitats shared the same coordinate. Human population density was calculated by averaging human population in a radius of 30 km from each site, rescaling it to $\log_{10}$ (individuals 100 km^{-2}), and then averaging across locations and regions. The raw human population data was obtained from the Gridded Population of the World (GPW), v4 (CIESIN, 2016). We used GLMs with gamma error distribution to model regional biomass and productivity, and Gaussian linear models to model regional average body length.

Modelling a coral reef fish assemblage

We used size-spectrum theory as a basis to derive theoretical expectations on the size structure of fish assemblages in our model (Andersen & Beyer, 2006; Edwards, Robinson, Plank, Baum, & Blanchard, 2017; Jennings & Dulvy, 2005). Size-spectrum expectations have been shown to accurately reflect the empirical size structure of coral reef fish assemblages (Dulvy, Polunin, Mill, & Graham, 2004; Graham, Dulvy, Jennings, & Polunin, 2005; Robinson et al., 2017; Wilson et al., 2010). Thus, we used the principles laid out by Edwards et al. (2017) to guide our model building. The bounded power law is defined by the probability density function:

$$f(L_i) = C{L_i}^{\lambda} \quad \text{(F1)}$$

where L_i represents the length of each individual fish, λ is the exponent governing the abundance-size relationship, and C is a constant relating the exponent to the maximum and minimum sizes, L_{min}^{n} and L_{max}^{n} (Edwards et al., 2017). We considered 5 cm total length (TL) as the minimum size of a fish in our modelled assemblage, and 100 cm TL as the maximum size. Fish smaller than 5 cm TL are not adequately surveyed by standard coral reef fish sampling procedures (e.g. visual surveys, Ackerman & Bellwood, 2000). Fish larger than 100 cm TL have very low abundances, encompassing a small fraction of what is normally detected in coral reef surveys. Sharks can be an exception to this, and large densities of sharks in remote coral reefs have been estimated using visual surveys (Sandin et al., 2008). However,

their high mobility and inquisitive behaviour likely result in overestimated counts by divers (Bradley et al., 2017; Ward-Paige, Flemming, & Lotze, 2010). Thus, we follow recent large-scale studies (e.g. Robinson et al., 2017; Williams et al., 2015) and do not consider sharks in our modelled assemblage. The exponent λ describing the shape of the size spectrum was set to the value of -2.7, based on the values for length size spectra in Robinson et al. (2017). Nevertheless, we have also considered different values of λ (see *Sensitivity Analyses* below). We used the inverse probability distribution function to randomly draw length values from the bounded power law in equation (F1), as described in Edwards et al. (2017). Our fish assemblage consisted of $n = 1000$ individuals with length values sampled by this method.

To be able to estimate individual somatic growth, and therefore productivity (**Chapter 3**), we had to assign a theoretical maximum size (total length) to which each individual i could grow, L_{max_i}. Because there are no mechanistic links between the size of a fish in a community and the maximum size it will potentially attain, we based this step on the distribution of maximum sizes of an empirical coral reef fish assemblage at Lizard Island, in the Great Barrier Reef (**Chapter 4**; Morais & Bellwood, 2019). We used a resampling procedure that combines multiple survey phases in one standardised area as described below (section *Simulating fishing on whole coral reef fish assemblages*). The resampled dataset included only individuals from species with $L_{max} \geq 6\ cm$ TL, thus allowing fish with 5 cm TL (i.e. the minimum size in our modelled assemblage) to grow at least 1 cm. We first created size-specific distributions of L_{max} by binning the sizes of the individuals on this dataset (5-10 cm, 11-20 cm, 21-30 cm, 31-50 cm and >50 cm). Then, for each individual in our simulated assemblage, we sampled a maximum size value from the size-specific L_{max} distribution that matched L_i, the size of that individual. For example, a fish with $L_i = 15\ cm$ would have its maximum size drawn from the empirical L_{max} distribution of the 11-20 cm size bin. The probability of drawing each L_{max} value in a size bin was proportional to the number of individuals from the empirical dataset that had that value, provided that $L_{max} \geq L_i$ (i.e. an individual could not attain a maximum size smaller than its actual size).

To estimate body mass values, we assigned length-weight regression parameters to each fish. These parameters were obtained from the same empirical assemblage as above. We started by testing

for potential relationships between the length-weight parameters a and b and individual size or maximum species size. Linear models did neither show evidence of size nor of maximum species size dependences on a or b, and therefore we used the model intercept estimates (i.e. average values) of $a = 0.019$ and $b = 3.04$ for all individuals. In essence, this means that all fishes in our model shared the same average body shape and did not significantly change this shape during their ontogeny (see Froese, 2006). These parameters were then used to estimate the mass of each individual following equation (12) in **Chapter 6**, and the biomass of the assemblage following equation (13) in **Chapter 6**.

To model the somatic growth of each individual, we first determined likely growth trajectories in the Von Bertalanffy Growth Model (VBGM) following Morais & Bellwood (2018). The theoretical maximum size of each individual assigned above, L_{max_i}, was used as the species maximum body size; and we assigned a temperature of 30°C to our simulated coral reef fish assemblage. This is a typical mean sea surface temperature to which reefs in the Coral Triangle are exposed (data extracted from Bio-Oracle, Tyberghein et al., 2012). Then, we used these values to predict growth for all combinations of trophic groups and positions relative to the reef. We further averaged the predictions across trophic groups and remaining positions relative to the reef to obtain K_{max_i}, *i.e.* the growth coefficient of an individual i from our modelled fish assemblage. By averaging across trophic groups and positions, we assume that all combinations of these traits can coexist in the modelled community. Nevertheless, the impact of any potential departure between the result of this step and the trophic structure of real assemblages is likely to be minor because dietary group and position relative to the reef explain, together, only about 6% of the variability in reef fish K_{max}. Body size and temperature are the primary drivers of fish growth, together explaining around 69% of its variability (**Chapter 2**; Morais & Bellwood, 2018). Finally, we used the derived parameters L_{max} and K_{max} to calculate the expected growth, in mass units, from equations (12) to (18) of **Chapter 6**.

Simulating coral reef fisheries impacts in our modelled assemblage

The next step to unveiling the potential mechanisms relating productivity-biomass relationships with human population density, was to simulate exploitation of our modelled fish assemblages, i.e. coral

reef fisheries. We did that by simulating the effect of different capture levels c with a size-dependent fishing probability function. We started by establishing $L_{max_{th}} = 20cm$, as an arbitrary threshold L_{max} for a fish to be considered as "fishable" or target for fisheries. Thus, any individuals with $L_{max_i} \geq L_{max_{thr}}$ were considered as targeted. We formulated our size-dependent fishing function as a mixed Power and Gompertz curve that should act over this pool of target fishes, n_{tar}. Within this function, we established a reference size, L_f, so that: 1) fish with 5 cm TL had zero chance of being captured; 2) fish with 6-10 cm TL had a negligible chance of being captured; and 3) fish with 11-L_f cm had an exponential increase in their chance of being captured, cp_{l_f}, up to $cp_{l_f} = 0.1$. Thus, from 5 cm to L_f the probability of being captured obeyed the Power part of the function (**Figure F17**). From L_f to L_{max}^n, the maximum size potentially found in our assemblage (*i.e.* 100 cm TL), our function followed a Gompertz curve. The Gompertz inflexion point was set at $2L_f$ and, given the mixed nature of the function, coincided with a $cp_{l_f} = 0.6$. Between $2L_f$ and L_{max}^n, cp_l would slowly grow in an asymptotic way (**Figure F17**). Finally, at L_{max}^n, the probability of capture was at its maximum value, $cp_{l_{max}} = 1$. The mathematical formulation of our function was, for $L_f < L \leq L_{max}^n$:

$$cp_l = I + \left[(S - I)e^{e^{-v\left(L-2L_f\right)}}\right] \tag{F2}$$

where L is length in cm, $L_f = 17$ cm, and the parameters I, S and k are fixed at $I = 1.25$, $S = 1$ and $v = 0.025$. For $L_{min}^n \leq L \leq L_f$:

$$cp_l = rL^h \tag{F3}$$

where h is fixed at $h = 6$ and r is a constant defined by $r = \frac{I+\left[(S-I)e^{e^{-v\left(L_f-2L_f\right)}}\right]}{{L_f}^h}$. The calculated cp vector was rescaled to assume values between 0 and 1, resulting in actual probability values. Sigmoidal size-susceptibility curves have been suggested for multiple gear types in coral reef fisheries, including

trawls, seines, traps and corrals (Dalzell, Polunin, & Roberts, 1996). Other gears, such as handlines or spearfishing select for carnivorous and/or large fish, and potentially also result in sigmoidal size-susceptibility curves.

We simulated fishing impacts by randomly withdrawing a proportion c of the n_{tar} individuals in our assemblage with the probability vector given by our size-dependent fishing probability function. A preliminary exploration showed that a value of c_{max} = 0.2 was sufficient to create a scenario of biomass depletion, with $B_{c_{max}} < 0.1\ B_0$, *i.e.* in which the final biomass was reduced to less than 10% of the initial biomass. Therefore, we simulated fishing at c = {0.01, 0.02, 0.03, ..., c_{max}= 0.2}, and measured the standing biomass, productivity and turnover rates of the resulting assemblage. We present our results relative to exploitation rate (Worm et al., 2009), which is given by:

$$E_c = 1 - \left(\frac{B_c}{B_0}\right) \tag{F4}$$

where E_c is exploitation rate at catch c, B_c is biomass at c, and B_0 is unfished biomass. Productivity was calculated from equations (12) to (18) in **Chapter 6**, and turnover rates were calculated as the ratio of productivity per biomass, rescaled to % year^{-1}.

Fishing was repeated for each capture level c for 200 iterations. Importantly, we simulated fishing captures acting over the initial (unfished) fish assemblage only. Our emphasis here is on the effects of "instantaneous fishing" on the biomass and productivity of coral fish assemblages. We acknowledge that other processes acting at larger time scales, such as behavioural responses to fishing, could additionally affect capture rates in a scenario of continue fishing, *i.e.* fishing over previously fished assemblages.

Measuring the steepening of the size-spectrum exponent and sensitivity analyses

One of the expected consequences of fishing is the steepening of the size spectrum exponent λ, *i.e.* λ becoming more negative (Dulvy et al., 2004; Jennings & Blanchard, 2004; Robinson et al., 2017). We evaluated if this prediction held in our simulations by estimating the exponent λ_c from our

assemblage after fishing for each c value. To do that, we calculated the log-likelihood of a broad range of candidate λ_c, and then searched for the value of λ_c that maximum the likelihood function. We employed the modified form of the likelihood function presented in Edwards et al. (2017):

$$\ln[\mathcal{L}(\lambda_c|\,\vec{L})] = n\ln\left(\frac{\lambda_c+1}{{L_{max}^n}^{\lambda_c+1} - {L_{min}^n}^{\lambda_c+1}}\right) + \lambda_c\sum_{i=1}^{n}\ln L_i \tag{F5}$$

where $\mathcal{L}$ denotes the likelihood function and $\vec{L}$ is the vector of observed fish lengths.

We also performed a series of sensitivity analyses to assess how relaxing certain assumptions could affect our conclusions. We re-ran all the analytical procedures by varying 1) the initial exponents of the size spectrum, λ; 2) the size thresholds for considering a fish as "fishable" or target, $L_{max_{thr}}$; and 3) the size-specific fishing function. We used λ = {-2.9, -2.7, -2.5, -2.3, -2.1}, which encompasses the range of the length size-spectrum exponent empirically reported for uninhabited coral reef fish assemblages in Robinson et al. (2017). We used $L_{max_{thr}}$ = {30, 25, 20, 15, 10} in cm, ranging from a scenario of selective fisheries (larger $L_{max_{thr}}$), normally characteristic of lightly fished coral reef systems, to a scenario of unselective fisheries (smaller $L_{max_{thr}}$), normally characteristic of heavily fished systems. The alternative size-dependent fishing probability functions employed varied in how they dealt with our size reference points L_f, $2L_f$, and L_{max}^n. All functions, however, had the same overall shape: the probability of being captured was very small at small sizes, growing quickly at intermediate sizes and slowing down towards the largest sizes. **Table F6** lists the functions used, their formulas and their fixed parameter values.

Simulating fishing on parrotfish assemblages

To evaluate whether the observed decreases in biomass and productivity with fishing in our model could arise from properties of our modelled fish assemblages, we simulated fishing in the parrotfish dataset. This procedure also involved applying a size-dependent fishing probability function

and simulating different capture intensities (see Methods, *Simulating the impact of coral reef fisheries on empirical fish assemblages*).

We started by subsampling the parrotfish assemblage of each region to include three samples from each of back, flat and crest reef habitats. Vanuatu was the only region where back reefs were not present, so we sampled six reef flats and three crests from this region instead. Samples were drawn from the available pool hierarchically by habitat, and randomly within habitats. We rescaled the outputs from a total sampled area of 10,575 m^2 for each region, to one hectare. In contrast to our modelled assemblages, each subsampled assemblage had different abundances, and so the maximum capture rate c_{max} could not be fixed. We chose c_{max} values for each region that allowed enough individuals to be captured and to result in a scenario of at least $B_{c_{max}} < 0.2\ B_0$. These c_{max_r} values varied from 0.25 to 0.55. We then simulated fishing, for each region, using c_r values that ranged from c_r = {0.01, 0.02, ..., c_{max_r}}. Each c intensity was simulated over 200 iterations for each region, with each iteration subsampling the parrotfish assemblages per region.

Parrotfish assemblages subjected to simulated fishing exhibited the same decoupled declines in biomass and productivity as the modelled assemblages (**Figure F18**). This happened irrespective of the regional-scale initial level of biomass depletion, although the capture rates required to trigger the most intense responses varied depending on the region (**Figure F19**). This reinforced the suggestion from our model that the initial size structure affects the intensity of the buffering response (see **Figure F8**). However, intrinsic size-structure differences between whole fish assemblages (i.e. our model) and selected groups (i.e. parrotfishes) could preclude generalising insights from simulating fishing on this dataset. To solve this potential issue, we simulated fishing over entire coral reef fish assemblages using empirical data from the Coral Triangle and the Great Barrier Reef.

Simulating fisheries impacts on whole coral reef fish assemblages

We simulated fishing on two high-resolution empirical datasets of entire coral reef fish assemblages from the Great Barrier Reef (Lizard Island) and the Coral Triangle (Raja Ampat, Indonesia). We first asked if the same decoupled productivity-biomass relationships were generated by

fishing these datasets, and then evaluated initial size structure features likely to affect the intensity of these decoupled relationships.

The Great Barrier Reef (GBR) dataset encompassed the same underwater visual counts of fish as used in **Chapter 4** (Morais & Bellwood, 2019). This included 36 fish counts obtained at Lizard Island, in the norther section of the GBR, distributed among four reef zones: outer slope, crest, flat and back reef. The Coral Triangle dataset was collected in the southern Raja Ampat's islands around Misool, in Indonesia's West Papua Province, using the same underwater visual count method. A total of eight counts were obtained from the crest/slope of fringing reefs at the same depth range (6-15 m). In these fringing reefs, the transition between the reef crest and slope was often not reliably identifiable. In both locations, surveys were undertaken primarily within no-take zones of Marine Protected Areas (the Great Barrier Reef Marine Park and the Misool Private Marine Reserve, respectively). Apart from limited poaching, there is virtually no fishing extraction in both locations, making them ideal for simulating the effects of fishing on reef fish assemblages.

The counts from both the GBR and the Coral Triangle were composed of four phases, each targeting fishes of different size ranges and behaviours. These phases were combined by using an algorithm that resamples proportionally to the abundance detected and area surveyed on each phase, providing an output relative to a standardised area (see **Chapter 4**). We chose a standardised area of 250 m^2, equal to area of the largest survey step, which included enough individuals to withstand simulated fishing with varying intensity. All coral reef fishes detected within the surveyed area at each phase were recorded and identified to the species or genus level. Because of significant differences in accessibility, we split the Lizard Island dataset in lagoon (flat and back reefs) and exposed habitats (crest and slopes). The three resulting datasets (lagoon and exposed reefs at Lizard Island, and Raja Ampat) were then filtered to include the same size range encompassed by our modelled assemblages (individuals with 5-100 cm TL, with $L_{max} \geq 6\ cm$). Bayesian length-weight parameters a and b and VBGM coefficients were obtained for each species using to the same procedures and methods described above for parrotfishes.

We then ran two sets of fishing simulations using the three datasets. First, to evaluate if decoupled responses from productivity and biomass to exploitation occurred at the regional scale, we combined

samples within each dataset into one large assemblage, and then simulated fishing on each of these regional assemblages. Then, we resampled one standardised area of 250 m^2 per dataset (i.e. lagoon and forereefs at Lizard Island, and Raja Ampat). Finally, we simulated fishing over a range of capture rates, c, ranging from c = {0.01, 0.02, 0.03, ..., c_{max}= 0.35}, that resulted in a biomass after fishing of $B_{c_{max}} < 0.1\ B_0$. These steps were repeated for each c for 200 iterations. Second, to compare the behaviour of modelled and empirical fish assemblages submitted to fishing, we resampled one standardised area of 250 m^2 per sample per dataset. This resulted in 44 fish assemblages (18 in the lagoon and 18 in the forereef of Lizard island, and eight on Raja Ampat). We then submitted each of these to fishing over a range of capture rates, c_r, that ranged from c_r = {0.01, 0.02, ..., c_{max_r}}. In this case, the maximum capture rate c_{max} could not be fixed and was chosen for each sample to result in a scenario of at least $B_{c_{max}} < 0.1\ B_0$. These c_{max_r} values varied from 0.11 to 0.3. Again, each c intensity was simulated over 200 iterations for each sample.

Comparing modelled and empirical buffering responses to exploitation

We used the transect-level set of fishing simulations above to compare features of the buffering responses to fishing between empirical and modelled fish assemblages. Specifically, we chose the maximum buffering productivity as a reference point with which to contrast modelled and empirical datasets. We first calculated the maximum value attained by the average buffering productivity curve across 200 iterations in our modelled fish assemblages while varying the size-spectrum exponent, with values of λ = {-5, -4.8, -4.6, ..., -1.8, -1.6, -1.4}. This interval was similar to the size-spectrum exponent interval comprised by the empirical fish assemblages before fishing. We term the maximum value of the buffering productivity curve the 'peak buffering productivity'. We hypothesized that the peak buffering productivity would respond to the size structure of the target component of the unfished assemblages. Therefore, we investigated how it related to λ, mean individual body size (in g), mean individual growth (in g day^{-1}) and biomass turnover rates in both the model and empirical fishing simulations. Importantly, these size-structure indicators (i.e. size spectrum exponent, mean body size and growth, and turnover) were calculated from fishable individuals, i.e. those larger than the minimum

fishing species size threshold of 20 cm TL. This resulted in both modelled and empirical target size-spectrum exponents, λ_{tar} shallower (i.e. less negative) than λ.

Due to extensive collinearity among variables (e.g. mean individual body size and growth, **Figure F16**), peak buffering productivity from empirical assemblages was modelled separately by each size structure indicator. We used Generalized Additive Models (GAMs) with thin plate regression splines as the smoothing basis and a maximum dimension of 10. Each GAM had peak buffering productivity as the response variable and one of the size structure indicators as the predictor. Posterior checking of the estimated degrees of freedom revealed that maximum dimension chosen performed consistently. For the modelled assemblages, we simply varied the initial size spectrum exponent over the same interval observed in the empirical assemblages and plotted the peak buffering response against each of the four indicators above. Empirical- and modelled-peak buffering productivity responses to each indicator were compared visually.

Model assumptions and stock-recruitment relationships

In this study, we consider that the variation in productivity as a function of biomass is likely driven by somatic growth rather than by recruitment. This can happen if recruitment saturates or peaks at low to intermediate biomass, with no recruitment gains (or decreases in recruitment) following further biomass increases. Fisheries models such as Beverton-Holt, Ricker, Deriso-Schnute and Shepherd commonly include an asymptotic or unimodal stock recruitment relationship that arises from post-recruitment density-dependent processes (Beverton & Holt, 1957; Hilborn & Walters, 1992; Subbey, Devine, Schaarschmidt, & Nash, 2014). Multiple lines of evidence suggest that a relationship like that is likely for reef fishes. For example, although the impacts of fishing on reproductive-biomass and -energy output are well documented (Barneche, Robertson, White, & Marshall, 2018; Hixon, Johnson, & Sogard, 2014; Scott, Marteinsdottir, & Wright, 1999), evidence for strong positive relationships between reproductive biomass and recruitment in marine fishes is weak, suggesting that any such relationships are likely small in magnitude (Munch, Giron-Nava, & Sugihara, 2018; Szuwalski, Vert-Pre, Punt, Branch, & Hilborn, 2015). A recent evaluation of stock-recruitment assumptions showed

that, for most fisheries stocks evaluated, recruitment was relatively independent of spawning biomass (Szuwalski et al., 2015). The authors of this study found that recruitment was, most often, explained by environmental variations (Szuwalski et al., 2015). Another meta-analysis on the subject detected higher coupling between stock size and recruitment, although stock size explained only a very small proportion of variation in recruitment (Munch et al., 2018). Importantly, neither of these two large-scale evaluations were based on multispecies stocks or included coral reef fish species.

Coral reef fishes have distinct life-histories and habitat relationships compared to temperate or tropical non-reef fishes, which predominate as fisheries stocks. The dual life cycle of reef fishes includes a pelagic larvae, but there is mixed evidence on the degree to which these populations are open or closed, and on the extent to which adult populations can affect recruitment (Mora & Sale, 2002). Intense pelagic mortality, for instance, can drive substantial decoupling in the magnitudes of spawning and recruitment (Doherty, 1991; Meekan, Milicich, & Doherty, 1993; Robertson, 1990). Furthermore, the degree of spawning-recruitment decoupling varies with body size among fish families globally (Brandl et al., 2019), with larger fishes having low recruitment despite high reproductive output, and smaller fishes the opposite pattern (Brandl et al., 2019). This implies that families of larger fishes that are most likely to drive buffering productivity do so despite limited inputs from recruitment. Thus, our assumption that recruitment saturates at relatively low biomass levels for coral reef fishes appears reasonable in light of the knowledge available.

By modelling the somatic component of productivity, we do not explicitly quantify settlement inputs and natural mortality. We believe that this is likely to have minimal consequences for the output values. First, the direct contribution of settlement to local biomass production is likely to be negligible. Because recruits are often just a small fraction of adult size (Leis, 1991; Victor, 1991), any fish in the range size targeted by coral reef fisheries undertakes the vast majority of their somatic growth post-recruitment. This point can be further illustrated if we consider a hypothetical parrotfish recruit with 1.7 cm TL (a conservative recruit size for this group, see Grutter et al., 2017) and apply average length-weight regression coefficients for the group ($a = 0.017$ and $b = 3.06$, Froese & Pauly, 2018; Froese et al., 2014) to estimate its body mass. The weight of this recruit, 0.086 g, would only be 0.33% of the weight of an individual (with the same length-weight regression coefficients) with the minimum length

susceptible to fishing in our model (11 cm TL), approximately 26 g. Thus, 303 recruits would be required to yield the weight of a single 11 cm-sized fish. Such a ratio of recruits is not ordinarily expected in coral reef fishes (Hixon & Webster, 2002), further supporting our assumption that recruitment is negligible as a direct source of standing biomass.

Second, natural mortality rates are small in the size range considered herein. Although coral reef fish recruits can have high (> 35%) daily mortality rates (Almany & Webster, 2006), these rates drop rapidly (to <0.2%) as the fishes grow above 42 mm (Goatley & Bellwood, 2016). Hence, fishes in the scope of this work have probably already overcome most of the natural mortality rates to which they would be subjected during their lives. At the sizes considered, fishing mortality is likely to dominate total mortality. Furthermore, spatial variation in natural mortality rates of parrotfishes has been attributed to either predation pressure or density-dependent processes (Gust, Choat, & Ackerman, 2002; Taylor et al., 2018). If differential predation pressure drives natural mortality variation, natural mortality would be expected to decrease at low biomass levels as large predatory fishes are depleted first with increasing fishing pressure (D'agata et al., 2016; Graham et al., 2017). Similarly, if density-dependent processes drive natural mortality, higher mortality would be expected under high biomass/high density than under low biomass/low density scenarios. In both cases, natural mortality would decrease as biomass is depleted. Our model therefore provides a conservative estimate of the effects of biomass depletion on fish productivity.

Relationship between buffering productivity and surplus production

Although buffering productivity may resemble the dynamic concept of surplus production (Schnute & Richards, 2002; Szuwalski et al., 2015), they differ in three fundamental ways. Firstly, while surplus production is a measure of net production, buffering productivity exclusively describes relative rates of productivity depletion: net production does decline with decreasing biomass (**Figure 4**, **Chapter 6**). Secondly, while surplus production curves are traditionally dome-shaped (Hilborn & Walters, 1992; Schnute & Richards, 2002), buffering productivity curves are left-skewed (**Figure 4**, **Chapter 6**). Finally, while surplus production models have been developed and are implemented predominantly at the population/stock level (Hilborn & Walters, 1992; Schnute & Richards, 2002),

buffering productivity is essentially an assemblage-level metric. Buffering productivity could arise, for example, as an emergent property of surplus production from multiple populations that vary in body size. When subjected to size-selective fisheries, these populations would be driven to different parts of their exploitation axis. As a consequence, while surplus production models predict, at high exploitation, a steep decline in productivity from its peak value, buffering productivity predicts only a small decline. Thus, its compensatory nature appears to be stronger.

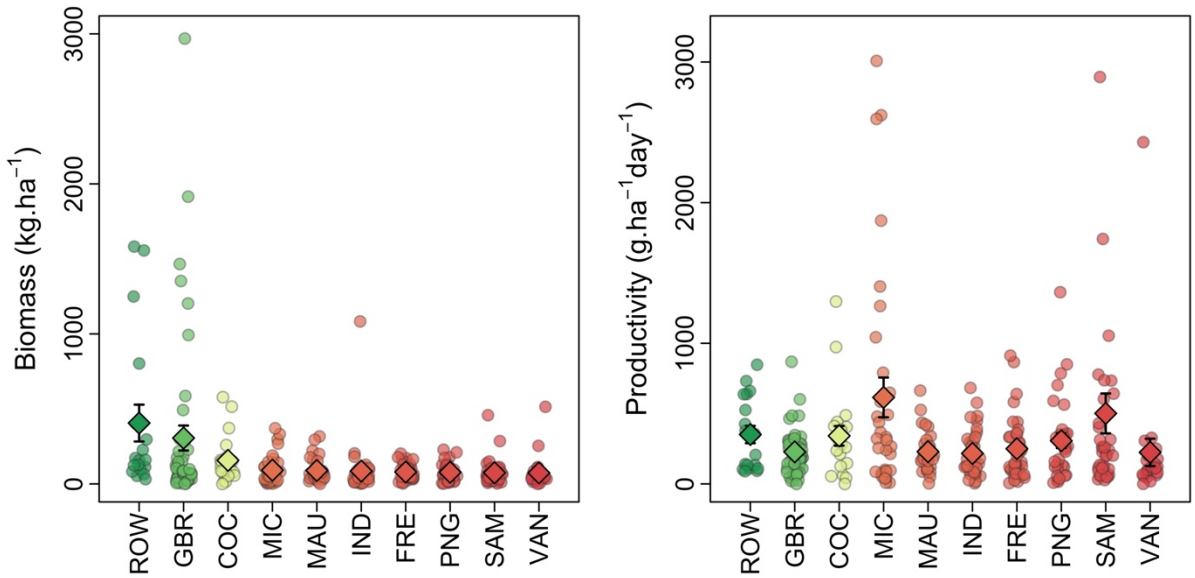

Figure F1: *The mismatch between biomass and productivity in parrotfish assemblages across the Indo-Pacific. Each circle is a sample, diamonds are the mean values, and error bars are the standard errors of the mean. Note that the axes were rescaled from Figure 1 to accommodate extreme values. ROW = Rowley Shoals; GBR = Great Barrier Reef; COC = Cocos (Keeling) Islands; MIC = Micronesia; MAU = Mauritius; IND = Indonesia; FRE = French Polynesia; PNG = Papua New Guinea; SAM = Samoa; VAN = Vanuatu.*

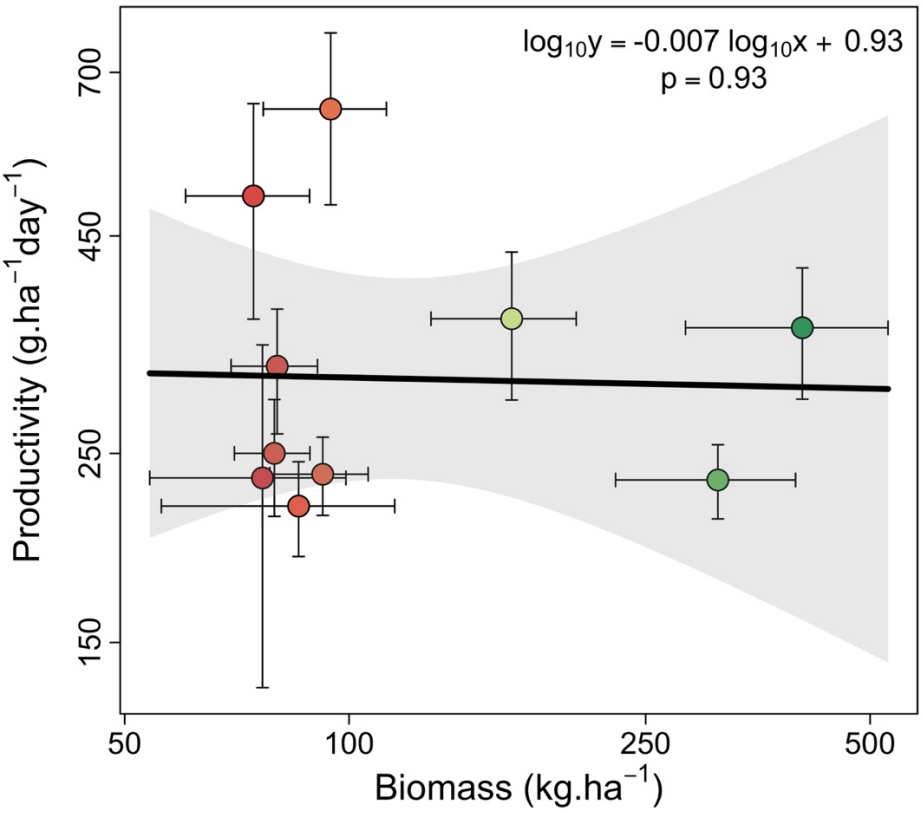

Figure F2: *Standing biomass did not predict parrotfish productivity across regions in the Indo-Pacific. The upper-right equation describes the output of a Generalized Linear Model (GLM) with gamma error distribution including biomass as the only potential predictor of productivity. Colours are proportional to the regional-level average biomass. Error bars represent the standard error of the mean. The grey band is the 95% confidence interval of the model.*

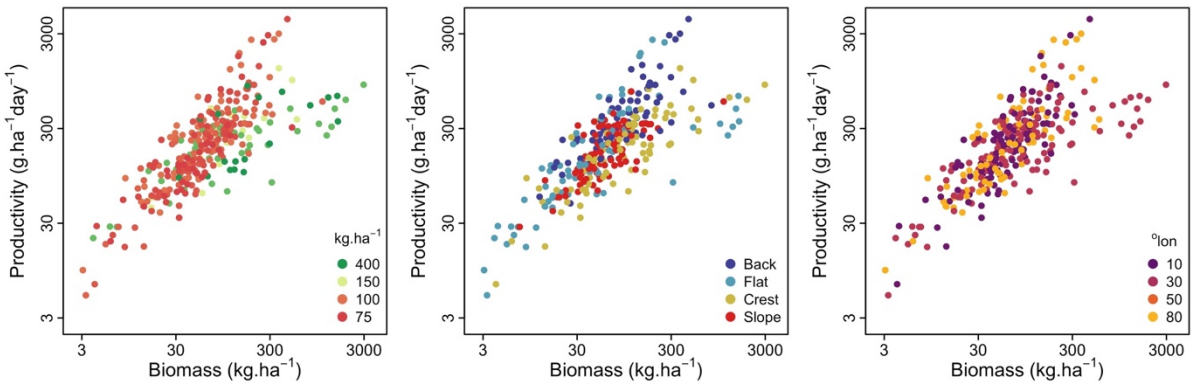

Figure F3: *The productivity-biomass relationship (at the site level) for Indo-Pacific parrotfish assemblages suggests different relationships for regions with high and low average biomass. Different habitats (central panel) and distances to the centre of the IAA (right panel) did not entail consistently distinct productivity-biomass slopes (see model in* ***Table F1*** *and* ***Table F6****).*

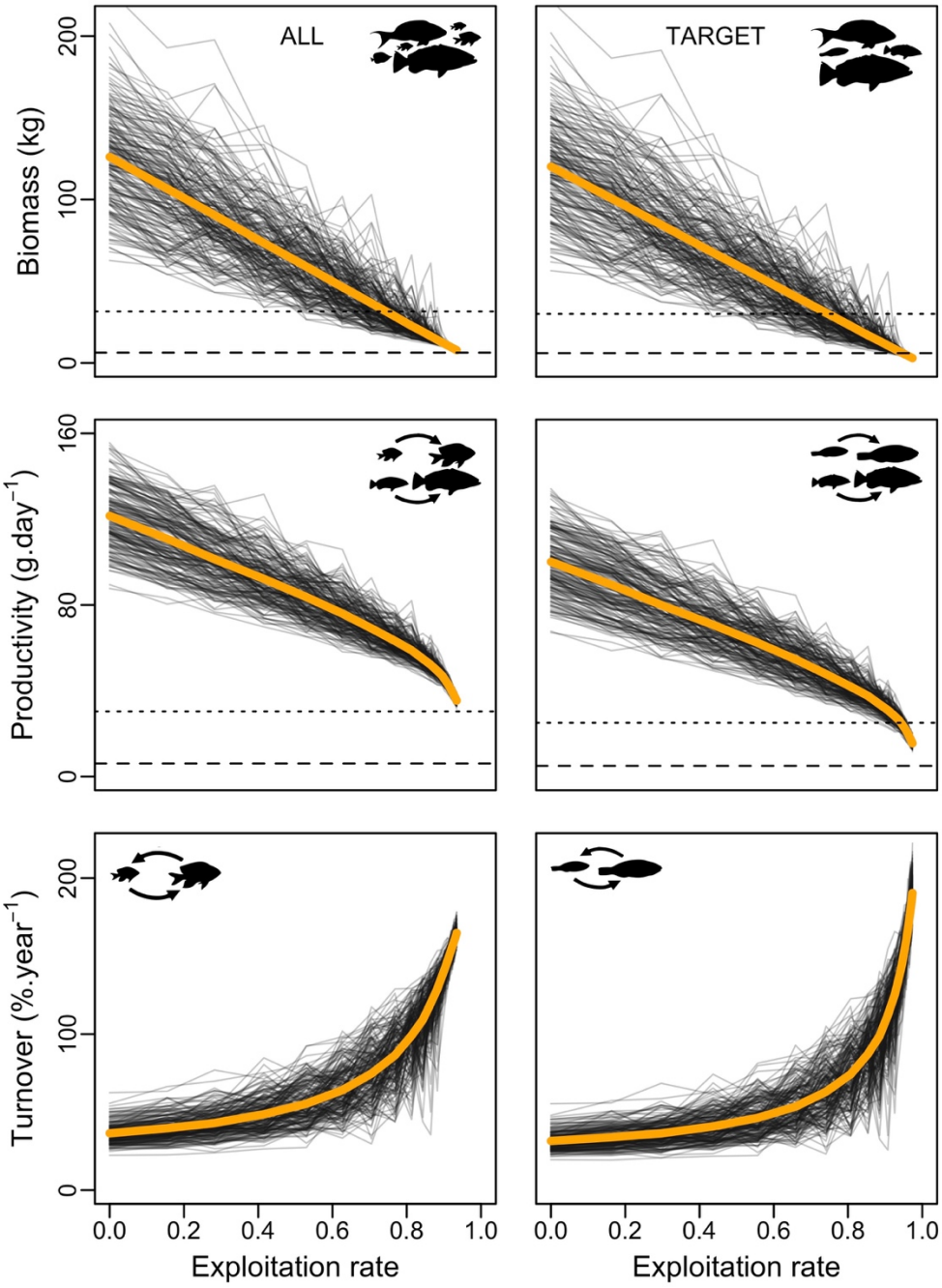

Figure F4: *Effects of increasing exploitation on the whole-assemblage and target fish biomass, productivity and turnover in modelled coral reef fish assemblages. At high exploitation, modelled coral reef fish biomass approaches zero (first row), yet productivity consistently remains higher (centre row). This happens because turnover steadily increases (bottom row). Black lines are the output of each fishing simulation and the orange lines are the average. The dotted and dashed horizontal lines represent, respectively, the 25% and 5% values of the unfished assemblage biomass or productivity. Left panels depict all fish and right panels target-species only.*

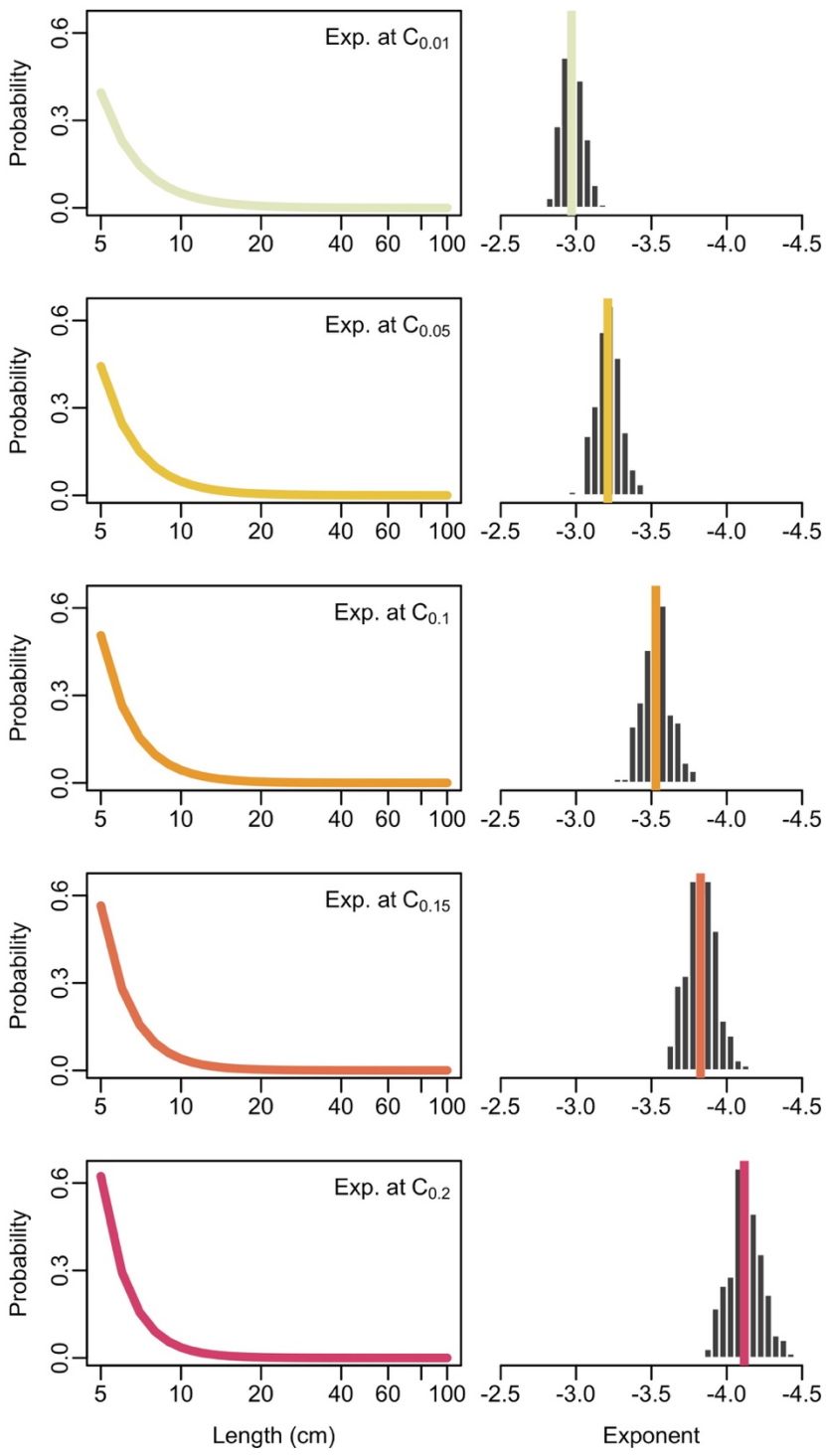

Figure F5: *Steepening of the size-spectrum exponent with increasing fishing intensity (capture rates) of modelled coral reef fish assemblages. Shown are the probability density functions (left panels) from the average size-spectrum exponents (coloured vertical line, right panels) across simulations (histogram, right panels) at different capture levels (from $C_{0.01}$ to $C_{0.2}$).*

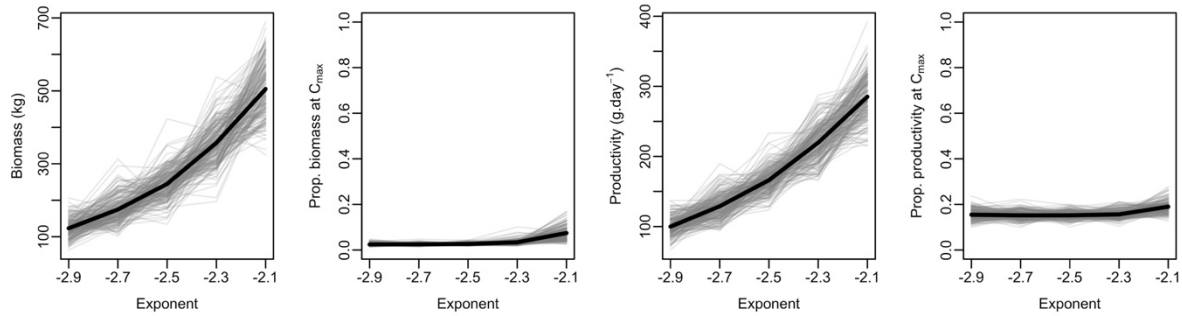

Figure F6: *The effect of varying the size-spectrum exponent on the biomass and productivity of modelled fish assemblages before and after fishing simulations. Initial total biomass and total productivity increase as assemblages become more size even (less negative exponents, left and middle-right panels). Although the proportion of initial biomass after simulating fishing at the maximum capture C_{max} (see Method of* ***Chapter 6****) increases for the more size even assemblages (middle-left), the proportion of initial productivity at C_{max} is fairly constant across exponents (right). Grey lines represent each simulation and black thick lines the average across simulations.*

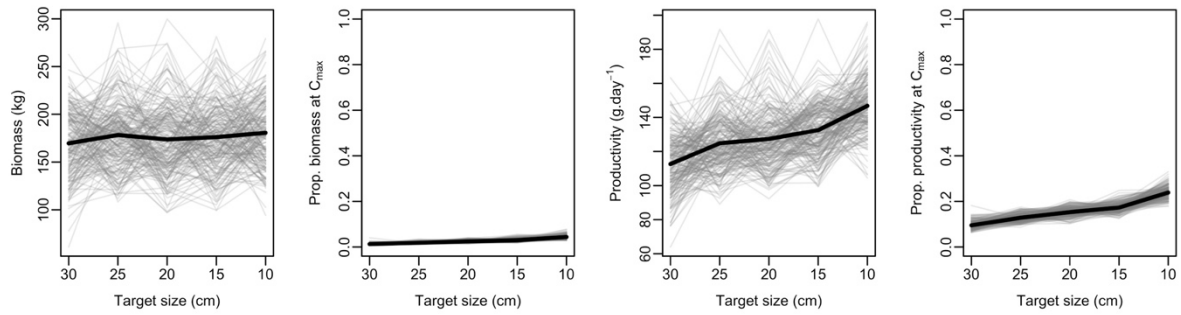

Figure F7: *The effect of varying the minimum size thresholds for exploitation on the biomass and productivity of modelled fish assemblages before and after fishing simulations. Neither the initial total biomass nor the proportion of initial biomass change after simulating fishing at the maximum capture C_{max} when fisheries target increasingly small individuals (left and middle-left panels). Contrarily, both the initial total productivity and the proportion of initial productivity at C_{max} increase as fisheries target smaller individuals (middle-right and right panels). This suggests that fisheries targeting smaller individuals will have larger disparities between the declining trajectories of biomass and productivity (buffering productivity). Grey lines represent each simulation and black thick lines the average across simulations.*

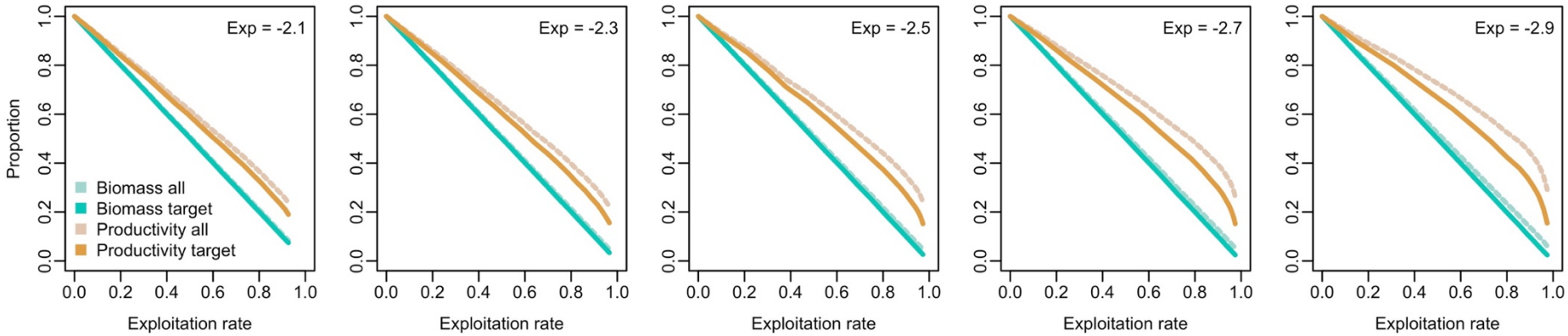

Figure F8: *The proportional decline in the biomass and productivity of modelled fish assemblages with increasing exploitation changes according to the initial size-spectrum exponents. The main overall effects of decreasing size evenness (more negative size-spectrum exponents) are increasing the disparity between the declining trajectories of biomass and productivity (buffering productivity), and between whole-assemblages and target species curves.*

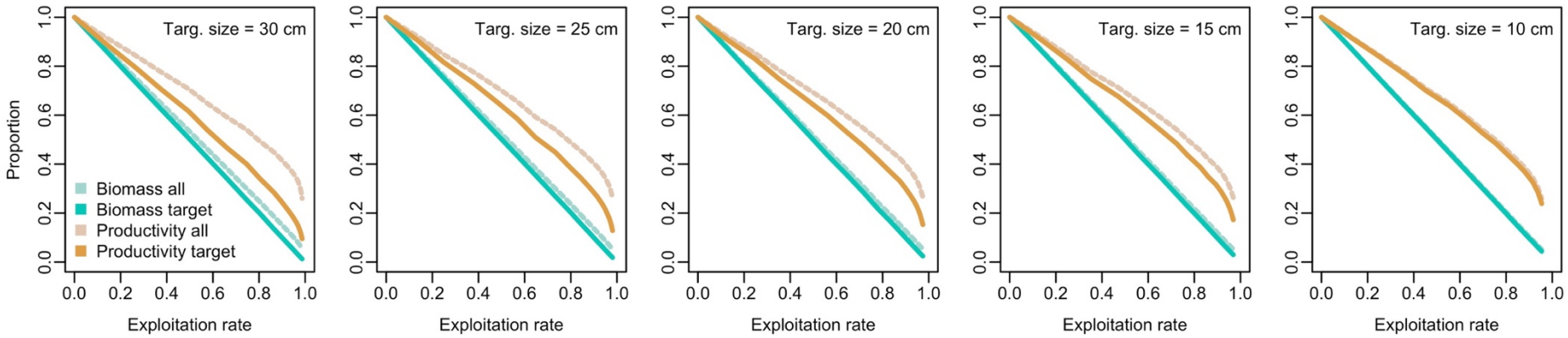

Figure F9: *The proportional decline in the biomass and productivity of modelled fish assemblages with increasing exploitation changes according to the minimum size thresholds for considering a fish as targeted by fisheries. The main overall effects of decreasing the minimum target size are increasing the similarity between the whole-assemblages and target species curves, as well as increasing the disparity between the declining trajectories of biomass and productivity (buffering productivity).*

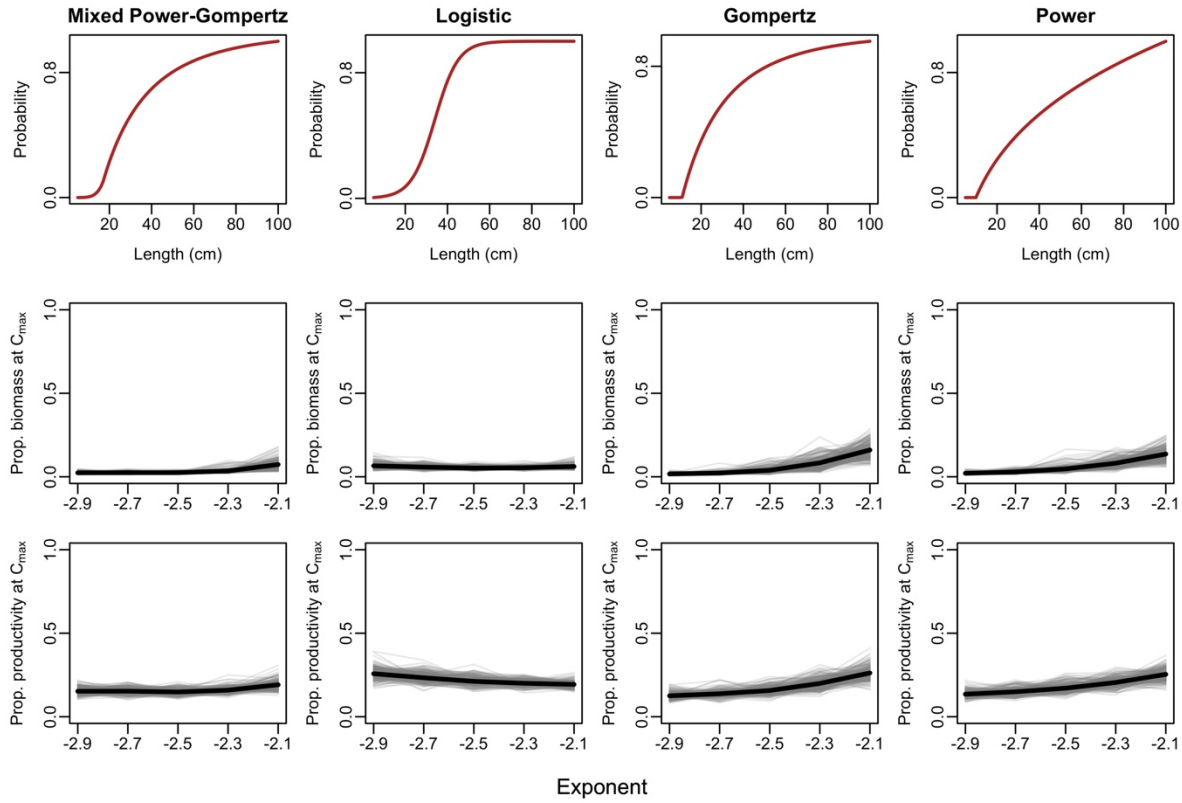

Figure F10: *The effect of changing the size-selective fishing function used to simulate fishing on modelled assemblages with varying size-spectrum exponents. Changing the shape of the size-selective function causes no changes in the biomass depletion of target species after fishing with a capture level of C_{max} at more negative size-spectrum exponents. At less negative exponents, biomass depletion is smaller for Gompertz and Power curves compared to the Logistic and the Mixed functions. A similar trend occurs with productivity, except that in no case productivity is depleted below 15% of the initial value. Buffering productivity, therefore, is a constant feature across size-spectrum exponents regardless of the fishing function used.*

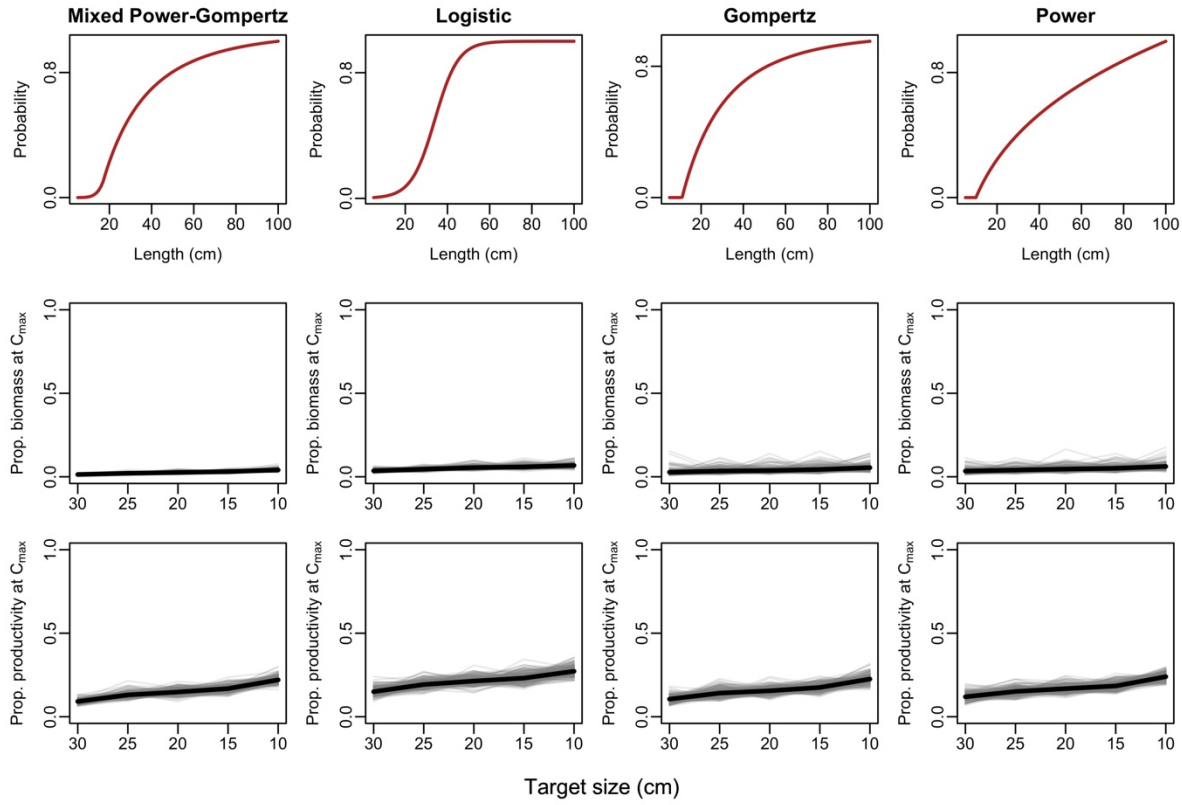

Figure F11: *The effect of changing the size-selective fishing function used to simulate fishing on modelled assemblages with varying minimum size thresholds for fisheries. Changing the shape of the size-selective function causes no changes in the biomass or productivity depletion for target species after fishing with a capture level of C_{max}. Buffering productivity, therefore, is a constant feature across minimum size thresholds for fisheries regardless of the fishing function used.*

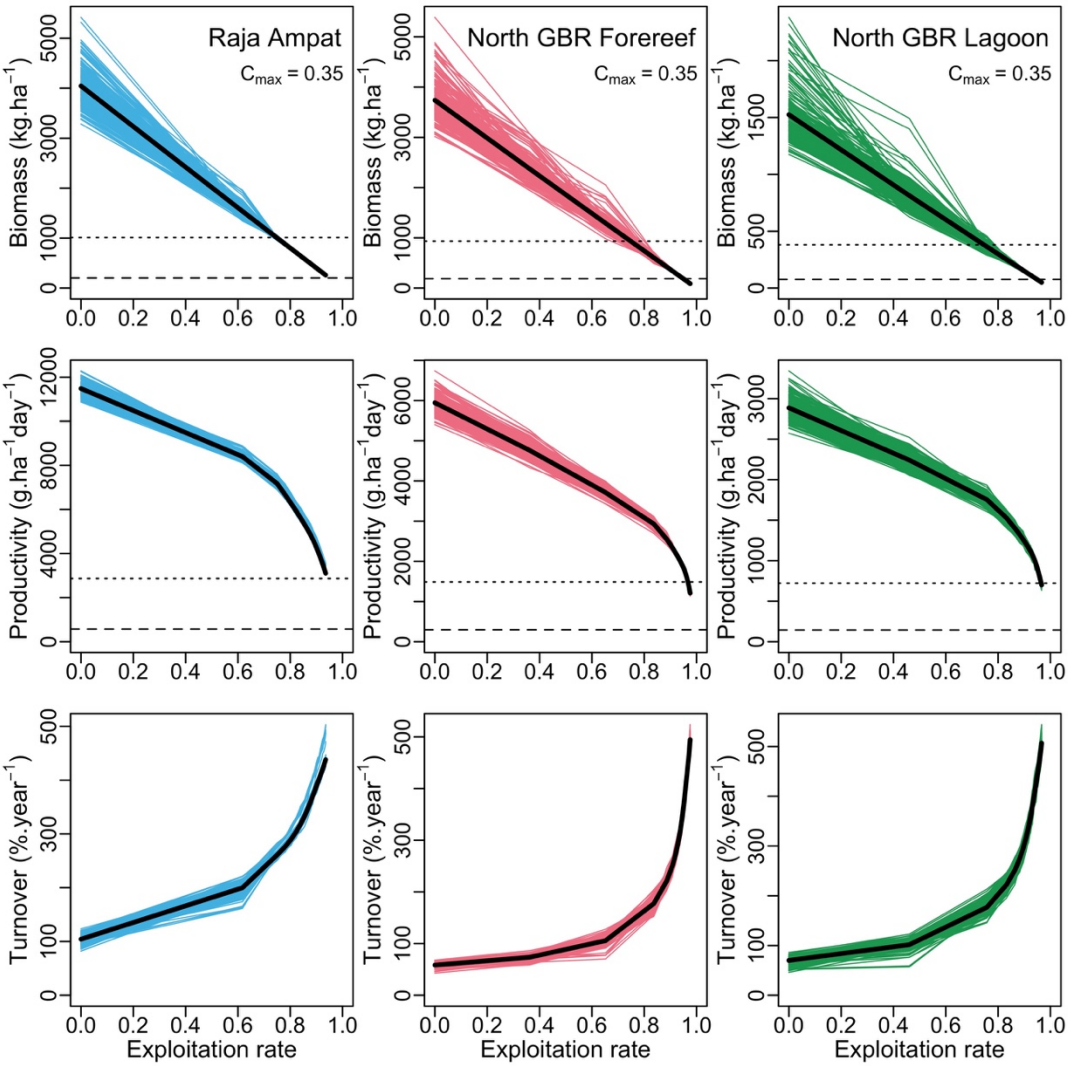

Figure F12: *Biomass, productivity and turnover of three entire coral reef fish assemblages with increasing exploitation. The observed patterns between assemblages remarkably mimic one another and the patterns observed both in the modelled (**Figure F4**) and in the parrotfish assemblages (**Figure F18**). C_{max} is the maximum capture level as a proportion of the initial abundance and varied across regions as depicted.*

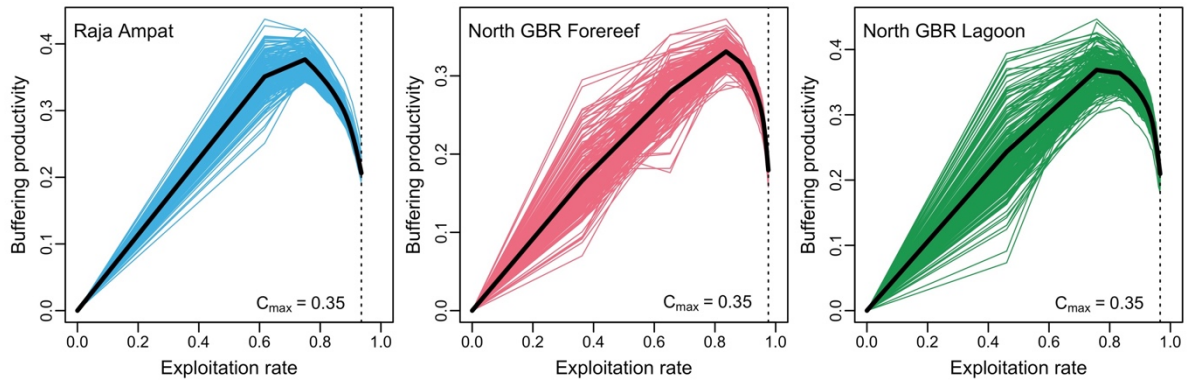

Figure F13: *The buffering productivity of entire coral reef fish assemblages with increasing exploitation. As exploitation increases, buffering productivity also increases until it reaches a peak value. The observed patterns between assemblages remarkably mimic one another and the patterns observed both in our modelled (**Figure F4**) and parrotfish assemblages (**Figure F19**). C_{max} is the maximum capture level as a proportion of initial abundance and varied across regions.*

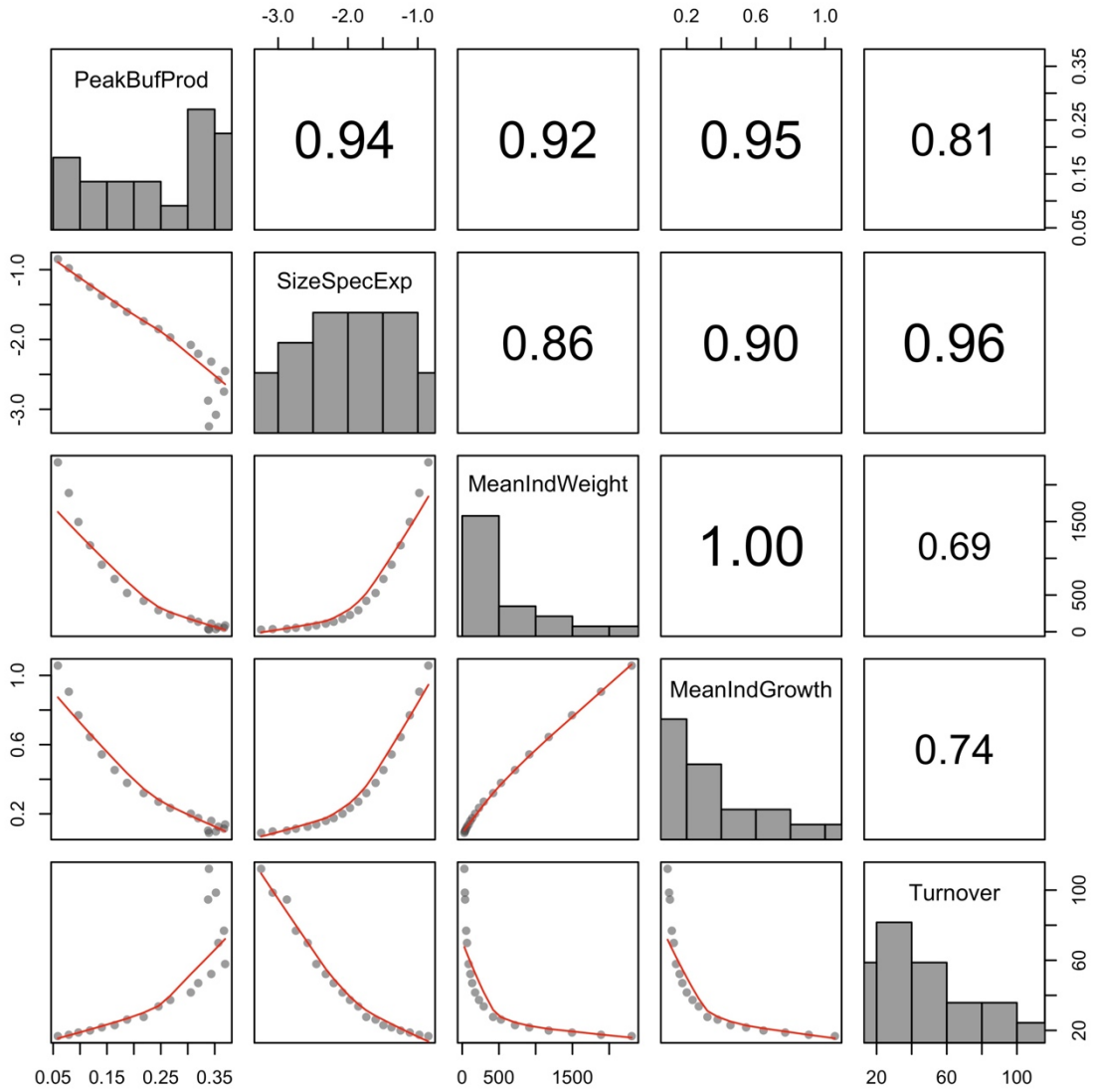

Figure F14: *Peak buffering productivity is highly correlated with features of the modelled fish assemblages before fishing simulations. These features include: a negative relationship with SizeSpecExp = size-spectrum exponent; a negative relationship with MeanIndWeight = mean individual weight in g; a negative relationship with MeanIndGrowth = mean individual growth in g day^{-1}; and a positive relationship with turnover in % year^{-1}. Most of the features also correlate among themselves. All features refer to the target portion of the fish assemblage only (see Methods of* ***Chapter 6****). Red lines are LOWESS smoothers. Numbers in the upper right panels are Pearson's correlation coefficient.*

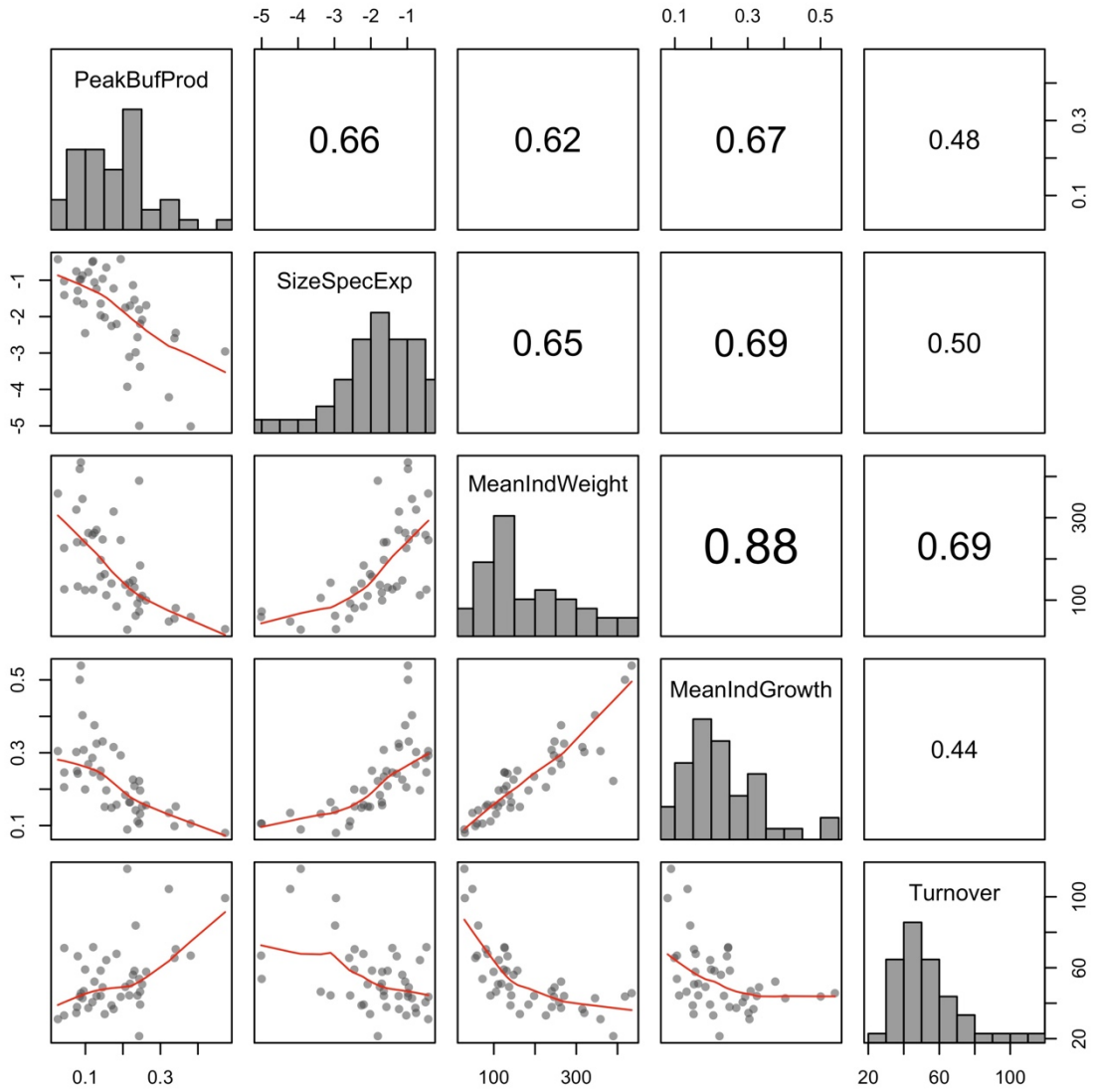

Figure F15: *Peak buffering productivity is correlated with features of empirical coral reef fish assemblages before fishing simulations. The directionality of these correlations is always the same as in our modelled fish assemblages (**Figure F14**). The correlated features include: a negative relationship with SizeSpecExp = size-spectrum exponent; a negative relationship with MeanIndWeight = mean individual weight in g; a negative relationship with MeanIndGrowth = mean individual growth in g day^{-1}; and a positive relationship with turnover in % year^{-1}. Some of the features also correlate among themselves, especially mean individual weight and mean individual growth. All features refer to the target portion of the fish assemblage only (see Methods of **Chapter 6**). Red lines are LOWESS smoothers. Numbers in the upper right panels are Pearson's correlation coefficient.*

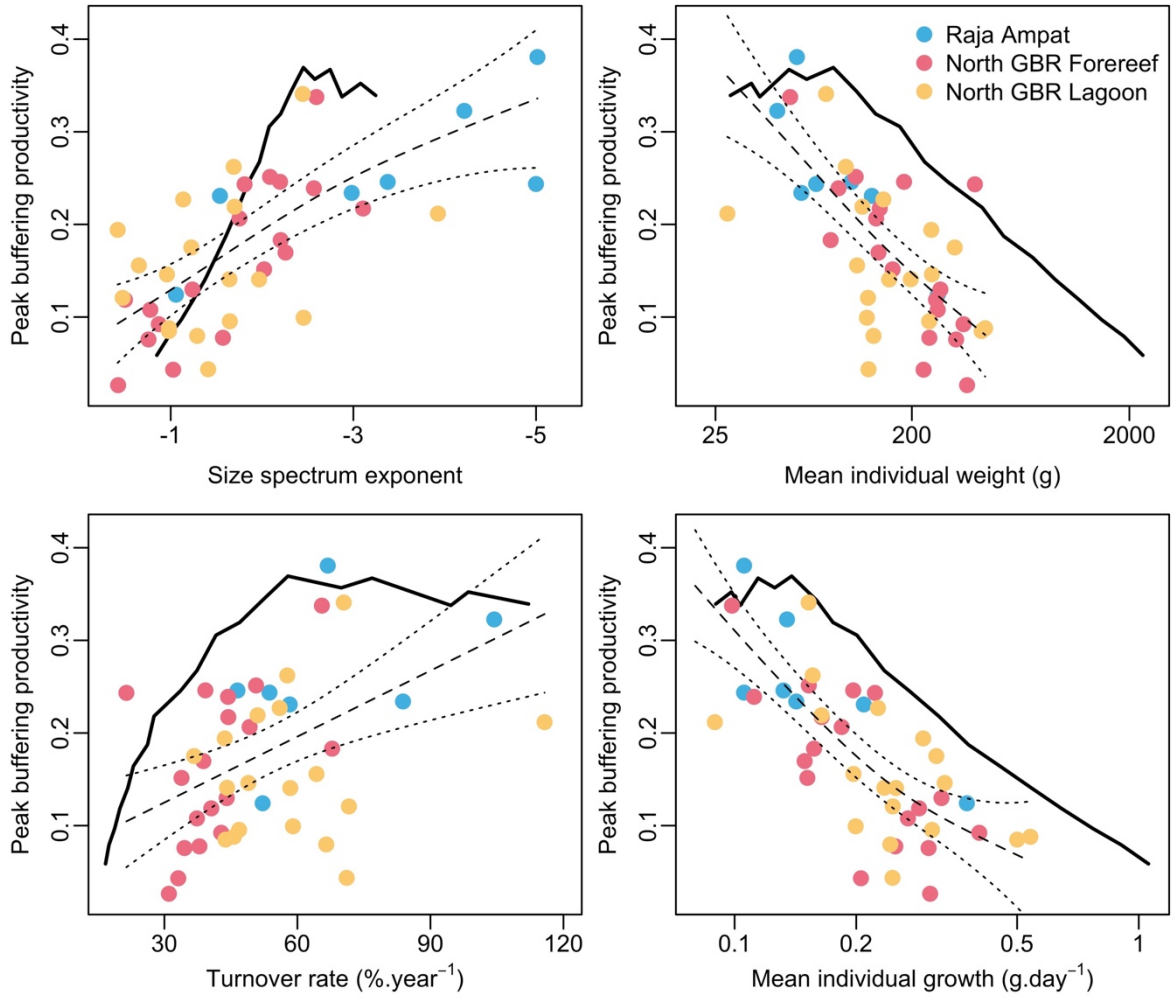

Figure F16: *The response of beak buffering productivity to features of the initial assemblages (before fishing simulations) in modelled versus empirical data. All features refer to the target portion of the fish assemblages only (see Methods of* ***Chapter 6****), both in the case of the modelled and the empirical data. Black continuous lines are peak buffering productivity from modelled assemblages and coloured dots from empirical data. Dashed and dotted lines are, respectively, Generalized Additive Model fits to the empirical data, and upper and lower 95% confidence intervals of these fits.*

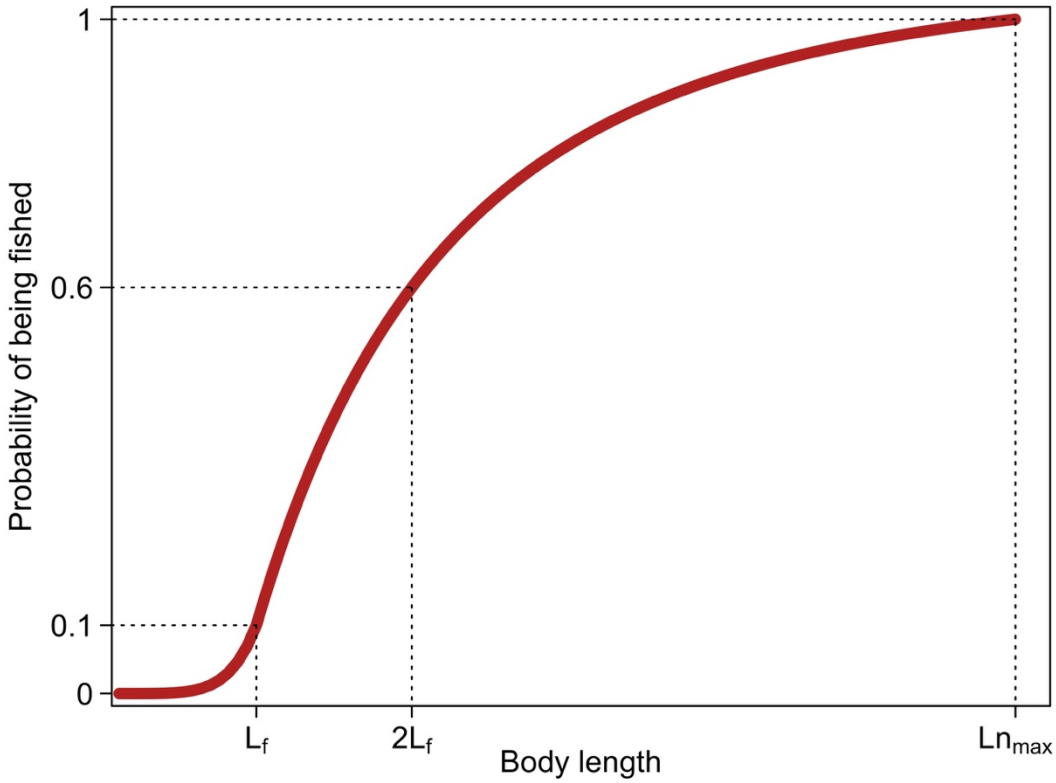

Figure F17: *The mixed Power and Gompertz size-specific fishing function used to simulate coral reef fisheries in both modelled and empirical fish assemblages. The body size (length) reference points represent: the transition size between the Power and the Gompertz components of the curve (L_f); the inflexion point of the Gompertz part of the curve ($2L_f$), and the maximum size potentially found in our assemblage (L^n_{max}).*

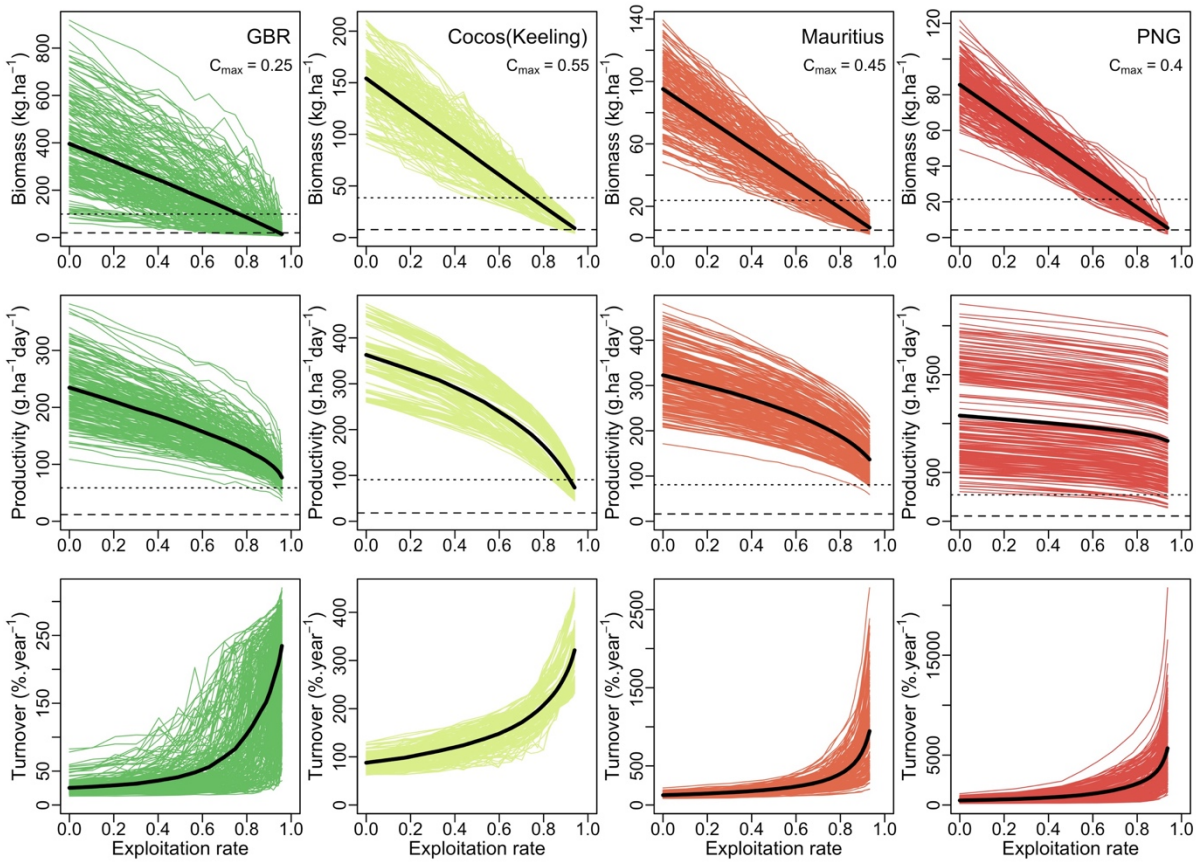

Figure F18: *Parrotfish biomass, productivity and turnover with increasing exploitation at four regions. Although with particularities in the scales of variation or magnitude of responses, the observed patterns between regions remarkably mimic one another and the patterns observed in the modelled (**Figure F4**) and whole empirical assemblages (**Figure F12**). C_{max} is the maximum capture level as a proportion of the initial abundance, varying with regions as shown.*

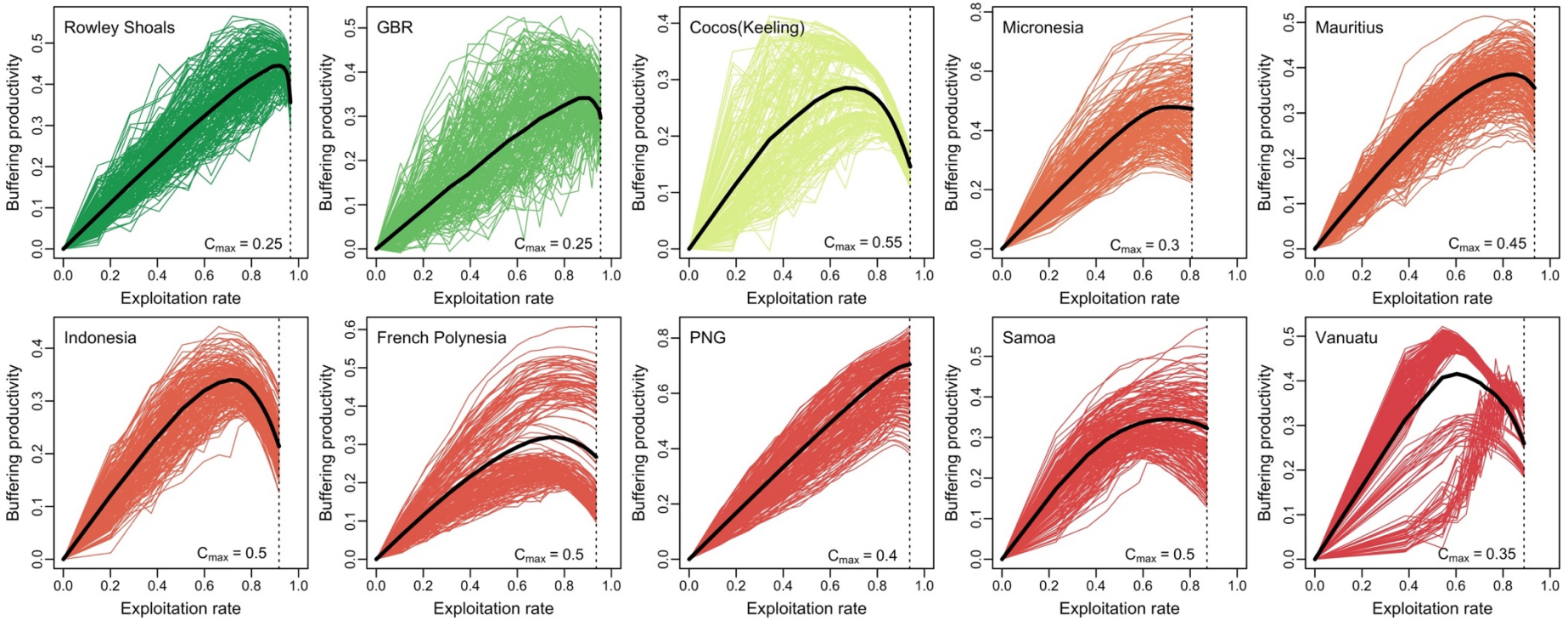

Figure F19: *The buffering productivity of parrotfish assemblages with increasing exploitation. As exploitation increases, buffering productivity also increases until it reaches a peak value. Although with particularities (e.g. scales of variation, peak value or exploitation rate at which buffering productivity starts to decline), the observed patterns between regions remarkably mimic one another and the patterns observed in our modelled (**Figure F4**) and whole empirical assemblages (**Figure F13**).* C_{max} *is the maximum capture level as a proportion of initial abundance and varied with regions as shown.*

Table F1: *Model selection table of sample-level parrotfish productivity as a function of biomass, region, habitat and distance to the centre of the IAA (linear fits). The models are ordered by AICc. Productivity (response variable) and biomass were log_{10}-transformed. Dist = distance to the centre of the IAA; Hab = habitat; Biom = biomass; Reg = region; df = degrees of freedom; logLik = log-likelihood.*

Dist	Hab	Biom	Reg	Dist:Biom	Hab:Biom	Biom:Reg	df	logLik	AICc	ΔAIC	wAIC
+	+	+	+			+	25	63.96	-73.3	0.00	0.463
	+	+	+			+	24	62.35	-72.4	0.85	0.303
+	+	+	+	+		+	26	64.15	-71.3	2.01	0.170
+	+	+	+		+	+	28	64.90	-67.9	5.35	0.032
	+	+	+		+	+	27	63.30	-67.2	6.12	0.022
+	+	+	+	+	+	+	29	64.96	-65.6	7.65	0.010
+	+	+	+	+			17	31.19	-26.3	47.03	0.000
+		+	+			+	22	35.74	-23.9	49.37	0.000
		+	+			+	21	34.50	-23.8	49.53	0.000
+		+	+	+		+	23	36.25	-22.6	50.69	0.000
+	+	+	+	+	+		20	31.79	-20.6	52.65	0.000
+	+	+	+				16	18.23	-2.6	70.71	0.000
	+	+	+				15	17.09	-2.5	70.77	0.000
+	+	+	+		+		19	20.05	0.5	73.84	0.000
	+	+	+		+		18	18.92	0.5	73.84	0.000
+		+	+	+			14	-0.74	30.9	104.21	0.000
+	+	+		+			8	-7.89	32.3	105.56	0.000
+	+	+		+	+		11	-6.90	36.7	109.99	0.000
		+	+				12	-16.38	57.8	131.12	0.000
+		+	+				13	-15.78	58.8	132.10	0.000
	+	+					6	-23.51	59.3	132.60	0.000
+	+	+					7	-22.80	60	133.27	0.000
	+	+			+		9	-21.79	62.2	135.47	0.000
+	+	+			+		10	-21.01	62.8	136.06	0.000
+		+		+			5	-36.07	82.3	155.63	0.000
+		+					4	-52.11	112.4	185.64	0.000
		+					3	-53.26	112.6	185.89	0.000
	+						5	-163.06	336.3	409.61	0.000
+	+						6	-162.87	338	411.31	0.000
	+		+				14	-157.16	343.8	417.05	0.000
+	+		+				15	-156.49	344.6	417.93	0.000
							2	-185.35	374.7	448.03	0.000
+							3	-185.33	376.7	450.04	0.000
			+				11	-177.21	377.3	450.60	0.000
+			+				12	-176.80	378.7	451.95	0.000

Table F2: *Sample-level parrotfish assemblage productivity as a function of biomass, region and habitat. The model presented was chosen among nested subsets of the complete model using model selection procedures. The full model and less informative nested models are in* ***Table F6****. Productivity and biomass have been log_{10}-transformed.*

Model	**Multiple R^2**	**Adjusted R^2**	**F-statistic**	**p-value**	
Prod ~ Biom * Reg + Hab	0.801	0.785	51.91	<0.0001	***
Coefficient	**Estimate**	**Std. Error**	**t-value**	**p-value**	
Intercept	1.669	0.239	6.98	<0.0001	***
Biomass	0.388	0.100	3.88	0.0001	***
Region (GBR)	-0.166	0.257	-0.65	0.5183	
Region (Cocos Keeling)	-0.877	0.342	-2.56	0.0109	*
Region (Micronesia)	-0.790	0.271	-2.92	0.0038	**
Region (Mauritius)	-0.537	0.323	-1.66	0.0976	
Region (Indonesia)	-0.669	0.268	-2.50	0.0130	*
Region (French Polyn.)	-1.237	0.298	-4.15	<0.0001	***
Region (PNG)	-1.008	0.292	-3.45	0.0007	***
Region (Samoa)	-1.027	0.280	-3.67	0.0003	***
Region (Vanuatu)	-0.783	0.305	-2.57	0.0107	*
Habitat (Flat)	-0.118	0.038	-3.12	0.0020	**
Habitat (Crest)	-0.258	0.036	-7.09	<0.0001	***
Habitat (Slope)	-0.197	0.035	-5.60	<0.0001	***
Biomass x Region (GBR)	0.058	0.111	0.53	0.5986	
Biomass x Region (Cocos Keeling)	0.484	0.155	3.12	0.0020	**
Biomass x Region (Micronesia)	0.601	0.124	4.85	<0.0001	***
Biomass x Region (Mauritius)	0.326	0.154	2.12	0.0353	*
Biomass x Region (Indonesia)	0.440	0.124	3.55	0.0005	***
Biomass x Region (French Polyn.)	0.687	0.141	4.88	<0.0001	***
Biomass x Region (PNG)	0.629	0.138	4.56	<0.0001	***
Biomass x Region (Samoa)	0.703	0.132	5.34	<0.0001	***
Biomass x Region (Vanuatu)	0.450	0.150	3.01	0.0028	**
Residual	-	0.205	-	-	

Table F3: *Region-level average biomass, body length and productivity of parrotfish assemblages as functions of human population density and distance to the centre of the Indo-Australian Archipelago (IAA). Models are Generalized Linear Models with gamma distribution (biomass and productivity) or gaussian distribution (length). Human population density was log10-transformed. Hum = human population density; Dist = distance to the centre of the IAA.*

Model	Coefficient	Estimate	Std. Error	t-value	p-value	
Biomass ~ Hum + Dist	Intercept	5.725	0.166	34.42	<0.0001	***
	Human Pop.	-0.397	0.067	-5.90	0.0006	***
	Dist. Cent. IAA	0.001	0.004	0.22	0.8354	
Length ~ Hum + Dist	Intercept	23.947	1.152	20.80	<0.0001	***
	Human Pop.	-1.911	0.467	-4.09	0.0046	**
	Dist. Cent. IAA	-0.002	0.028	-0.06	0.9518	
Productivity ~ Hum + Dist	Intercept	5.792	0.310	18.66	<0.0001	***
	Human Pop.	-0.005	0.126	-0.04	0.9710	
	Dist. Cent. IAA	0.000	0.008	0.03	0.9790	

Table F4: *Peak buffering productivity as a function of features of two empirical coral reef fish assemblages (Raja Ampat, Indonesia, and Lizard Island, Great Barrier Reef) before fishing simulations. Models are Generalized Additive Models with gaussian distribution, and only statistics from the smoothers are shown. SizeSpecExp = size-spectrum exponent; MeanIndWeight = mean individual weight; MeanIndGrow = mean individual growth; edf = estimated degrees of freedom. MeanIndWeight and MeanIndGrow are* log_{10}*-transformed.*

Model	Adjusted R^2	Dev. expl.	Smoother edf	F-statistic	p-value
PeakBP ~ s(SizeSpecExp)	0.441	46.2%	1.605	17.06	<0.0001
PeakBP ~ s(MeanIndWeight)	0.511	52.8%	1.492	26.25	<0.0001
PeakBP ~ s(MeanIndGrow)	0.581	59.9%	1.892	25.32	<0.0001
PeakBP ~ s(Turnover)	0.212	23.1%	1	12.58	0.0009

Table F5: *Number of parrotfish counts per reef habitat, for each location, among the ten sampled regions across the Indo-Pacific.*

Region	Location	Back	Flat	Crest	Slope
Rowley Shoals	Clerke Reef	4	4	5	5
GBR	Day Reef	4	4	4	4
GBR	Hicks Reef	4	4	4	4
GBR	Yonge Reef	4	4	4	4
Cocos (Keeling)	South Keeling	4	4	6	6
Micronesia	Kosrae	5	4	4	4
Micronesia	Pohnpei	4	4	4	4
Mauritius	Mauritius	4	4	4	4
Mauritius	Rodrigues	4	4	4	4
Indonesia	North Sulawesi	-	5	6	6
Indonesia	Togean	3	4	4	8
French Polynesia	Moorea	4	4	6	4
French Polynesia	Tahiti	4	4	4	4
Papua New Guinea	North Kavieng	4	4	4	4
Papua New Guinea	South Kavieng	4	4	4	4
Samoa	Apia	6	4	4	5
Samoa	Nu'utele	5	4	4	4
Vanuatu	Efate	-	4	4	4
Vanuatu	Nguna	-	4	4	4

Table F6: *Alternative size-selective fishing functions used to simulate fishing on modelled fish assemblages, including conditions, formulas and values of fixed parameters.*

Function	Condition	Formula	Parameters
Logistic	-	$cp_l = \frac{s}{\left[1 + e^{-v(L-2L_f)}\right]}$	$S = 1; v = 0.18; L_f = 17$
Gompertz	For $L < 12$ cm	$cp_l = 0$	$S = 1; I = 1.25; v = 0.025;$ $L_f = 15$
	For $L \geq 12$ cm	$cp_l = I + \left[(S - I)e^{e^{-v(L-2L_f)}}\right]$	
Power	For $L < 10$ cm	$cp_l = 0$	$r = 200; h = 4$
	For $L \geq 10$ cm	$cp_l = rL^h$	

Appendix F References

Ackerman, J. L., & Bellwood, D. R. (2000). Reef fish assemblages: A re-evaluation using enclosed rotenone stations. *Marine Ecology Progress Series*, *206*(1954), 227–237. doi: 10.3354/meps206227

Allen, G. R. (2008). Conservation hotspots of biodiversity and endemism for Indo-Pacific coral reef fishes. *Aquatic Conservation: Marine and Freshwater Ecosystems*, *18*(5), 541–556. doi: 10.1002/aqc.880

Allen, G. R., & Erdmann, M. V. (2009). Reef fishes of the Bird's Head Peninsula, West Papua, Indonesia. *Check List*, *5*(3), 587–628. doi: 10.15560/5.3.587

Almany, G. R., & Webster, M. S. (2006). The predation gauntlet: early post-settlement mortality in reef fishes. *Coral Reefs*, *25*(1), 19–22. doi: 10.1007/s00338-005-0044-y

Andersen, K. H., & Beyer, J. E. (2006). Asymptotic Size Determines Species Abundance in the Marine Size Spectrum. *The American Naturalist*, *168*(1), 54–61. doi: 10.1086/504849

Barneche, D. R., Robertson, D. R., White, C. R., & Marshall, D. J. (2018). Fish reproductive-energy output increases disproportionately with body size. *Science*, *360*(6389), 642–645. doi: 10.1126/science.aao6868

Bartoń, K. (2016). *MuMIn: Multi-Model Inference*. R package version 1.15.6.

Bellwood, D. R., Hoey, A. S., & Choat, J. H. (2003). Limited functional redundancy in high diversity systems: Resilience and ecosystem function on coral reefs. *Ecology Letters*, *6*(4), 281–285. doi: 10.1046/j.1461-0248.2003.00432.x

Bellwood, D. R., Hoey, A. S., & Hughes, T. P. (2012). Human activity selectively impacts the ecosystem roles of parrotfishes on coral reefs. *Proceedings of the Royal Society B: Biological Sciences*, *279*(1733), 1621–1629. doi: 10.1098/rspb.2011.1906

Bellwood, D. R., Hughes, T. P., Folke, C., & Nyström, M. (2004). Confronting the coral reef crisis. *Nature*, *429*(6994), 827–833. doi: 10.1038/nature02691

Bellwood, D. R., & Wainwright, P. (2001). Locomotion in labrid fishes: Implications for habitat use and cross-shelf biogeography on the Great Barrier Reef. *Coral Reefs*, *20*(2), 139–150. doi: 10.1007/s003380100156

Beverton, R. J. H., & Holt, S. J. (1957). On the Dynamics of Exploited Fish Populations. In *Fisheries Investigations Series 2: Sea Fisheries* (Vol. 4). doi: 10.1007/978-94-011-2106-4

Bonaldo, R. M., Hoey, A. S., & Bellwood, D. R. (2014). The Ecosystem Roles of Parrotfishes on Tropical Reefs. *Oceanography and Marine Biology: An Annual Review*, *52*, 81–132.

Bradley, D., Conklin, E., Papastamatiou, Y. P., McCauley, D. J., Pollock, K., Pollock, A., … Caselle, J. E. (2017). Resetting predator baselines in coral reef ecosystems. *Scientific Reports*, *7*(1), 43131. doi: 10.1038/srep43131

Brandl, S. J., Tornabene, L., Goatley, C. H. R., Casey, J. M., Morais, R. A., Côté, I. M., … Bellwood, D. R. (2019). Demographic dynamics of the smallest marine vertebrates fuel coral reef ecosystem functioning. *Science*, *364*(6446), 1189–1192. doi: 10.1126/science.aav3384

Burnham, K. P., & Anderson, D. R. (2002). *Model Selection and Multimodel Inference A Practical Information-Theoretic Approach* (2nd ed.). New York: Springer-Verlag.

Choat, J. H., Axe, L. M., & Lou, D. C. (1996). Growth and longevity in fishes of the family Scaridae. *Marine Ecology Progress Series*, *145*(1–3), 33–41. doi: 10.3354/meps145033

Choat, J. H., & Robertson, D. R. (2002). Age-Based Studies. In Peter F Sale (Ed.), *Coral reef fishes: dynamics and diversity in a complex ecosystem* (pp. 57–80). Burlington, San Diego, London: Academic Press.

CIESIN. (2016). Gridded Population of the World, Version 4 (GPWv4): Population Density. Retrieved from Center for International Earth Science Information Network Columbia University website: http://dx.doi.org/10.7927/H4NP22DQ

Condy, M., Cinner, J. E., McClanahan, T. R., & Bellwood, D. R. (2015). Projections of the impacts of gear-modification on the recovery of fish catches and ecosystem function in an impoverished fishery. *Aquatic Conservation: Marine and Freshwater Ecosystems*, *25*(3), 396–410. doi: 10.1002/aqc.2482

D'agata, S., Mouillot, D., Wantiez, L., Friedlander, A. M., Kulbicki, M., & Vigliola, L. (2016). Marine reserves lag behind wilderness in the conservation of key functional roles. *Nature Communications*, *7*(May), 12000. doi: 10.1038/ncomms12000

Dalzell, P., Polunin, N. V. C., & Roberts, C. M. (1996). Reef Fisheries. In N. V. C. Polunin & C. M.

Roberts (Eds.), *Reef Fisheries*. doi: 10.1007/978-94-015-8779-2

DeMartini, E., Andrews, A., Howard, K., Taylor, B., Lou, D., & Donovan, M. (2017). Comparative growth, age at maturity and sex change and longevity of Hawaiian parrotfishes with bomb radiocarbon validation. *Canadian Journal of Fisheries an Aquatic Sciences*, *15*(51), 1–31. doi: 10.1139/cjfas-2016-0523

Doherty, P. J. (1991). Spatial and Temporal Patterns in Recruitment. In P F Sale (Ed.), *The ecology of fishes on coral reefs* (pp. 261–293). San Diego: Academic Press.

Dulvy, N. K., Polunin, N. V. C., Mill, A. C., & Graham, N. A. J. (2004). Size structural change in lightly exploited coral reef fish communities: evidence for weak indirect effects. *Canadian Journal of Fisheries and Aquatic Sciences*, *61*(3), 466–475. doi: 10.1139/f03-169

Edwards, A. M., Robinson, J. P. W., Plank, M. J., Baum, J. K., & Blanchard, J. L. (2017). Testing and recommending methods for fitting size spectra to data. *Methods in Ecology and Evolution*, *8*(1), 57–67. doi: 10.1111/2041-210X.12641

Froese, R., & Pauly, D. (2018). FishBase. World Wide Web page. http://www.fishbase.org.

Froese, R., Thorson, J. T., & Reyes, R. B. (2014). A Bayesian approach for estimating length-weight relationships in fishes. *Journal of Applied Ichthyology*, *30*(1), 78–85. doi: 10.1111/jai.12299

Goatley, C. H. R., & Bellwood, D. R. (2016). Body size and mortality rates in coral reef fishes : a three-phase relationship. *Proceedings of the Royal Society B: Biological Sciences*, *283*, 20161858. doi: 10.1098/rspb.2016.1858

Graham, N. A. J., Dulvy, N., Jennings, S., & Polunin, N. (2005). Size-spectra as indicators of the effects of fishing on coral reef fish assemblages. *Coral Reefs*, *24*(1), 118–124. doi: 10.1007/s00338-004-0466-y

Graham, N. A. J., McClanahan, T. R., MacNeil, M. A., Wilson, S. K., Cinner, J. E., Huchery, C., & Holmes, T. H. (2017). Human Disruption of Coral Reef Trophic Structure. *Current Biology*, *27*(2), 231–236. doi: 10.1016/j.cub.2016.10.062

Grutter, A. S., Blomberg, S. P., Fargher, B., Kuris, A. M., McCormick, M. I., & Warner, R. R. (2017). Size-related mortality due to gnathiid isopod micropredation correlates with settlement size in coral reef fishes. *Coral Reefs*, *36*(2), 549–559. doi: 10.1007/s00338-016-1537-6

Gust, N., Choat, J. H., & Ackerman, J. L. (2002). Demographic plasticity in tropical reef fishes. *Marine Biology*, *140*(5), 1039–1051. doi: 10.1007/s00227-001-0773-6

Hamilton, R. J., Almany, G. R., Stevens, D., Bode, M., Pita, J., Peterson, N. A., & Choat, J. H. (2016). Hyperstability masks declines in bumphead parrotfish (*Bolbometopon muricatum*) populations. *Coral Reefs*, *35*(3), 751–763. doi: 10.1007/s00338-016-1441-0

Hilborn, R., & Walters, C. J. (1992). *Quantitative Fisheries Stock Assessment*. Boston: Springer US. doi: 10.1007/978-1-4615-3598-0

Hixon, M. A., Johnson, D. W., & Sogard, S. M. (2014). BOFFFFs: on the importance of conserving old-growth age structure in fishery populations. *ICES Journal of Marine Science*, *71*(8), 2171–2185. doi: 10.1093/icesjms/fst200

Hixon, M. A., & Webster, M. S. (2002). Density dependence in reef fish populations. In P. Sale (Ed.), *Coral reef fishes: dynamics and diversity in a complex ecosystem* (pp. 303–325). Burlington, San Diego, London: Academic Press.

Hoey, A. S., Taylor, B. M., Hoey, J., & Fox, R. J. (2018). Parrotfishes, are We Still Scraping the Surface? Emerging Topics and Future Research Directions. In *Biology of Parrotfishes* (pp. 407–416). doi: 10.1201/9781315118079-17

Houk, P., Rhodes, K., Cuetos-Bueno, J., Lindfield, S., Fread, V., & McIlwain, J. L. (2012). Commercial coral-reef fisheries across Micronesia: A need for improving management. *Coral Reefs*, *31*(1), 13–26. doi: 10.1007/s00338-011-0826-3

Jennings, S., & Blanchard, J. L. (2004). Fish abundance with no fishing: predictions based on macroecological theory. *Journal of Animal Ecology*, *73*(4), 632–642. doi: 10.1111/j.0021-8790.2004.00839.x

Jennings, S., & Dulvy, N. K. (2005). Reference points and reference directions for size-based indicators of community structure. *ICES Journal of Marine Science*, *62*(3), 397–404.

Leis, J. M. (1991). The Pelagic Stage of Reef Fishes: The Larval Biology of Coral Reef Fishes. In P F Sale (Ed.), *The ecology of fishes on coral reefs* (pp. 183–230). San Diego: Academic Press.

McClanahan, T. R. (2018). Multicriteria estimate of coral reef fishery sustainability. *Fish and Fisheries*, *19*(5), 807–820. doi: 10.1111/faf.12293

Meekan, M., Milicich, M., & Doherty, P. (1993). Larval production drives temporal patterns of larval supply and recruitment of a coral reef damselfish. *Marine Ecology Progress Series*, *93*(17), 217–225. doi: 10.3354/meps093217

Mora, C., & Sale, P. F. (2002). Are populations of coral reef fish open or closed? *Trends in Ecology & Evolution*, *17*(9), 422–428. doi: http://dx.doi.org/10.1016/S0169-5347(02)02584-3

Morais, R. A., & Bellwood, D. R. (2018). Global drivers of reef fish growth. *Fish and Fisheries*, *19*(5), 874–889. doi: 10.1111/faf.12297

Morais, R. A., & Bellwood, D. R. (2019). Pelagic subsidies underpin fish productivity on a degraded coral reef. *Current Biology*, *29*(9), 1521–1527. doi: 10.1016/j.cub.2019.03.044

Munch, S. B., Giron-Nava, A., & Sugihara, G. (2018). Nonlinear dynamics and noise in fisheries recruitment: A global meta-analysis. *Fish and Fisheries*, *19*(6), 964–973. doi: 10.1111/faf.12304

Rhodes, K. L., Tupper, M. H., & Wichilmel, C. B. (2008). Characterization and management of the commercial sector of the Pohnpei coral reef fishery, Micronesia. *Coral Reefs*, *27*(2), 443–454. doi: 10.1007/s00338-007-0331-x

Robertson, D. R. (1990). Differences in the seasonalities of spawning and recruitment of some small neotropical reef fishes. *Journal of Experimental Marine Biology and Ecology*, *144*(1), 49–62.

Robinson, J. P. W., Williams, I. D., Edwards, A. M., McPherson, J., Yeager, L., Vigliola, L., … Baum, J. K. (2017). Fishing degrades size structure of coral reef fish communities. *Global Change Biology*, *23*(3), 1009–1022. doi: 10.1111/gcb.13482

Sandin, S. A., Smith, J. E., DeMartini, E. E., Dinsdale, E. A., Donner, S. D., Friedlander, A. M., … Sala, E. (2008). Baselines and degradation of coral reefs in the Northern Line Islands. *PLoS ONE*, *3*(2), e1548. doi: 10.1371/journal.pone.0001548

Schnute, J. T., & Richards, L. (2002). Surplus production models. In P. H. & J. Reynolds (Ed.), *Handbook of Fish Biology & Fisheries* (pp. 105–126). Blackwell Publishing Ltd.

Scott, B., Marteinsdottir, G., & Wright, P. (1999). Potential effects of maternal factors on spawning stock–recruitment relationships under varying fishing pressure. *Canadian Journal of Fisheries and Aquatic Sciences*, *56*(10), 1882–1890. doi: 10.1139/f99-125

Subbey, S., Devine, J. A., Schaarschmidt, U., & Nash, R. D. M. (2014). Modelling and forecasting

stock-recruitment: current and future perspectives. *ICES Journal of Marine Science*, *71*(8), 2307–2322. doi: 10.1093/icesjms/fsu148

Szuwalski, C. S., Vert-Pre, K. A., Punt, A. E., Branch, T. A., & Hilborn, R. (2015). Examining common assumptions about recruitment: a meta-analysis of recruitment dynamics for worldwide marine fisheries. *Fish and Fisheries*, *16*(4), 633–648. doi: 10.1111/faf.12083

Taylor, B. M., Brandl, S. J., Kapur, M., Robbins, W. D., Johnson, G., Huveneers, C., … Choat, J. H. (2018). Bottom-up processes mediated by social systems drive demographic traits of coral-reef fishes. *Ecology*, *99*(3), 642–651. doi: 10.1002/ecy.2127

Taylor, B. M., Lindfield, S. J., & Choat, J. H. (2015). Hierarchical and scale-dependent effects of fishing pressure and environment on the structure and size distribution of parrotfish communities. *Ecography*, *38*(5), 520–530. doi: 10.1111/ecog.01093

Tyberghein, L., Verbruggen, H., Pauly, K., Troupin, C., Mineur, F., & De Clerck, O. (2012). Bio-ORACLE: a global environmental dataset for marine species distribution modelling. *Global Ecology and Biogeography*, *21*(2), 272–281. doi: 10.1111/j.1466-8238.2011.00656.x

Victor, B. C. (1986). Larval Settlement and Juvenile Mortality in a Recruitment-Limited Coral Reef Fish Population. *Ecological Monographs*, *56(2)*, 145–160. doi: 10.2307/1942506

Victor, B. C. (1991). Settlement Strategies and Biogeography of Reef Fishes. In P F Sale (Ed.), *The ecology of fishes on coral reefs* (pp. 231–260). San Diego: Academic Press.

Ward-Paige, C., Flemming, J. M., & Lotze, H. K. (2010). Overestimating fish counts by non-instantaneous visual censuses: Consequences for population and community descriptions. *PLoS ONE*, *5*(7), e11722. doi: 10.1371/journal.pone.0011722

Williams, I. D., Baum, J. K., Heenan, A., Hanson, K. M., Nadon, M. O., & Brainard, R. E. (2015). Human, Oceanographic and Habitat Drivers of Central and Western Pacific Coral Reef Fish Assemblages. *PLoS ONE*, *10*(4), e0120516. doi: 10.1371/journal.pone.0120516

Wilson, S. K., Fisher, R., Pratchett, M. S., Graham, N. A. J., Dulvy, N. K., Turner, R. A., … Polunin, N. V. C. (2010). Habitat degradation and fishing effects on the size structure of coral reef fish communities. *Ecological Applications*, *20*(2), 442–451. doi: 10.1890/08-2205.1

Worm, B., Hilborn, R., Baum, J. K., Branch, T. A., Collie, J. S., Costello, C., … Zeller, D. (2009).

Rebuilding Global Fisheries. *Science*, *325*(5940), 578–585. doi: 10.1126/science.1173146